NASA TECHNICAL MEMORANDUM

NASA TM X-3423

NASA TM X-3423

# WAVE REFRACTION DIAGRAMS FOR THE BALTIMORE CANYON REGION OF THE MID-ATLANTIC CONTINENTAL SHELF COMPUTED BY USING THREE BOTTOM TOPOGRAPHY APPROXIMATION TECHNIQUES

*Lamont R. Poole*

*Langley Research Center*
*Hampton, Va. 23665*

NATIONAL AERONAUTICS AND SPACE ADMINISTRATION • WASHINGTON, D. C. • DECEMBER 1976

| 1. Report No. | 2. Government Accession No. | 3. Recipient's Catalog No. |
|---|---|---|
| NASA TM X-3423 | | |

| 4. Title and Subtitle | 5. Report Date |
|---|---|
| WAVE REFRACTION DIAGRAMS FOR THE BALTIMORE CANYON REGION OF THE MID-ATLANTIC CONTINENTAL SHELF COMPUTED BY USING THREE BOTTOM TOPOGRAPHY APPROXIMATION TECHNIQUES | December 1976 |
| | 6. Performing Organization Code |

| 7. Author(s) | 8. Performing Organization Report No. |
|---|---|
| Lamont R. Poole | L-11004 |
| | 10. Work Unit No. |
| 9. Performing Organization Name and Address | 161-07-02-03 |
| NASA Langley Research Center<br>Hampton, VA 23665 | 11. Contract or Grant No. |
| | 13. Type of Report and Period Covered |
| 12. Sponsoring Agency Name and Address | Technical Memorandum |
| National Aeronautics and Space Administration<br>Washington, DC 20546 | 14. Sponsoring Agency Code |

15. Supplementary Notes

16. Abstract

The Langley Research Center and Virginia Institute of Marine Science wave refraction computer model was applied to the Baltimore Canyon region of the mid-Atlantic continental shelf. Wave refraction diagrams for a wide range of normally expected wave periods and directions were computed by using three bottom topography approximation techniques: quadratic least squares, cubic least squares, and constrained bicubic interpolation. Mathematical or physical interpretation of certain features appearing in the computed diagrams is discussed.

17. Key Words (Suggested by Author(s))

Wave refraction
Bottom topography approximation
Baltimore Canyon region

18. Distribution Statement

Unclassified - Unlimited

Subject Category 48

| 19. Security Classif. (of this report) | 20. Security Classif. (of this page) | 21. No. of Pages | 22. Price* |
|---|---|---|---|
| Unclassified | Unclassified | 155 | $6.25 |

* For sale by the National Technical Information Service, Springfield, Virginia 22161

# WAVE REFRACTION DIAGRAMS FOR THE BALTIMORE CANYON REGION OF THE MID-ATLANTIC CONTINENTAL SHELF COMPUTED BY USING THREE BOTTOM TOPOGRAPHY APPROXIMATION TECHNIQUES

Lamont R. Poole
Langley Research Center

## SUMMARY

Wave refraction diagrams were computed by applying the Langley Research Center and Virginia Institute of Marine Science wave refraction computer model to the Baltimore Canyon region of the mid-Atlantic continental shelf. Diagrams were presented for a wide range of normally expected wave periods and directions. For each combination of period and direction, diagrams were computed by using each of three commonly used bottom topography approximation techniques (quadratic least squares, cubic least squares, and constrained bicubic interpolation), and all these diagrams are presented with the exception of cases in which essentially identical diagrams resulted from the three techniques. Certain features of the computed diagrams were discussed with respect to physical or mathematical interpretation, but no conclusions were drawn.

## INTRODUCTION

Man's increasing use of continental shelf regions of the world has stimulated the development of analytical models to aid in the study of the physical processes affecting offshore and coastal activities. One such analytical tool is the wave refraction model, which describes the behavior of surface waves propagating through areas of irregular bottom topography. The Langley

Research Center (LaRC) and the Virginia Institute of Marine Science (VIMS) have, in a cooperative effort, developed a large-scale refraction model (ref. 1) for application to the Virginian Sea, a region of the mid-Atlantic continental shelf from Cape Hatteras to Cape Henlopen. Computer resource requirements for applying the model to a large geographical region were significantly reduced by the subsequent incorporation of a random-access technique for modular storage and retrieval of bathymetry data (ref. 2). Recently the model has been modified to employ, on option, three commonly used techniques for approximating local ocean bottom topography. Two of these techniques are quadratic least squares and cubic least squares, both of which provide some smoothing of the discrete bathymetry data but do not insure continuity in the depth or its derivatives. The third technique, constrained bicubic interpolation, provides continuity without smoothing. Incorporation of all three techniques stemmed from a small-scale refraction study (ref. 3) in which it was concluded that the best approximation technique for use in future studies could not be determined without extensive comparison of computed results with quantitative experimental data. In lieu of such a comparison, refraction diagrams can be computed by using each of the techniques. Then more confidence can be placed in the computed results if no significant discrepancies exist among the three diagrams.

The purpose of this paper is to present wave refraction diagrams computed by applying the LaRC-VIMS model to an area of the mid-Atlantic shelf called the Baltimore Canyon region after a prominent regional submarine geological feature. Extending from near Wachapreague Inlet, Virginia, to near Manasquan Inlet, New Jersey, the region is of particular current interest with regard to offshore petroleum deposits and is one of a series of model regions which together provide broad-scale refraction modeling capability from Cape Hatteras to Montauk Point, New York (ref. 4). An immediate application of the computed diagrams is planned by the Philadelphia District and the Coastal Engineering Research

Center of the U.S. Army Corps of Engineers; these results will be used to furnish initial conditions for a fine-scale refraction study in the nearshore region off Ocean City, New Jersey.

## DATA INPUT

The bathymetry data array for the Baltimore Canyon region was developed by first constructing a special transverse Mercator map projection with a central meridian at 75° west, similar to the one constructed for the Virginian Sea region. (See ref. 1 for details.) The projection was then overlaid with a 0.5-nautical-mile square grid pattern extending for 150 nautical miles from north to south and for 127 nautical miles from west to east. Depth values at the 76 200 nodes (300 rows by 254 columns) of the square grid pattern were determined by using sounding charts and other data in a manner analogous to that used in developing the Virginian Sea bathymetry data grid (ref. 1). A three-dimensional computer-drawn plot of the Baltimore Canyon region bathymetry data grid (with a vertical exaggeration of approximately 300 to 1) is shown in figure 1. The regional array was then divided into a series of smaller modules for use with the random-access data storage and retrieval technique described in reference 2. The module size was selected as 42 rows by 32 columns to minimize computer cost, resulting in a series of 72 overlapped bathymetry data modules. (See ref. 2 for sequencing and overlapping details.) As a final adjustment to the input bathymetry data, the program input parameter for tide was set so that the input depth values would correspond to mean low water.

A range of wave direction and period was desired which would provide meaningful refraction diagrams while being realistic from the standpoint of normally occurring real-life wave conditions. With these requirements in mind, the selected input wave directions ranged from 0° (from due north) through 90° (from due east) to 180° (from due south). Input directions from the west were not deemed significant for this study because of the limiting fetch for

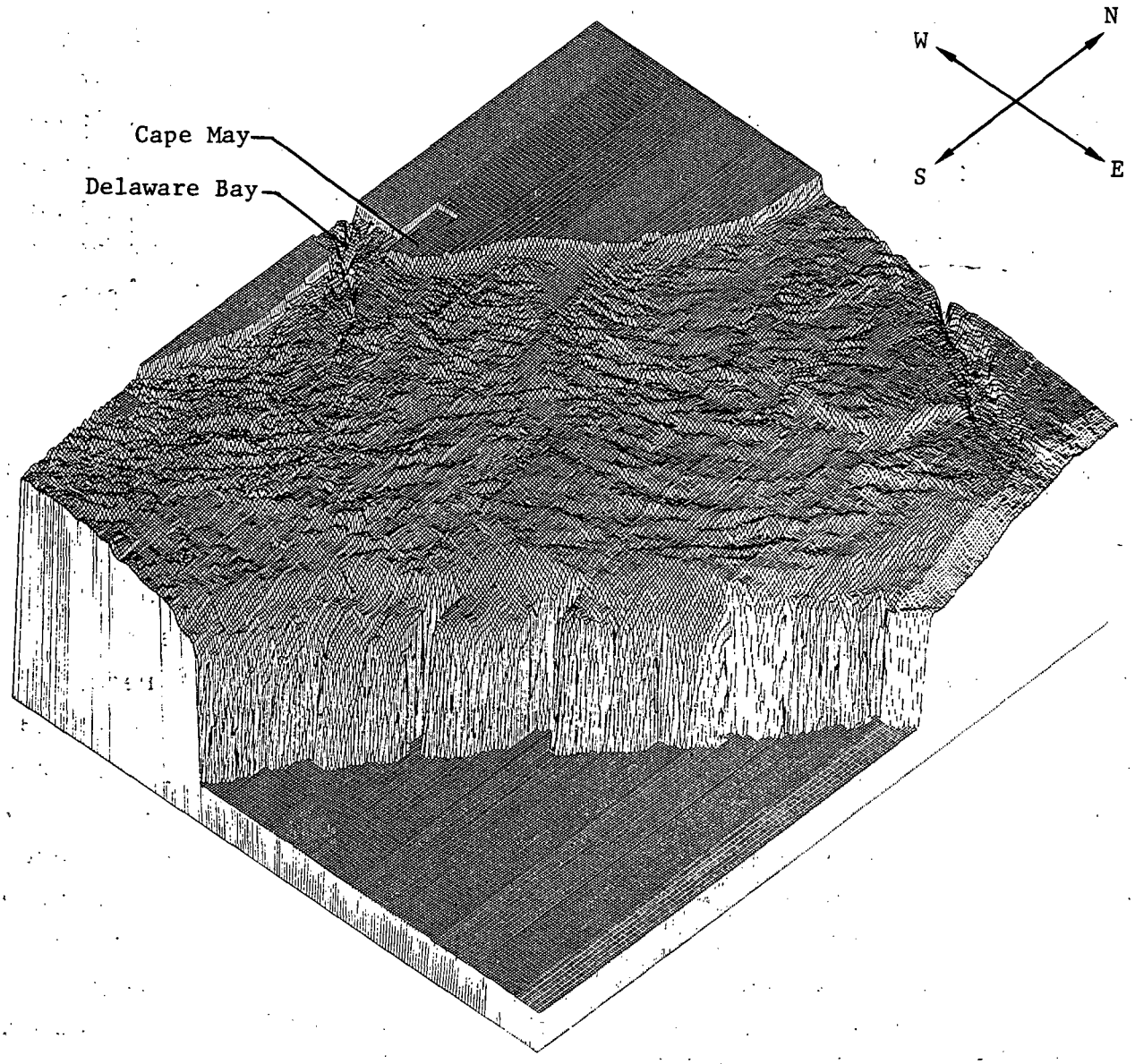


Figure 1.- Three-dimensional computer-drawn plot of the Baltimore Canyon region bathymetry data grid. Vertical exaggeration, 300 to 1.

physical wave generation. Within the selected direction range, input directions were chosen at 22.5° increments (i.e., N, NNE, NE, etc.) as was done in the study presented in reference 1. Input wave periods were selected in 2-second increments from 6 seconds to 16 seconds. On the basis of results of reference 1, waves of periods less than 6 seconds were expected to undergo very little, if any, refraction; thus, refraction diagrams for these periods

would be of little meaning. It was also felt that waves of periods greater than 16 seconds would occur so infrequently in nature that their inclusion in this study was not justified. As a final input, the initial wave height was fixed arbitrarily at 0.3 meter for all cases since, according to linear wave theory, wave height does not affect the refraction pattern for a given combination of wave period and direction.

## WAVE REFRACTION DIAGRAMS

Wave refraction diagrams for the Baltimore Canyon region were computed for the input range of wave period and direction by using quadratic least squares, cubic least squares, and constrained bicubic interpolation techniques for approximating local bottom topography. The initial separation distance between wave rays was selected as 3 nautical miles to provide adequate overall resolution without cluttering the diagrams. Computations were required to begin in deep water, which, for the purposes of this paper, was considered to be a water depth greater than one-fourth the initial wavelength for the particular wave period being considered. (See ref. 1 for discussion.) Tick marks were drawn along each computed ray at points equally spaced in time, with the time increment varied with wave period to provide relatively uniform spatial resolution among cases of different periods. By connecting corresponding tick marks on adjacent rays so that the connecting curve is orthogonal to each ray, wave crest patterns can be derived.

Computed refraction diagrams are presented in figures 2 to 52 in the sequence given in table I. Diagrams computed for a wave direction of $0^{\circ}$ and periods of 12, 14, and 16 seconds have been omitted because only one or two rays met the deep-water condition for initiating computations. Unless noted otherwise, each figure consists of three parts: part (a) presents the diagram computed by using the quadratic least squares technique for approximating bottom topography; part (b) presents the diagram computed by using the cubic least squares technique; and part (c) presents the dia-

gram computed by using the constrained bicubic interpolation technique. When essentially identical diagrams resulted from the three techniques, only the one computed by using the quadratic least squares technique is presented.

Some general comments are in order as an aid to potential users in interpreting the various diagrams. Since the tick marks along each ray denote equal time spacing, an increase in the spatial density of tick marks as a ray approaches the shore indicates decreasing wave phase speed. Convergence of a group of neighboring rays indicates an area of relatively high wave energy, whereas a sparsity of rays indicates relatively low energy. On occasion, individual rays stop abruptly in an area of relatively deep water (ray 23 in fig. 20(a), for example). Such ray terminations indicate failure to converge on a proper value for local ray curvature or calculation of a physically unrealistic value for wave height and, as such, should be considered of no physical significance. In several instances, individual rays undergo abrupt changes in direction relative to the mean direction of neighboring rays (ray 40 in fig. 32(c), for example). These abrupt changes are induced by sharp gradients in the local bottom topography, which are influenced, in turn, by the technique selected for approximating the topography within the finite-mesh bathymetry grid. Since use of the constrained bicubic interpolation technique results in a surface which passes directly through the bathymetry data points, sharp topography gradients tend to occur more often with this technique than with the two least squares techniques, both of which provide some smoothing of the data.

TABLE I.- SEQUENCE OF WAVE REFRACTION DIAGRAMS

| Figure | Wave direction, α, degrees | Wave period, T, seconds | Figure | Wave direction, α, degrees | Wave period, T, seconds |
|---|---|---|---|---|---|
| 2 | 0 | [a]6 | 28 | 90 | 16 |
| 3 | 0 | [a]8 | 29 | 112.5 | 6 |
| 4 | 0 | 10 | 30 | 112.5 | 8 |
| 5 | 22.5 | [a]6 | 31 | 112.5 | 10 |
| 6 | 22.5 | 8 | 32 | 112.5 | 12 |
| 7 | 22.5 | 10 | 33 | 112.5 | 14 |
| 8 | 22.5 | 12 | 34 | 112.5 | 16 |
| 9 | 22.5 | 14 | 35 | 135 | 6 |
| 10 | 22.5 | 16 | 36 | 135 | 8 |
| 11 | 45 | 6 | 37 | 135 | 10 |
| 12 | 45 | 8 | 38 | 135 | 12 |
| 13 | 45 | 10 | 39 | 135 | 14 |
| 14 | 45 | 12 | 40 | 135 | 16 |
| 15 | 45 | 14 | 41 | 157.5 | 6 |
| 16 | 45 | 16 | 42 | 157.5 | 8 |
| 17 | 67.5 | 6 | 43 | 157.5 | 10 |
| 18 | 67.5 | 8 | 44 | 157.5 | 12 |
| 19 | 67.5 | 10 | 45 | 157.5 | 14 |
| 20 | 67.5 | 12 | 46 | 157.5 | 16 |
| 21 | 67.5 | 14 | 47 | 180 | 6 |
| 22 | 67.5 | 16 | 48 | 180 | 8 |
| 23 | 90 | 6 | 49 | 180 | 10 |
| 24 | 90 | 8 | 50 | 180 | 12 |
| 25 | 90 | 10 | 51 | 180 | 14 |
| 26 | 90 | 12 | 52 | 180 | 16 |
| 27 | 90 | 14 | | | |

[a]Only the diagram computed by using the quadratic least squares technique is given because no resolvable difference existed among diagrams computed by using the three approximation techniques.

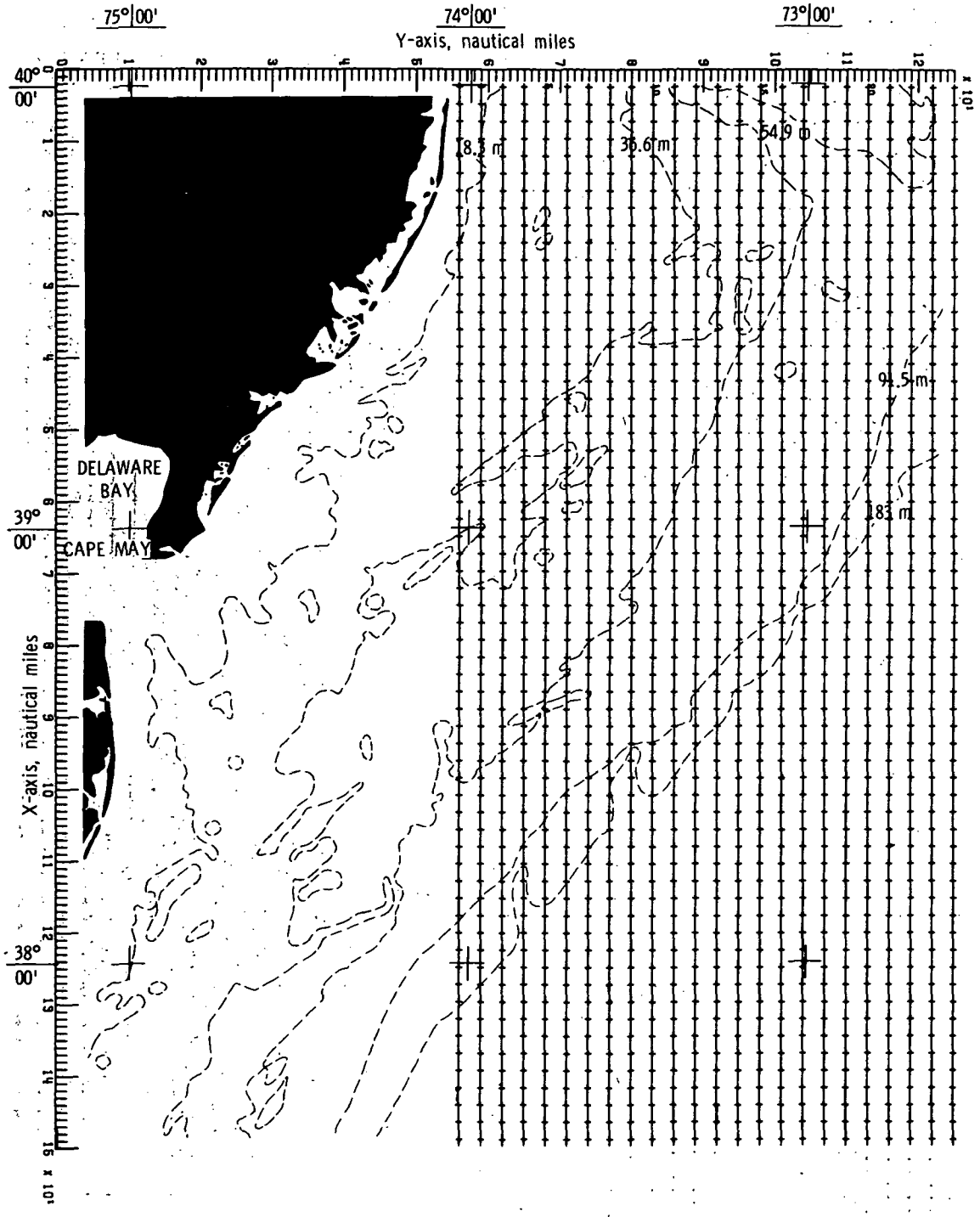


Figure 2.- Wave refraction diagram. $\alpha = 0^{\circ}$; T = 6 seconds. Bottom topography approximated by quadratic least squares technique.

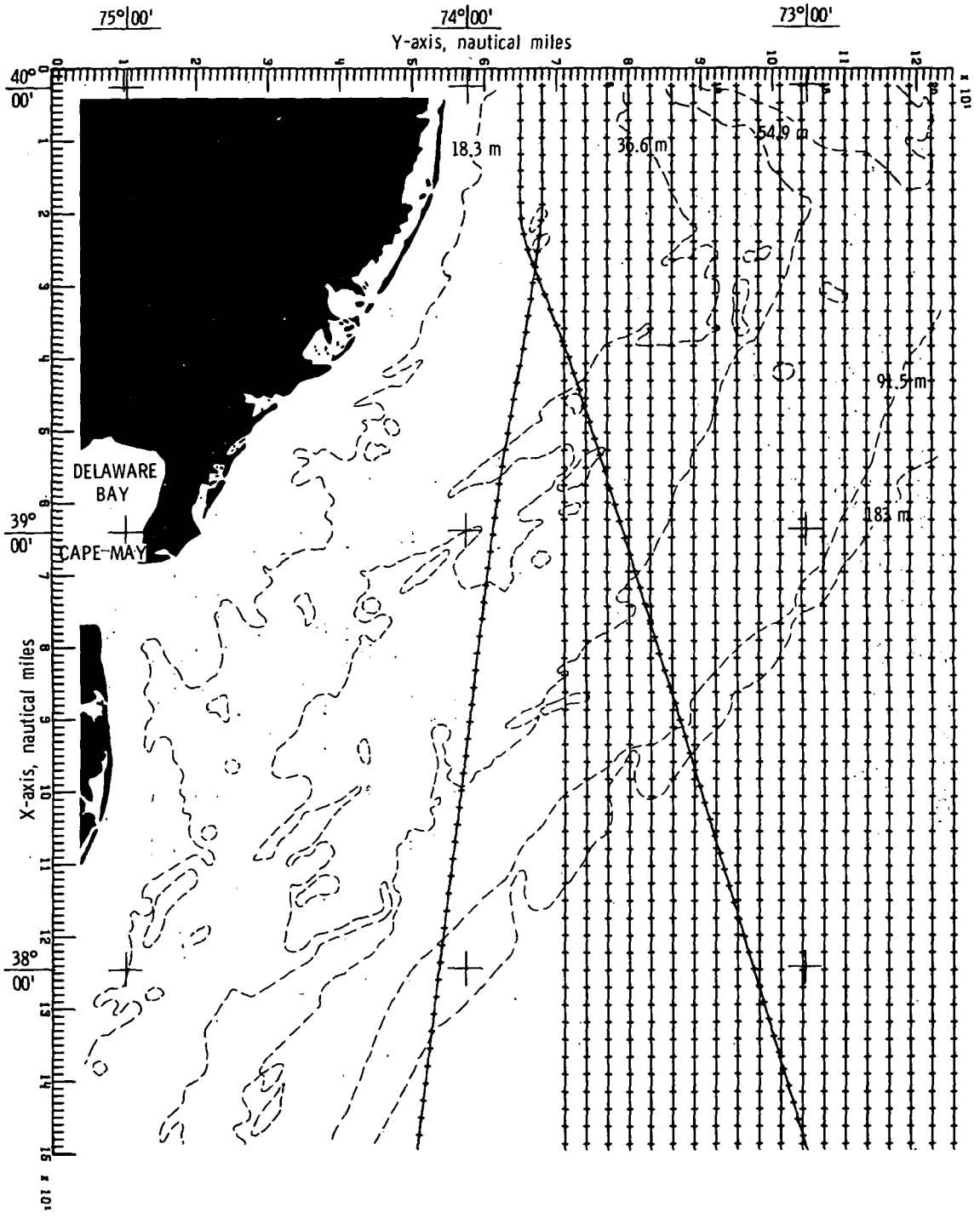


Figure 3.- Wave refraction diagram. $\alpha = 0^{\circ}$; $T = 8$ seconds. Bottom topography approximated by quadratic least squares technique.

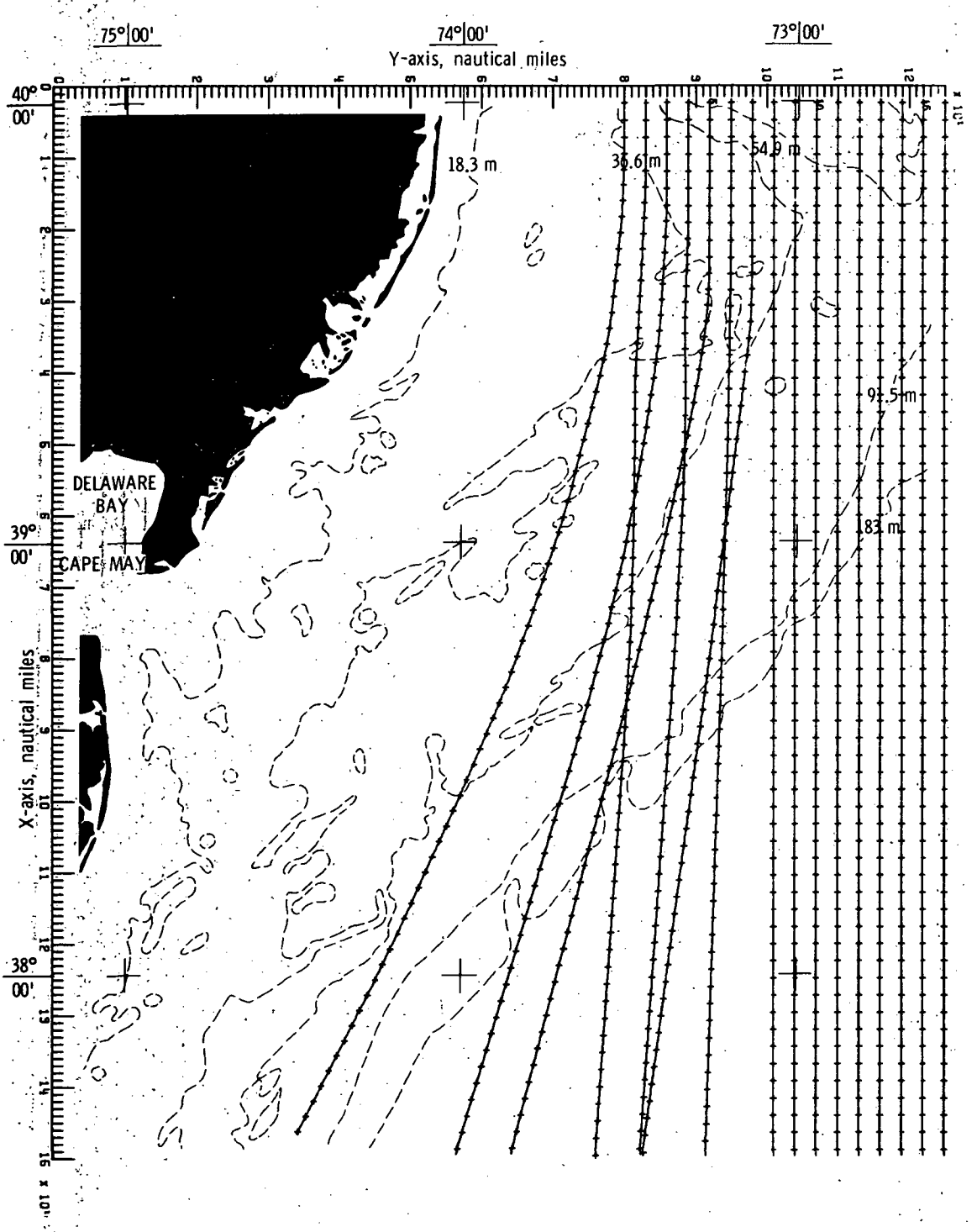


(a) Bottom topography approximated by quadratic least squares technique.

Figure 4.- Wave refraction diagrams. $\alpha = 0^{o}$; T = 10 seconds.

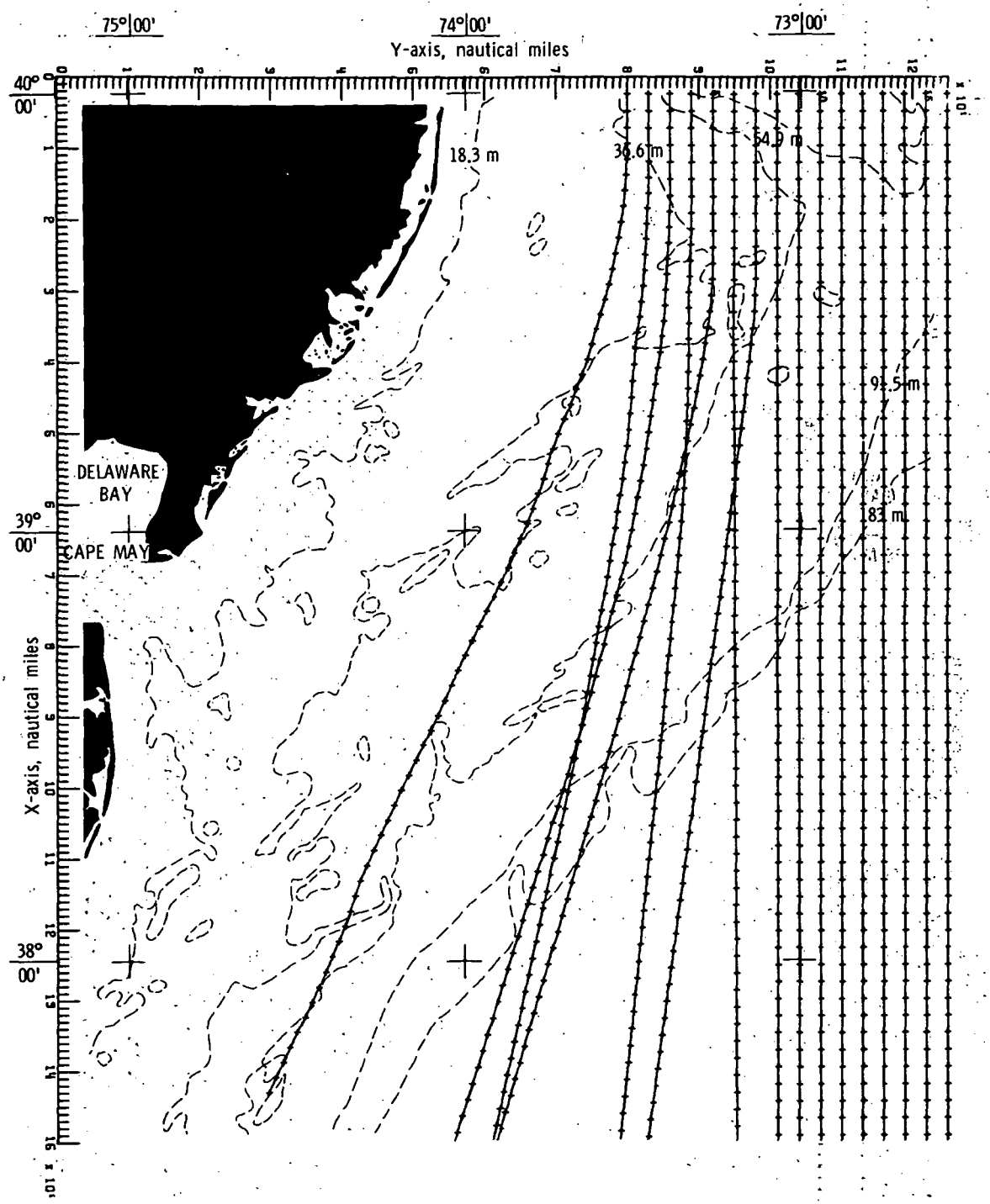


(b) Bottom topography approximated by cubic least squares technique.

Figure 4.- Continued.

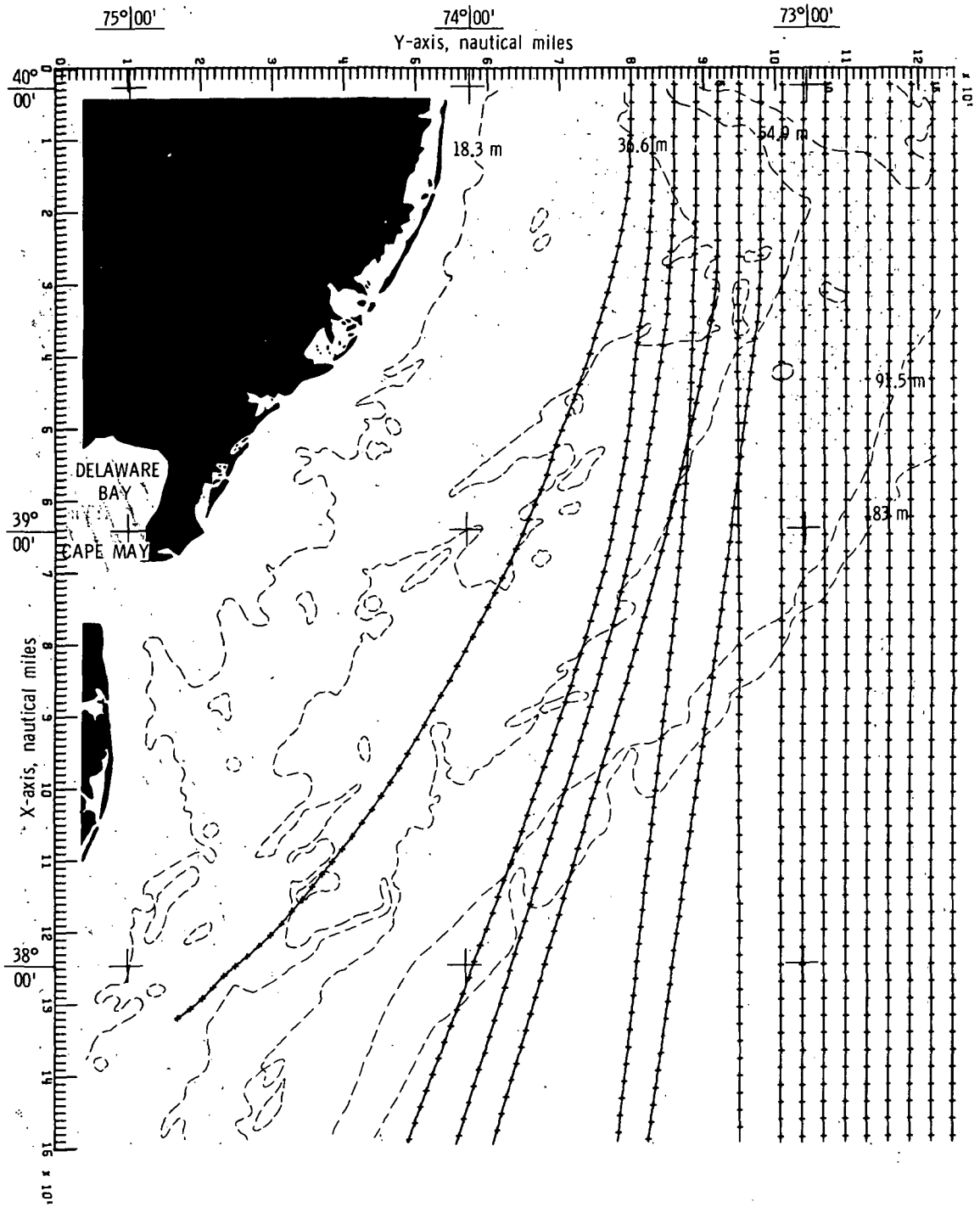


(c) Bottom topography approximated by constrained bicubic interpolation technique.

Figure 4.- Concluded.

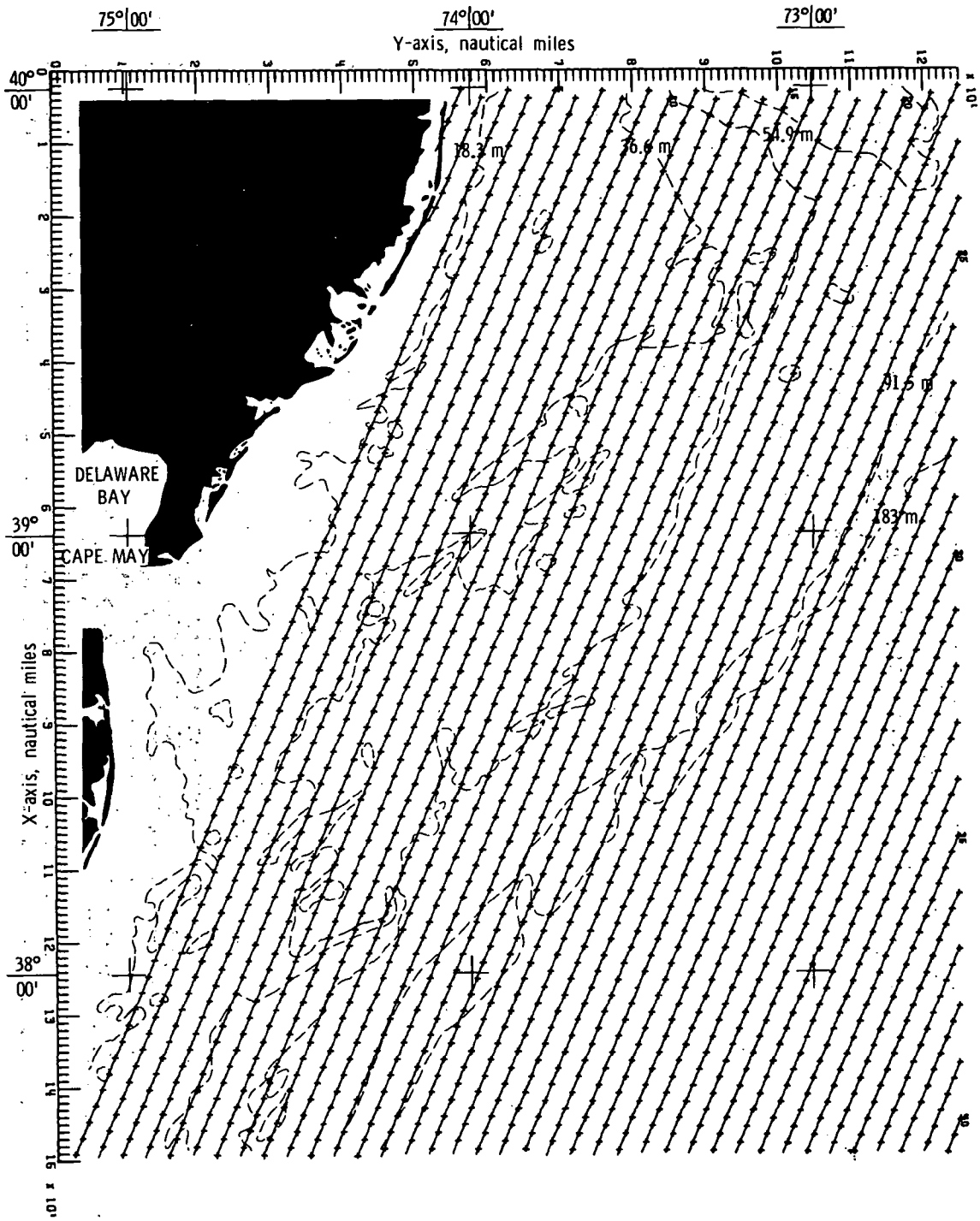


Figure 5.- Wave refraction diagram. $\alpha = 22.5^{\circ}$; T = 6 seconds. Bottom topography approximated by quadratic least squares technique.

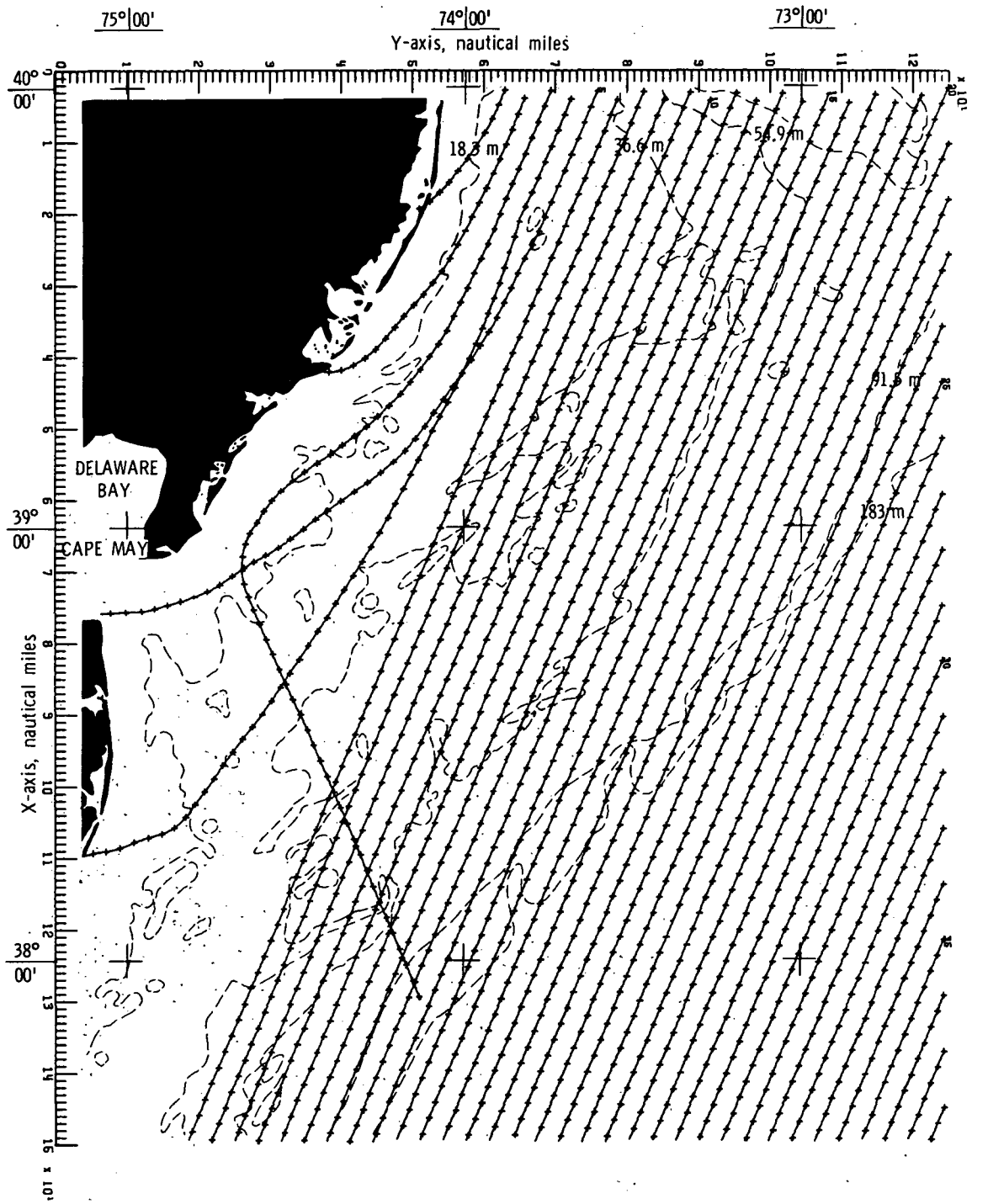


(a) Bottom topography approximated by quadratic least squares technique.

Figure 6.- Wave refraction diagrams. $\alpha = 22.5^{o}$; T = 8 seconds.

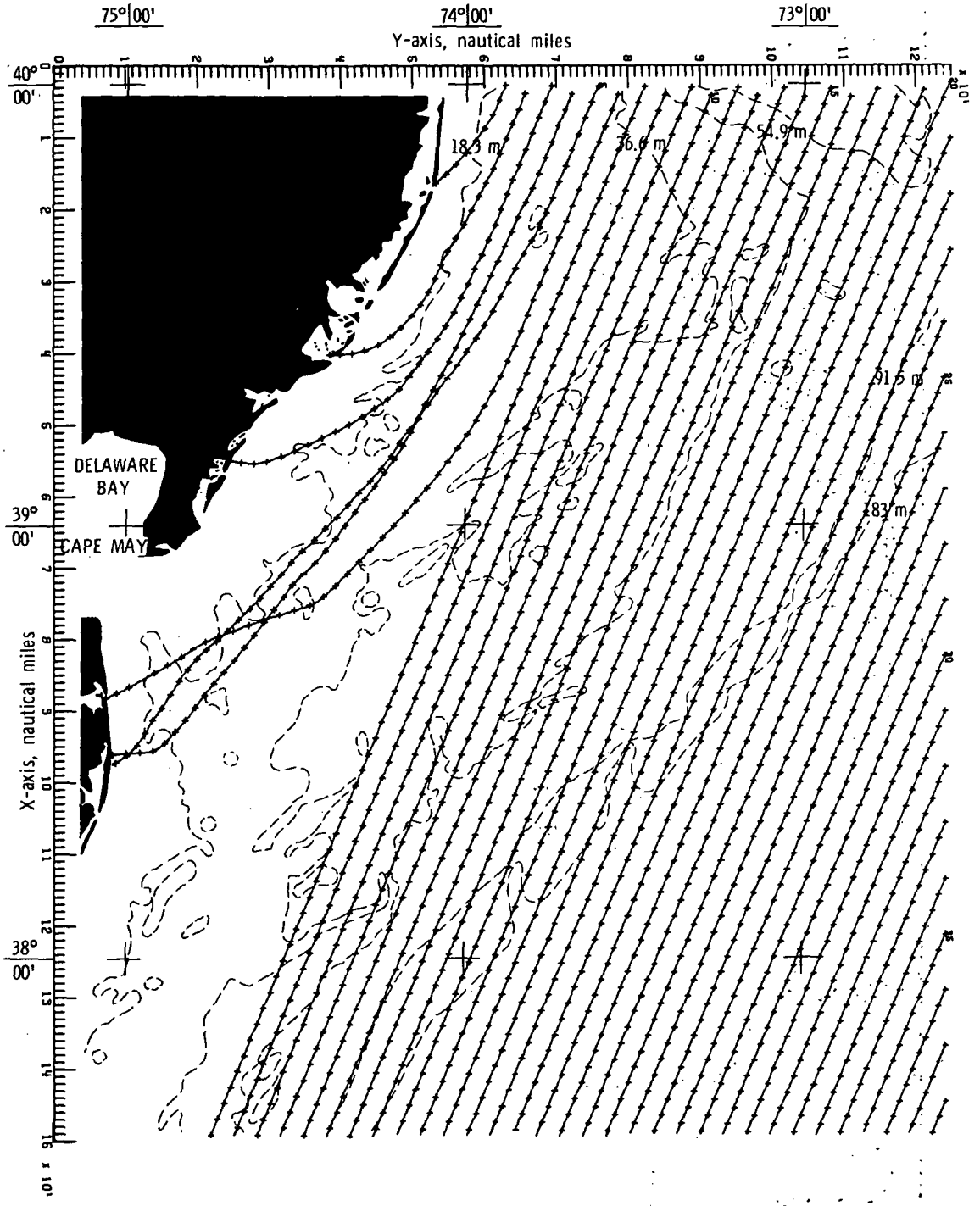


(b) Bottom topography approximated by cubic least squares technique.

Figure 6.- Continued.

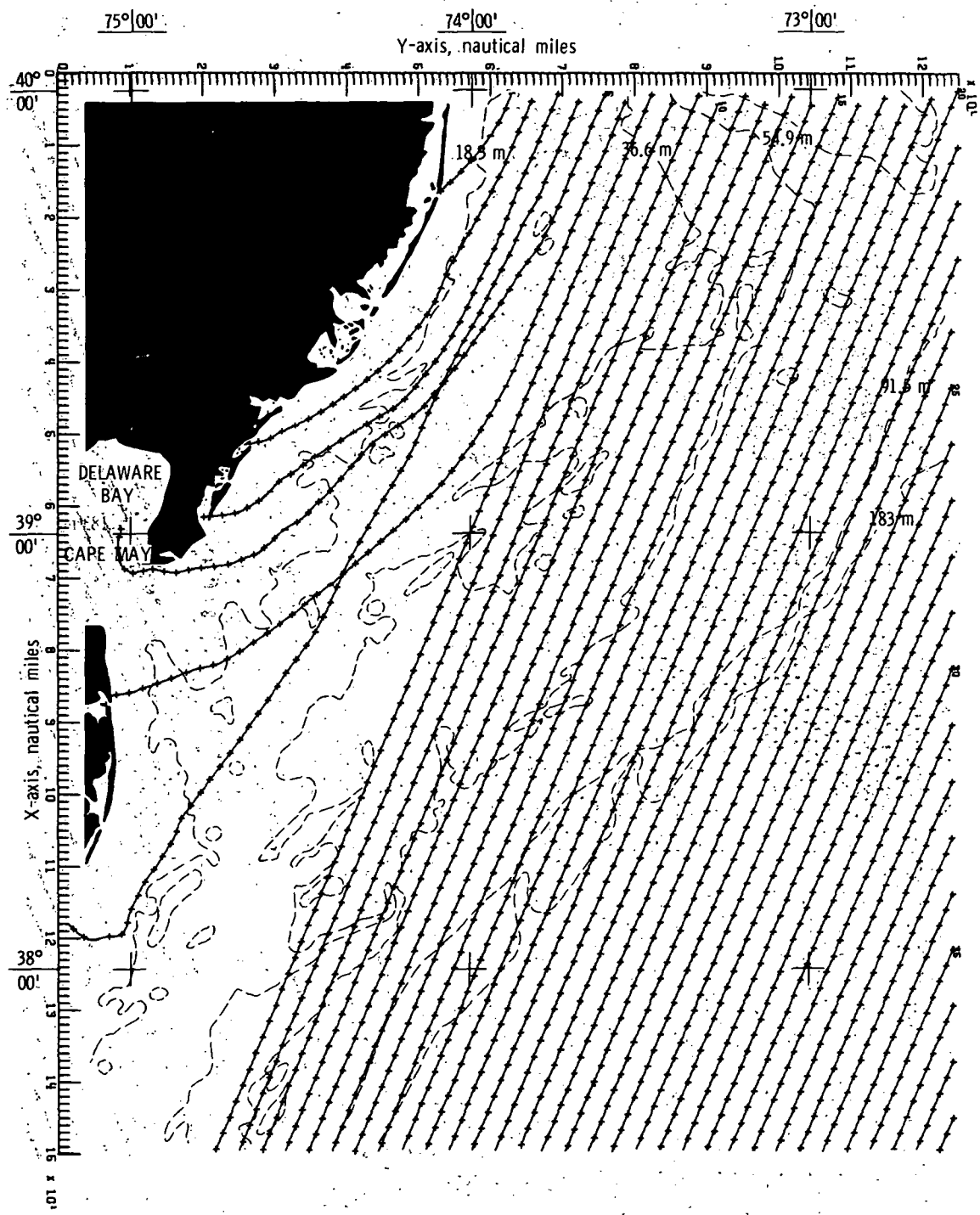


(c) Bottom topography approximated by constrained bicubic interpolation technique.

Figure 6.- Concluded.

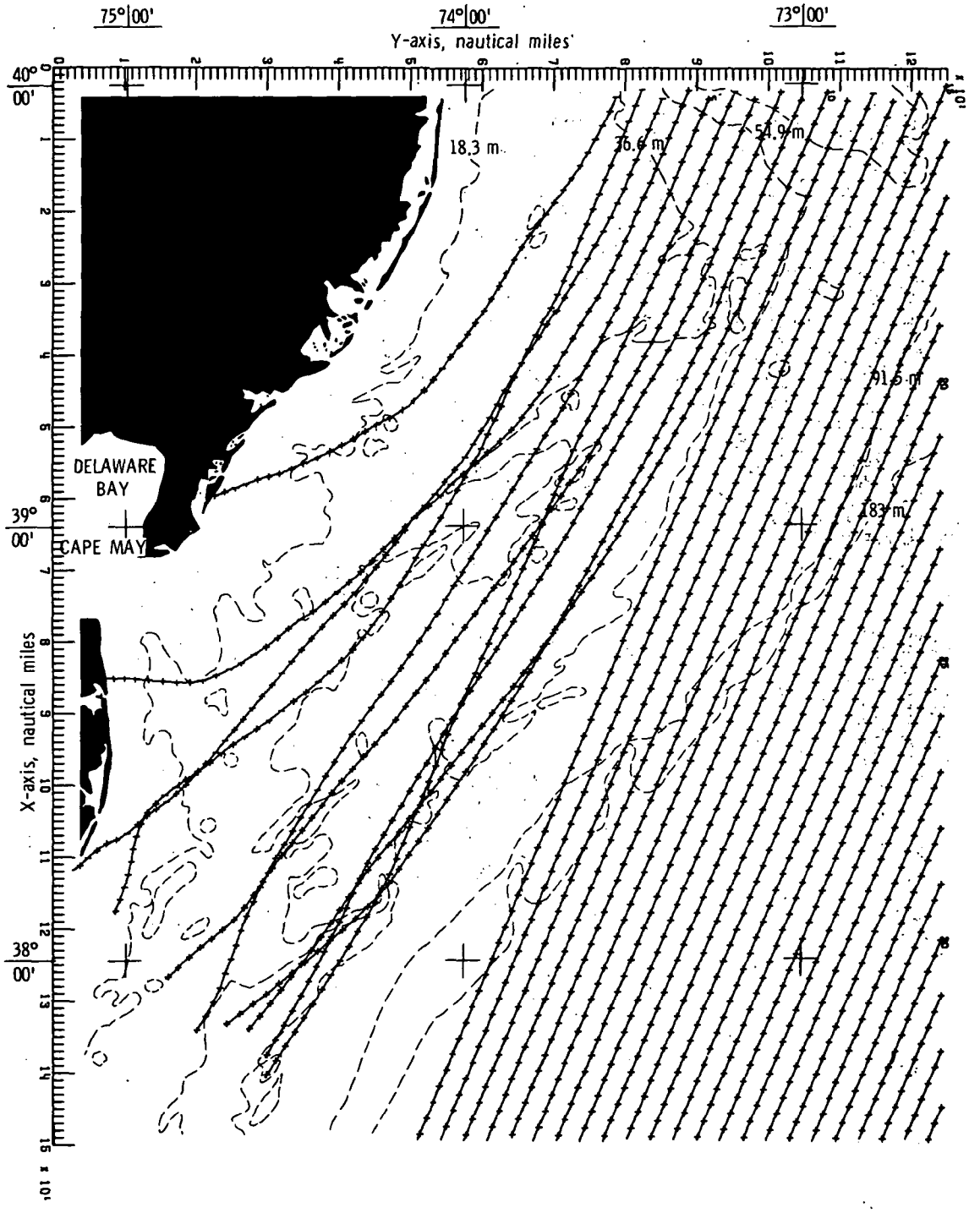


(a) Bottom topography approximated by quadratic least squares technique.

Figure 7.- Wave refraction diagrams. $\alpha = 22.5^{o}$; T = 10 seconds.

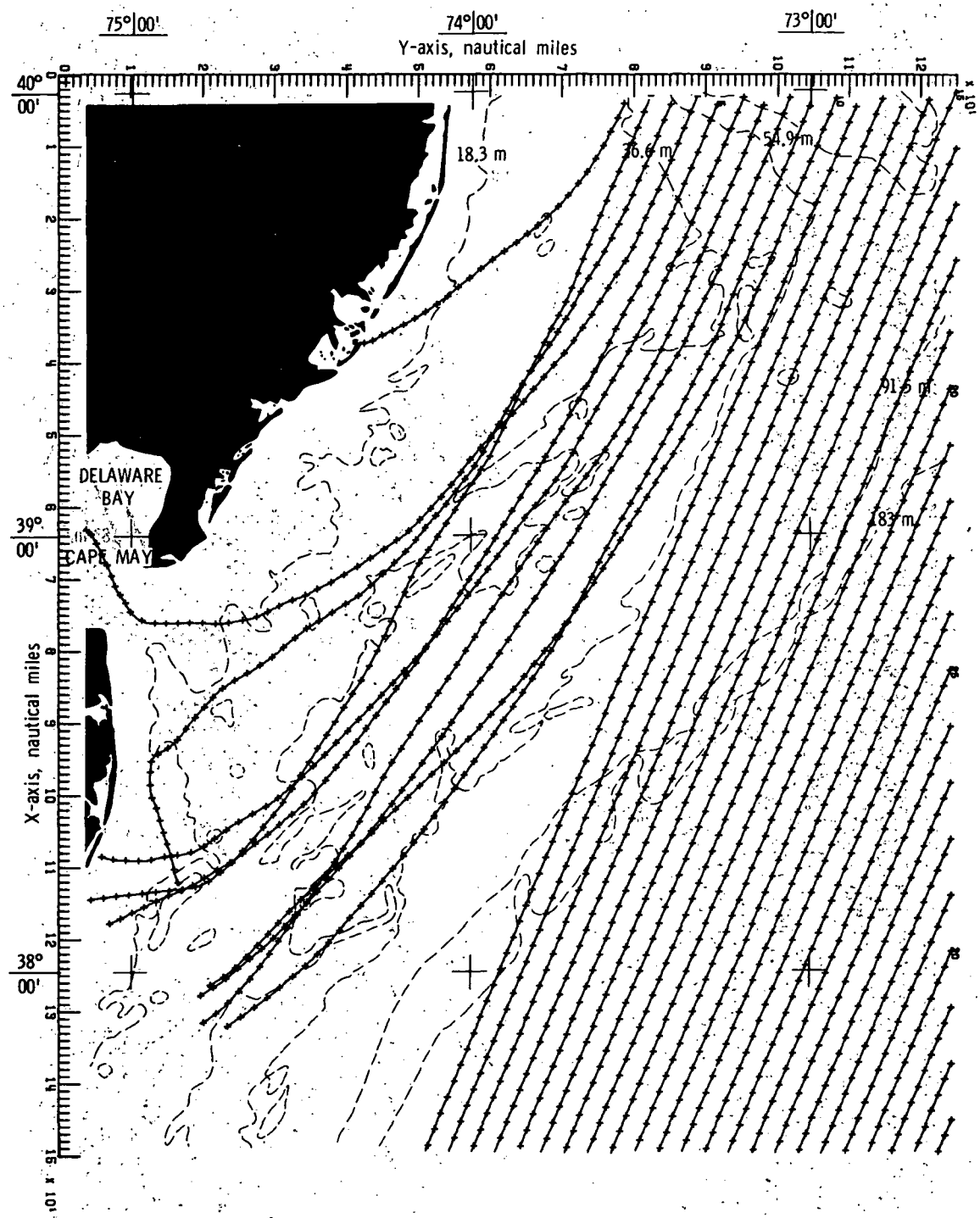


(b) Bottom topography approximated by cubic least squares technique.

Figure 7.- Continued.

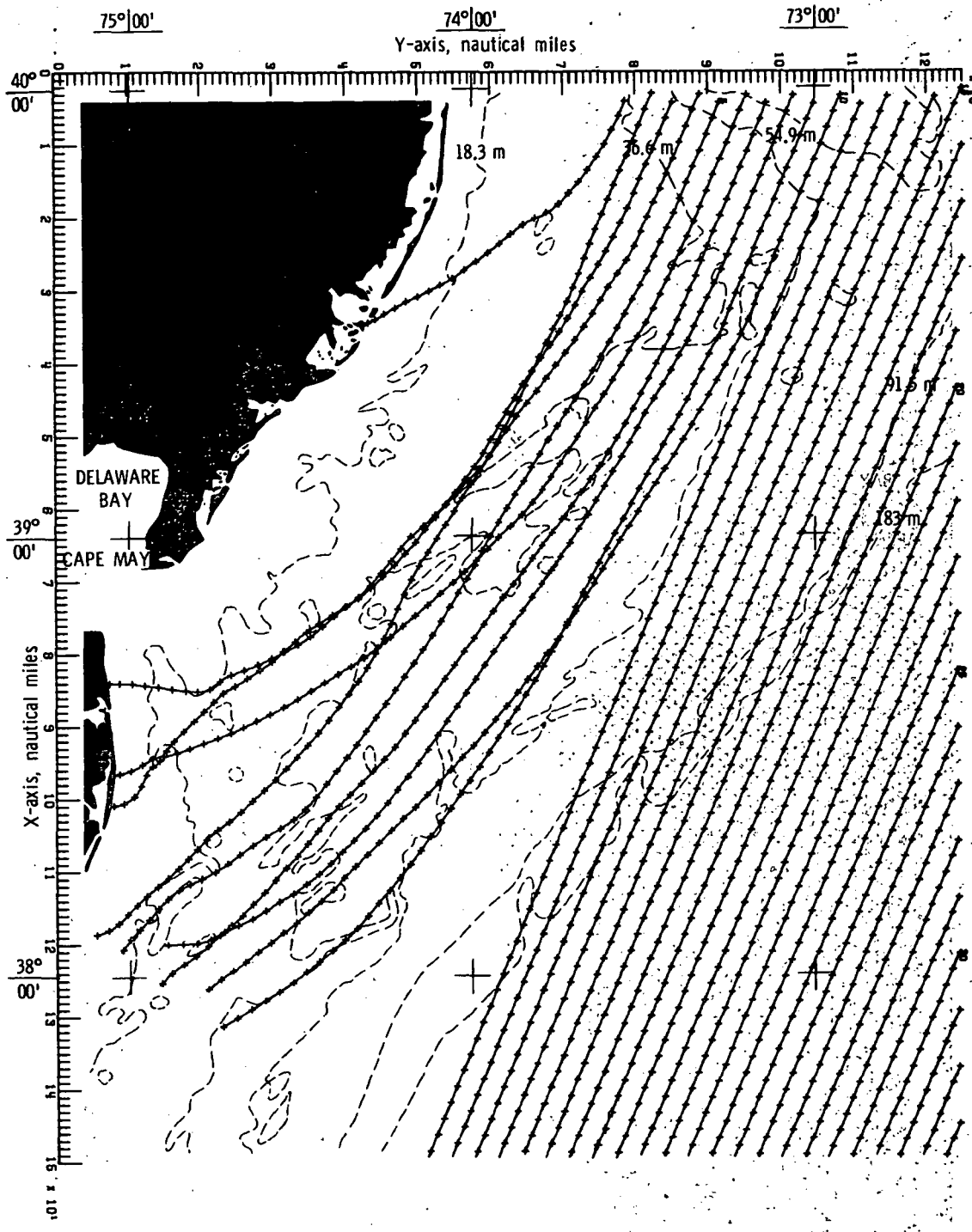


(c) Bottom topography approximated by constrained bicubic interpolation technique.

Figure 7.- Concluded.

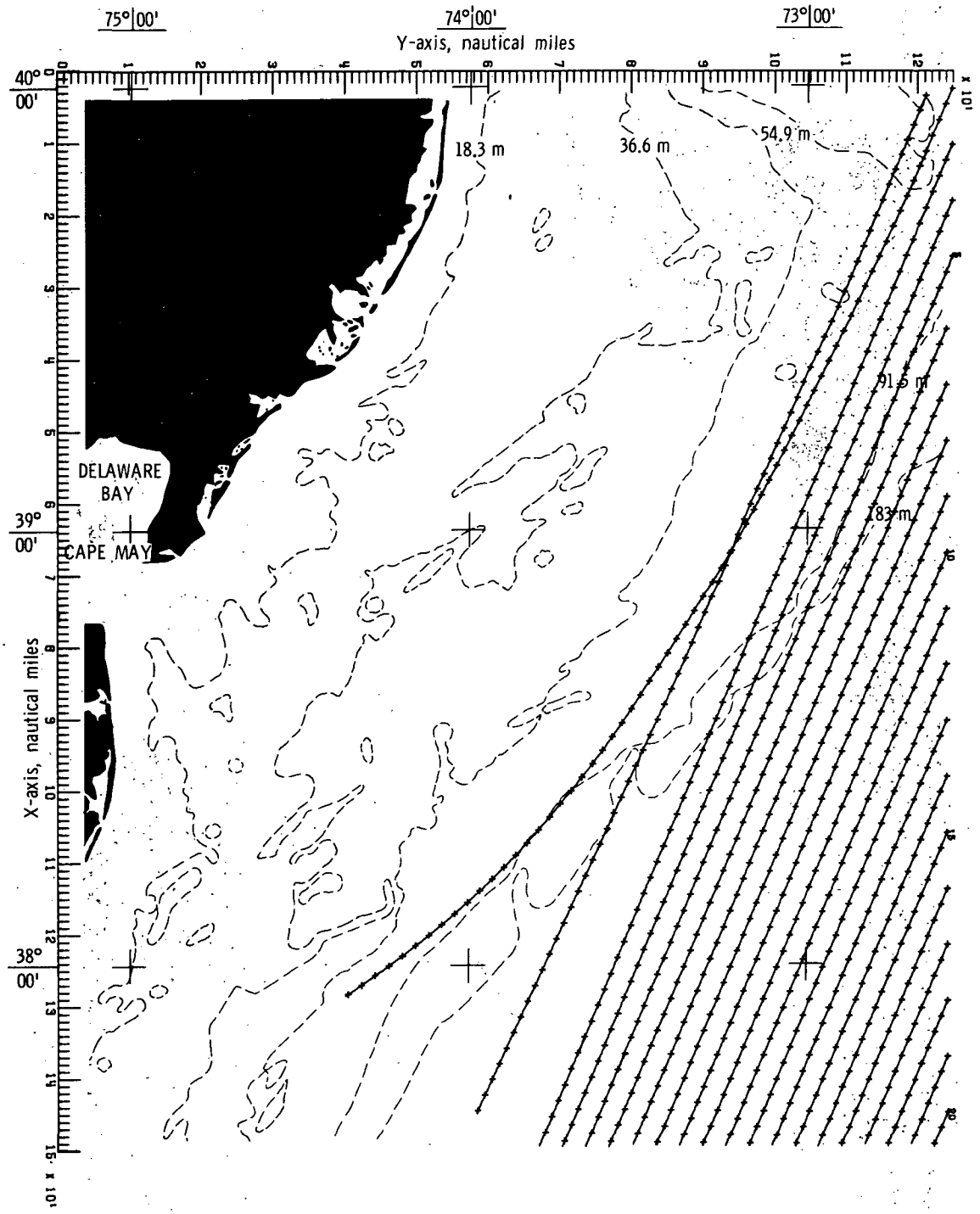


(a) Bottom topography approximated by quadratic least squares technique.

Figure 8.- Wave refraction diagrams. $\alpha$ = 22.5°; T = 12 seconds.

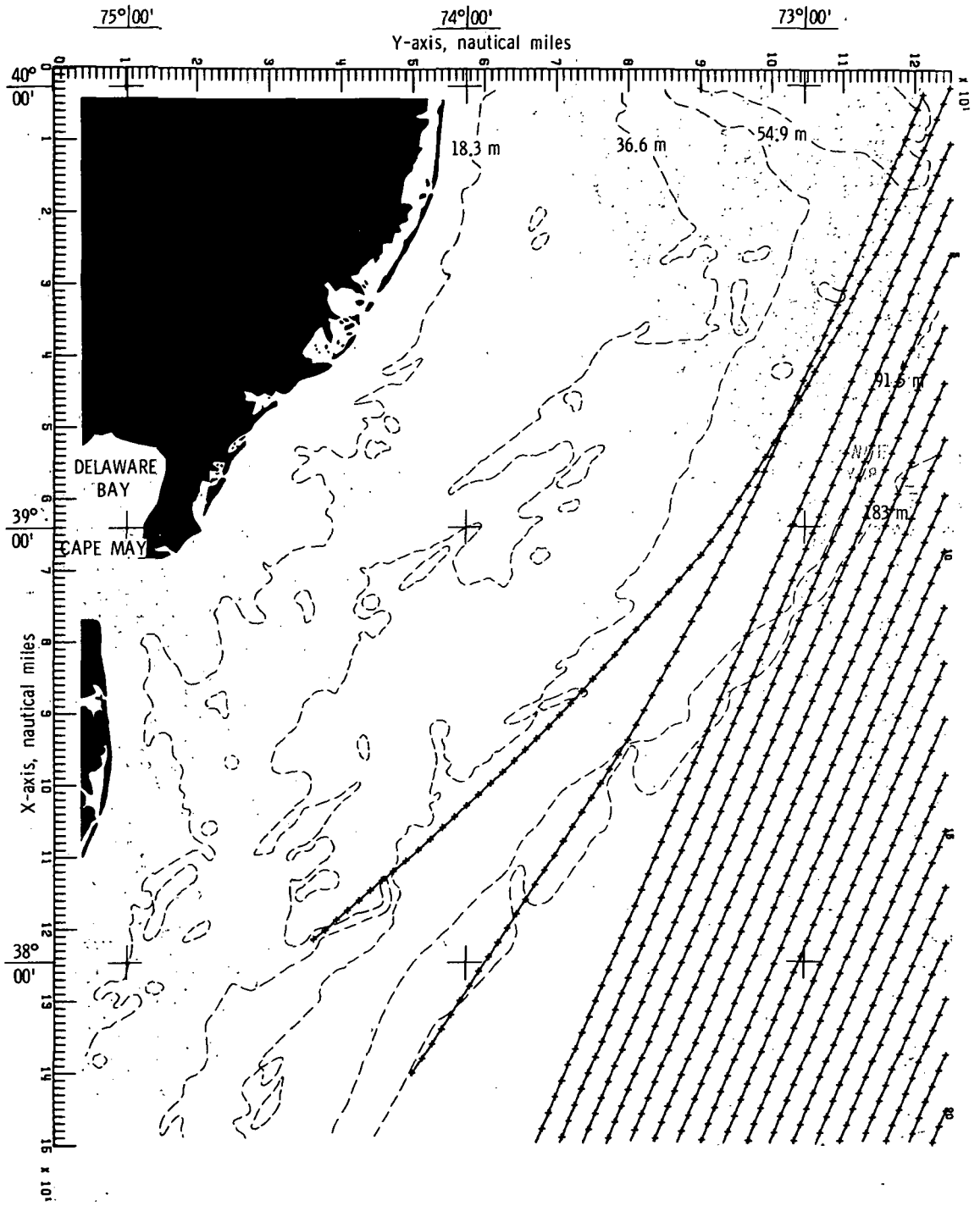


(b) Bottom topography approximated by cubic least squares technique.

Figure 8.- Continued.

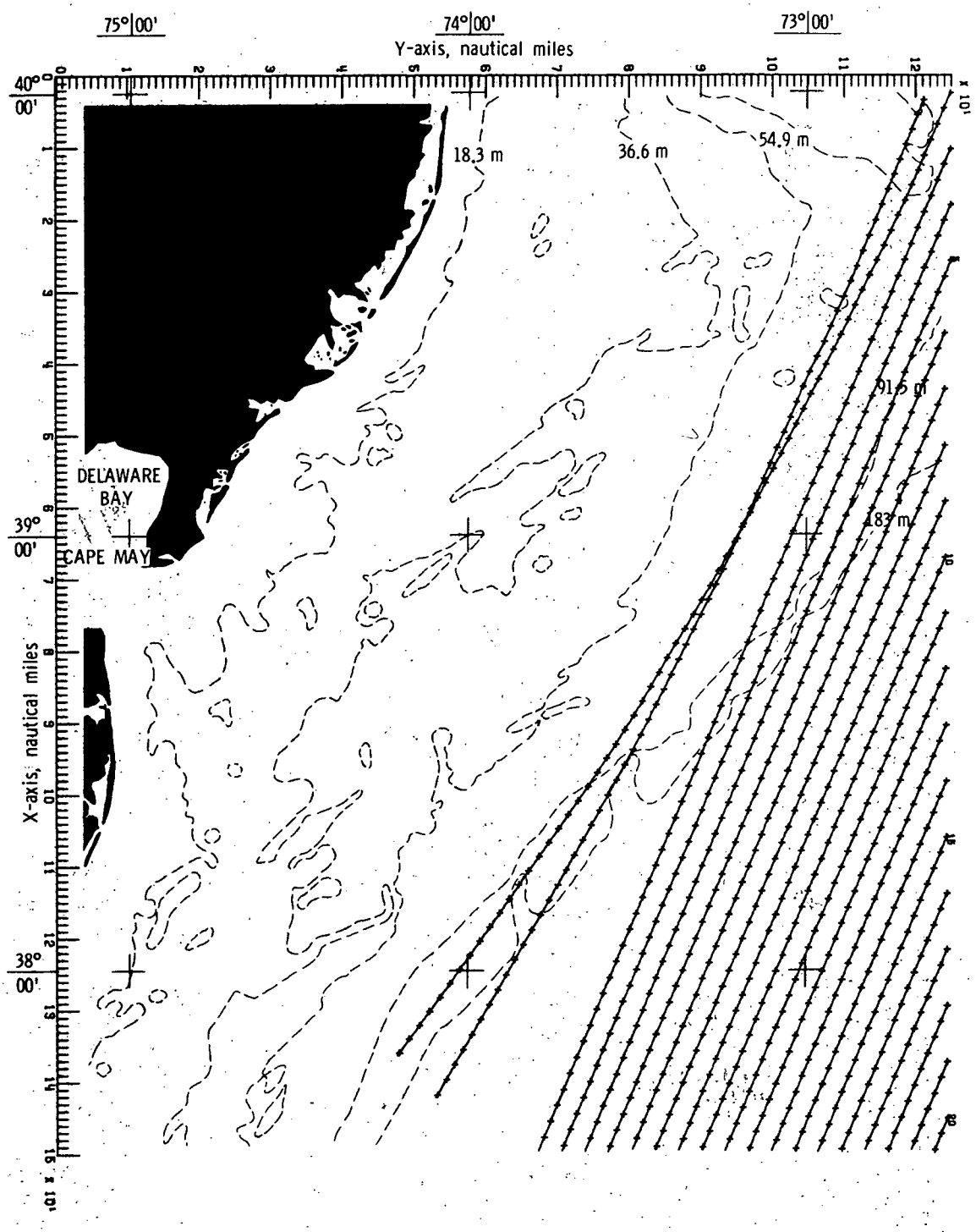


(c) Bottom topography approximated by constrained bicubic interpolation technique.

Figure 8.- Concluded.

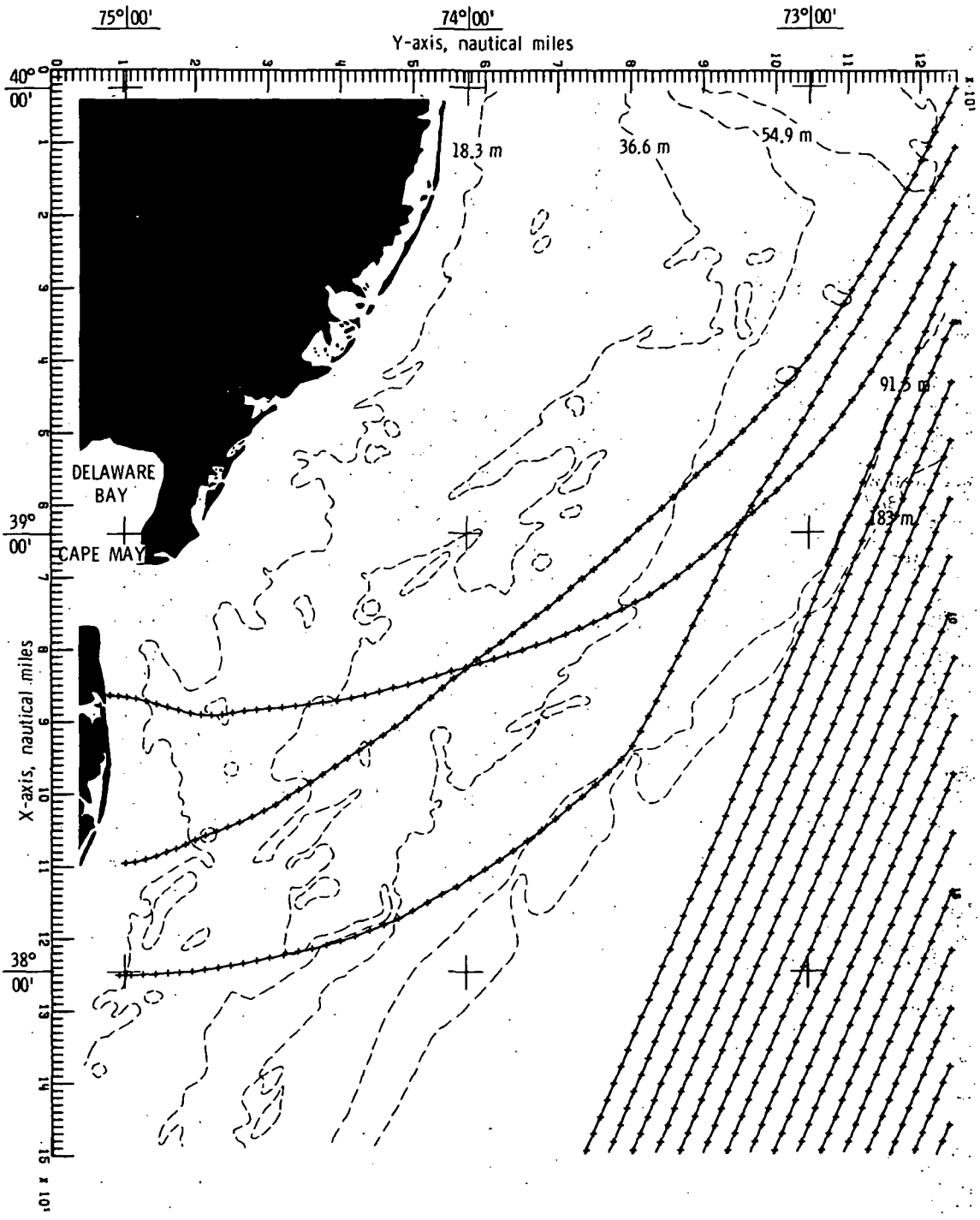


(a) Bottom topography approximated by quadratic least squares technique.

Figure 9.- Wave refraction diagrams. $\alpha = 22.5^{o}$; T = 14 seconds.

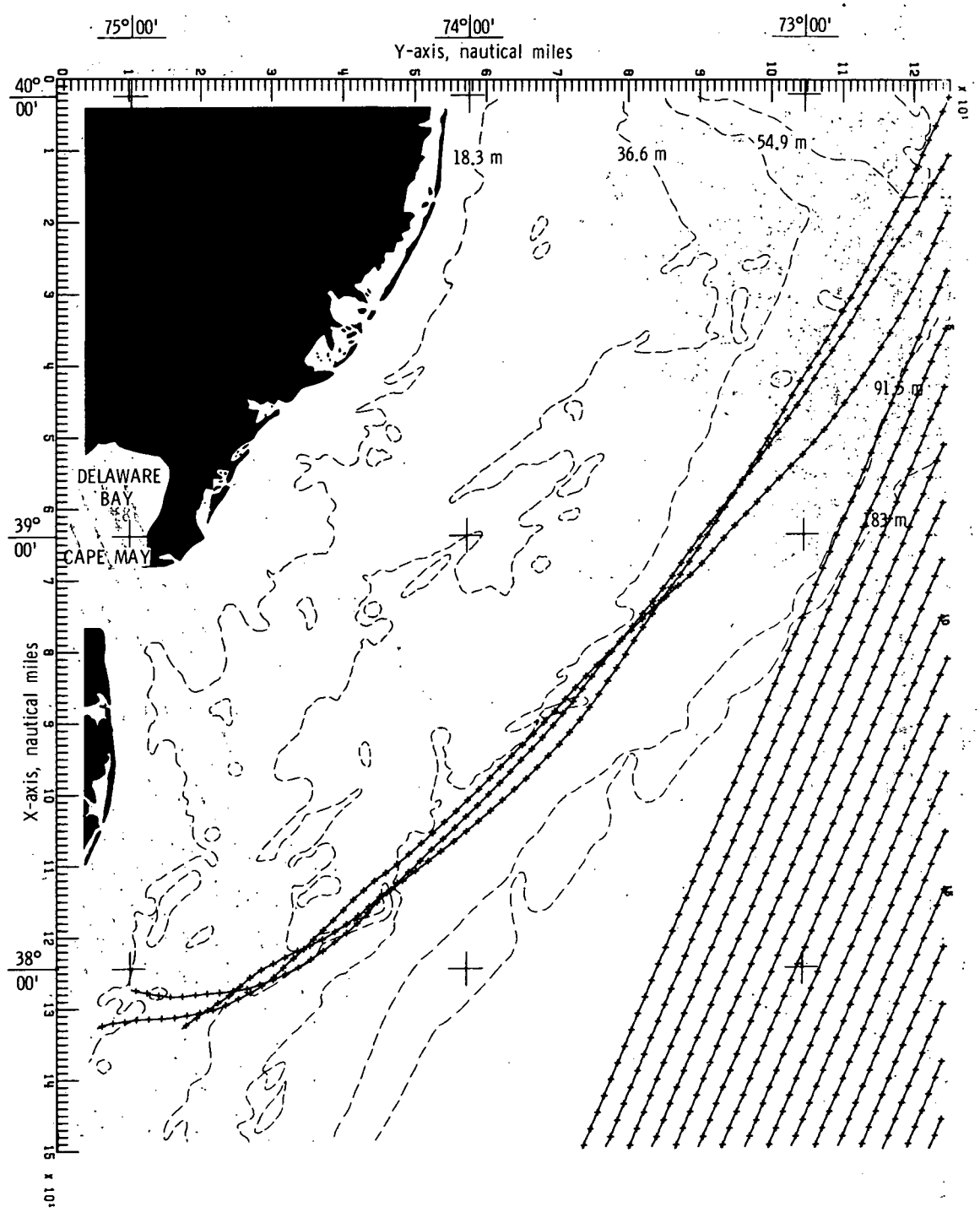


(b) Bottom topography approximated by cubic least squares technique.

Figure 9.- Continued.

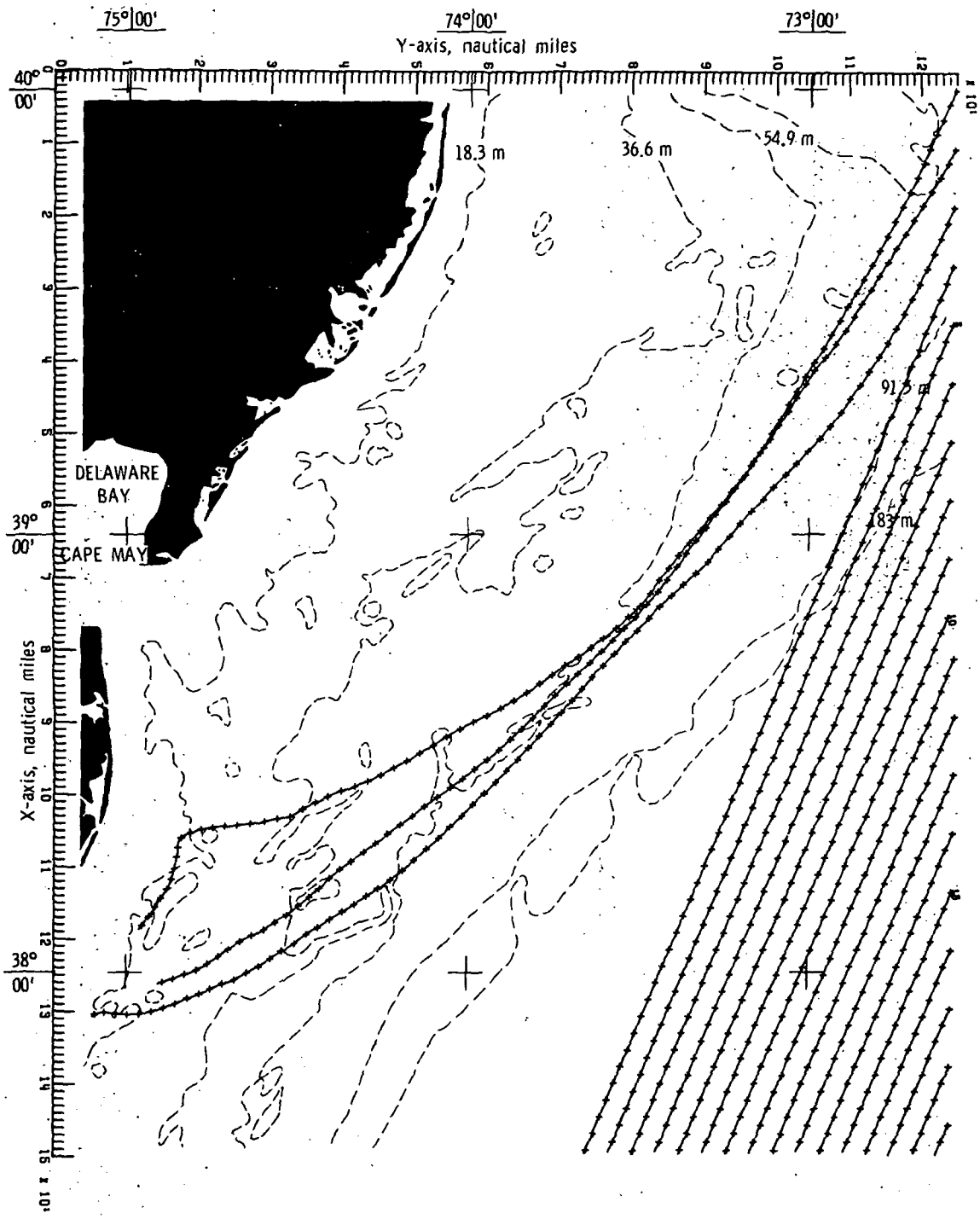


(c) Bottom topography approximated by constrained bicubic interpolation technique.

Figure 9.- Concluded.

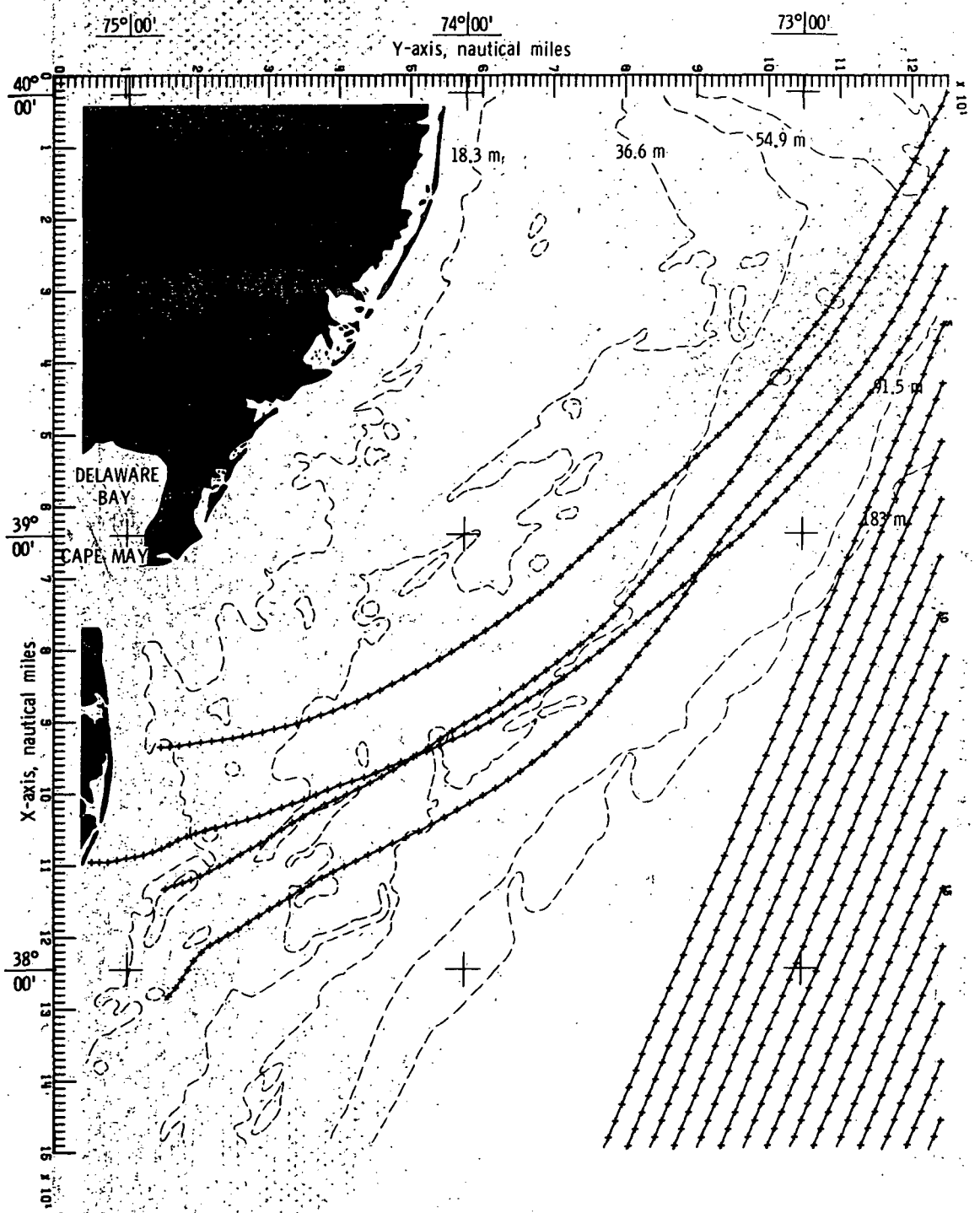


(a) Bottom topography approximated by quadratic least squares technique.

Figure 10.- Wave refraction diagrams. $\alpha = 22.5^{\circ}$; T = 16 seconds.

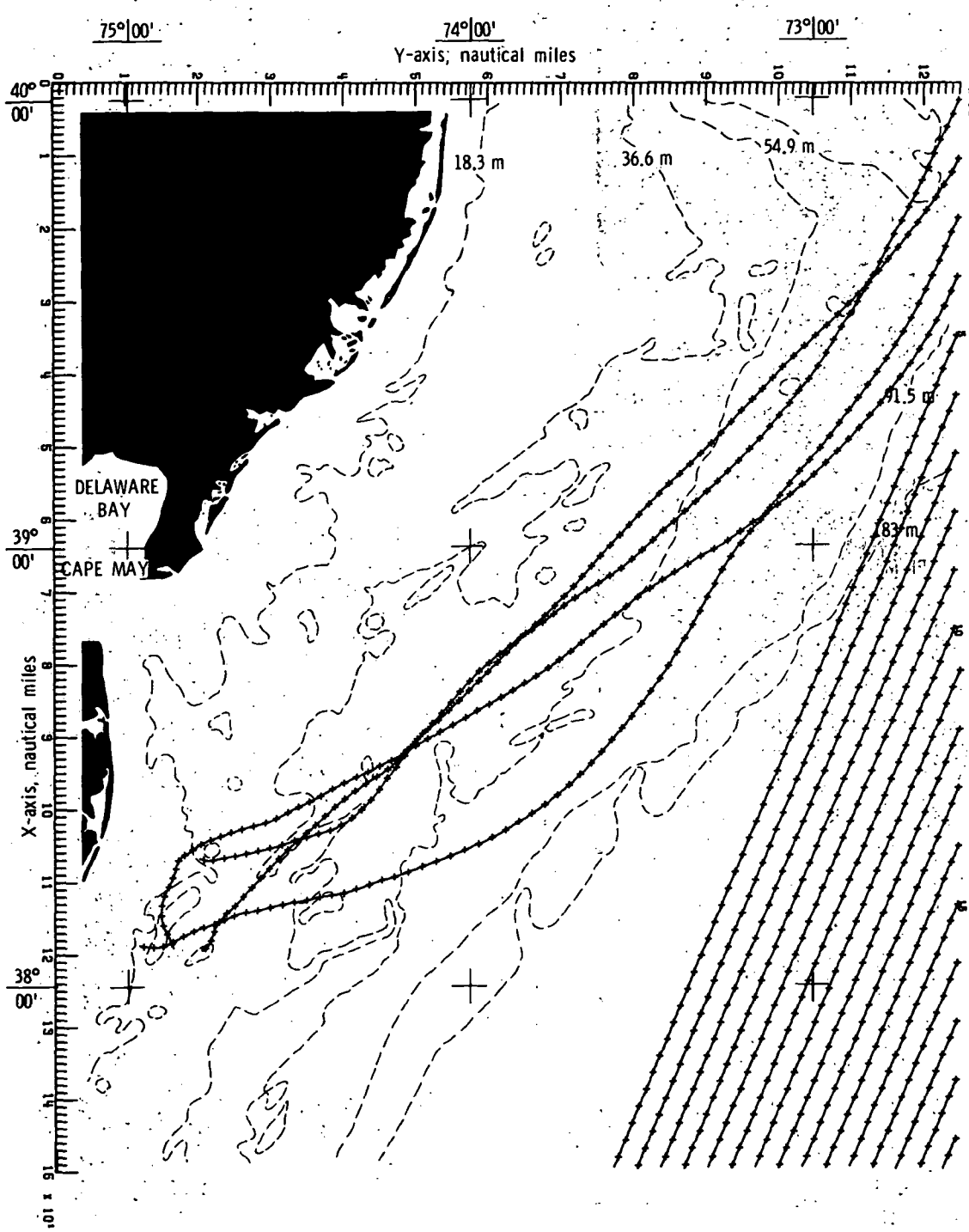


(b) Bottom topography approximated by cubic least squares technique.

Figure 10.- Continued.

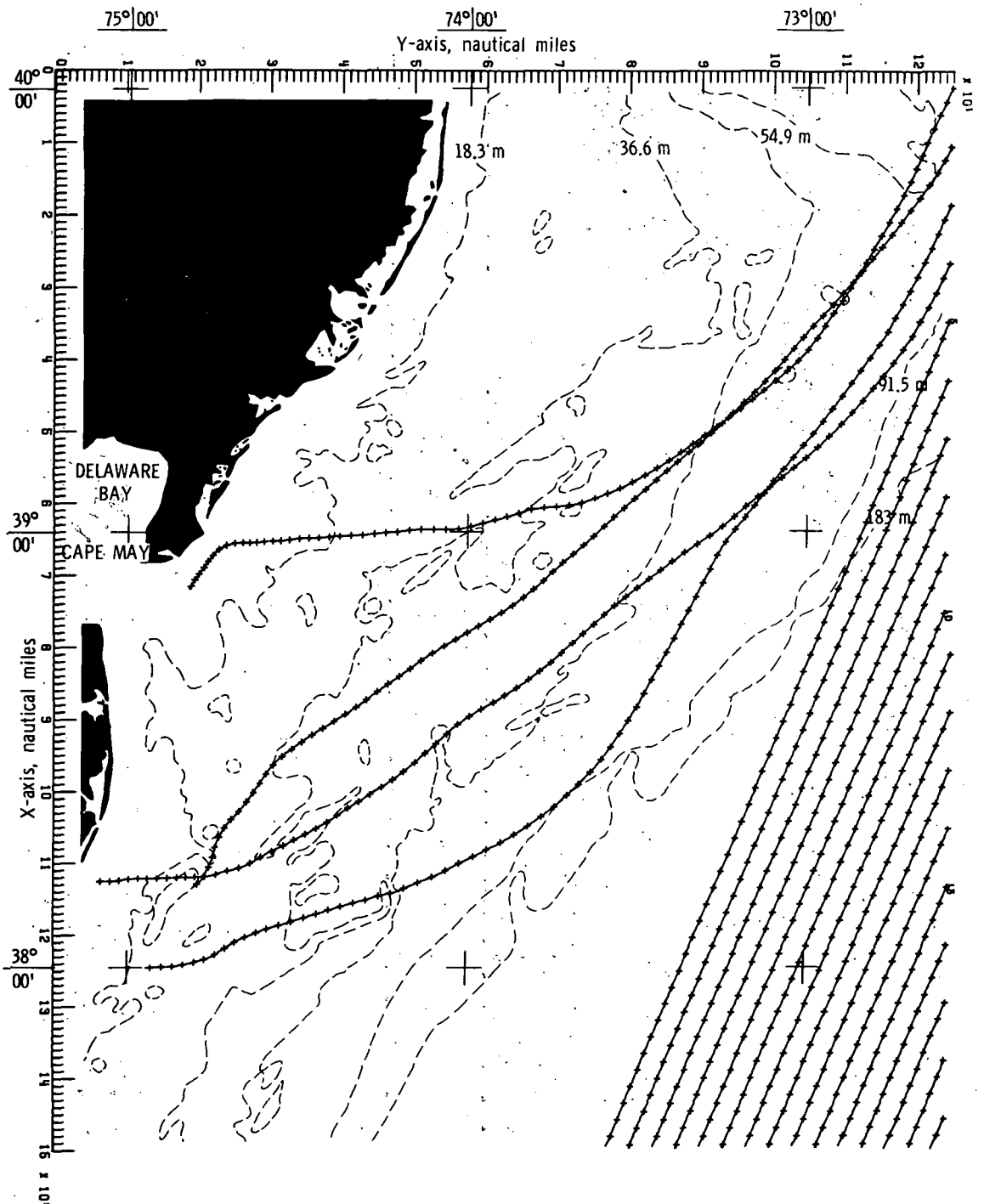


(c) Bottom topography approximated by constrained bicubic interpolation technique.

Figure 10.- Concluded.

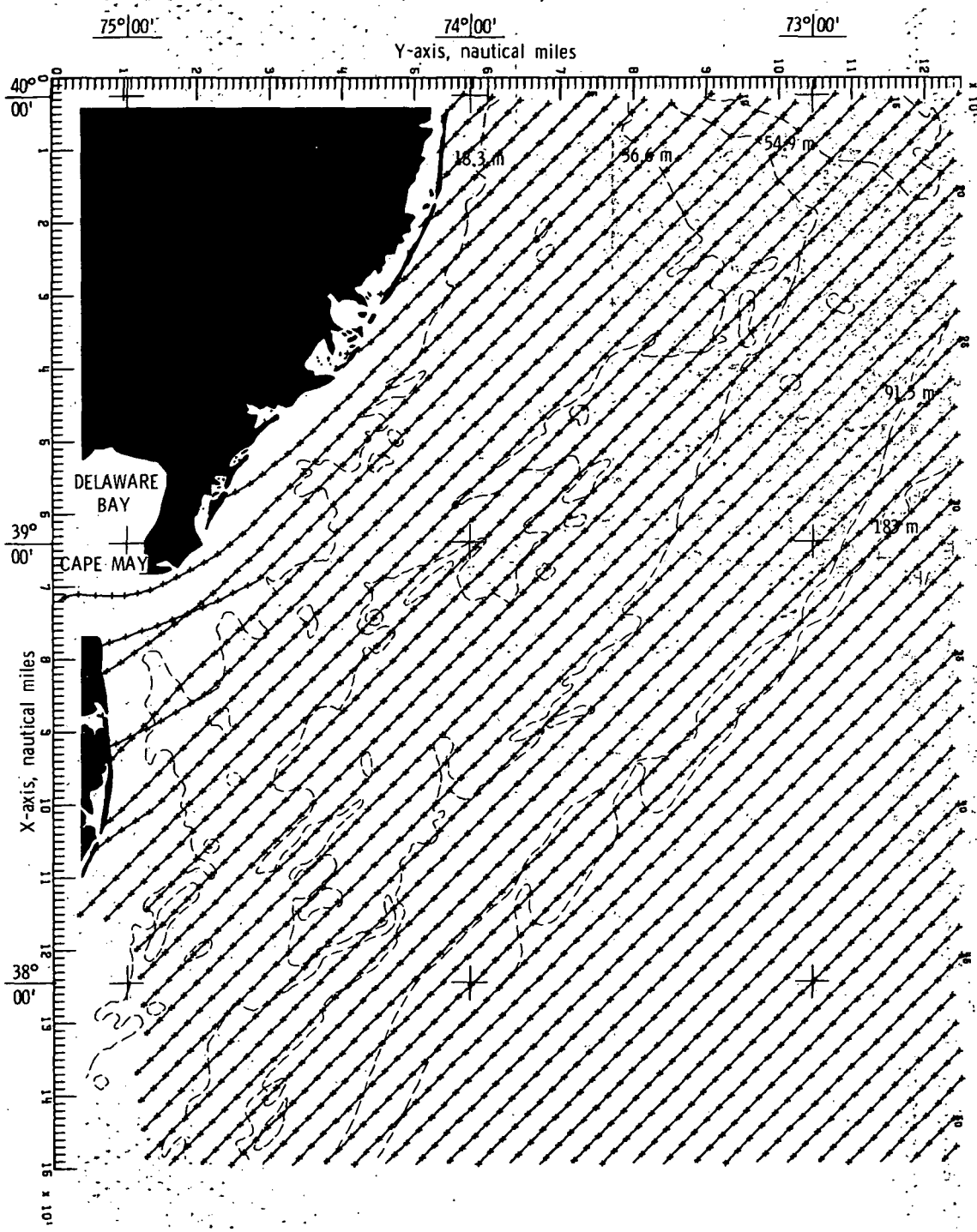


(a) Bottom topography approximated by quadratic least squares technique.

Figure 11. - Wave refraction diagrams. $\alpha = 45^{\circ}$; $T = 6$ seconds.

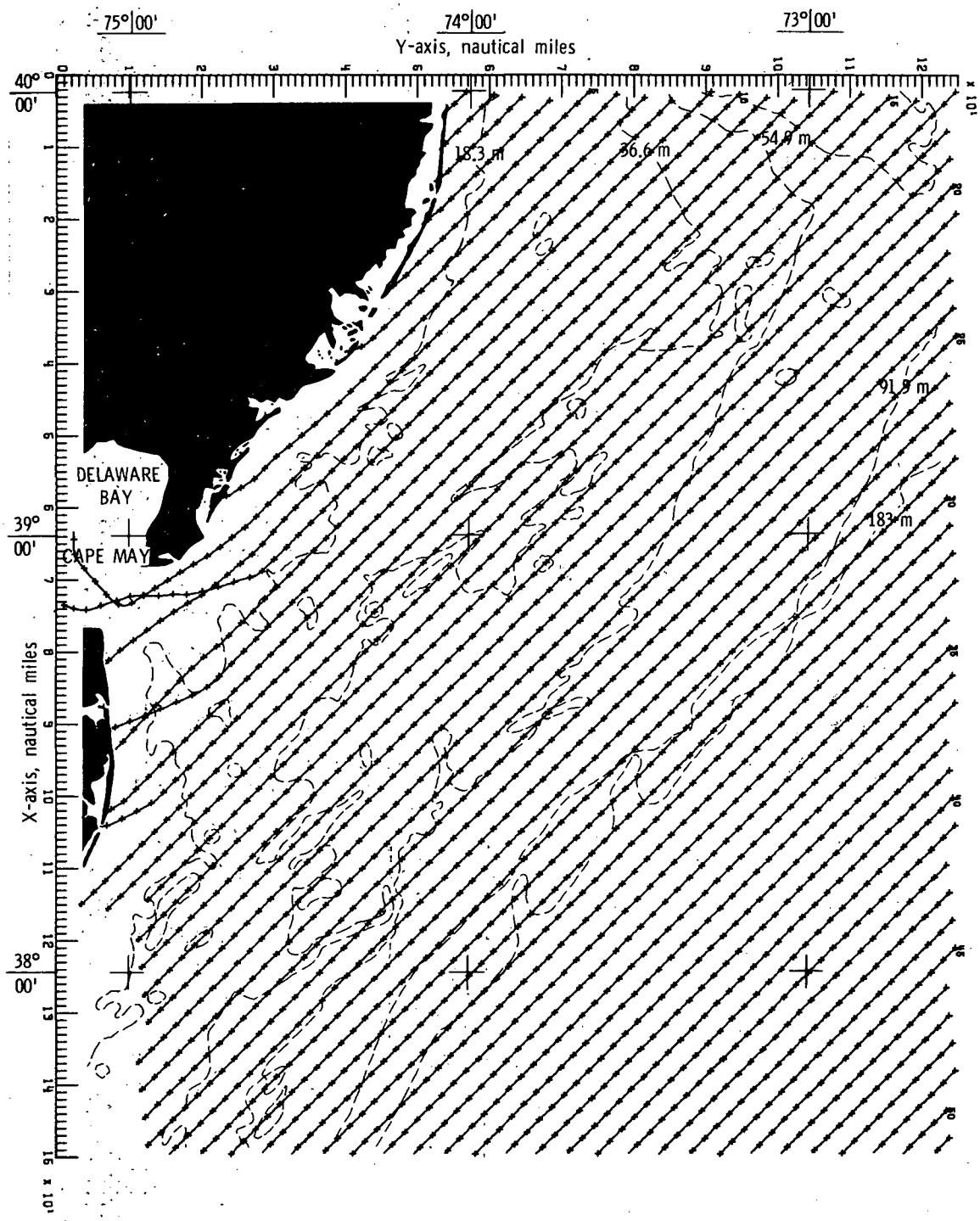


(b) Bottom topography approximated by cubic least squares technique.

Figure 11.- Continued.

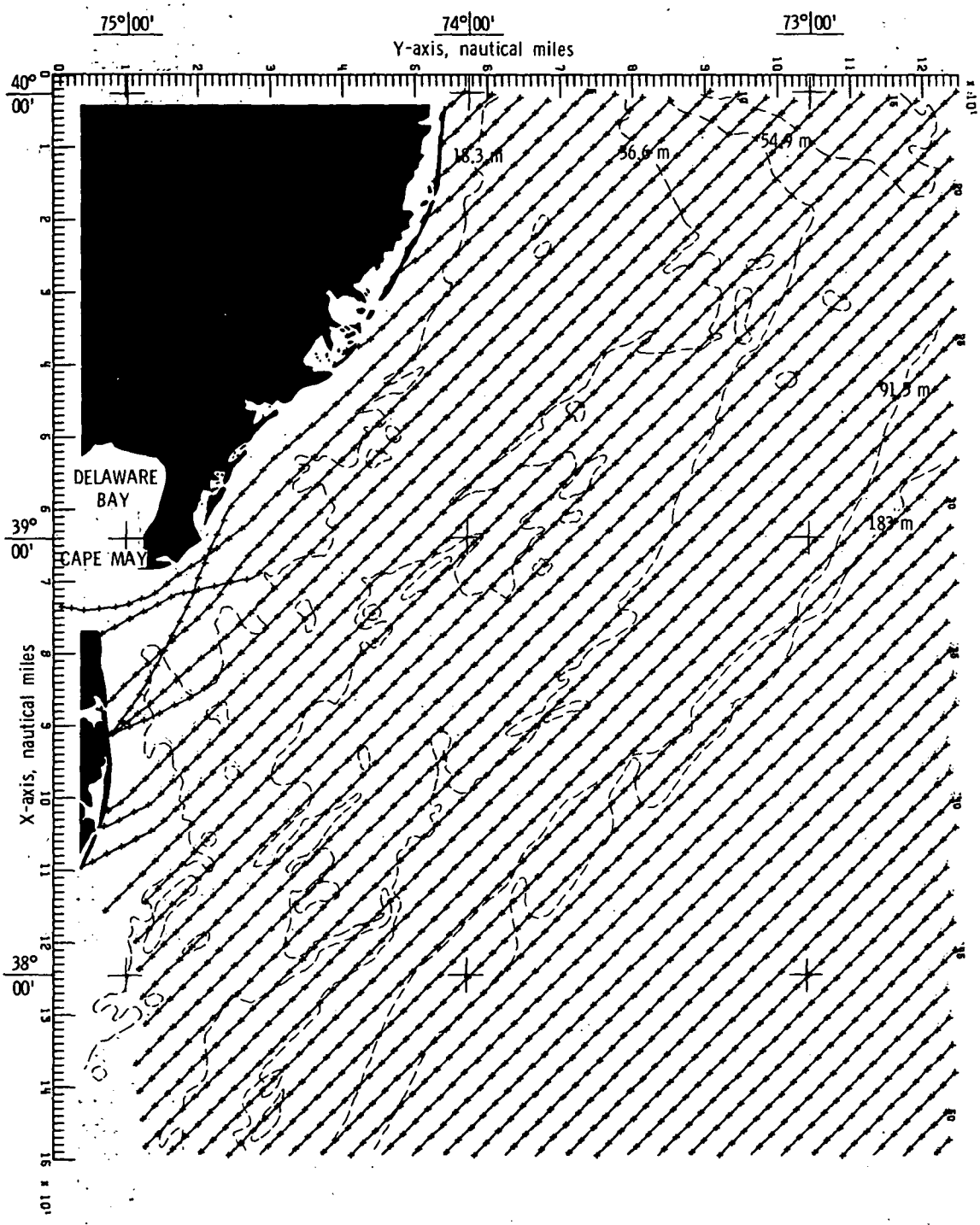


(c) Bottom topography approximated by constrained bicubic interpolation technique.

Figure 11.- Concluded.

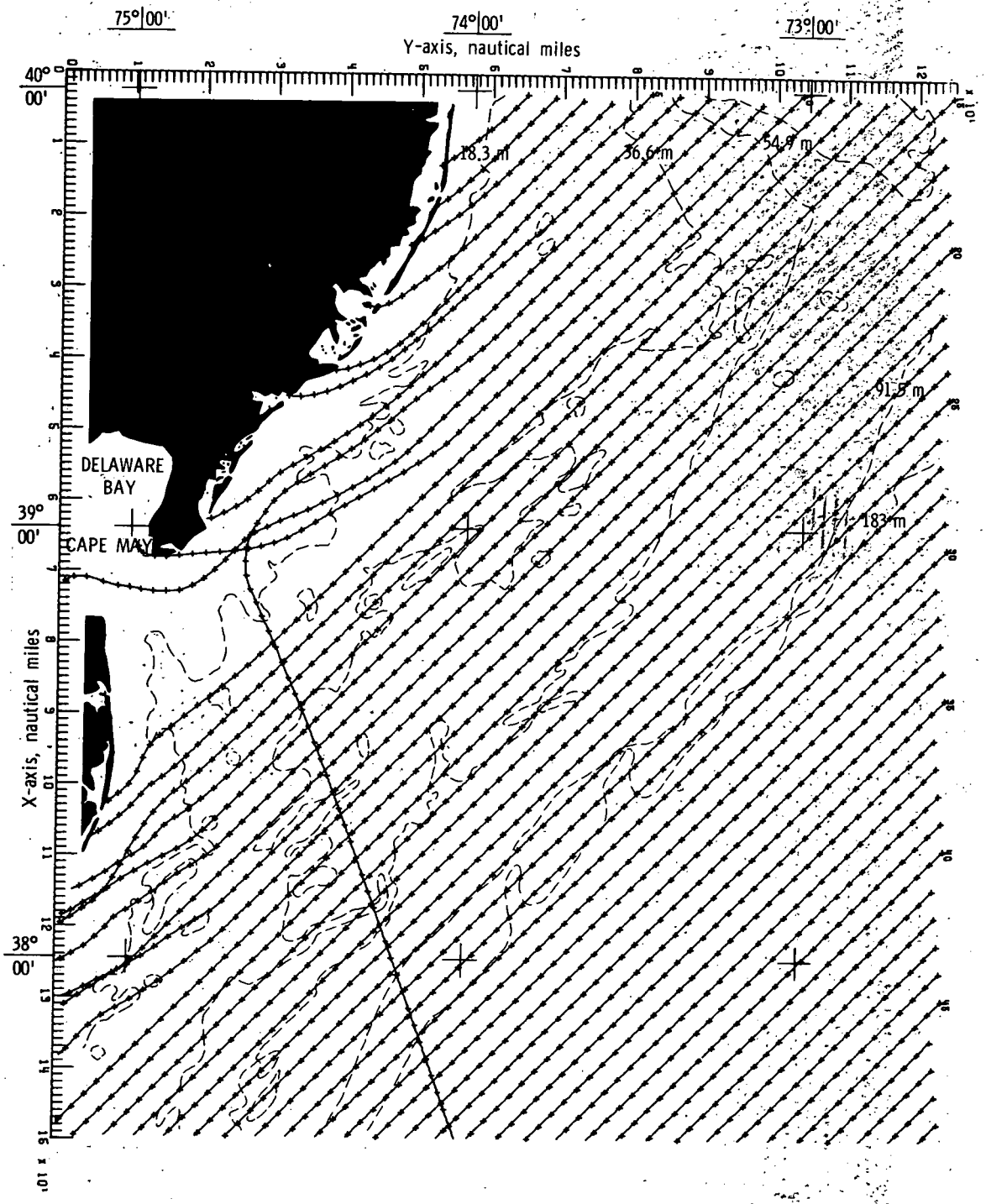


(a) Bottom topography approximated by quadratic least squares technique.

Figure 12.- Wave refraction diagrams. $\alpha = 45°$; $T = 8$ seconds.

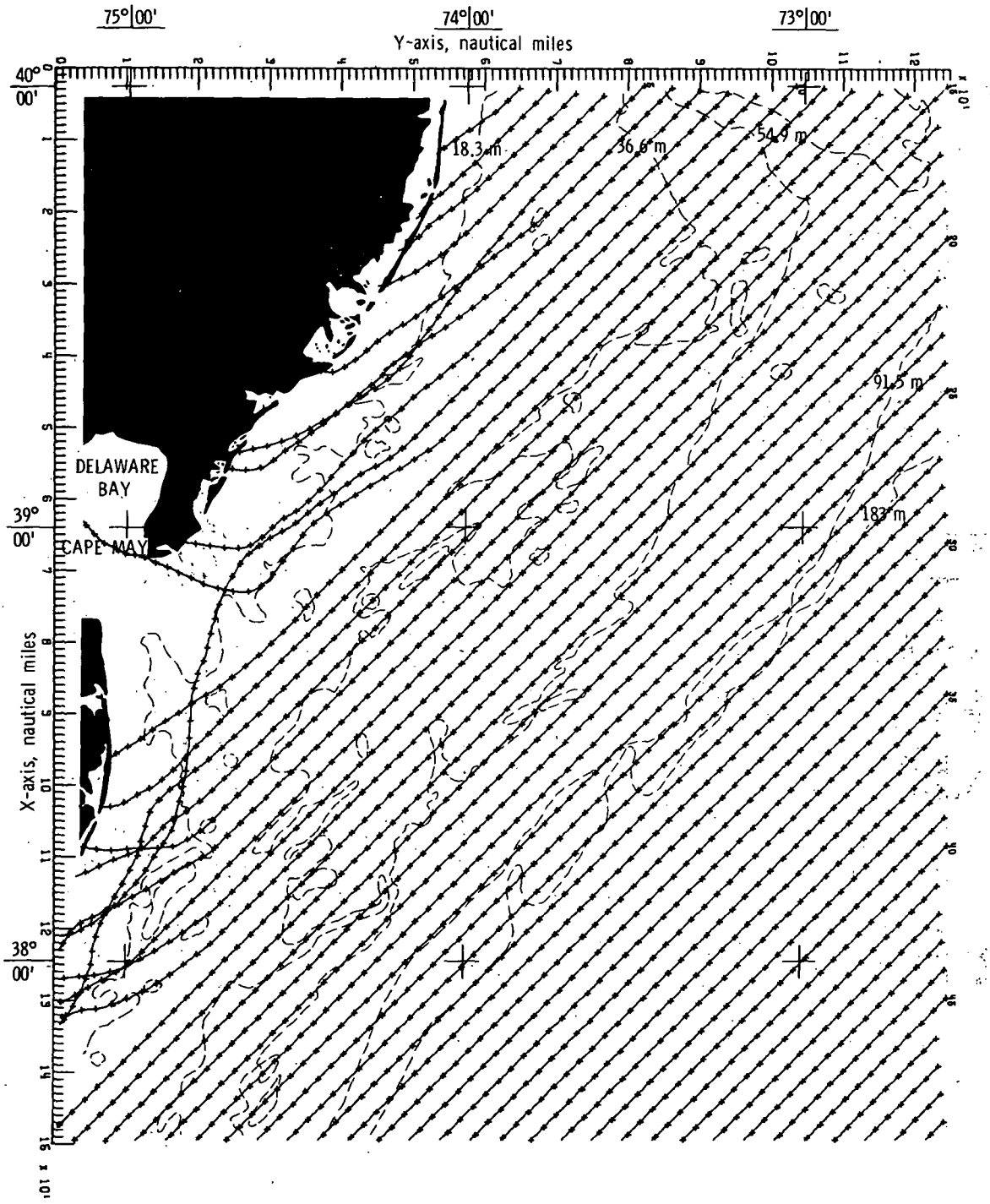


(b) Bottom topography approximated by cubic least squares technique.

Figure 12.- Continued.

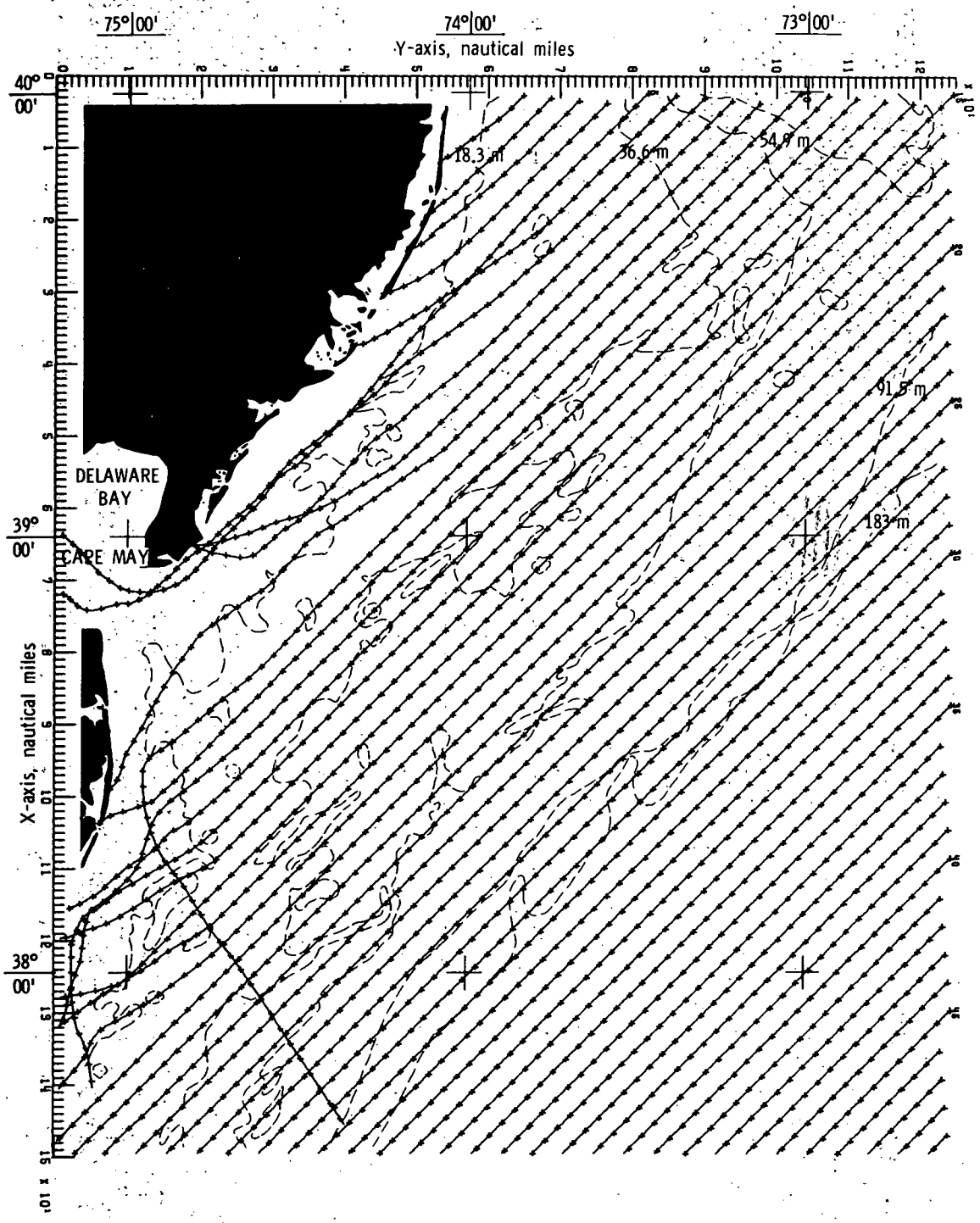


(c) Bottom topography approximated by constrained bicubic interpolation technique.

Figure 12.- Concluded.

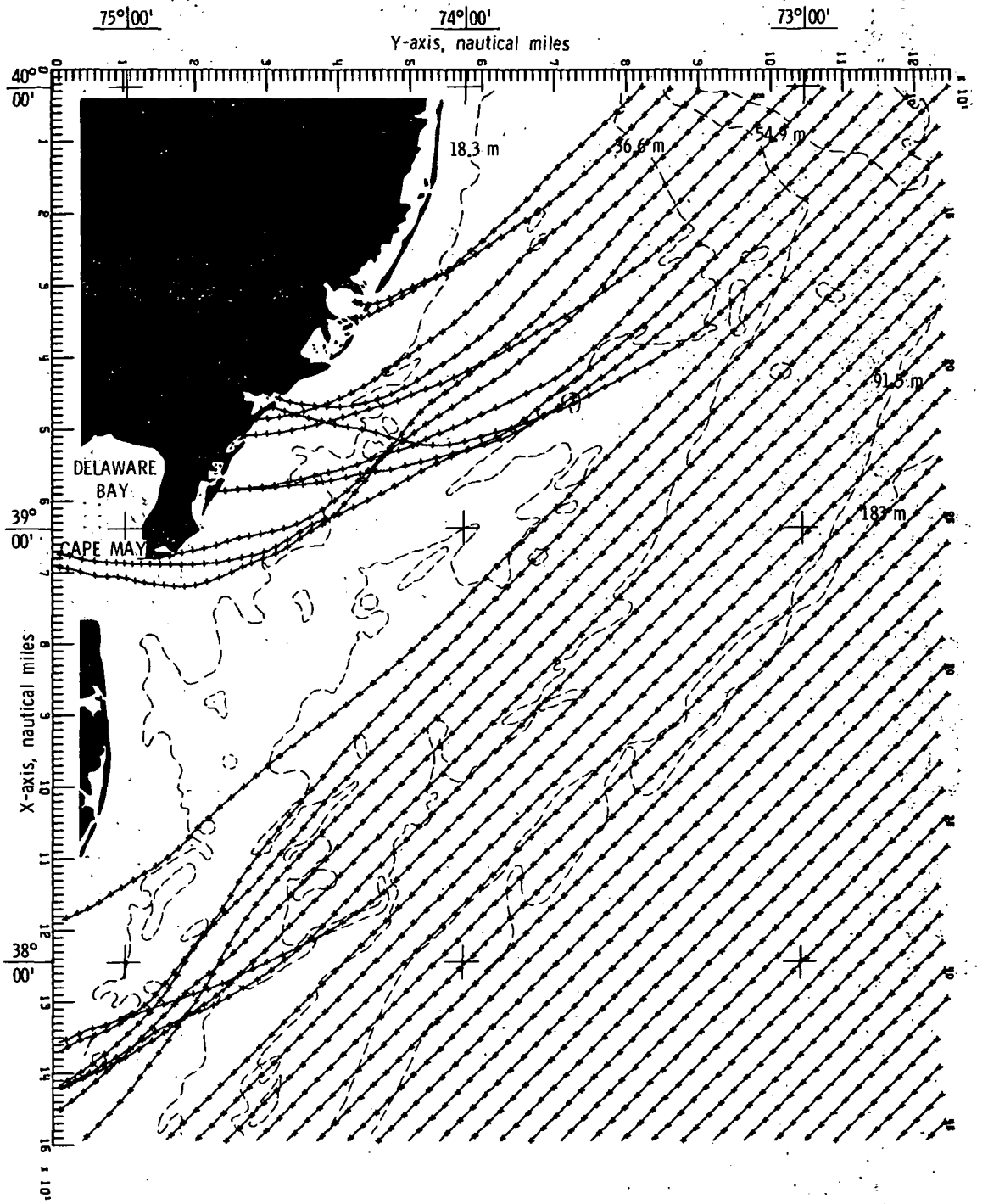


(a) Bottom topography approximated by quadratic least squares technique.

Figure 13.- Wave refraction diagrams. $\alpha = 45^{\circ}$; T = 10 seconds.

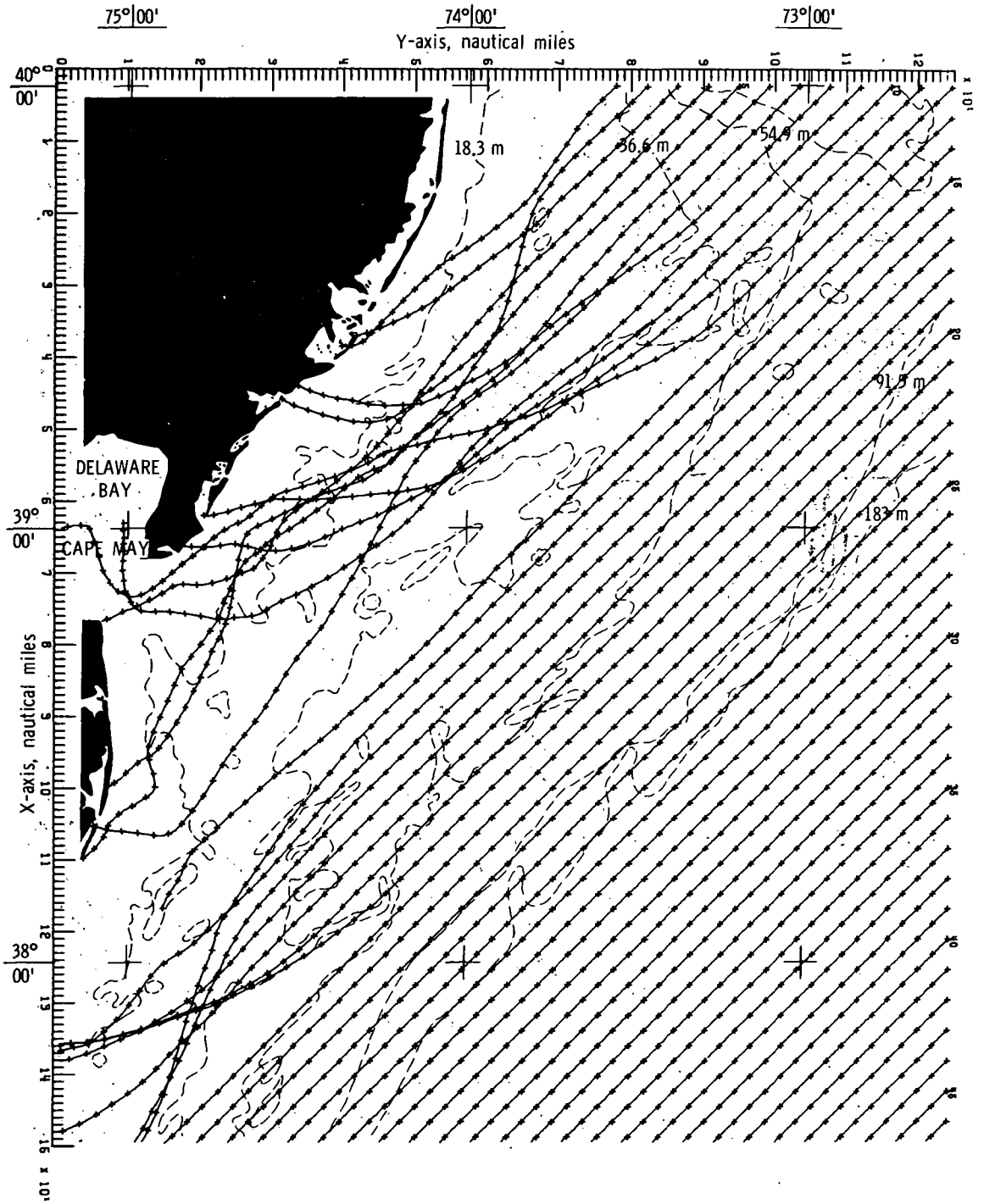


(b) Bottom topography approximated by cubic least squares technique.

Figure 13.- Continued.

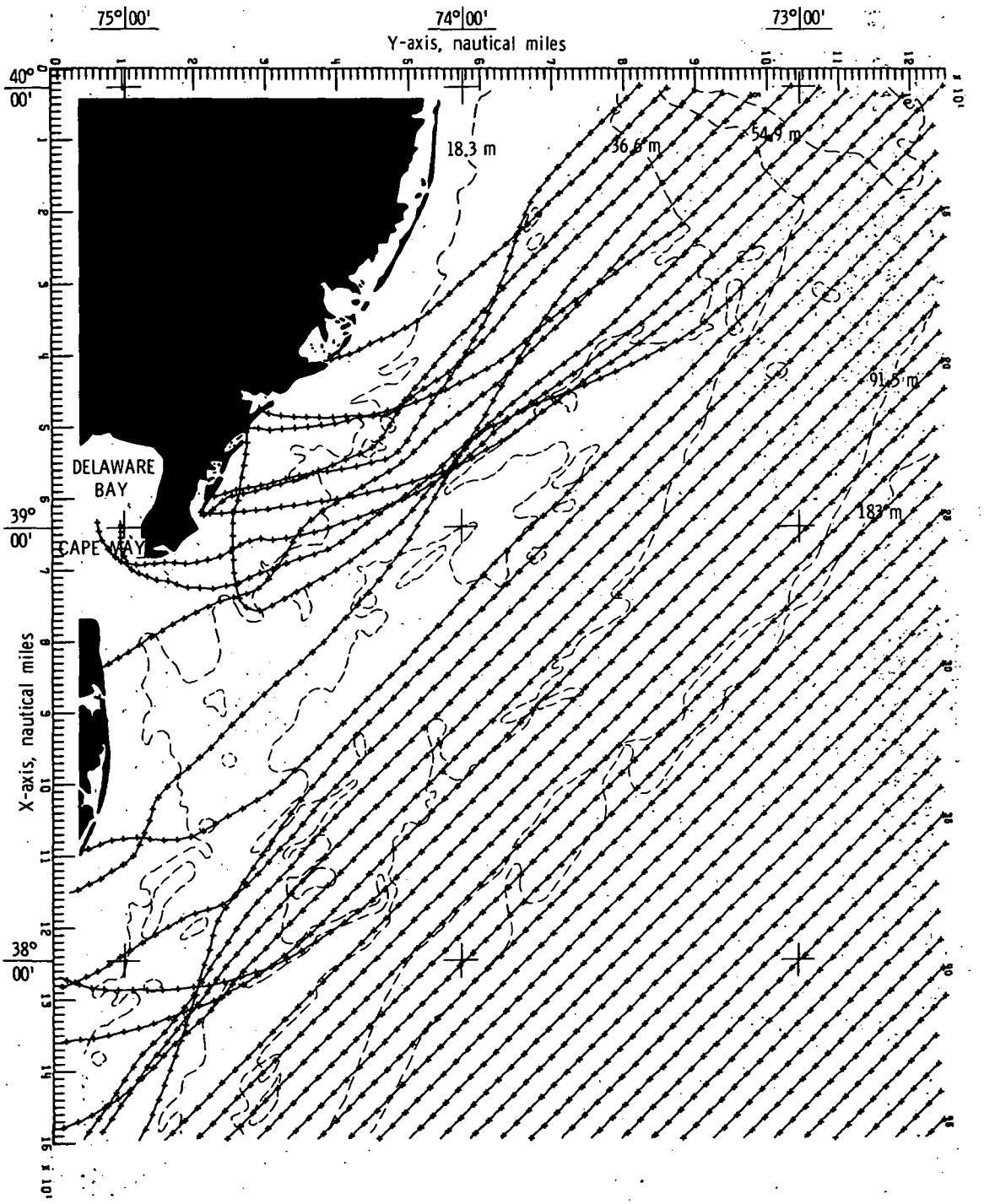


(c) Bottom topography approximated by constrained bicubic interpolation technique.

Figure 13.- Concluded.

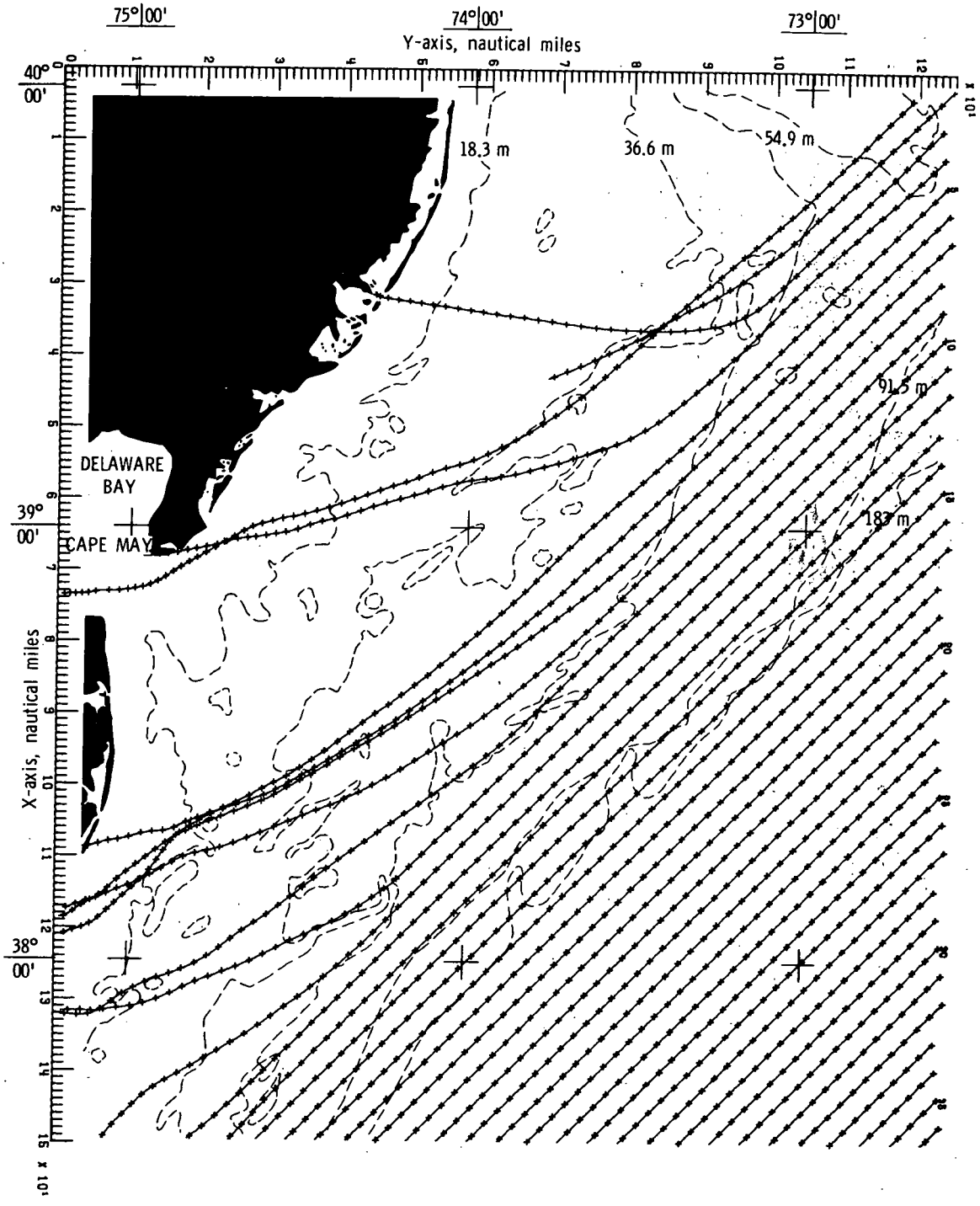


(a) Bottom topography approximated by quadratic least squares technique.

Figure 14.- Wave refraction diagrams. $\alpha$ = 45°; T = 12 seconds.

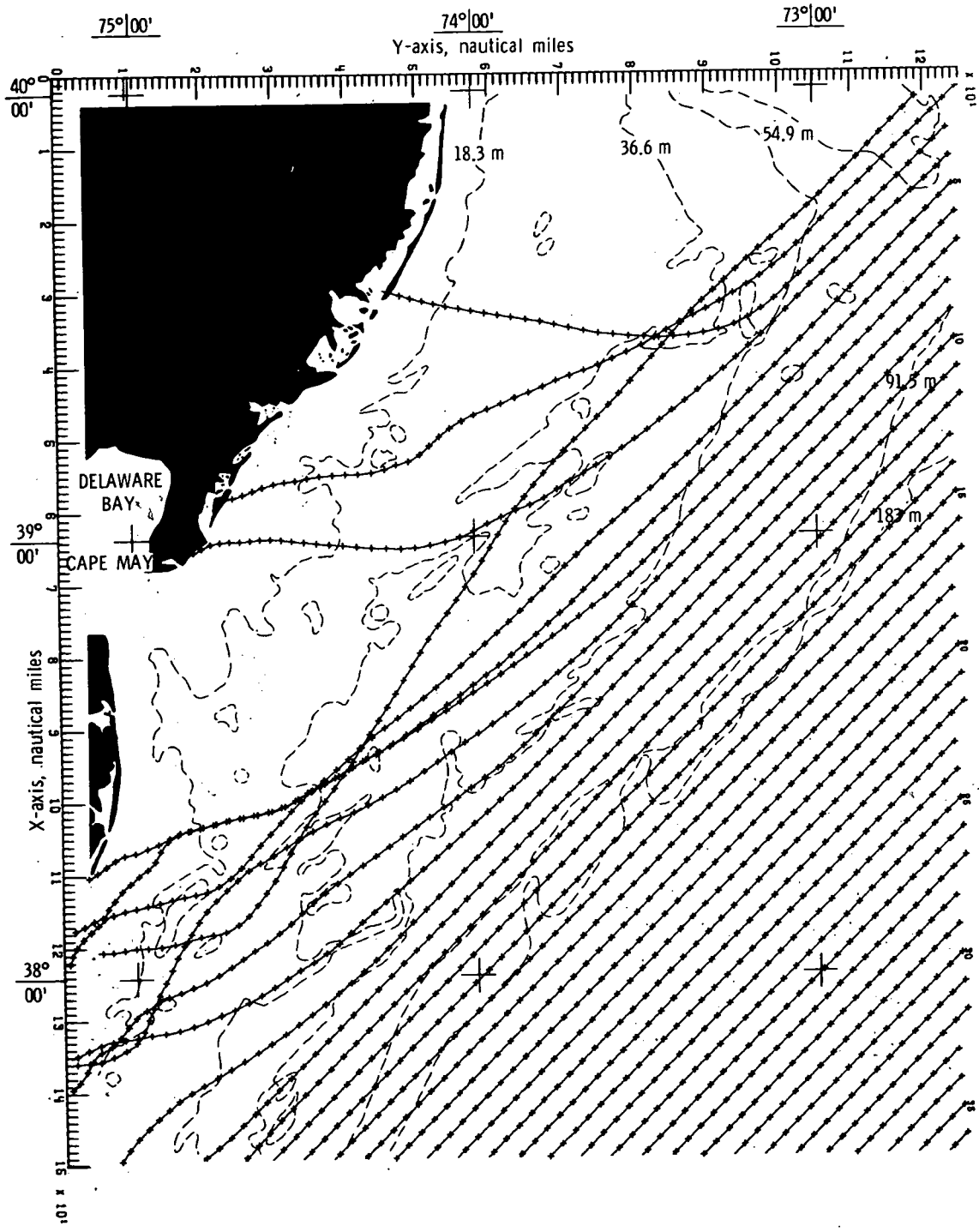


(b) Bottom topography approximated by cubic least squares technique.

Figure 14.- Continued.

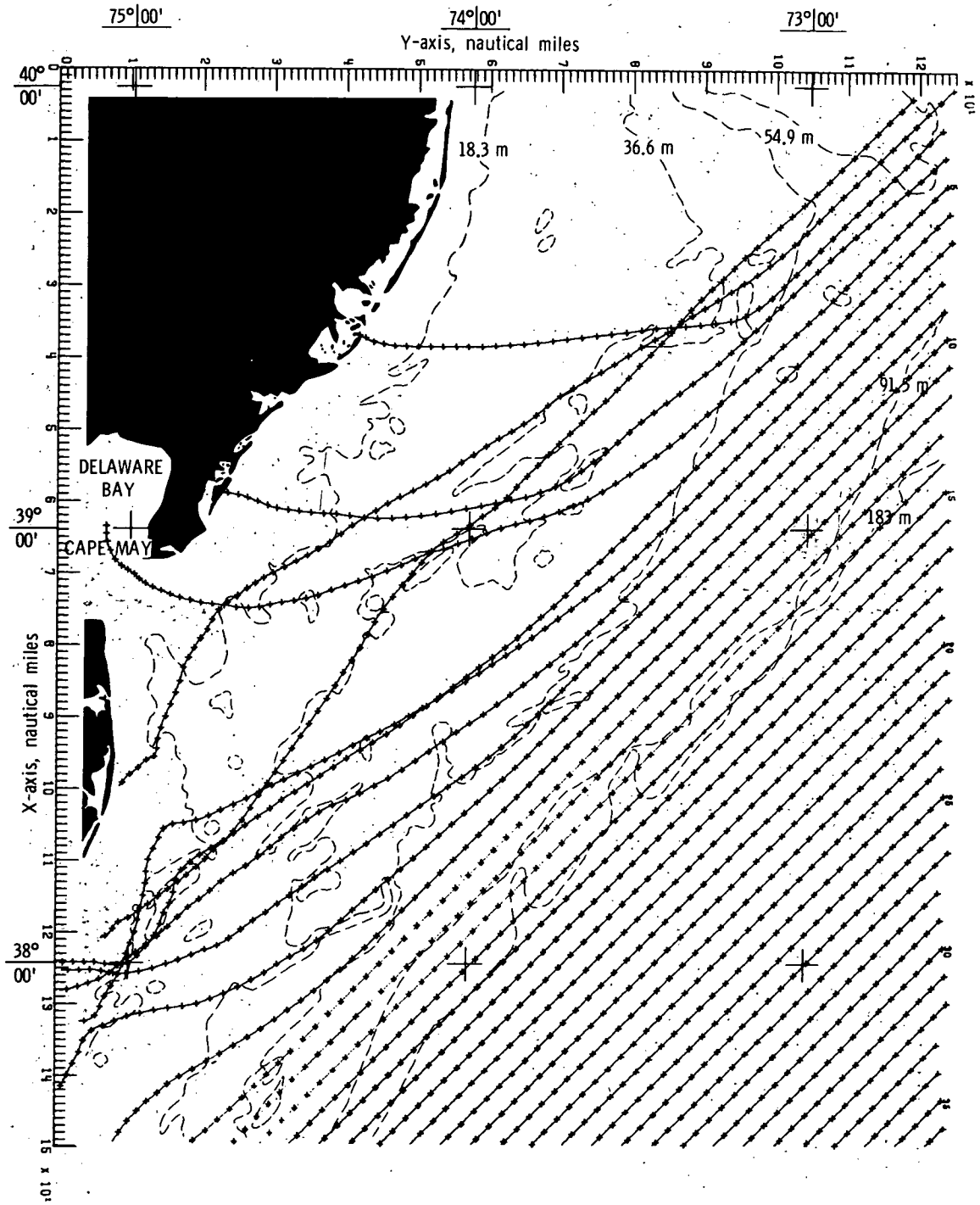


(c) Bottom topography approximated by constrained bicubic interpolation technique.

Figure 14.- Concluded.

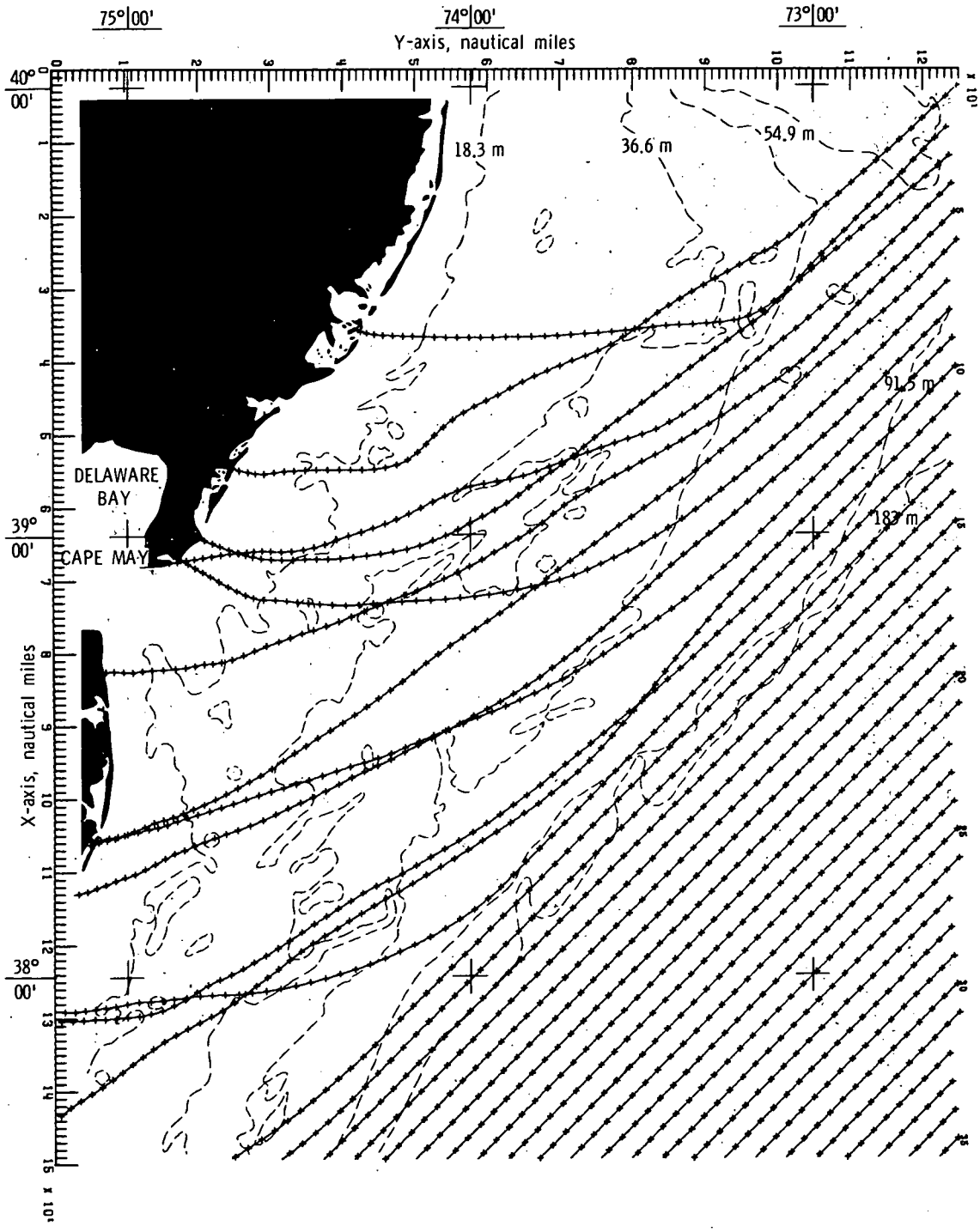


(a) Bottom topography approximated by quadratic least squares technique.

Figure 15.- Wave refraction diagrams. $\alpha = 45^{\circ}$; T = 14 seconds.

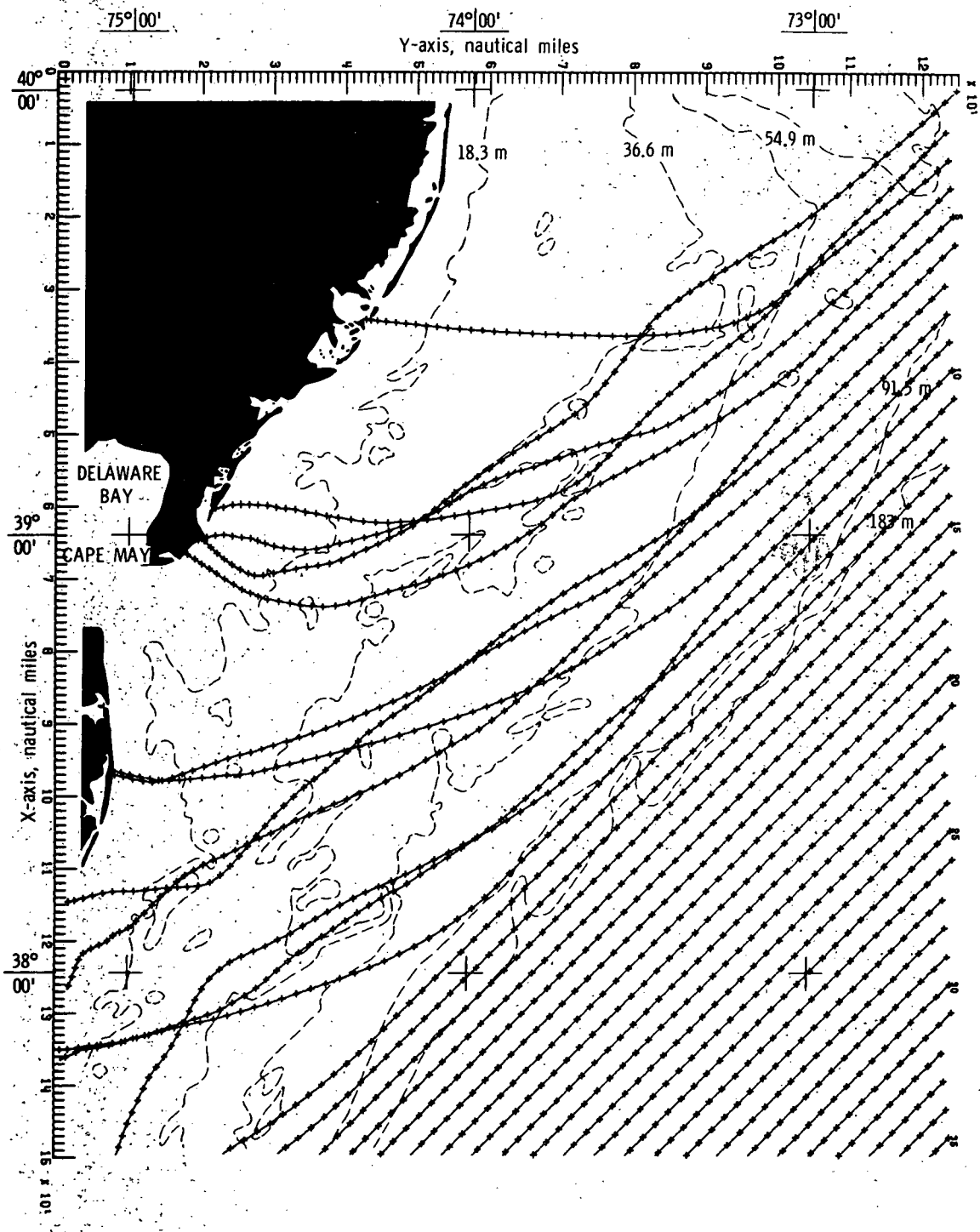


(b) Bottom topography approximated by cubic least squares technique.

Figure 15.- Continued.

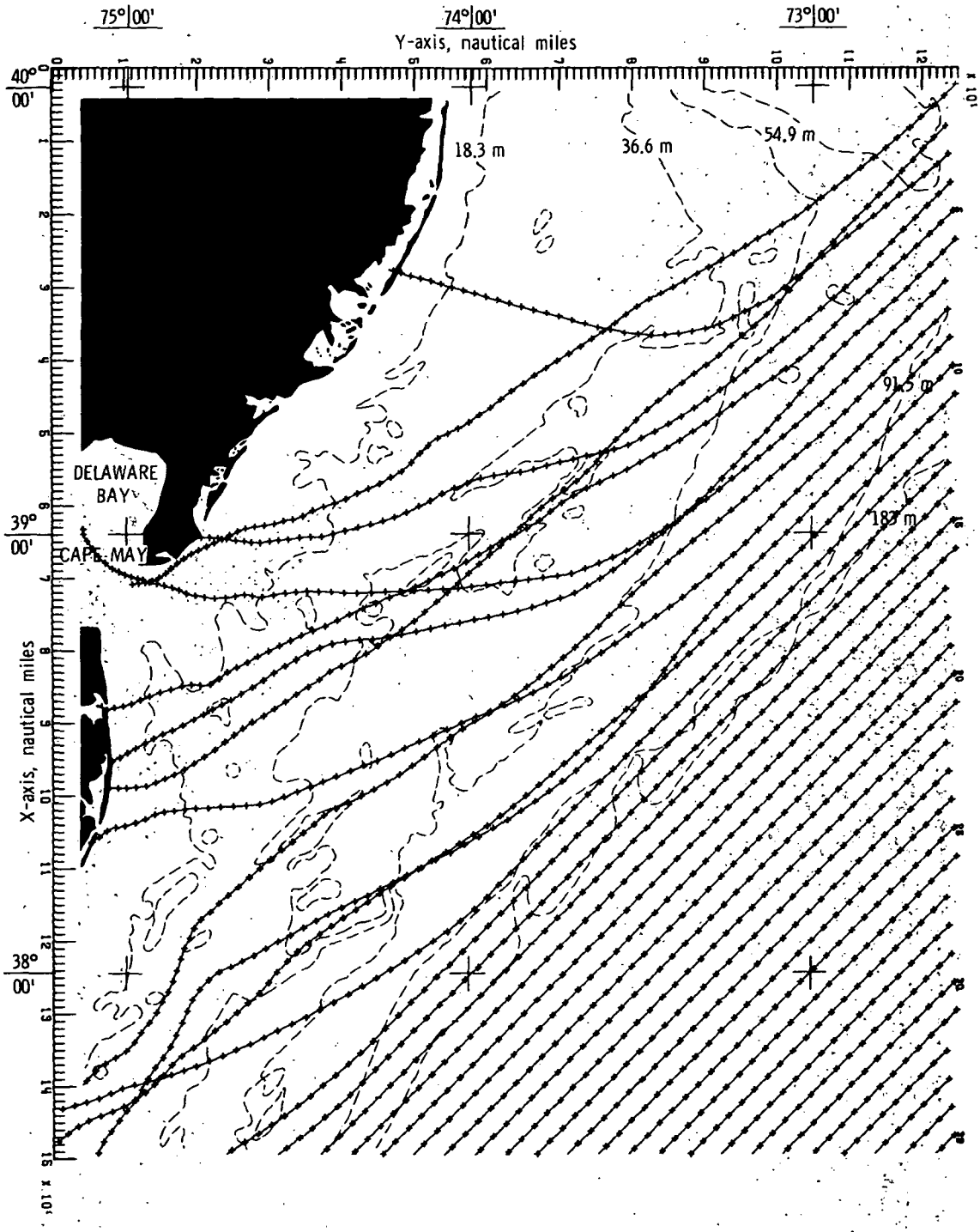


(c) Bottom topography approximated by constrained bicubic interpolation technique.

Figure 15.- Concluded.

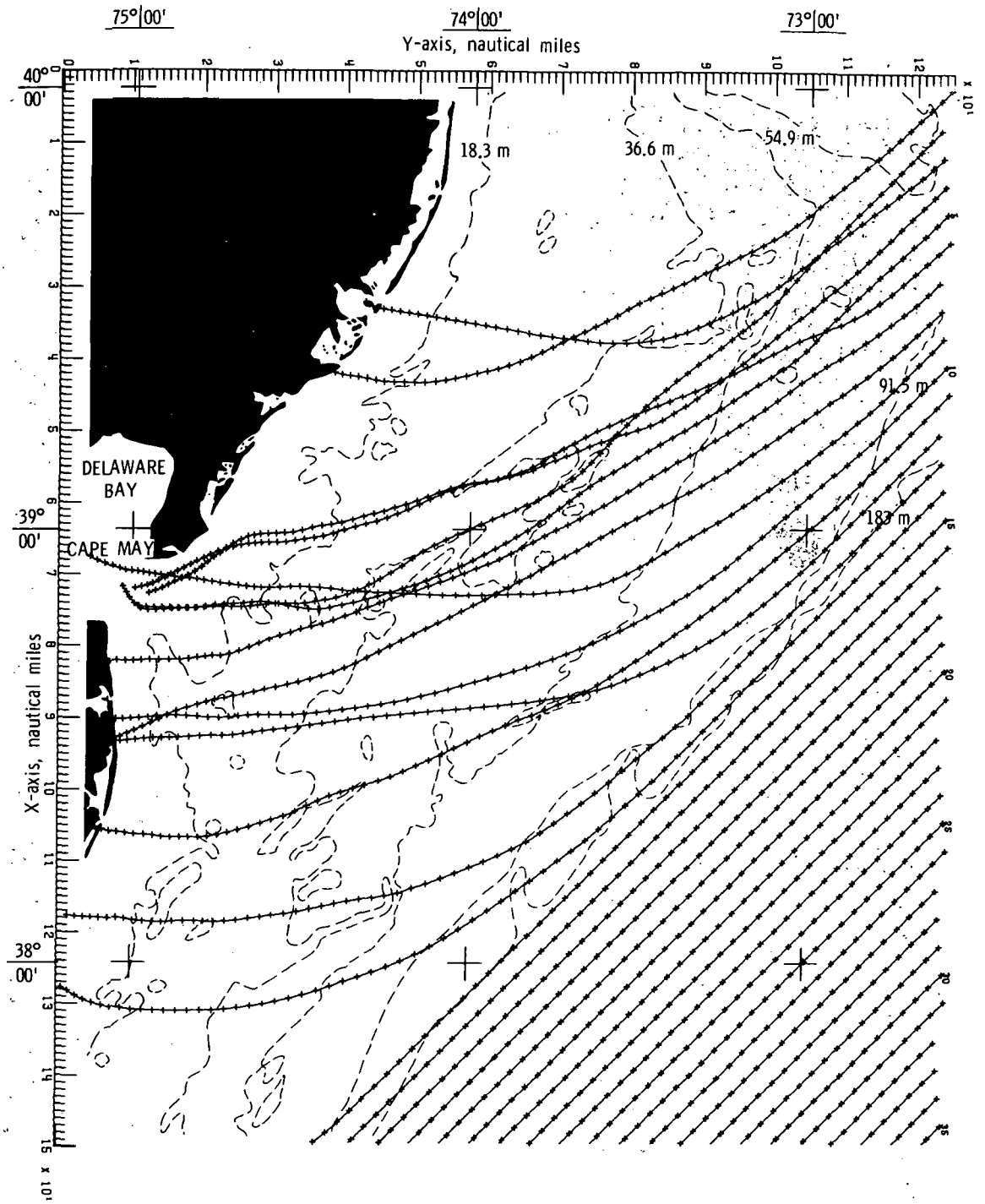


(a) Bottom topography approximated by quadratic least squares technique.

Figure 16.- Wave refraction diagrams. $\alpha_o = 45^o$; T = 16 seconds.

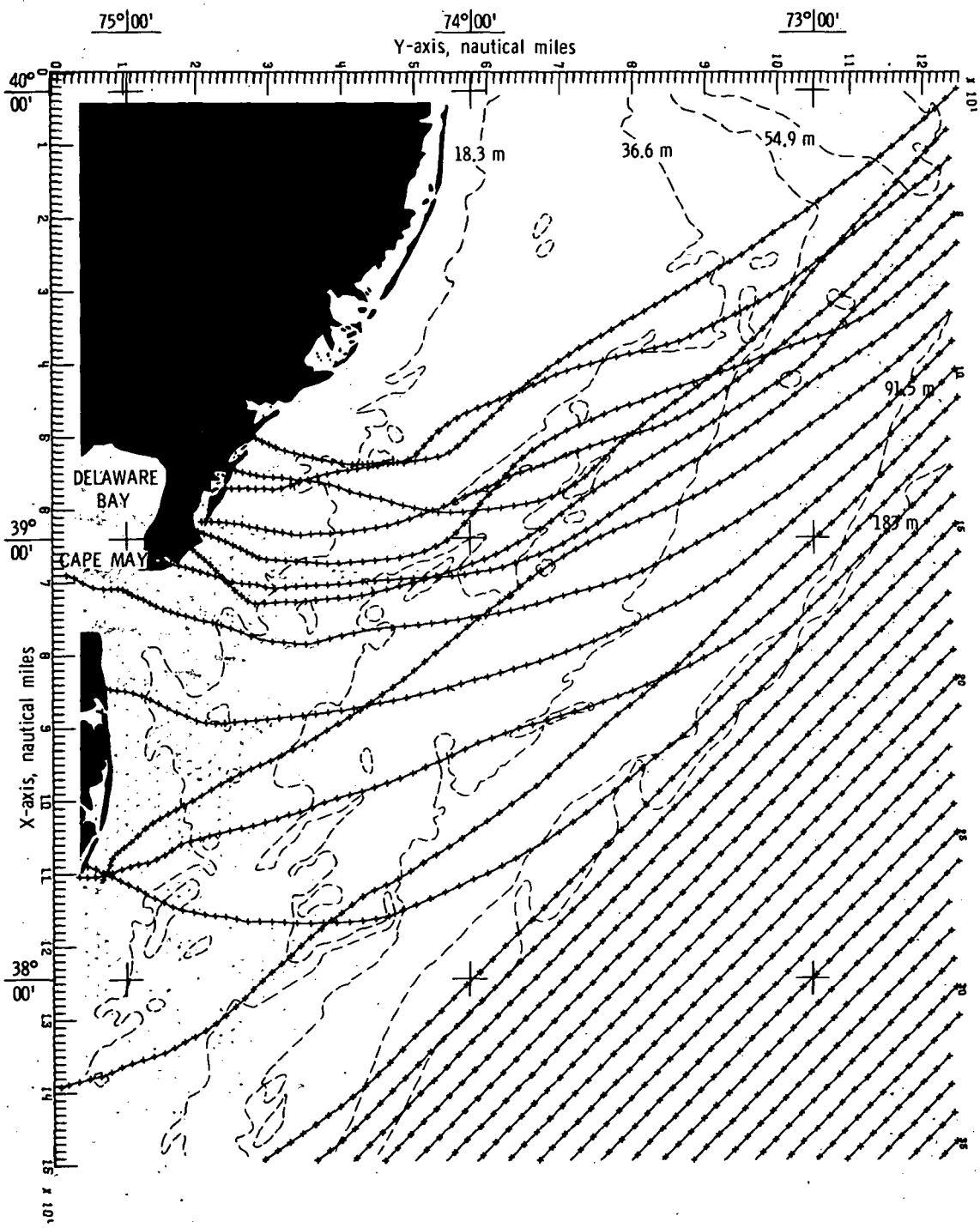


(b) Bottom topography approximated by cubic least squares technique.

Figure 16.- Continued.

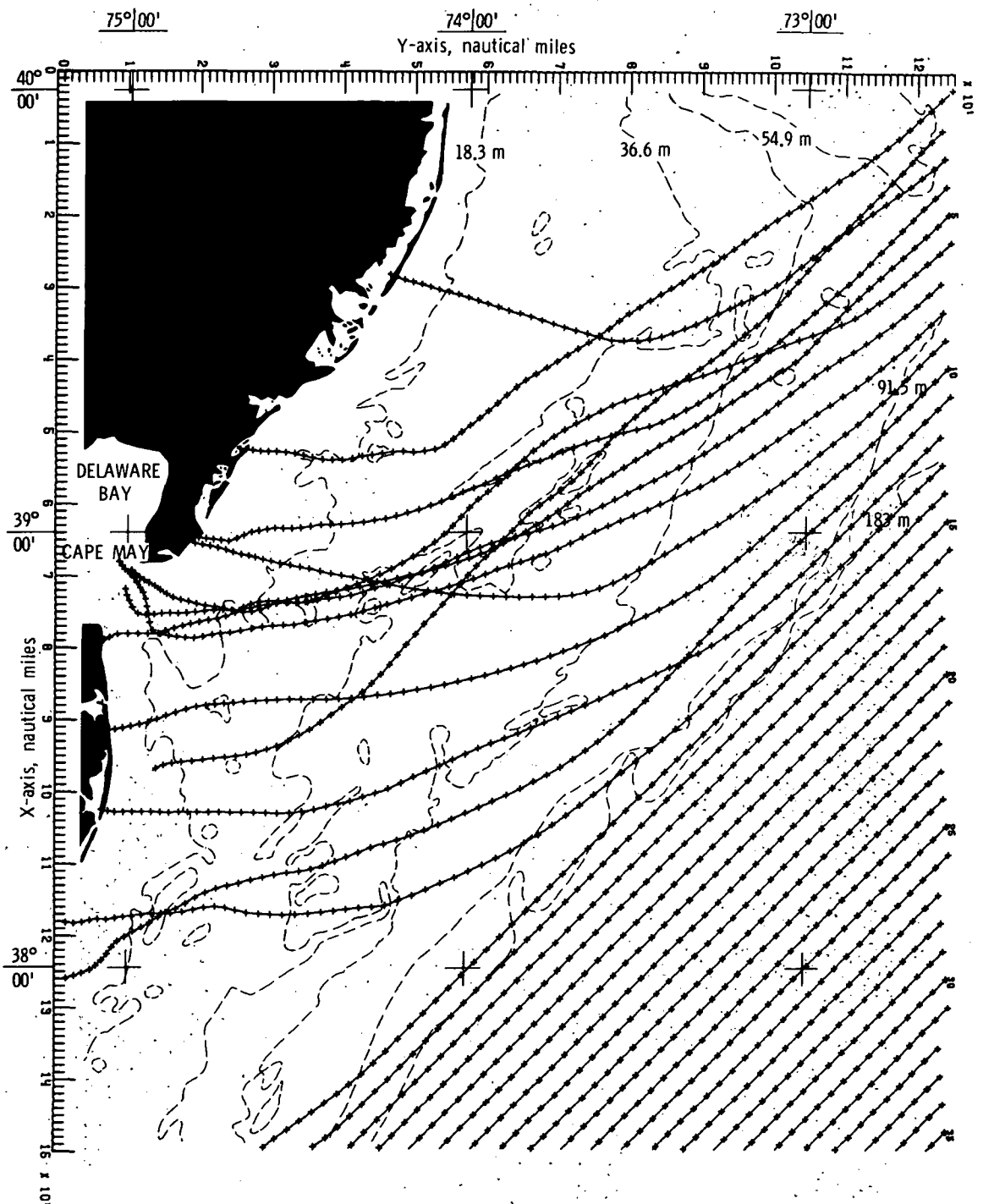


(c) Bottom topography approximated by constrained bicubic interpolation technique.

Figure 16.- Concluded.

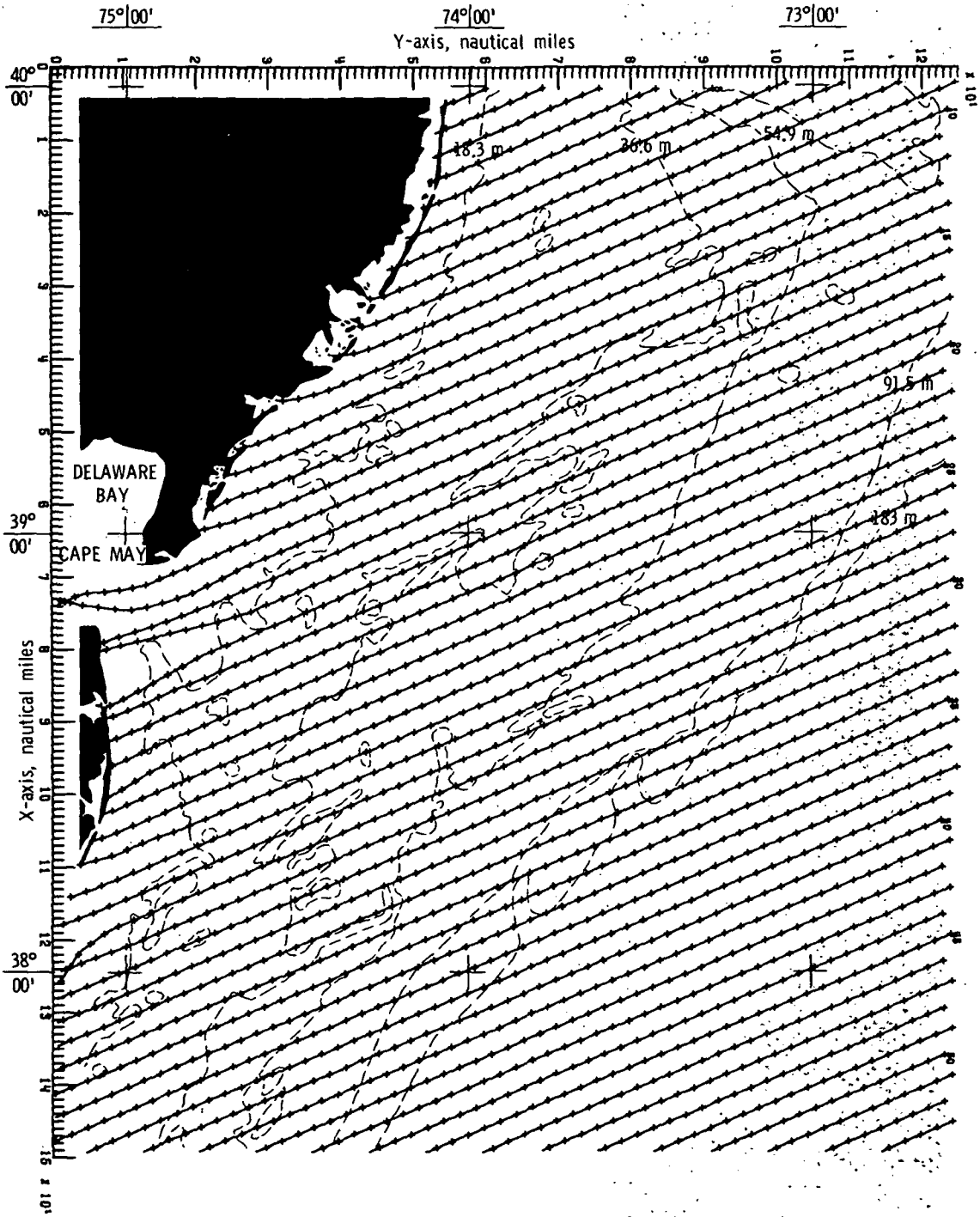


(a) Bottom topography approximated by quadratic least squares technique.

Figure 17.- Wave refraction diagrams. $\alpha = 67.5^{\circ}$; $T = 6$ seconds.

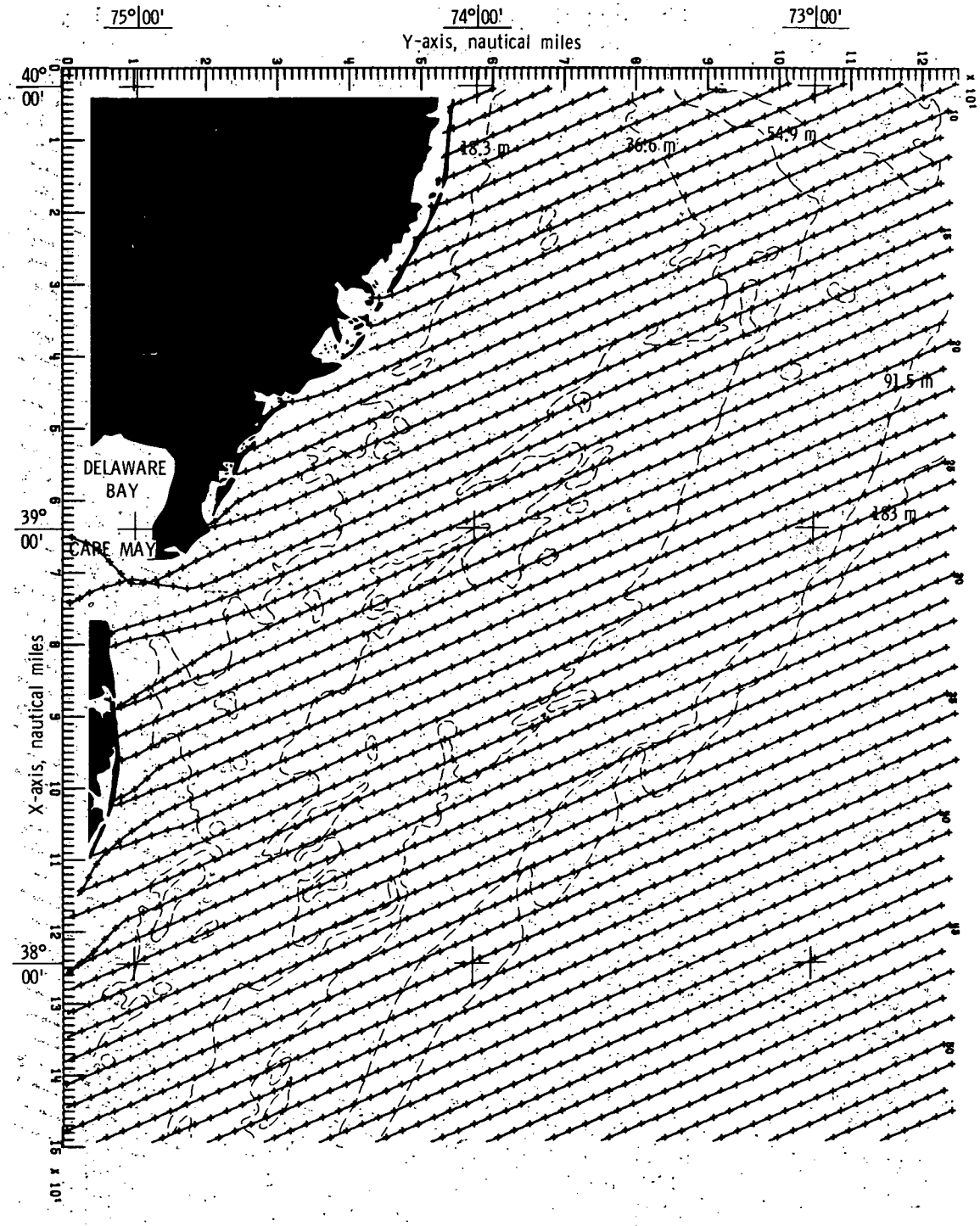


(b) Bottom topography approximated by cubic least squares technique.

Figure 17.- Continued.

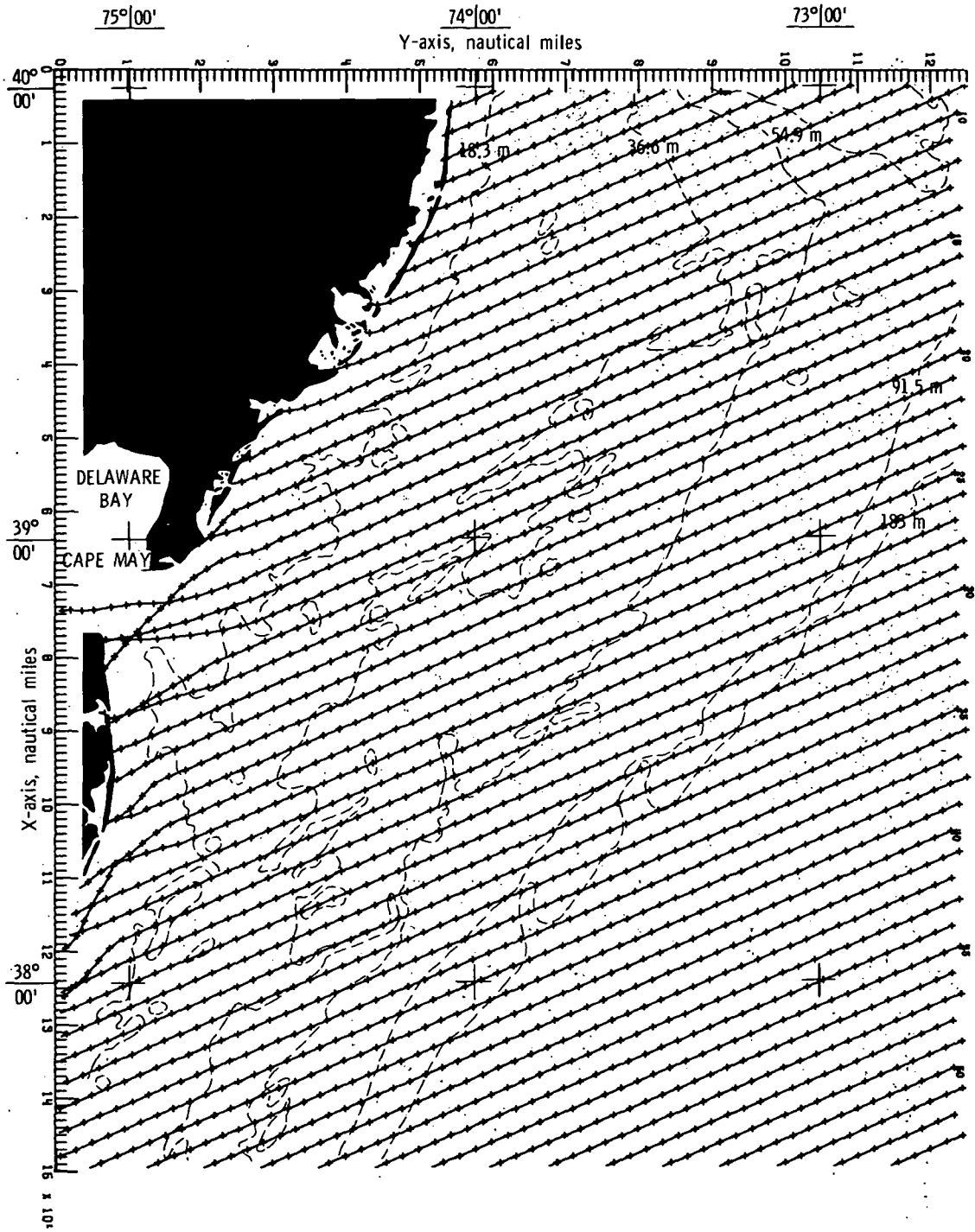


(c) Bottom topography approximated by constrained bicubic interpolation technique.

Figure 17.- Concluded.

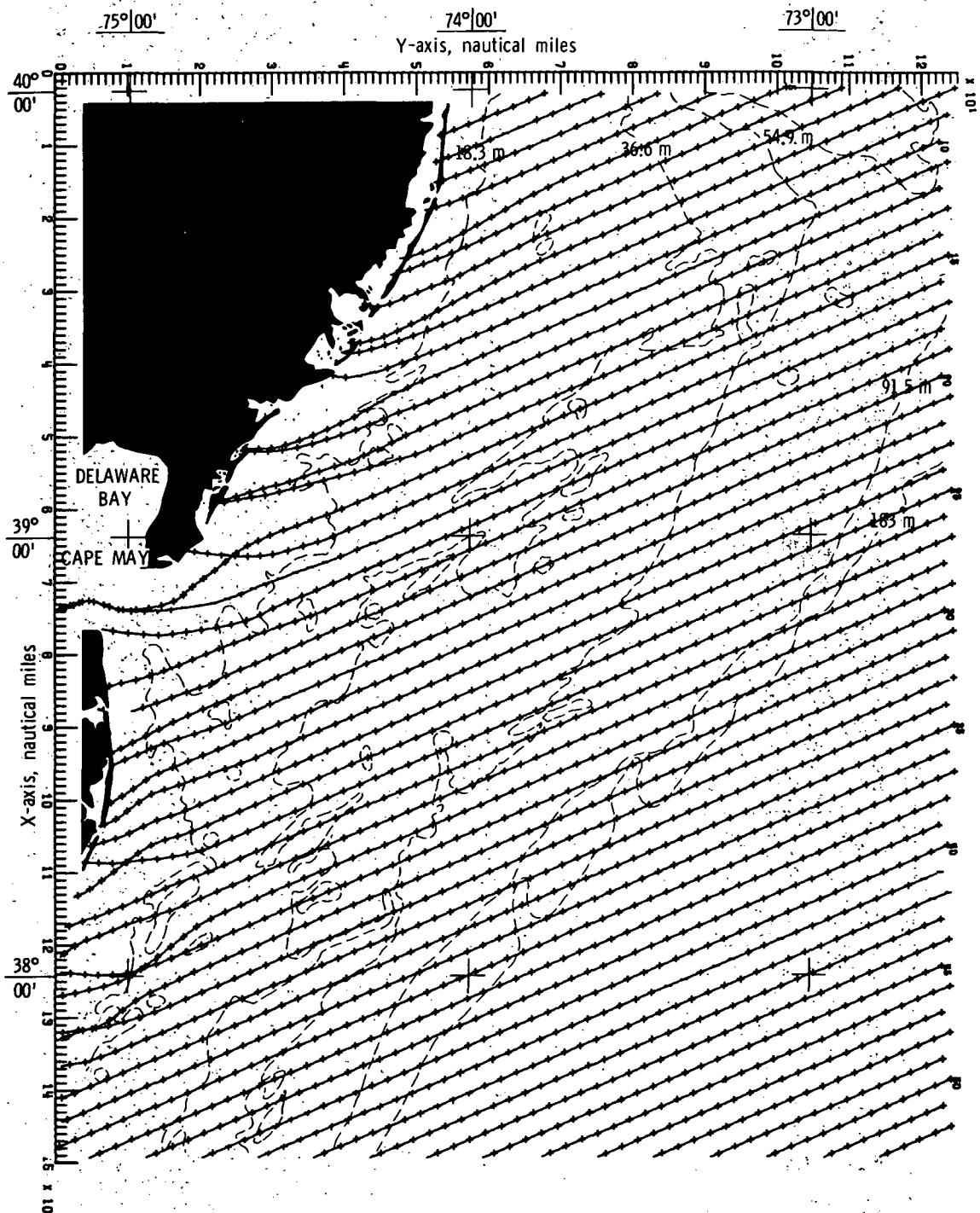


(a) Bottom topography approximated by quadratic least squares technique.

Figure 18.- Wave refraction diagrams. $\alpha = 67.5^{\circ}$; $T = 8$ seconds.

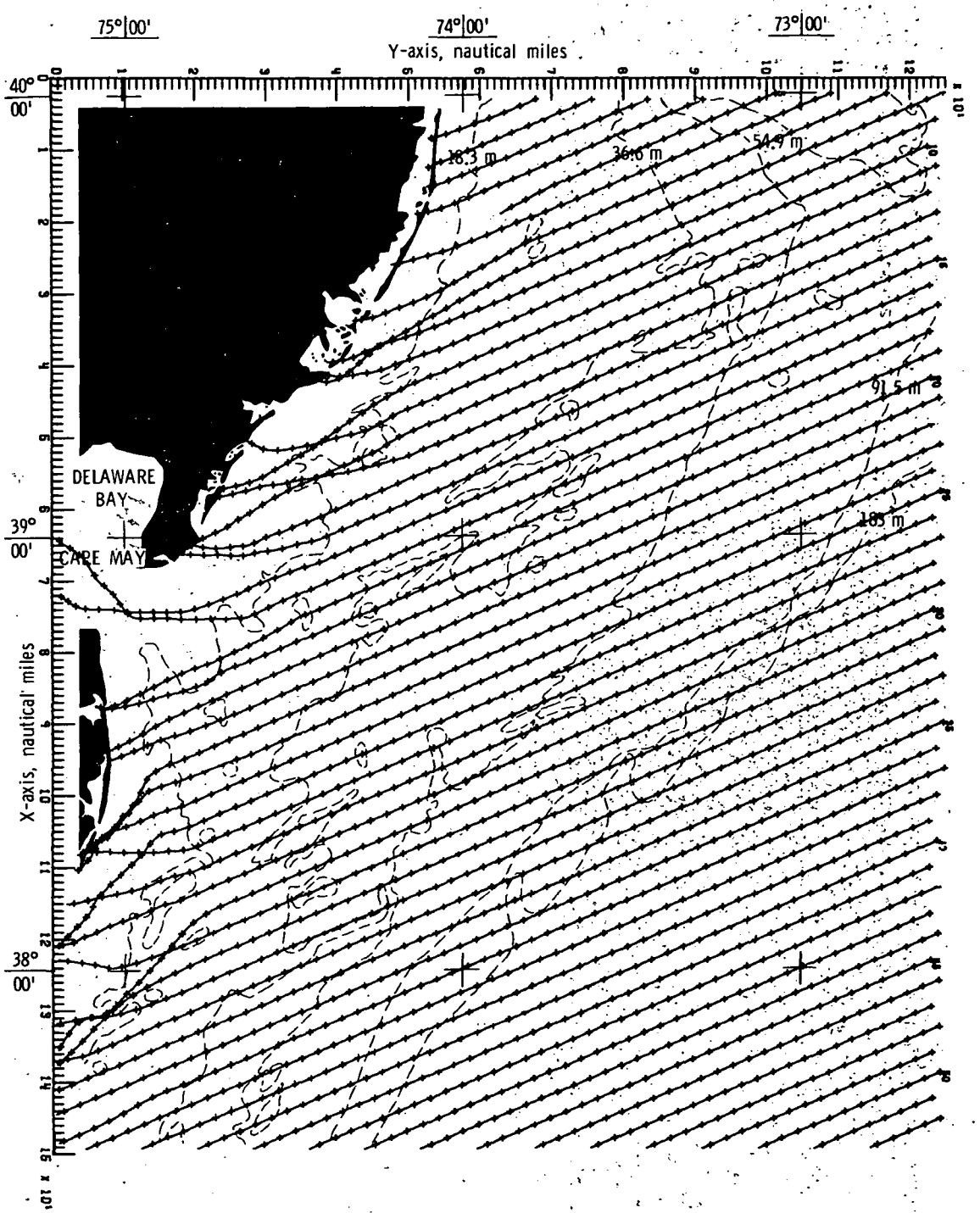


(b) Bottom topography approximated by cubic least squares technique.

Figure 18.- Continued.

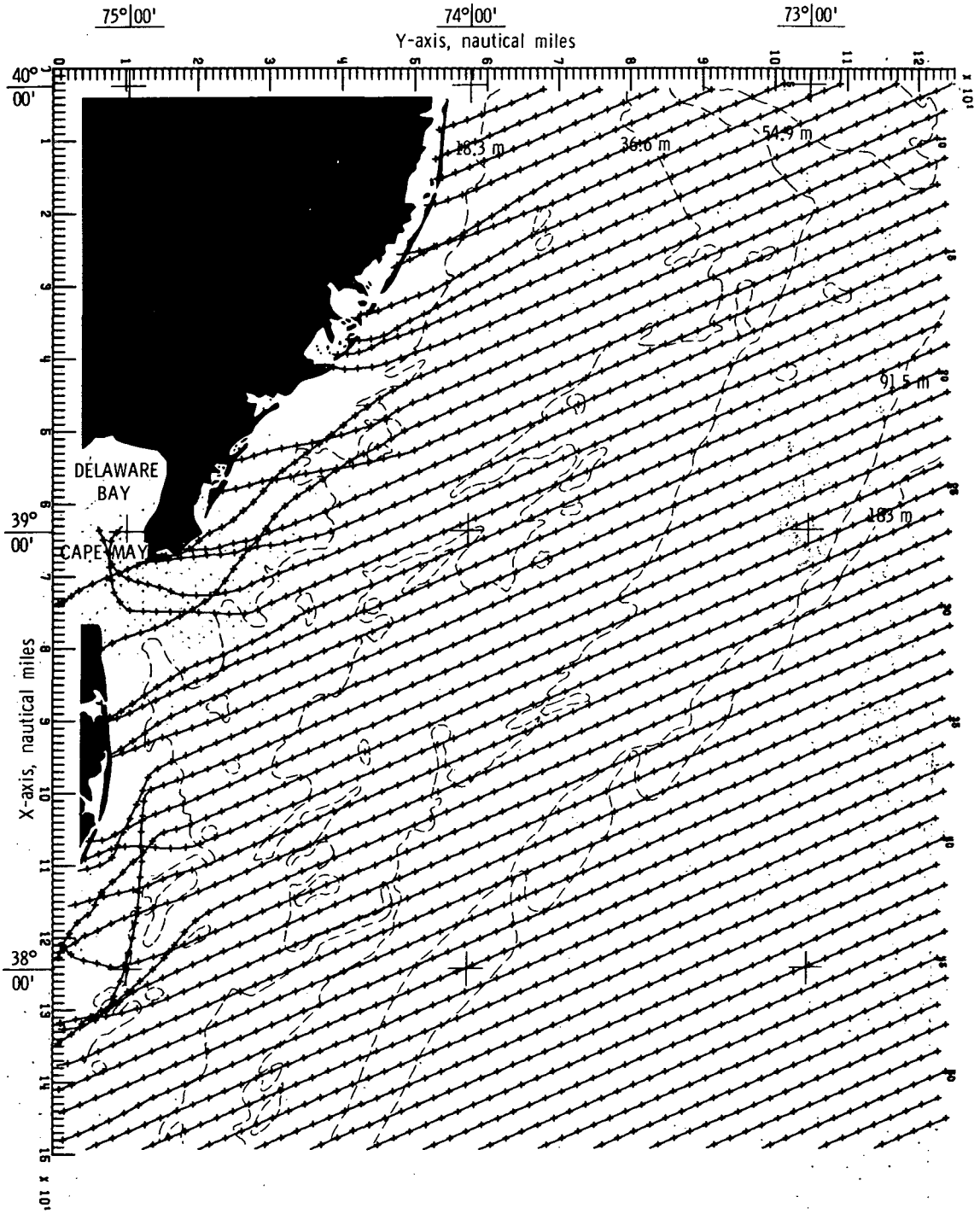


(c) Bottom topography approximated by constrained bicubic interpolation technique.

Figure 18.- Concluded.

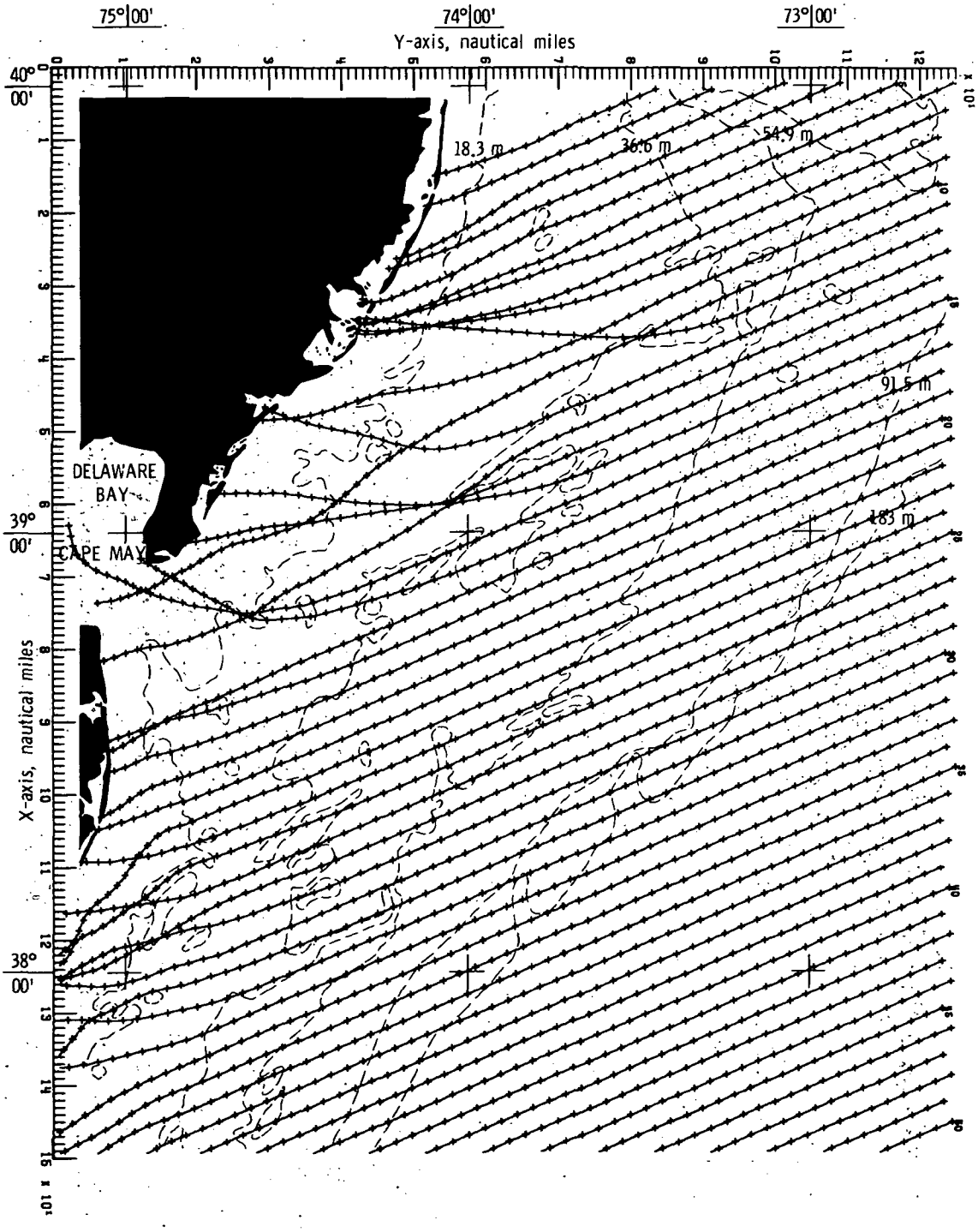


(a) Bottom topography approximated by quadratic least squares technique.

Figure 19.- Wave refraction diagrams. $\alpha = 67.5^{o}$; $T = 10$ seconds.

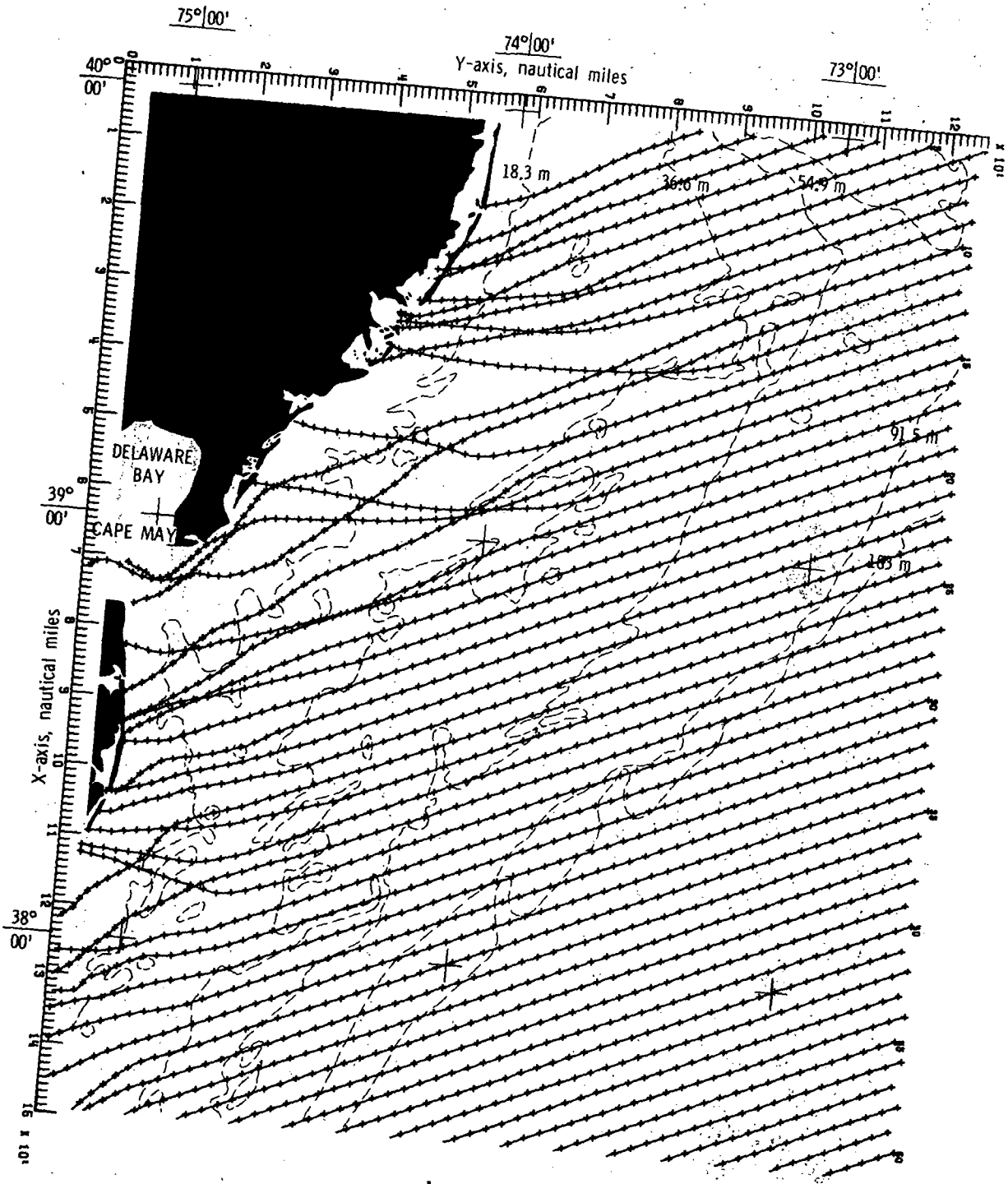


(b) Bottom topography approximated by cubic least squares technique.

Figure 19.- Continued.

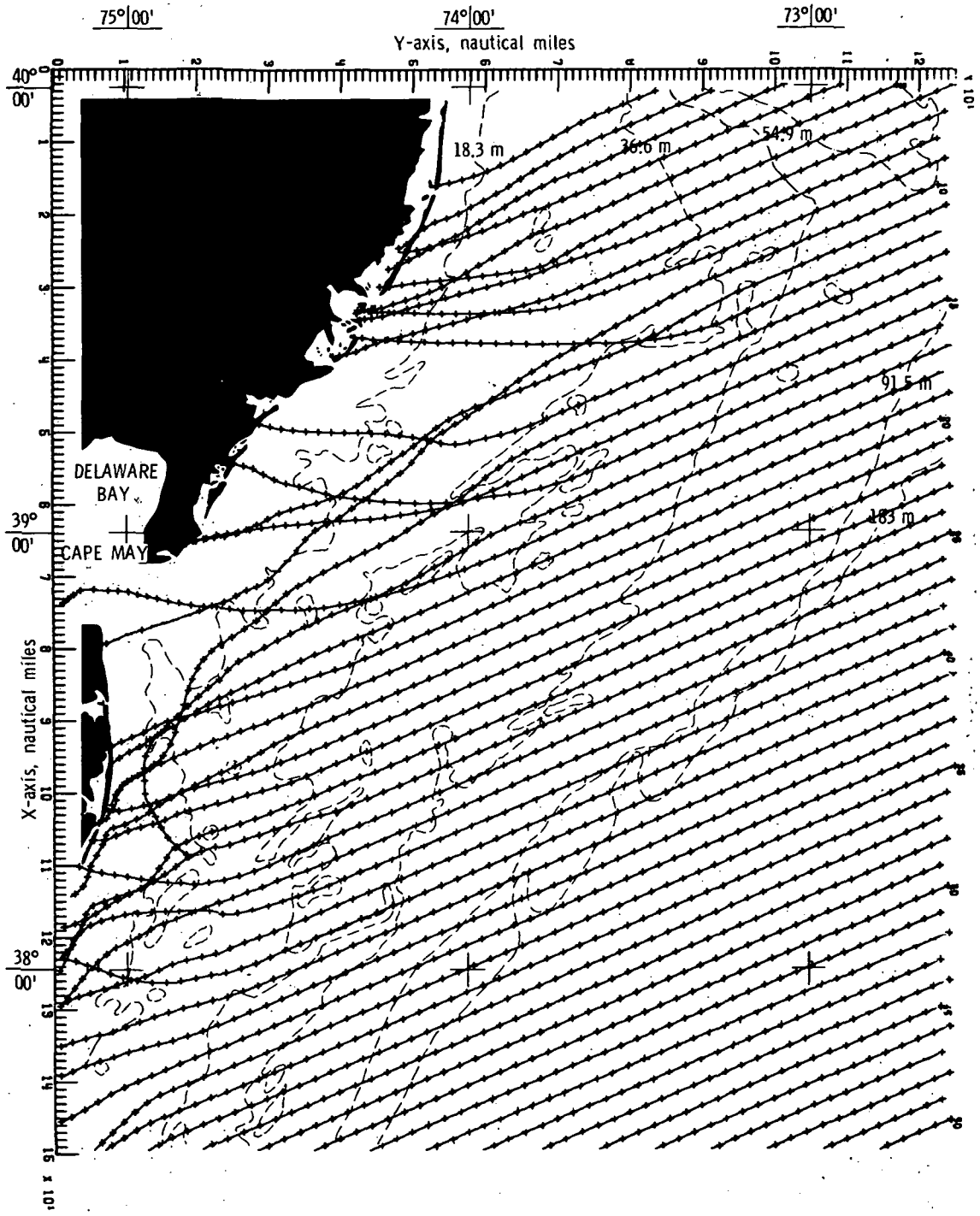


(c) Bottom topography approximated by constrained bicubic interpolation technique.

Figure 19.- Concluded.

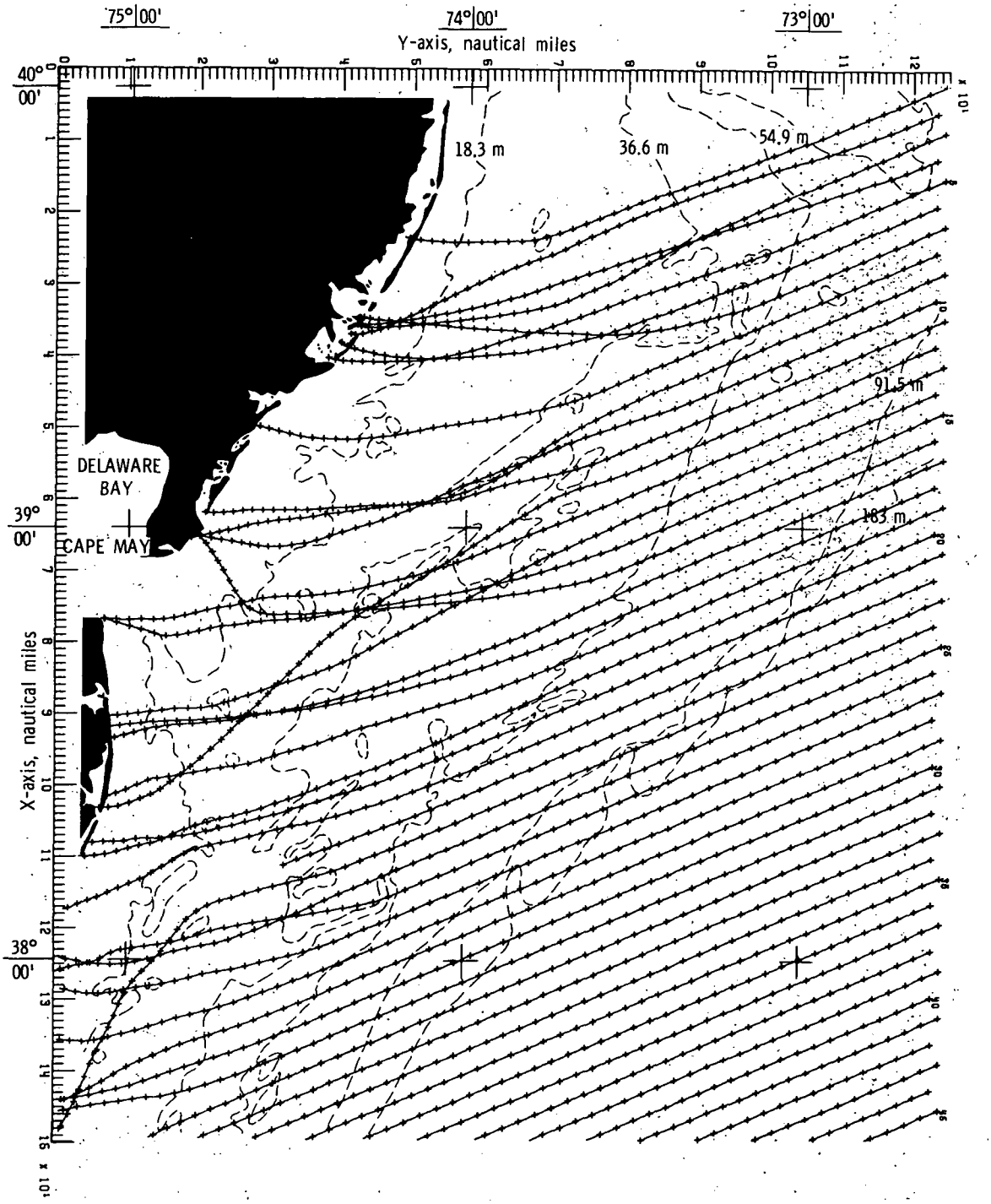


(a) Bottom topography approximated by quadratic least squares technique.

Figure 20.- Wave refraction diagrams. $\alpha = 67.5^{\circ}$; T = 12 seconds.

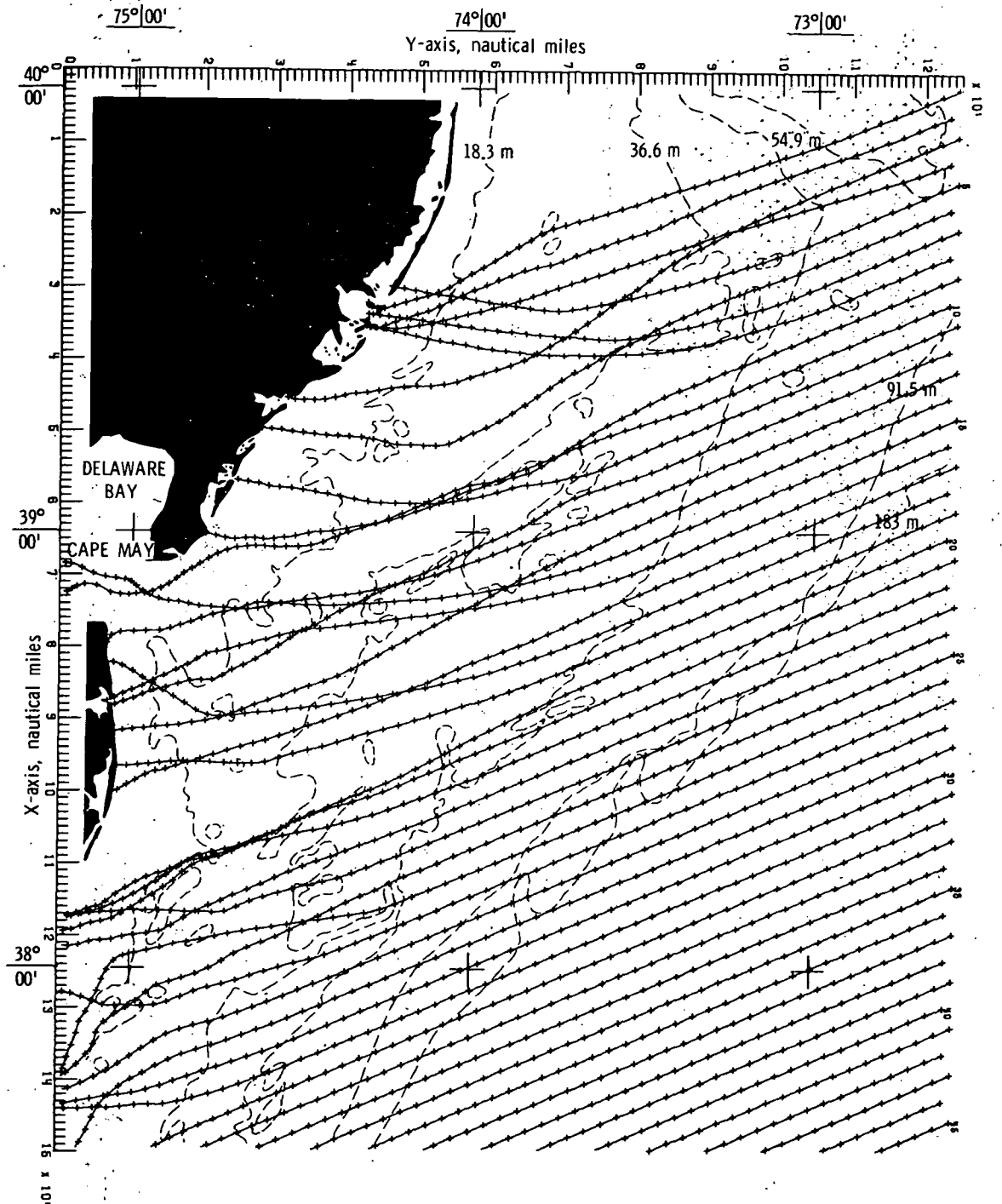


(b) Bottom topography approximated by cubic least squares technique.

Figure 20.- Continued.

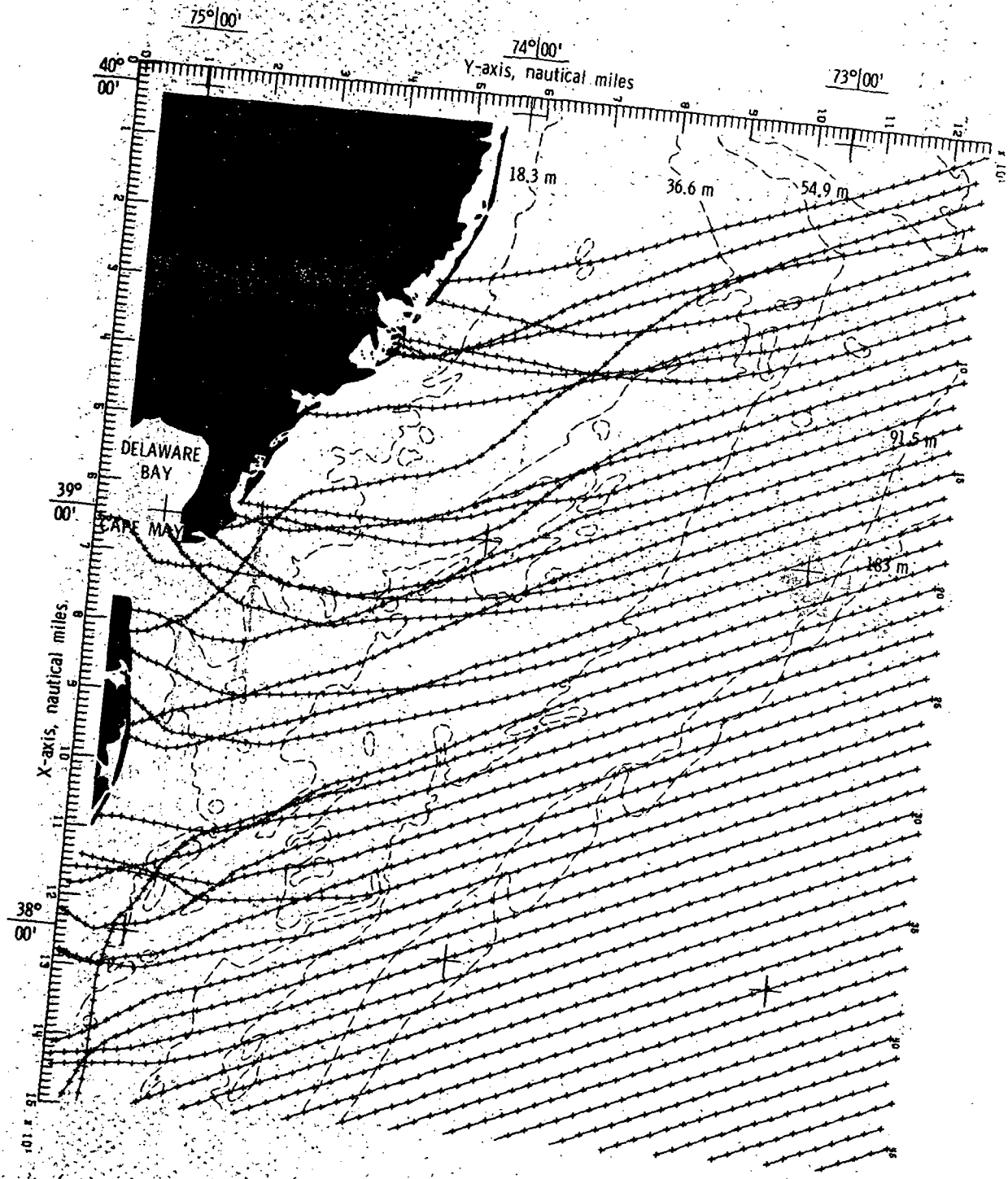


(c) Bottom topography approximated by constrained bicubic interpolation technique.

Figure 20.- Concluded.

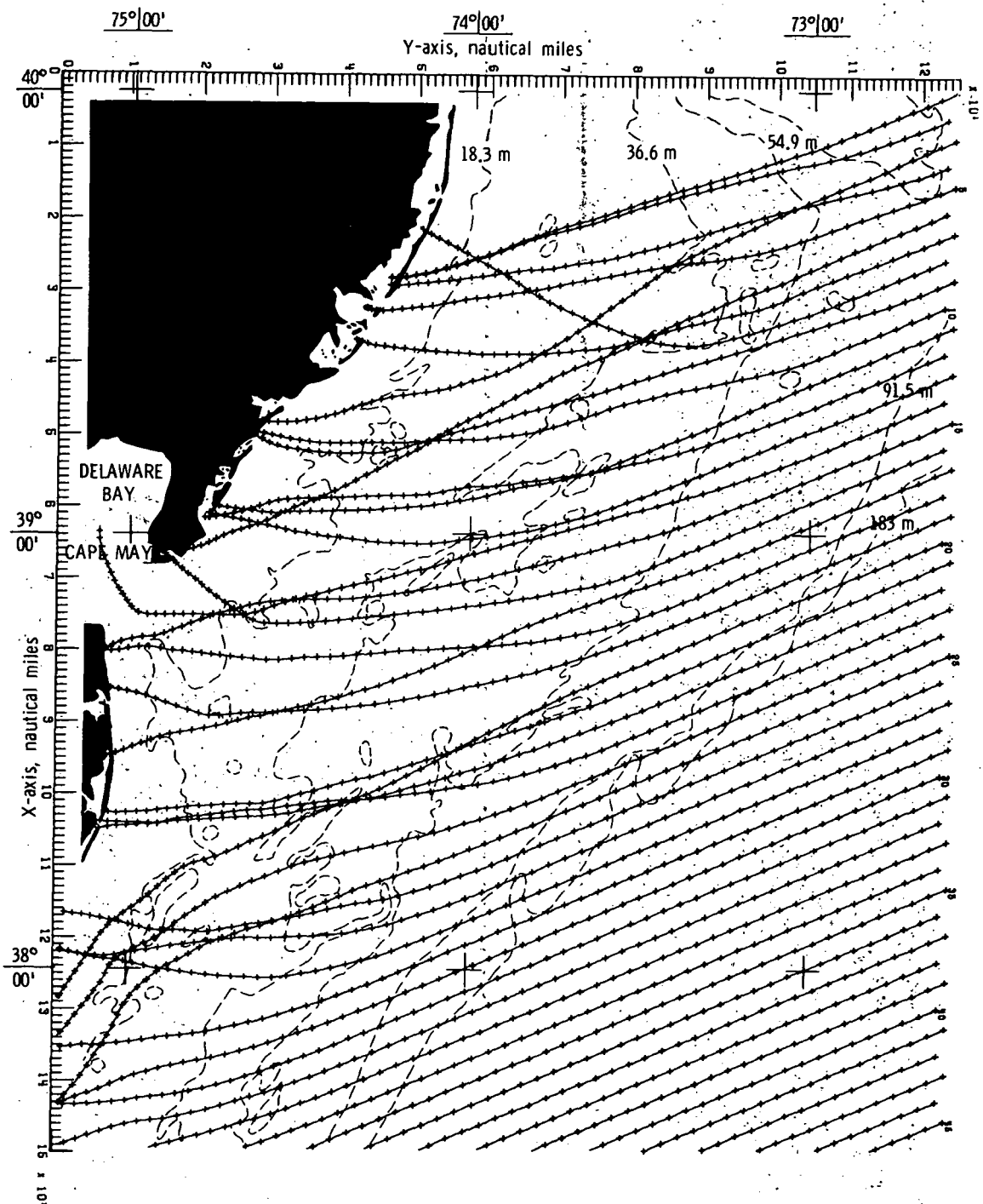


(a) Bottom topography approximated by quadratic least squares technique.

Figure 21.- Wave refraction diagrams. $\alpha = 67.5^{o}$; $T = 14$ seconds.

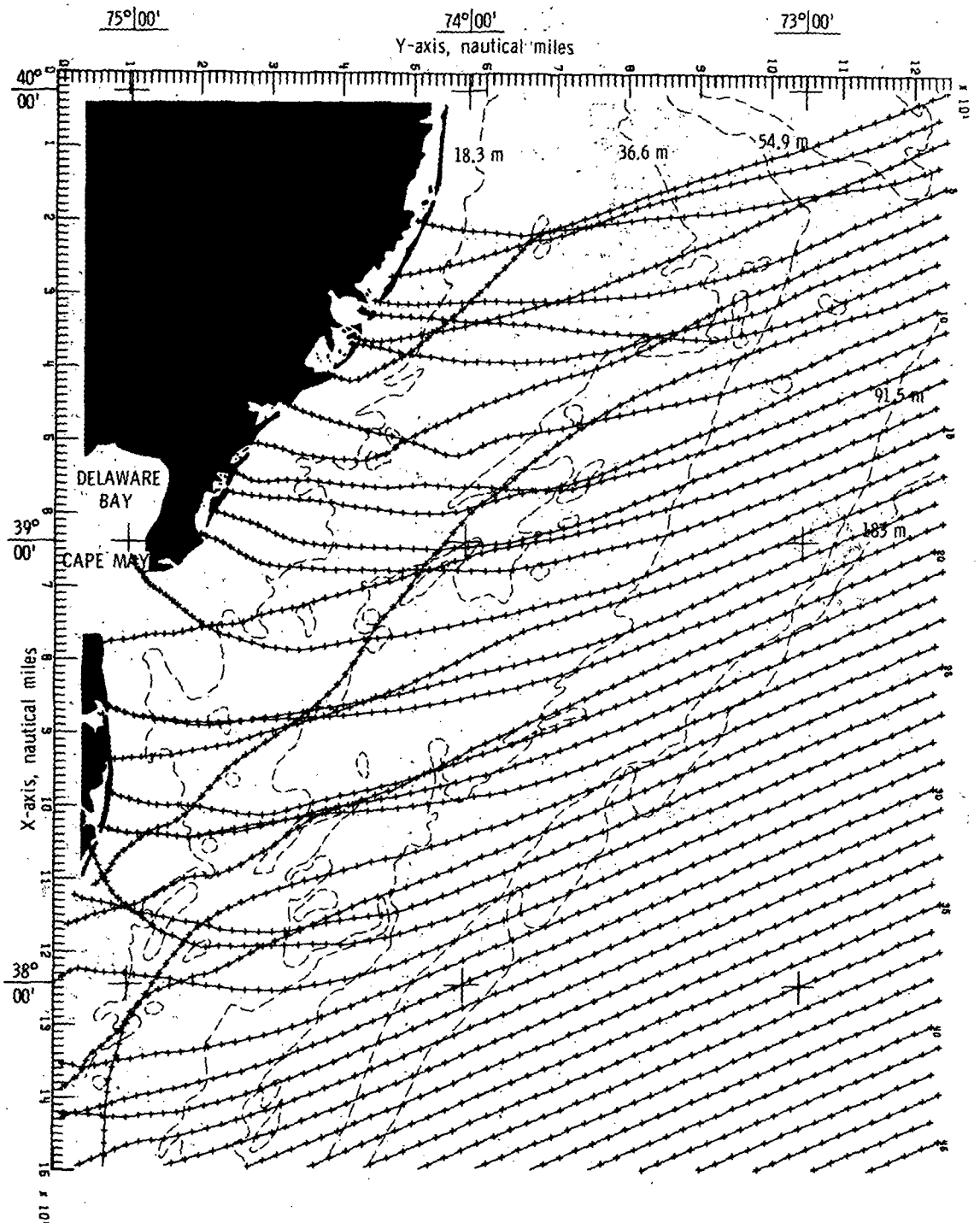


(b) Bottom topography approximated by cubic least squares technique.

Figure 21.- Continued.

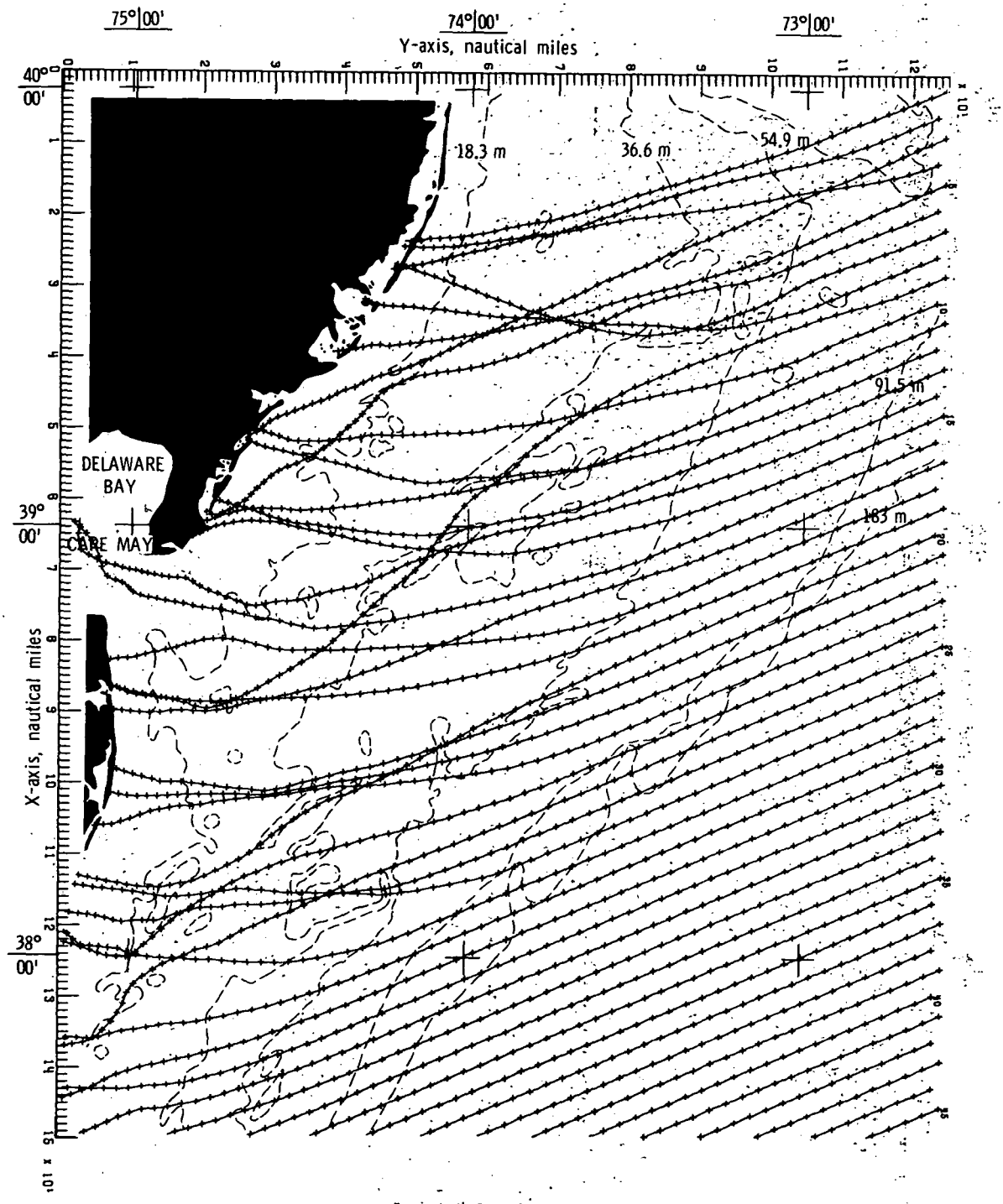


(c) Bottom topography approximated by constrained bicubic interpolation technique.

Figure 21.- Concluded.

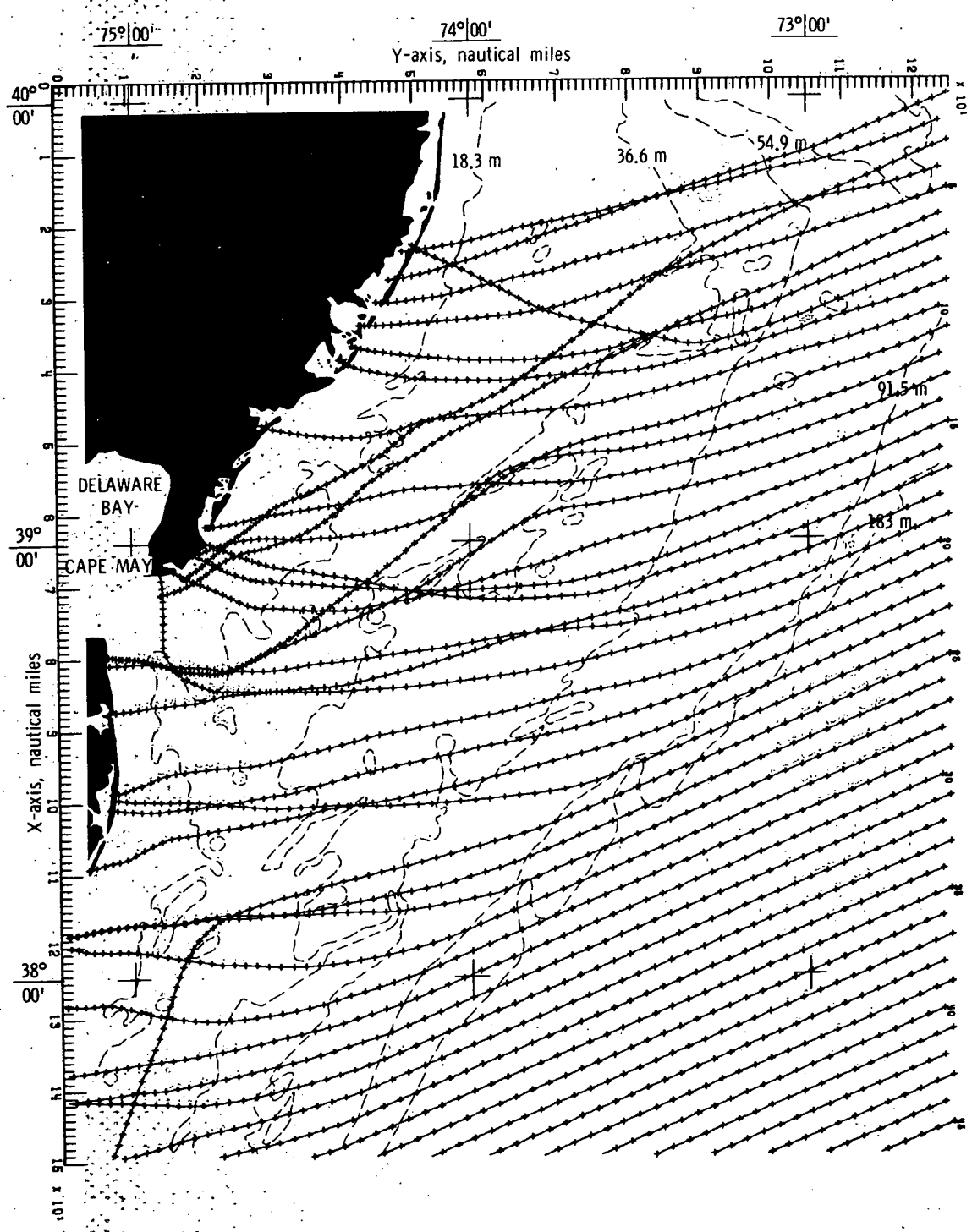


(a) Bottom topography approximated by quadratic least squares technique.

Figure 22.- Wave refraction diagrams. $\alpha = 67.5^{o}$; T = 16 seconds.

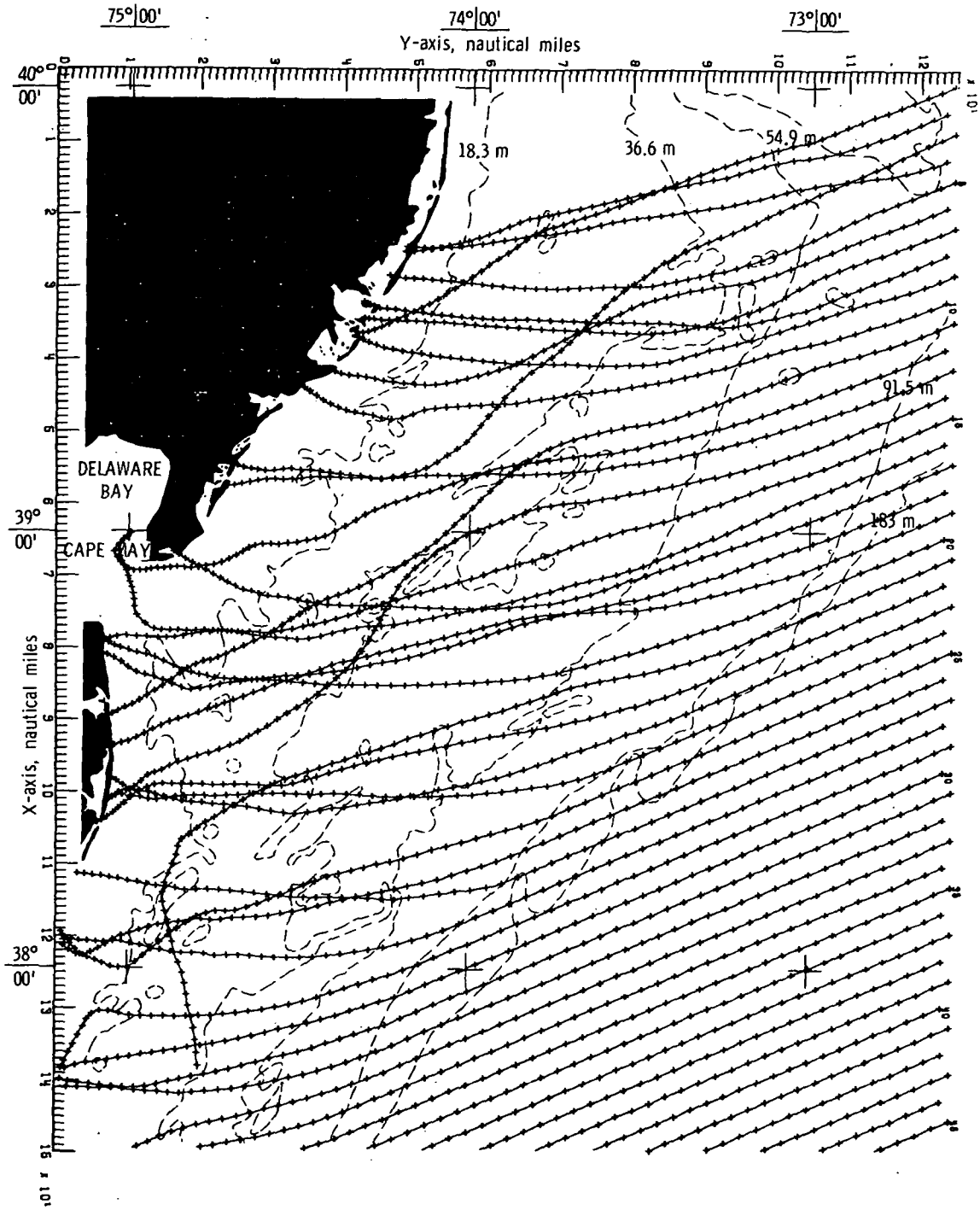


(b) Bottom topography approximated by cubic least squares technique.

Figure 22.- Continued.

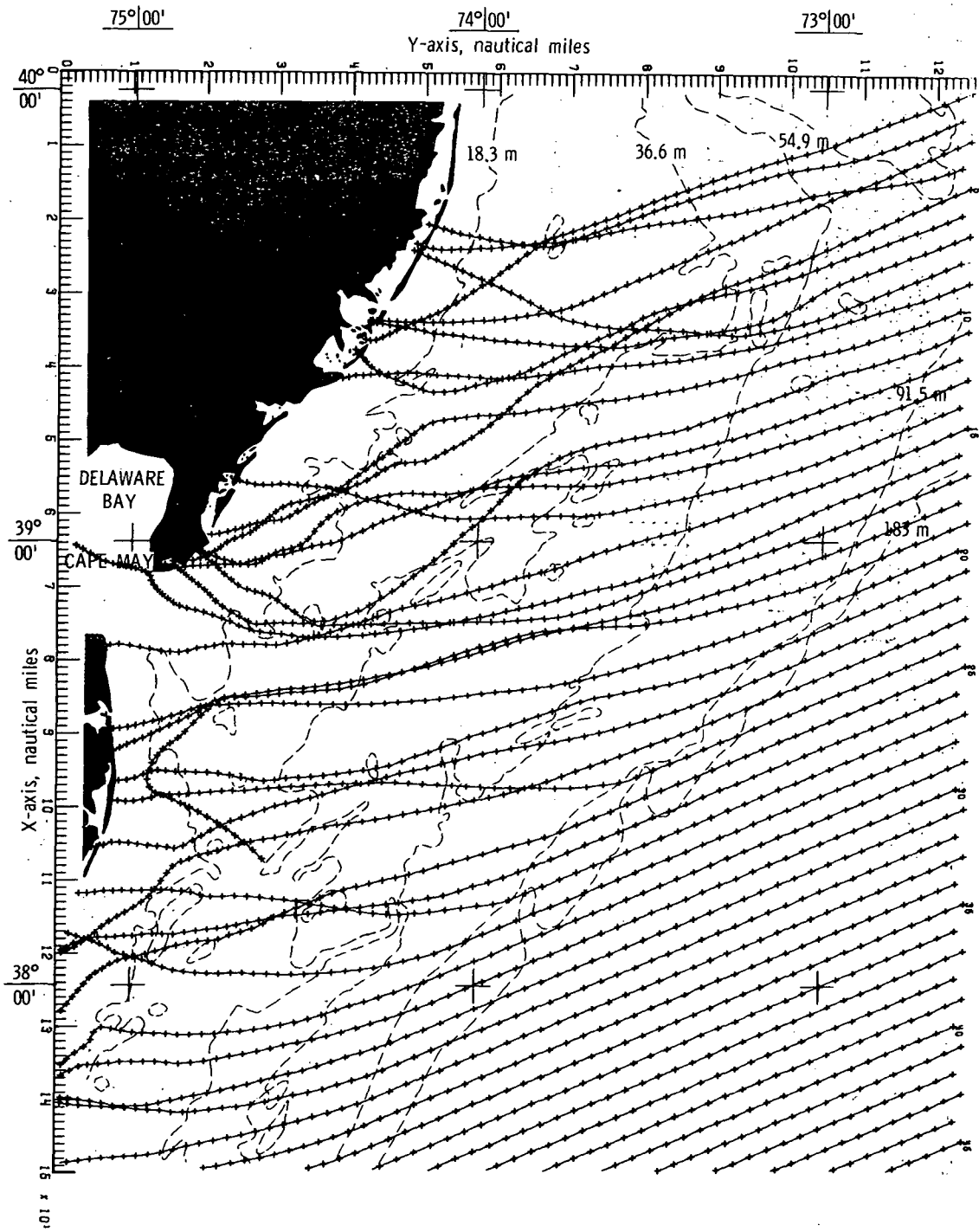


(c) Bottom topography approximated by constrained bicubic interpolation technique.

Figure 22.- Concluded.

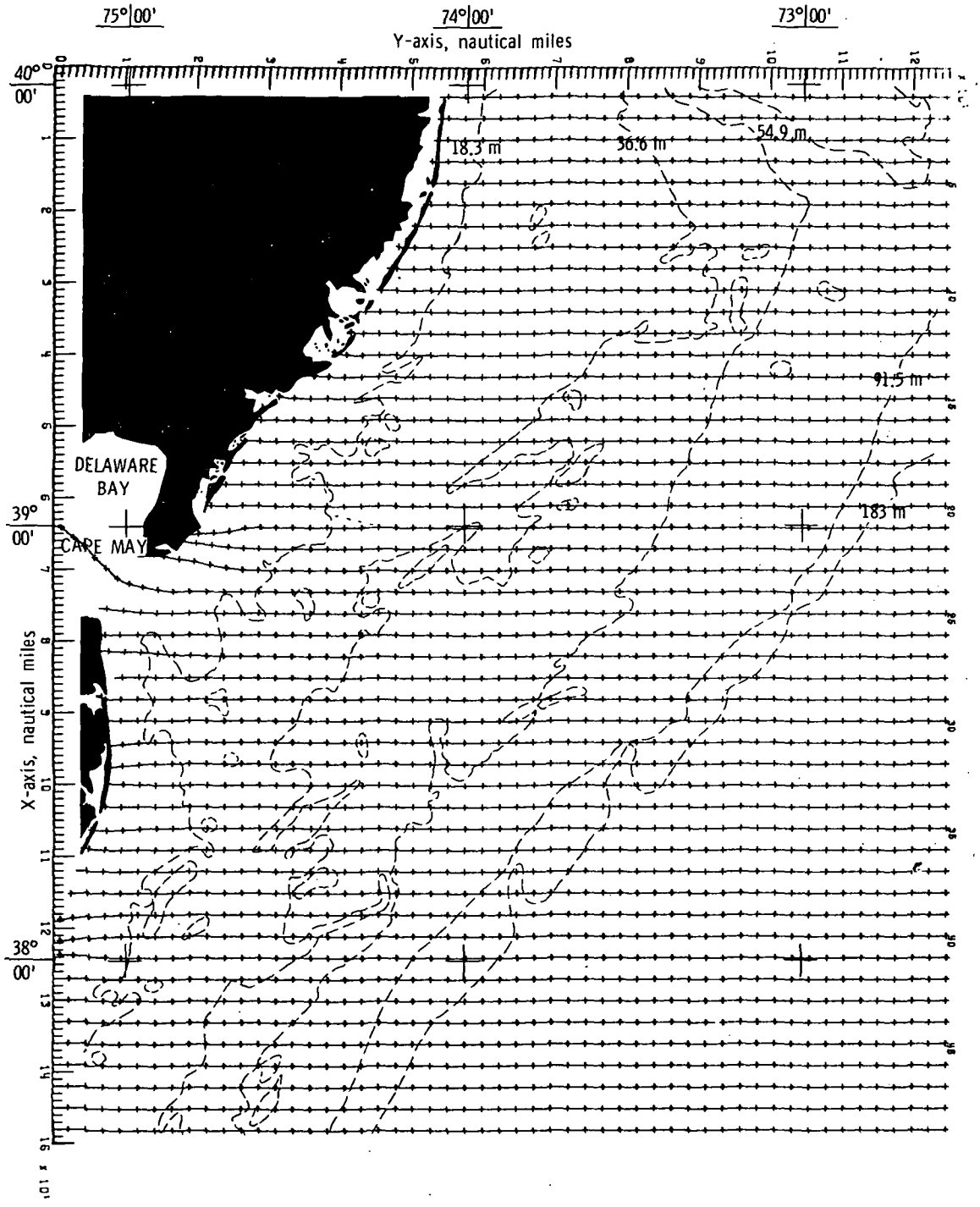


(a) Bottom topography approximated by quadratic least squares technique.

Figure 23.- Wave refraction diagrams. $\alpha = 90^{o}$; T = 6 seconds.

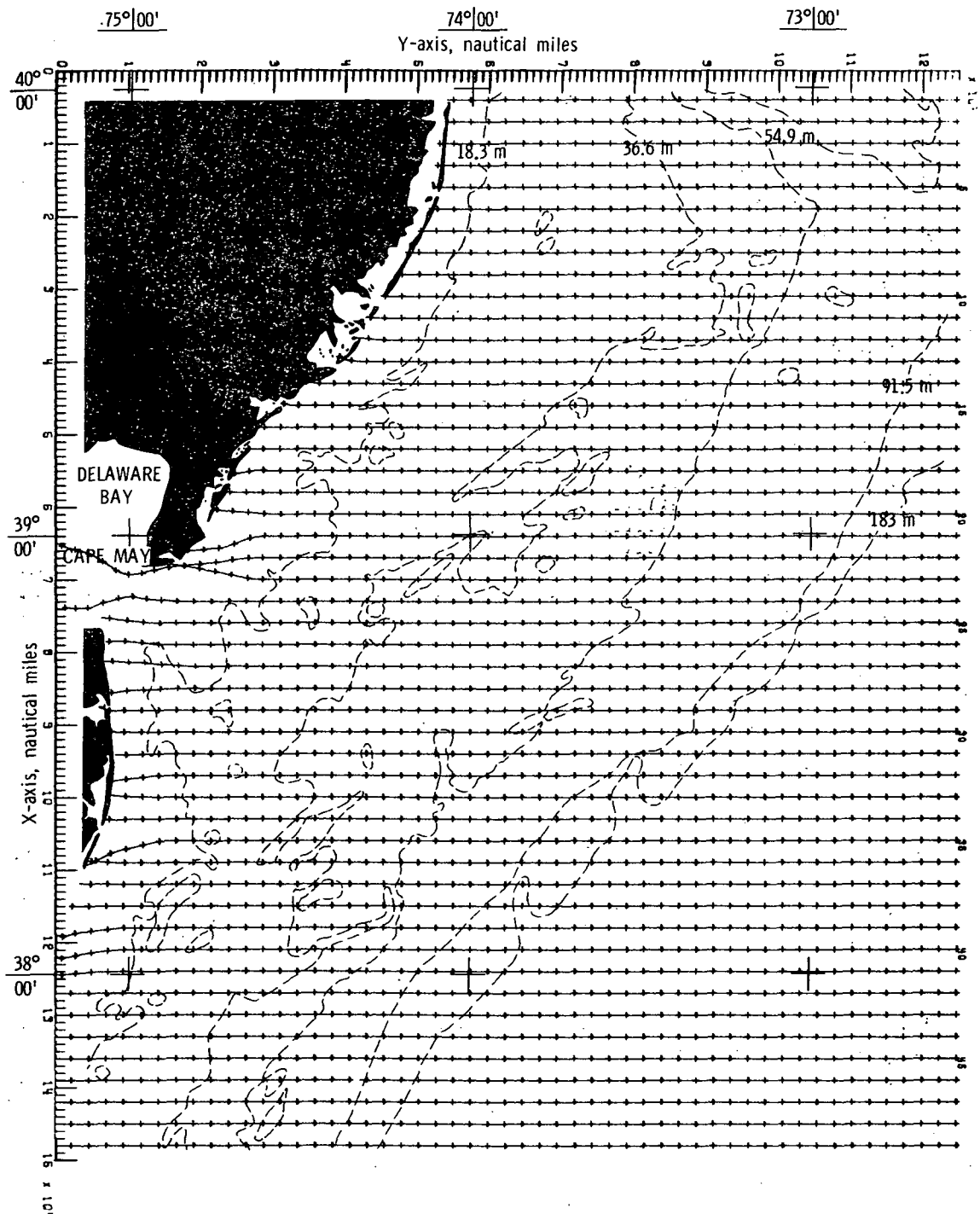


(b) Bottom topography approximated by cubic least squares technique.

Figure 23.- Continued.

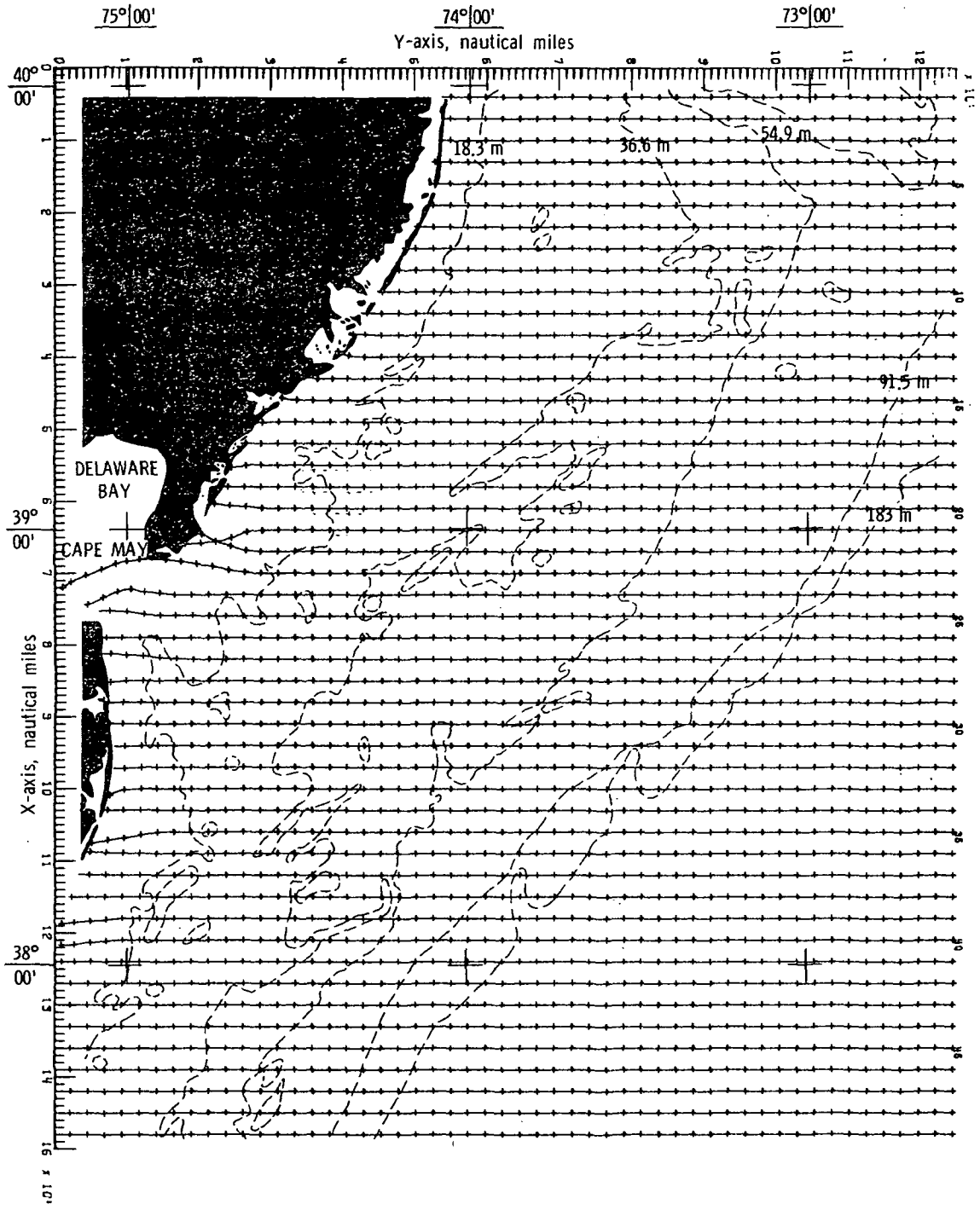


(c) Bottom topography approximated by constrained bicubic interpolation technique.

Figure 23.- Concluded.

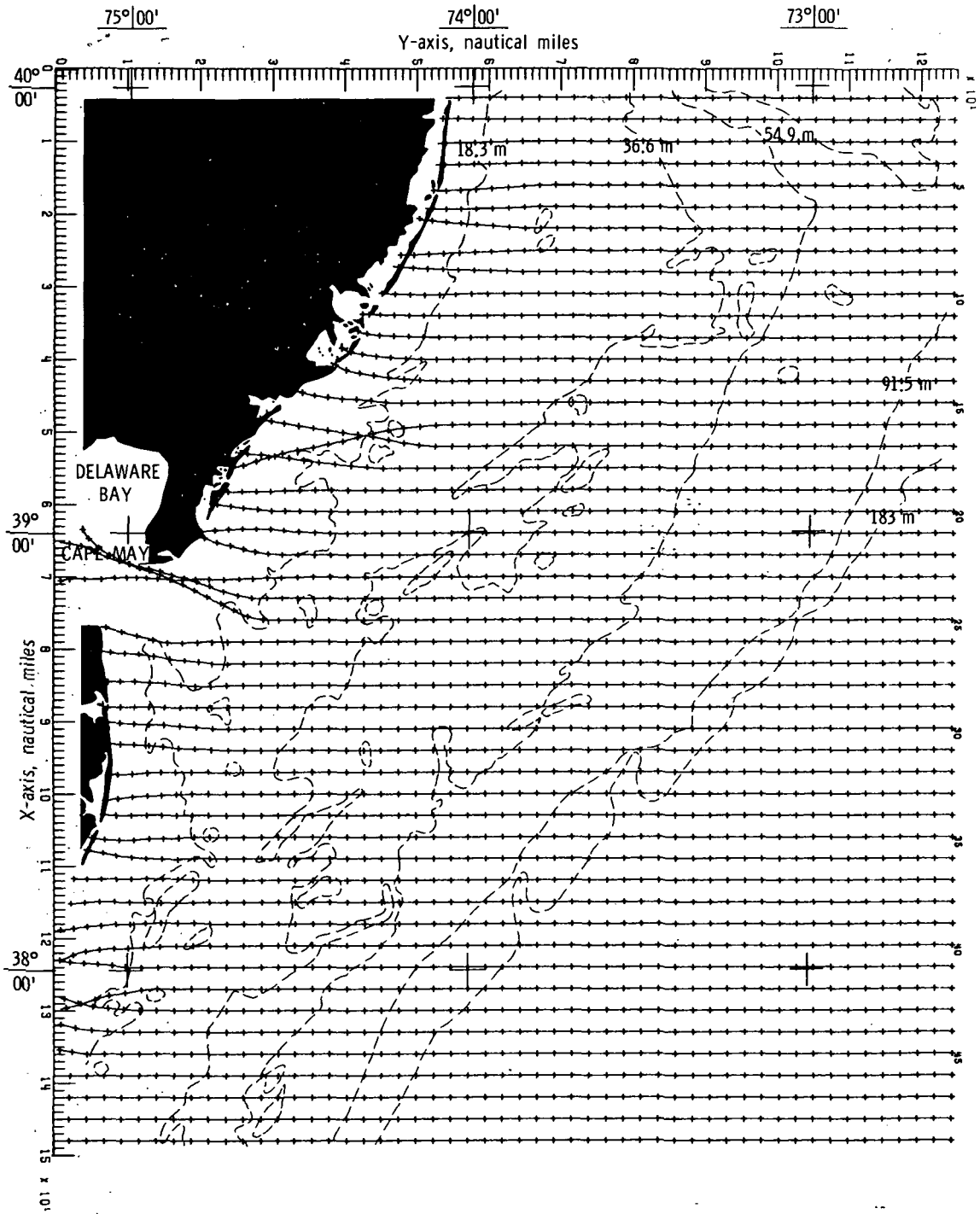


(a) Bottom topography approximated by quadratic least squares technique.

Figure 24.- Wave refraction diagrams. $\alpha = 90^{o}$; T = 8 seconds.

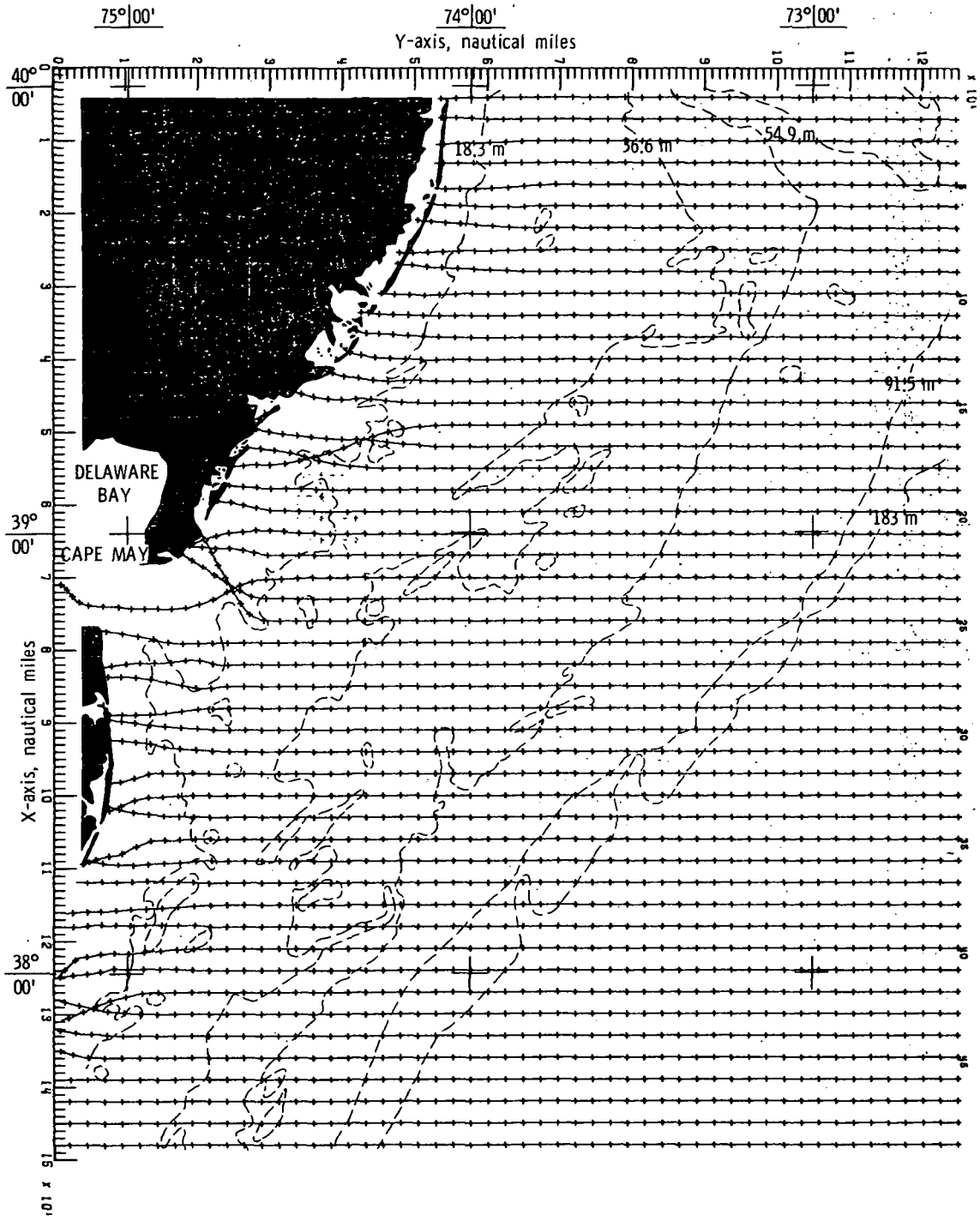


(b) Bottom topography approximated by cubic least squares technique.

Figure 24.- Continued.

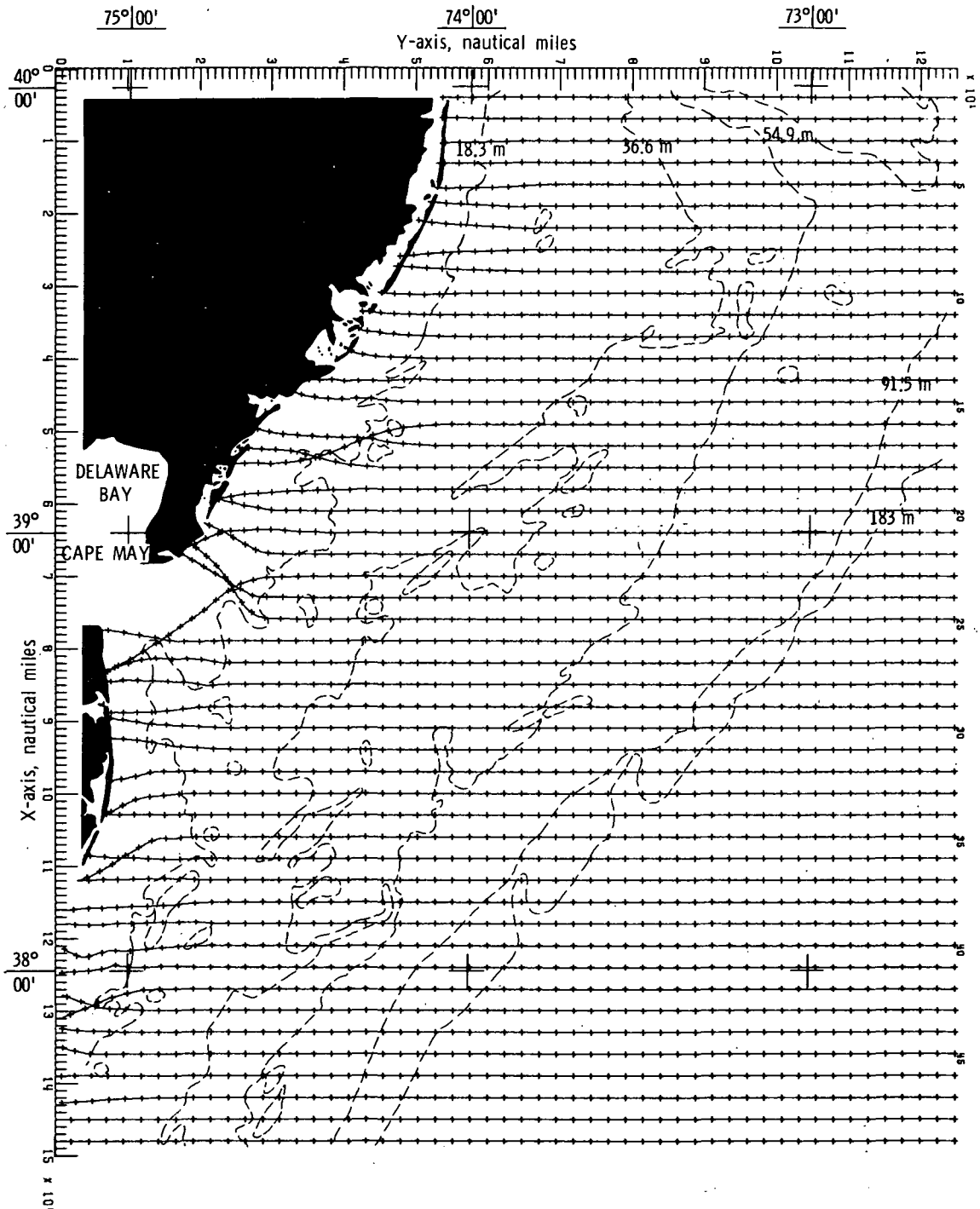


(c) Bottom topography approximated by constrained bicubic interpolation technique.

Figure 24.- Concluded.

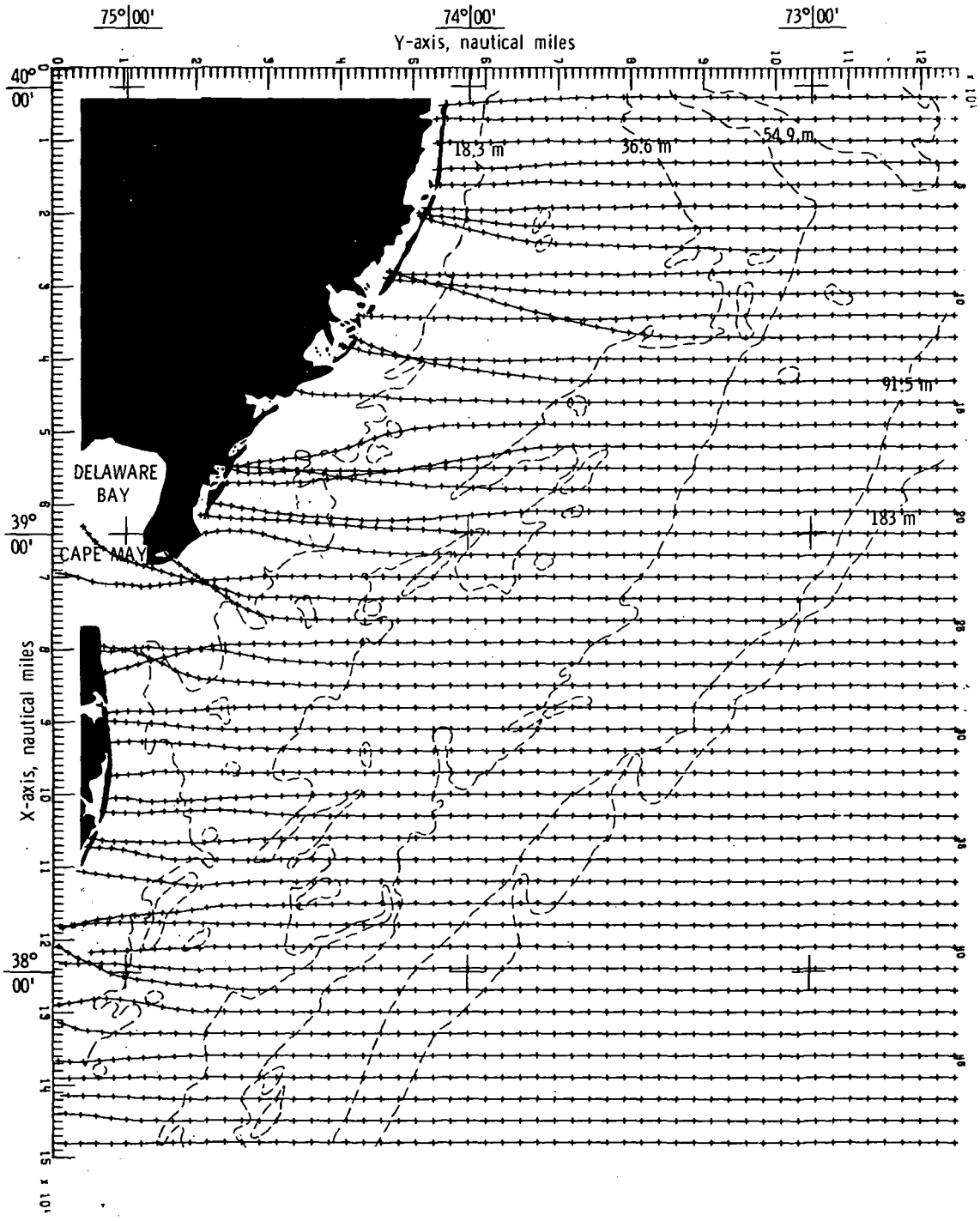


(a) Bottom topography approximated by quadratic least squares technique.

Figure 25.- Wave refraction diagrams. $\alpha = 90^{o}$; T = 10 seconds.

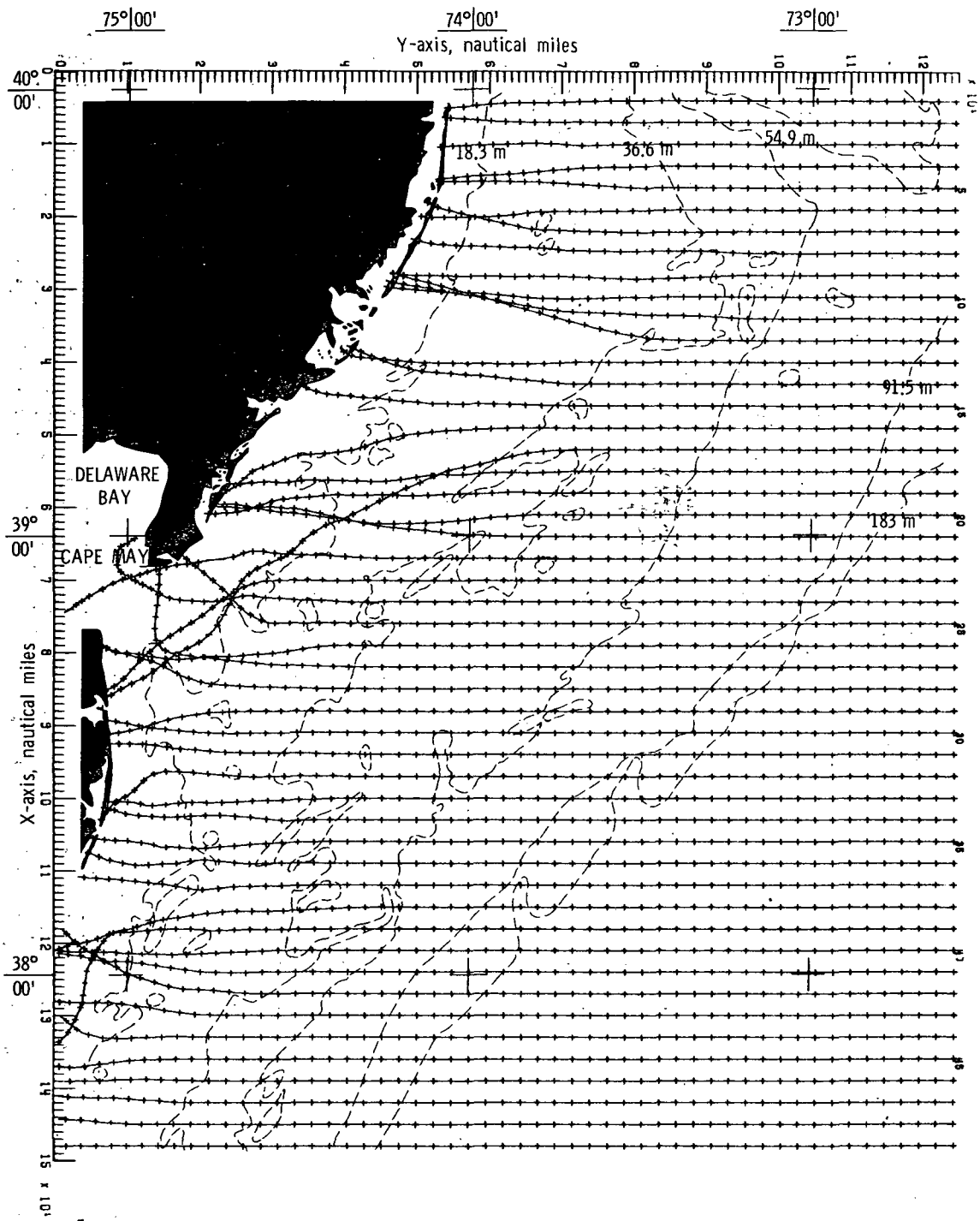


(b) Bottom topography approximated by cubic least squares technique.

Figure 25.- Continued.

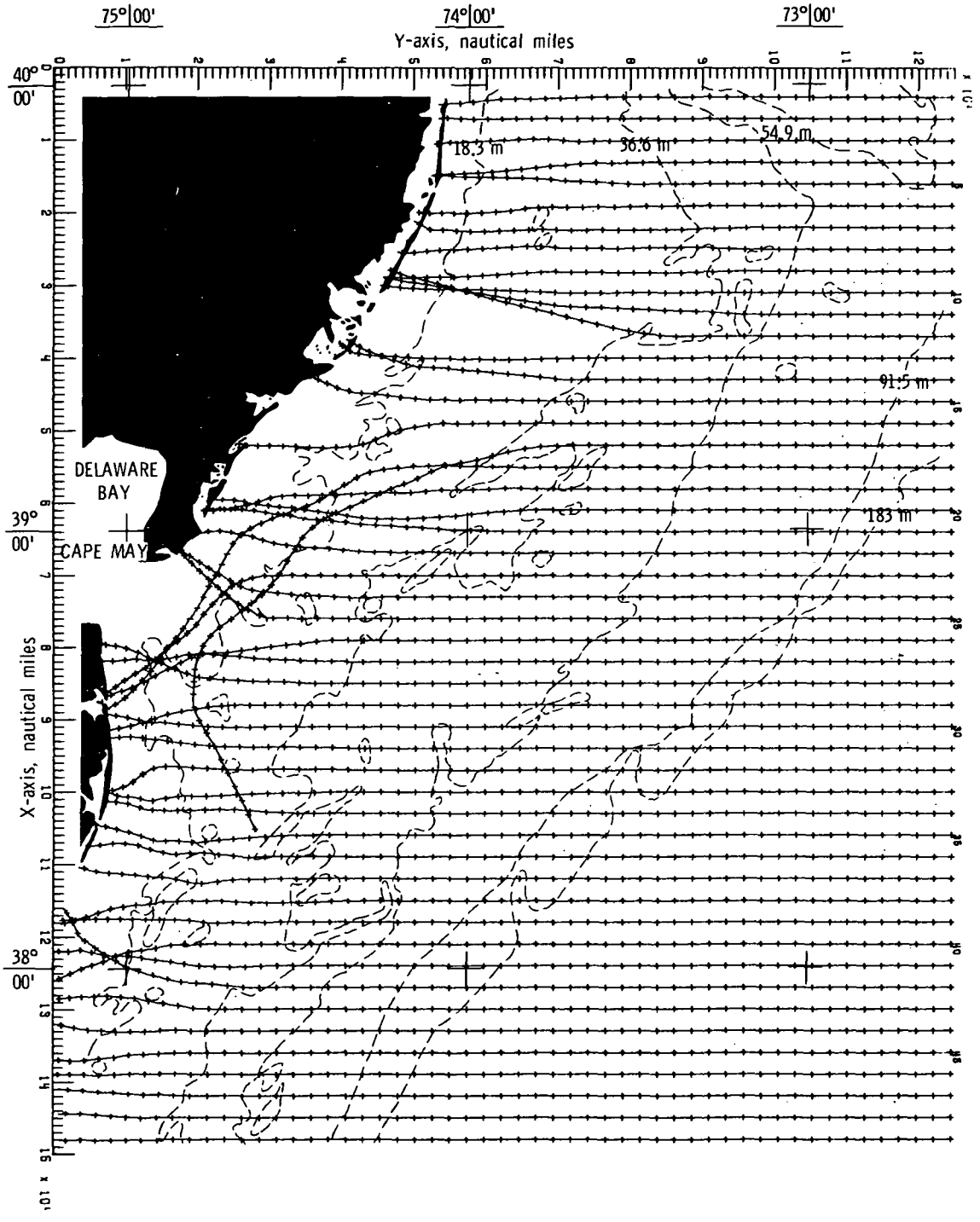


(c) Bottom topography approximated by constrained bicubic interpolation technique.

Figure 25.- Concluded.

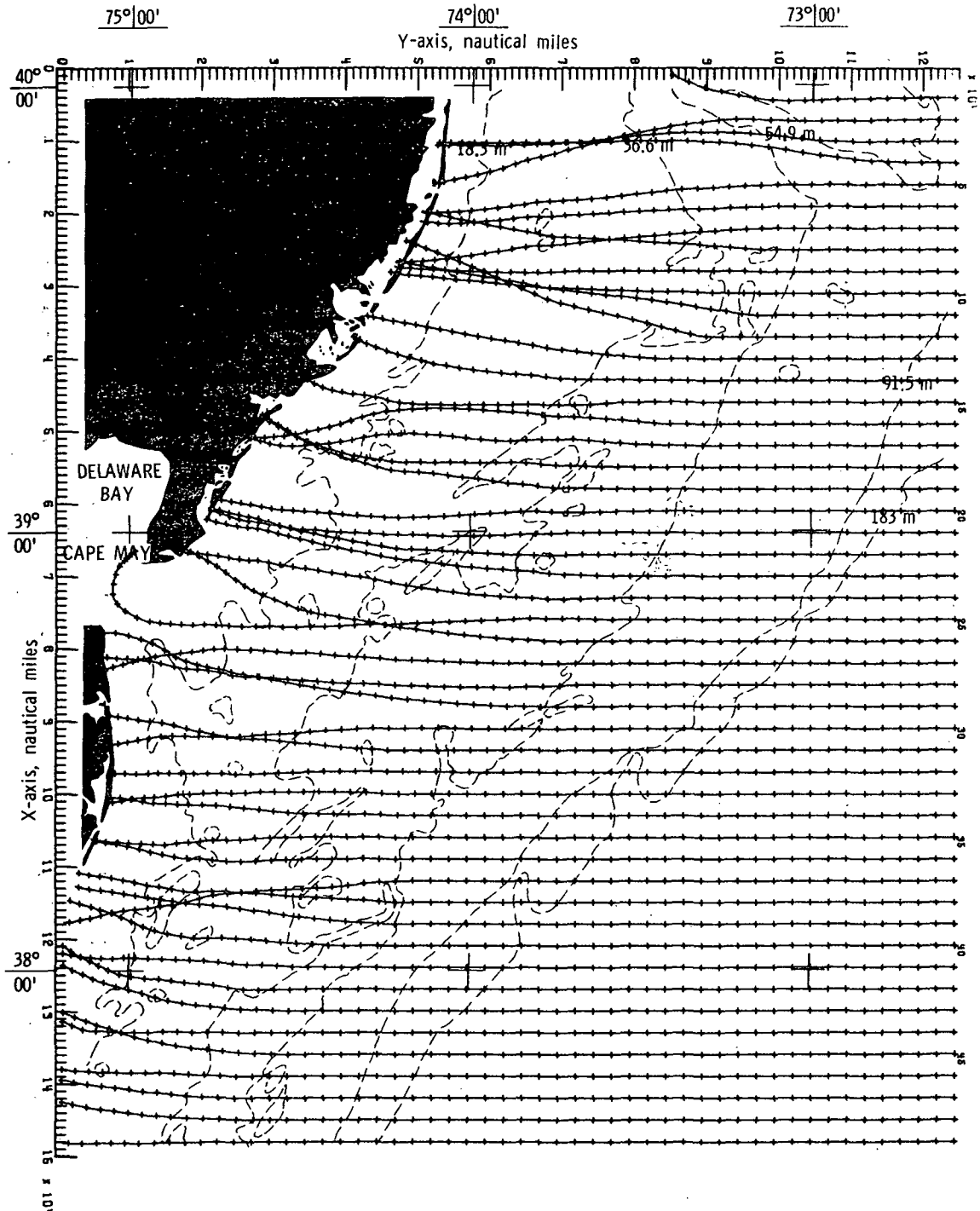


(a) Bottom topography approximated by quadratic least squares technique.

Figure 26.- Wave refraction diagrams. $\alpha = 90^{\circ}$; T = 12 seconds.

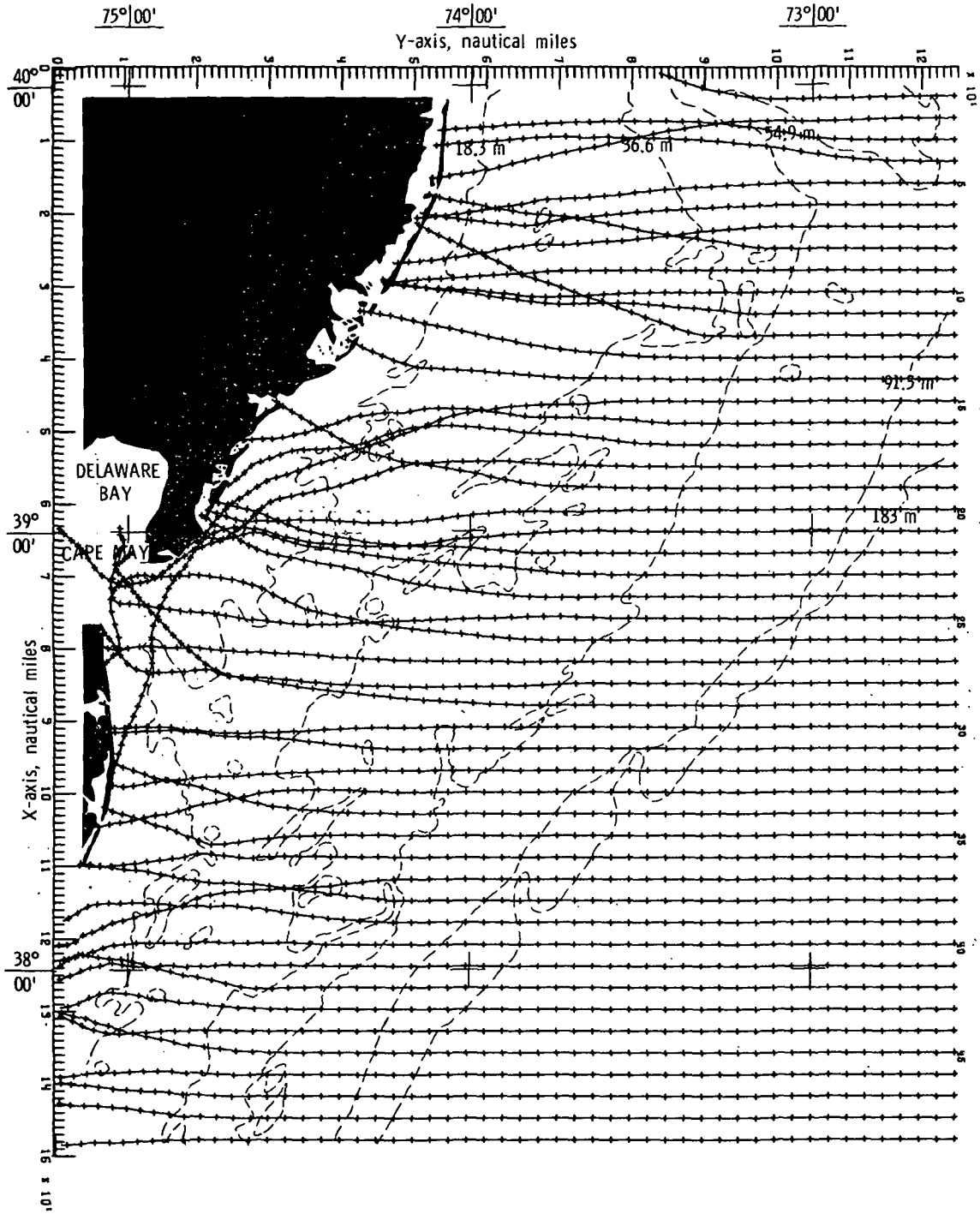


(b) Bottom topography approximated by cubic least squares technique.

Figure 26.- Continued.

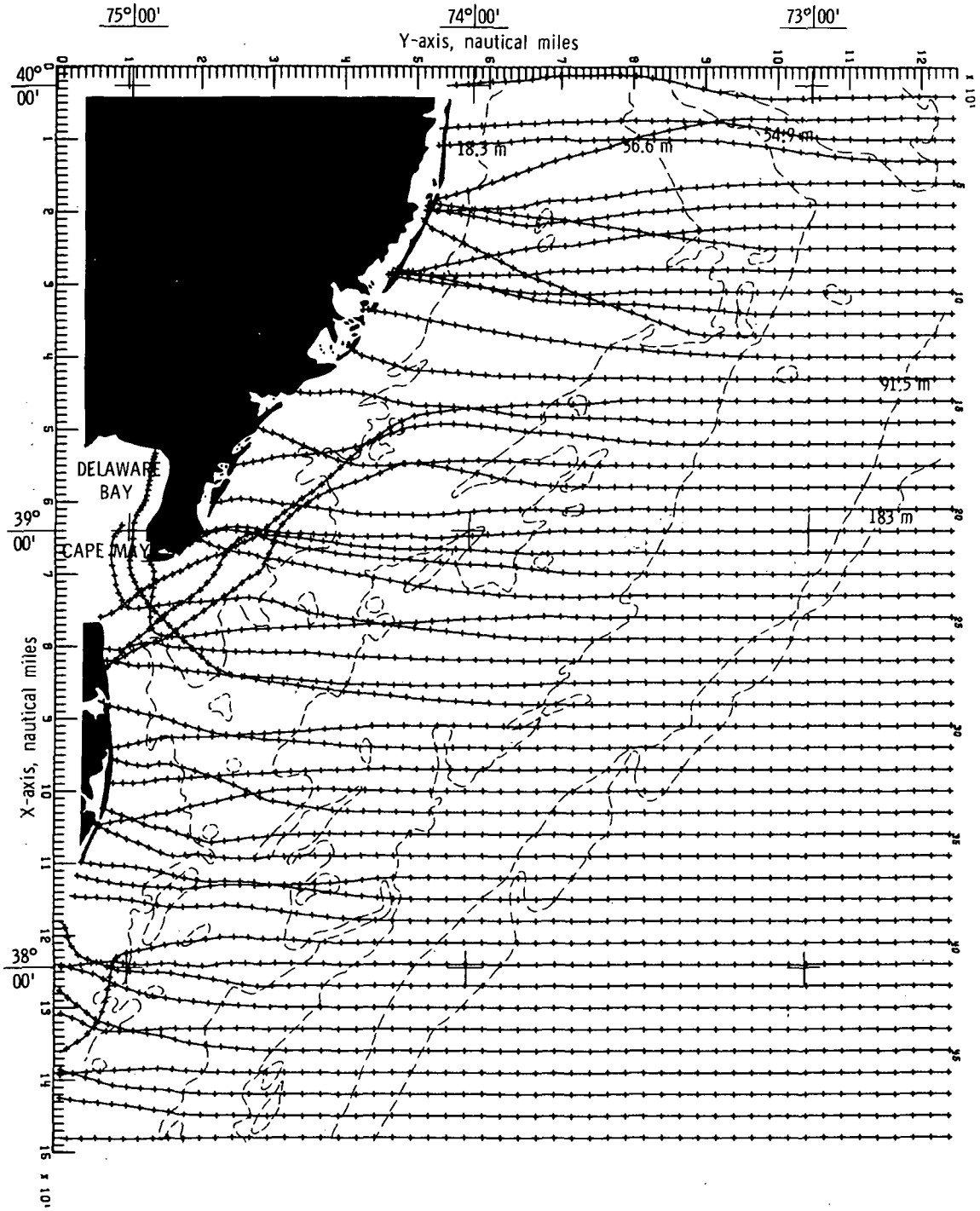


(c) Bottom topography approximated by constrained bicubic interpolation technique.

Figure 26.- Concluded.

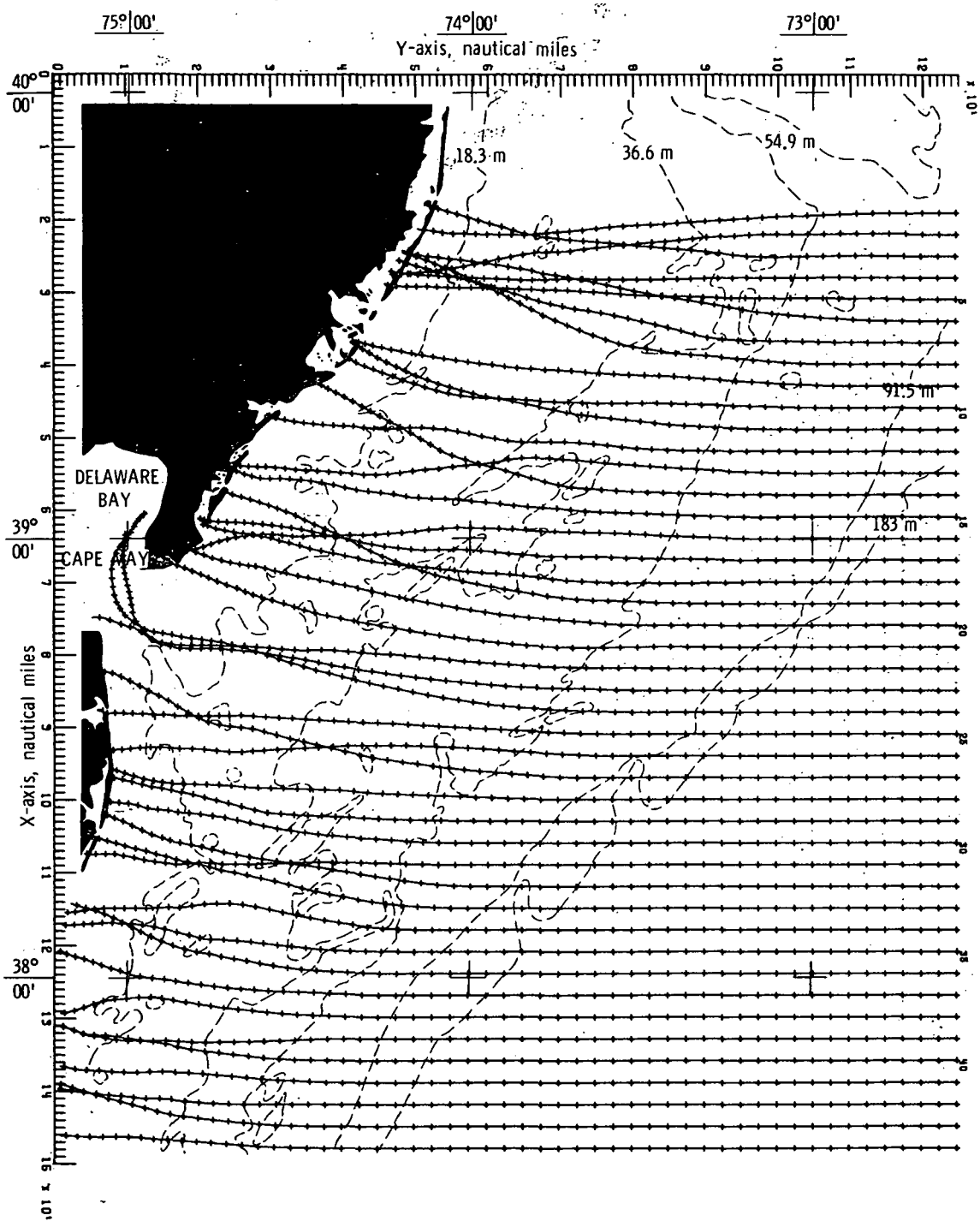


(a) Bottom topography approximated by quadratic least squares technique.

Figure 27.- Wave refraction diagrams. $\alpha = 90^{o}$; T = 14 seconds.

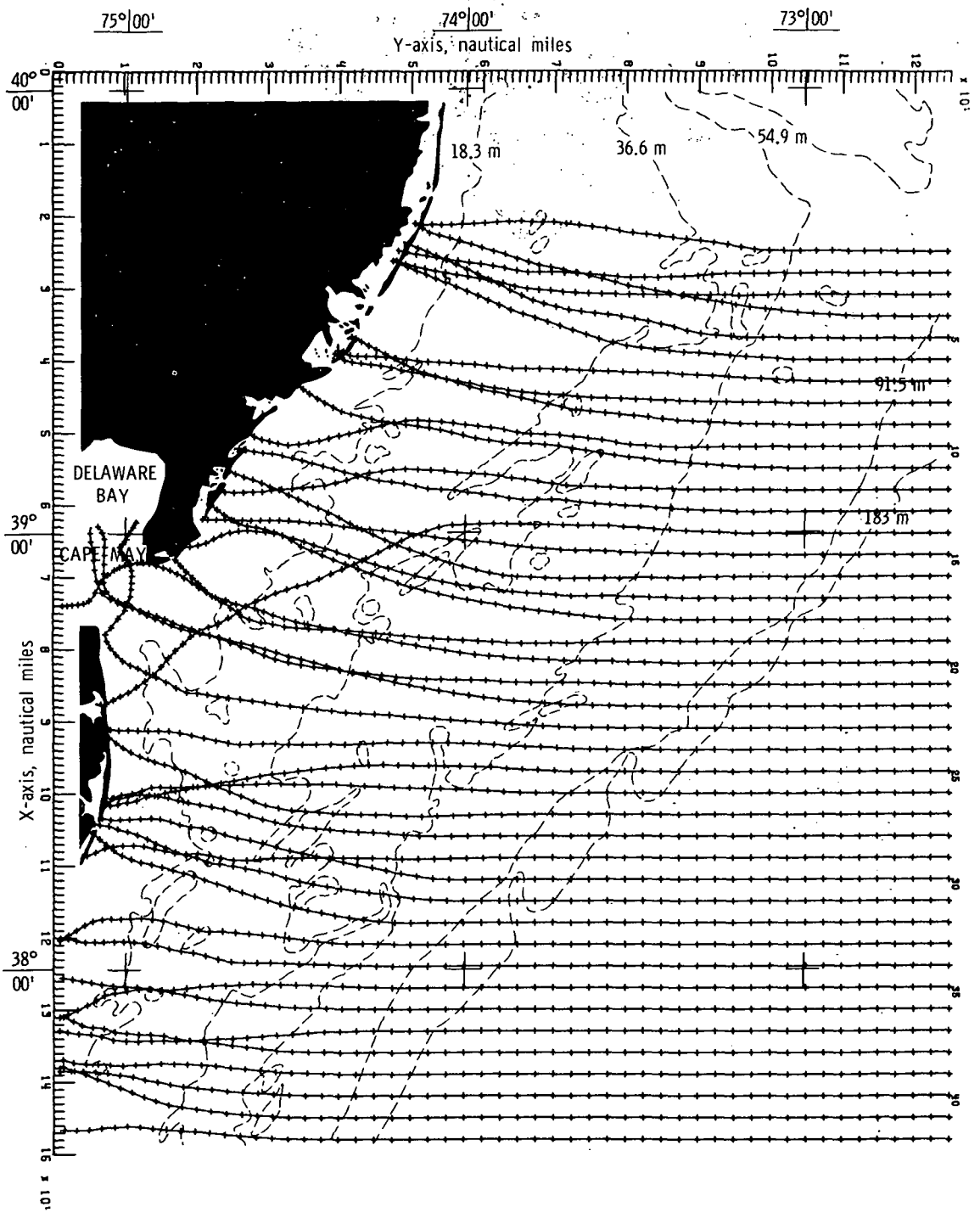


(b) Bottom topography approximated by cubic least squares technique.

Figure 27.- Continued.

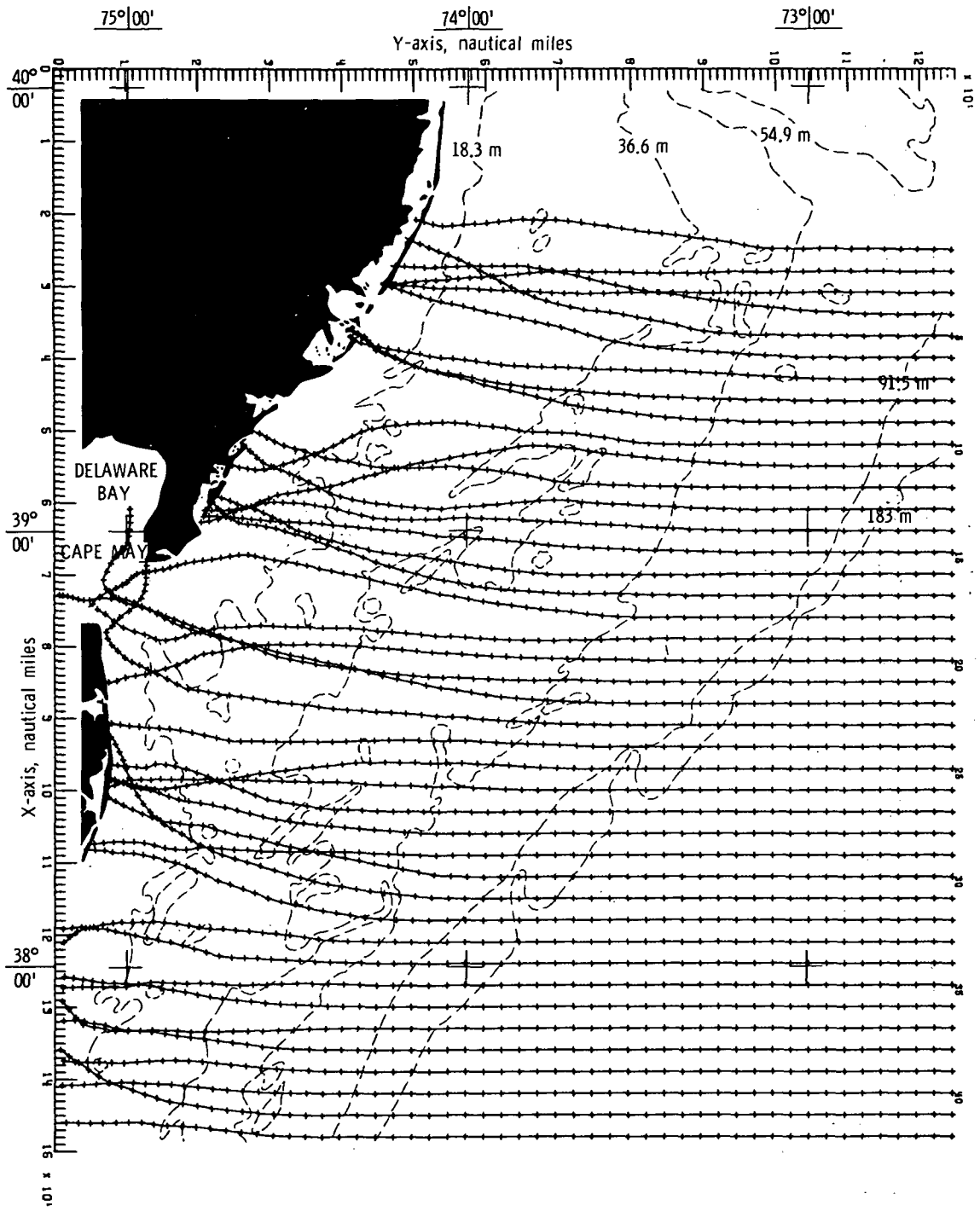


(c) Bottom topography approximated by constrained bicubic interpolation technique.

Figure 27.- Concluded.

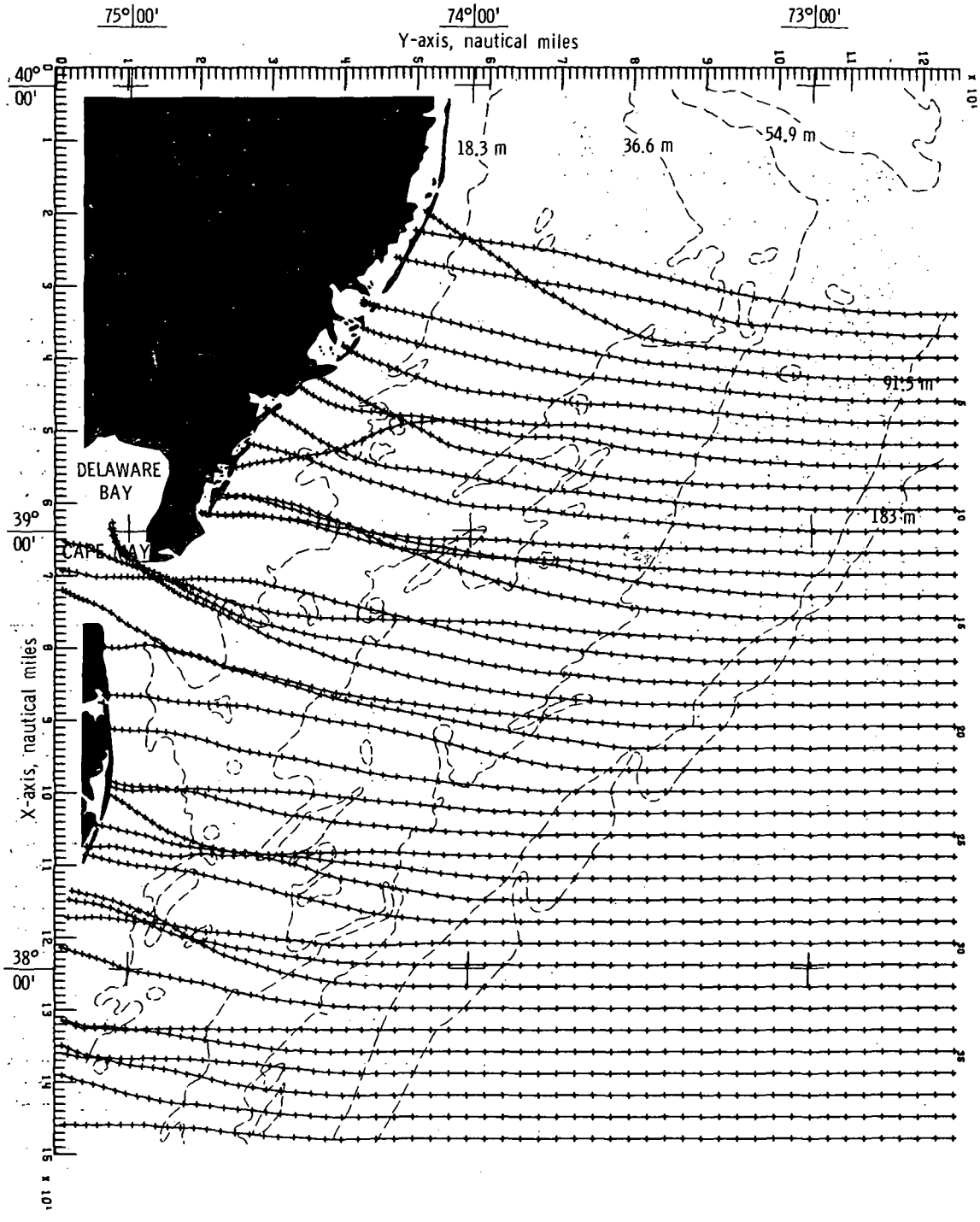


(a) Bottom topography approximated by quadratic least squares technique.

Figure 28.- Wave refraction diagrams. $\alpha = 90^{o}$; T = 16 seconds.

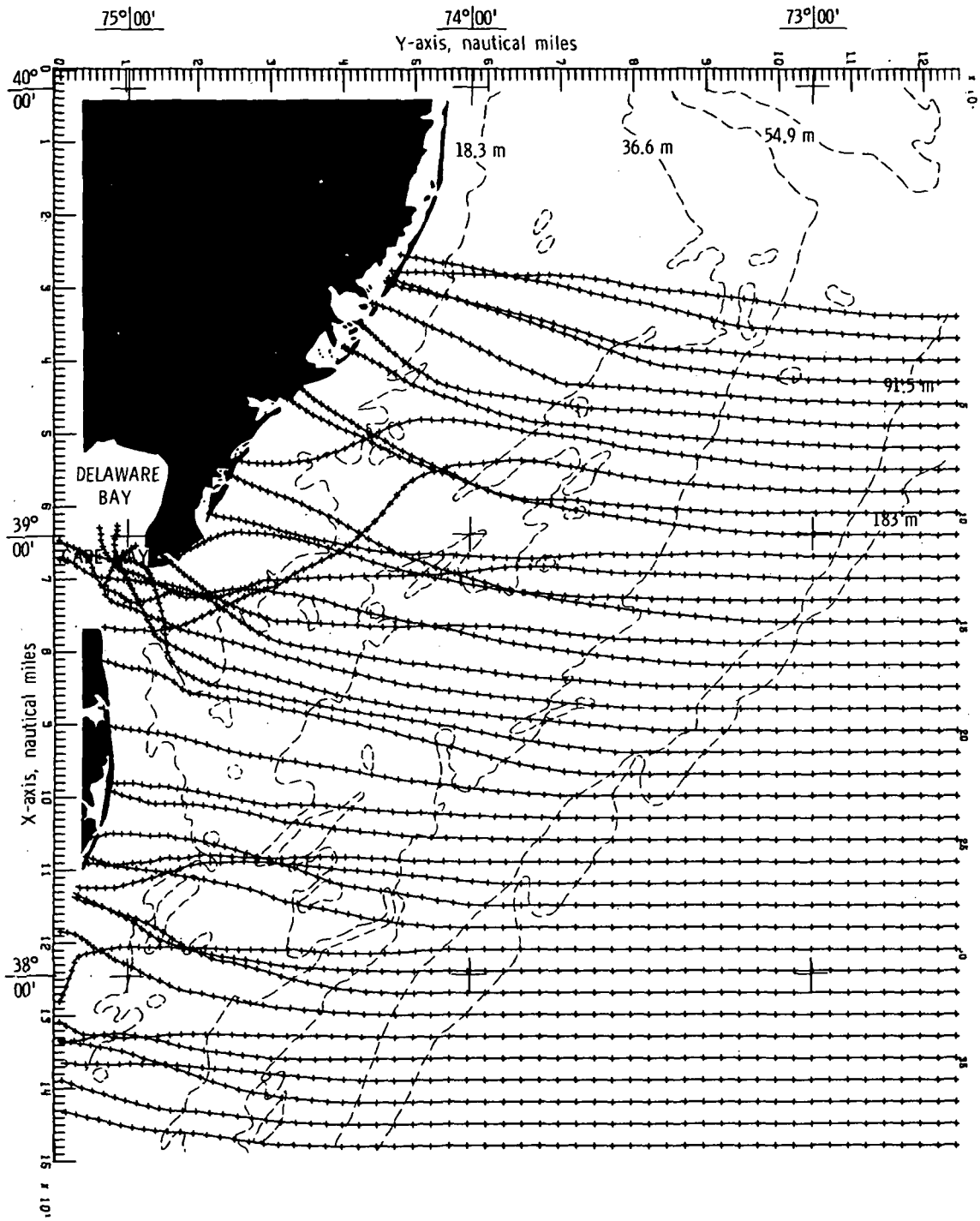


(b) Bottom topography approximated by cubic least squares technique.

Figure 28.- Continued.

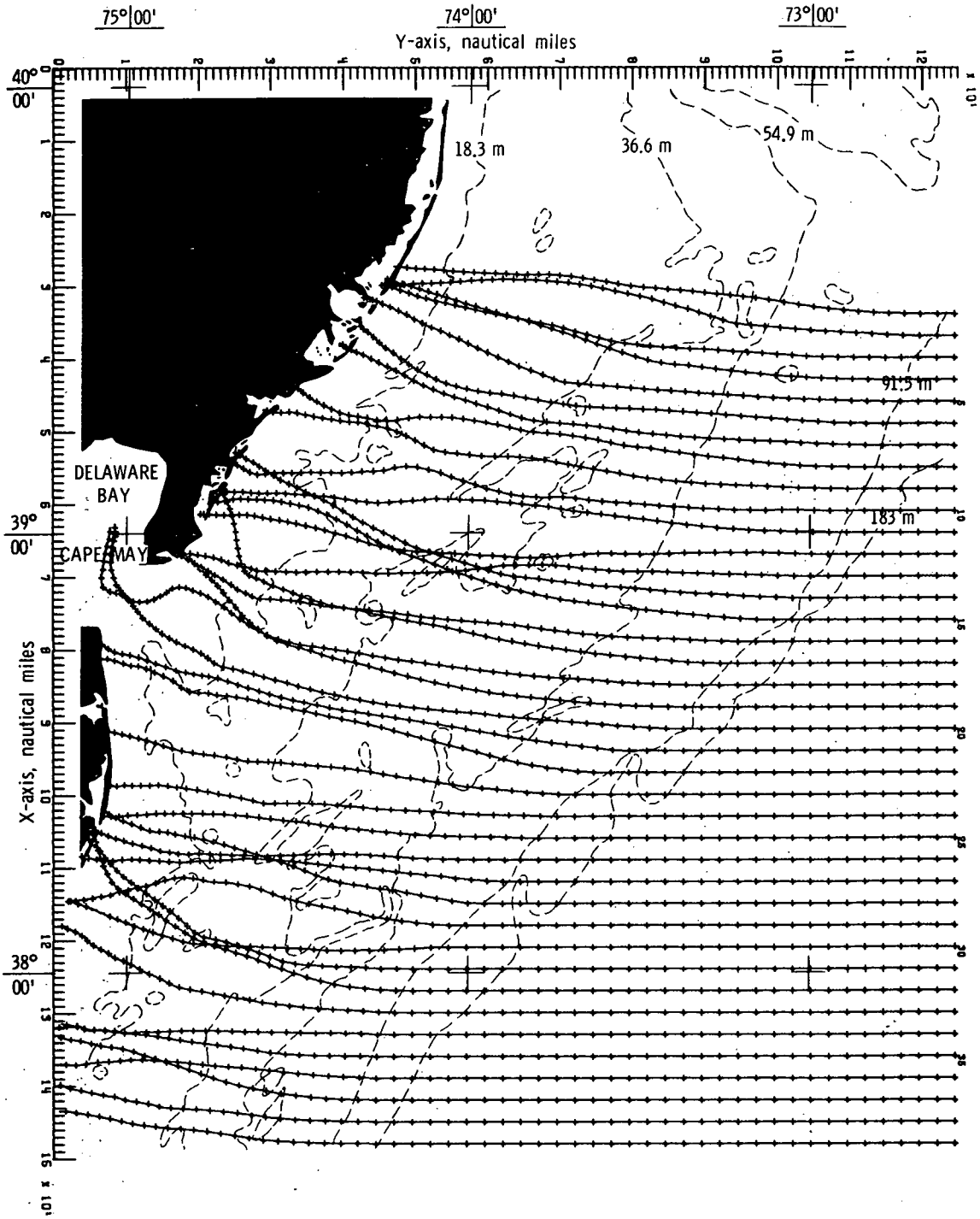


(c) Bottom topography approximated by constrained bicubic interpolation technique.

Figure 28.- Concluded.

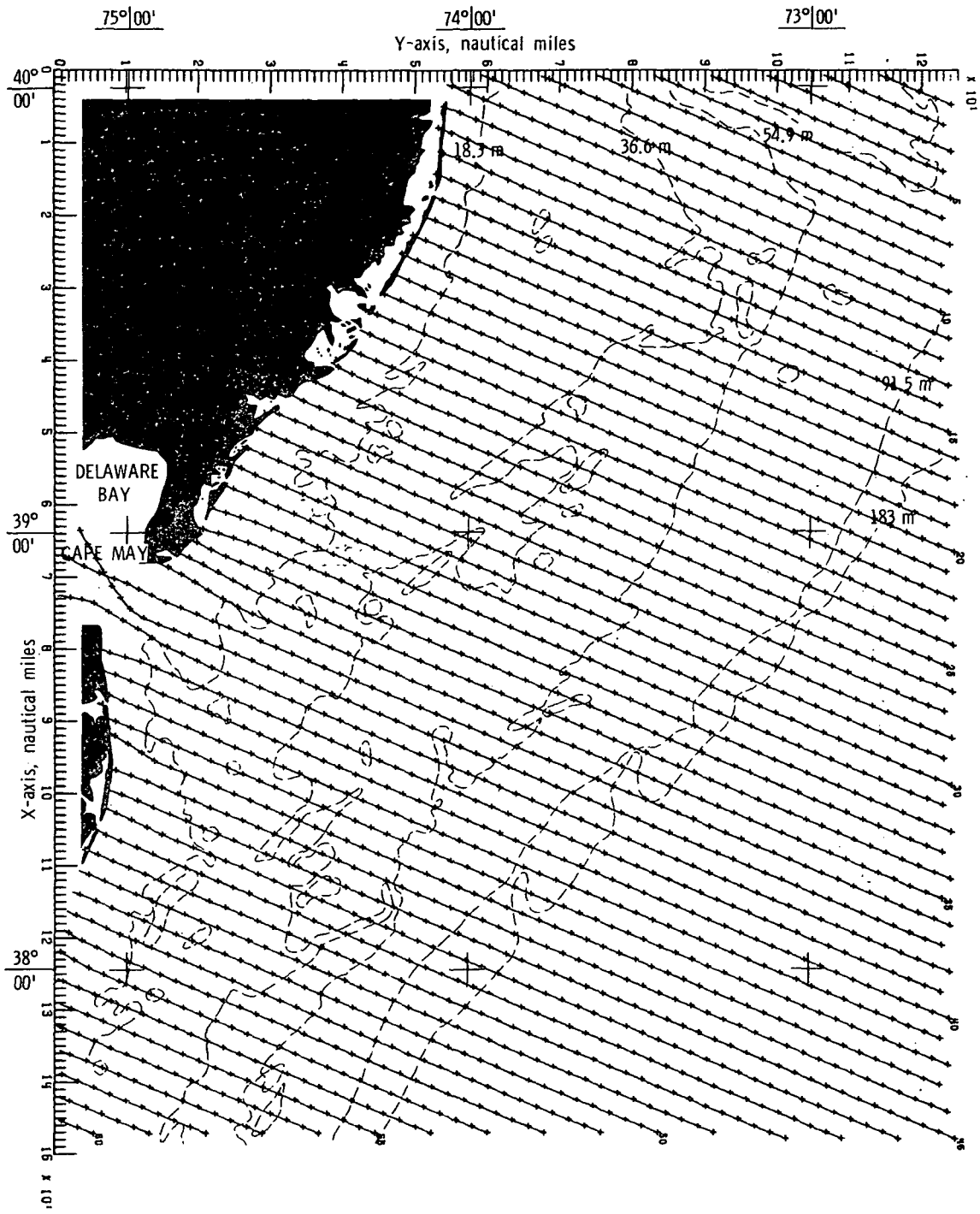


(a) Bottom topography approximated by quadratic least squares technique.

Figure 29.- Wave refraction diagrams. $\alpha = 112.5^{o}$; T = 6 seconds.

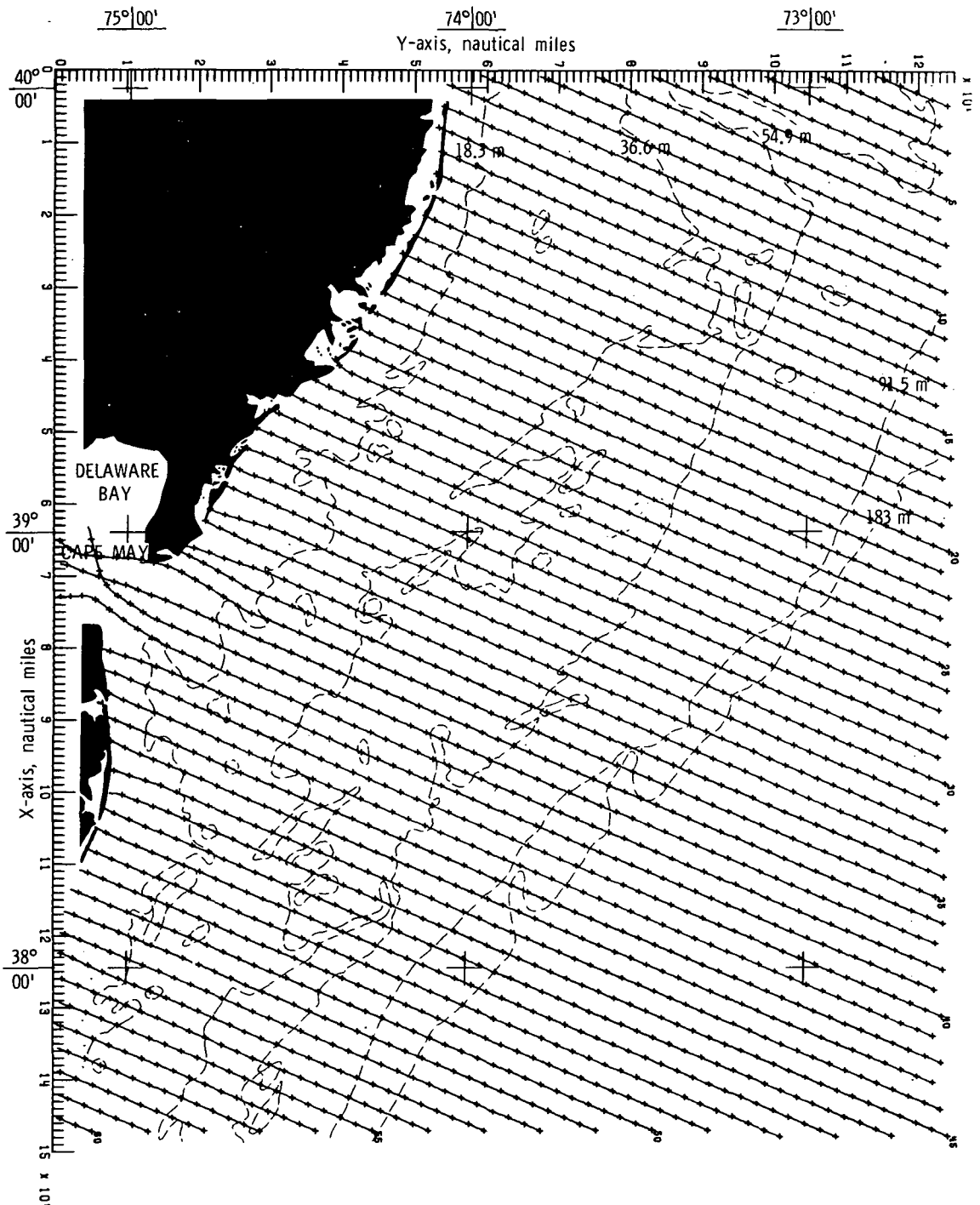


(b) Bottom topography approximated by cubic least squares technique.

Figure 29.- Continued.

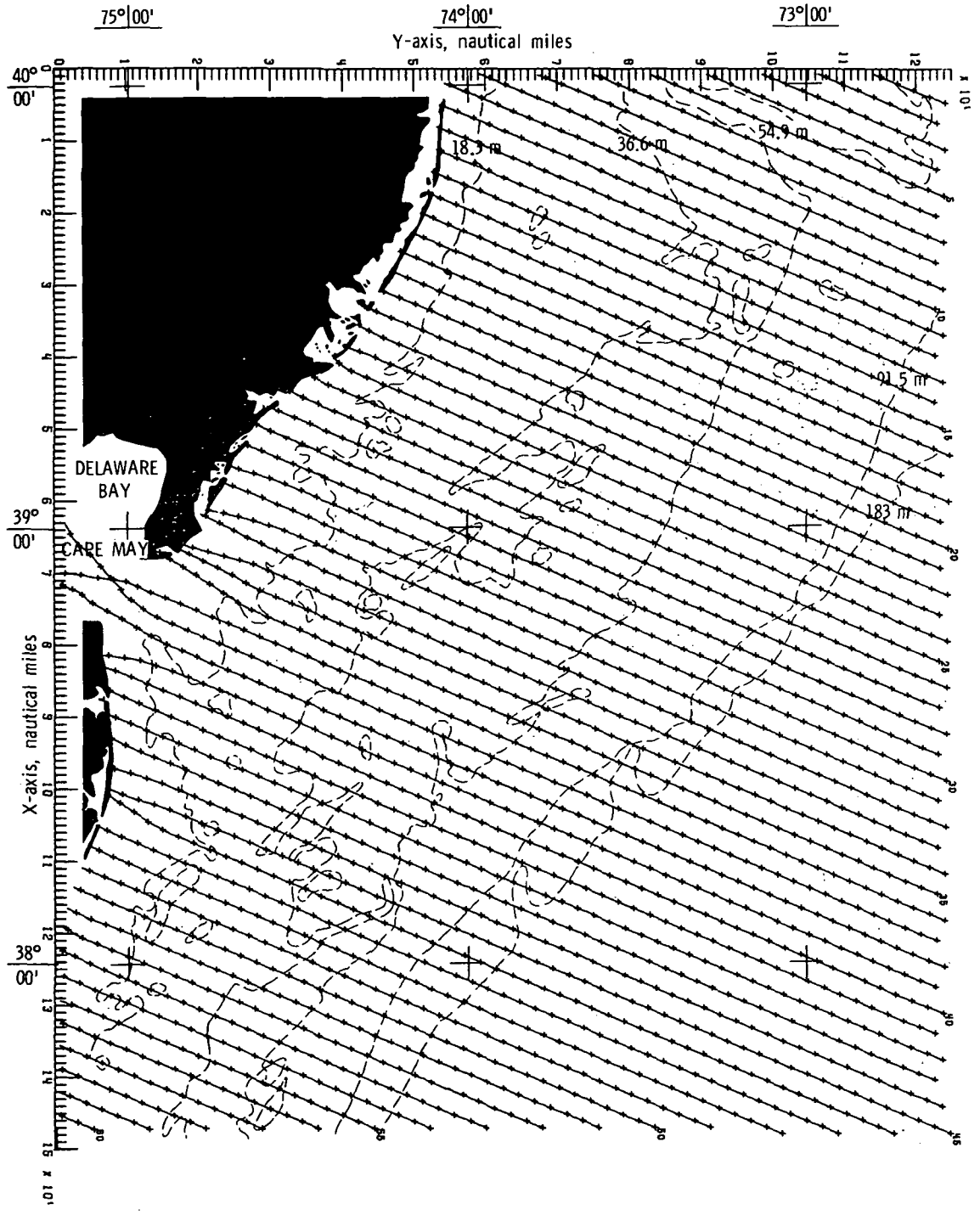


(c) Bottom topography approximated by constrained bicubic interpolation technique.

Figure 29.- Concluded.

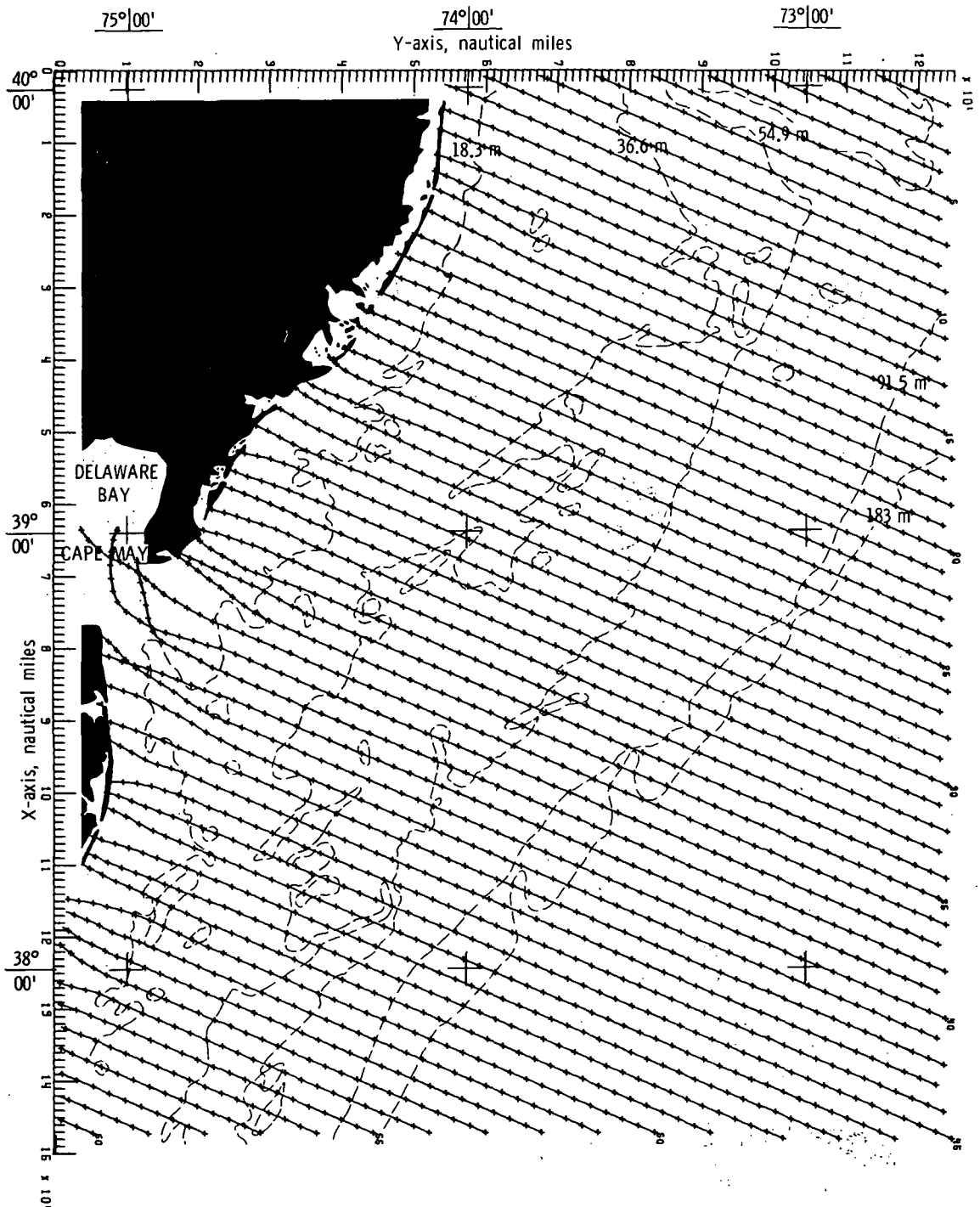


(a) Bottom topography approximated by quadratic least squares technique.

Figure 30.- Wave refraction diagrams. $\alpha$ = 112.5°; T = 8 seconds.

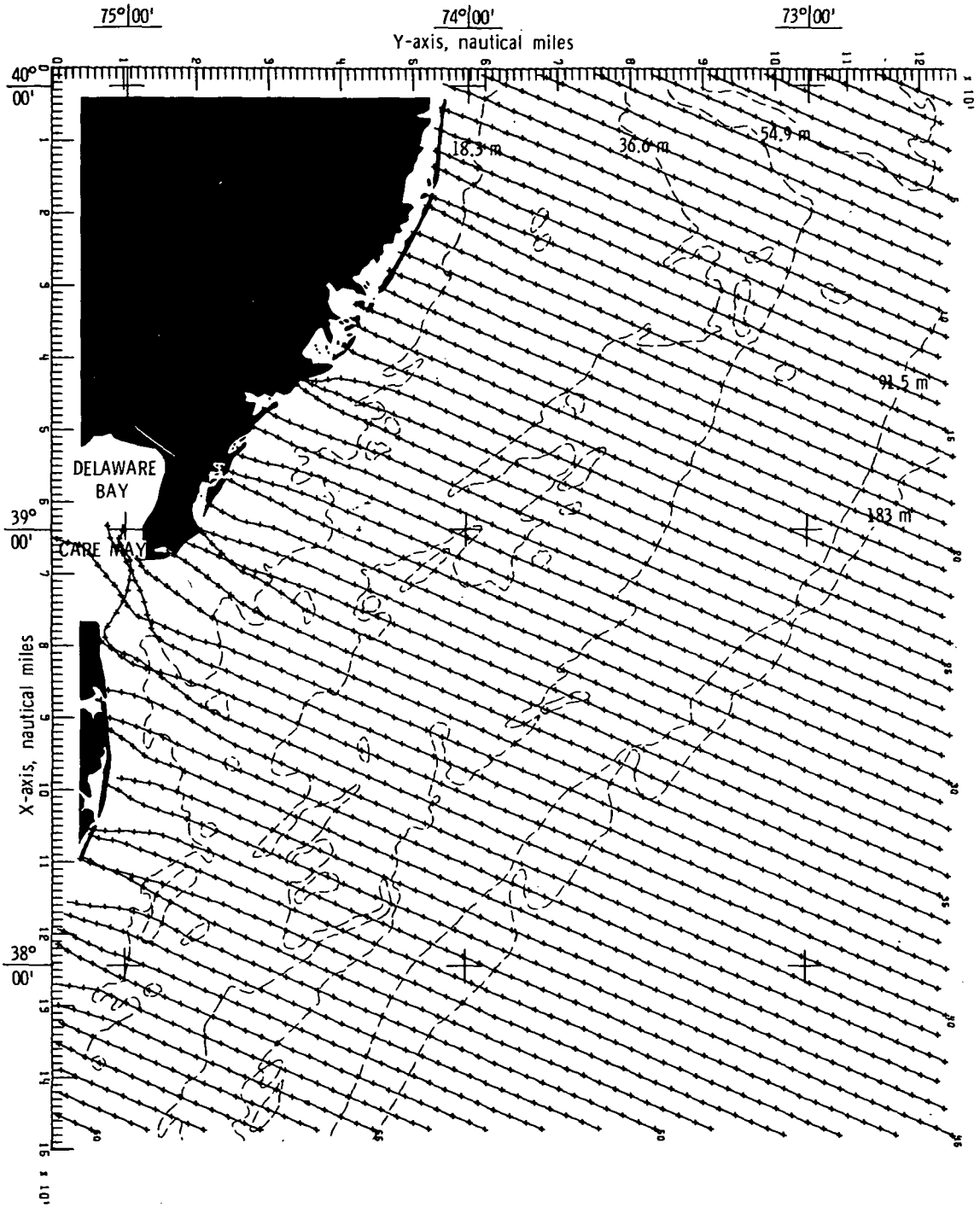


(b) Bottom topography approximated by cubic least squares technique.

Figure 30.- Continued.

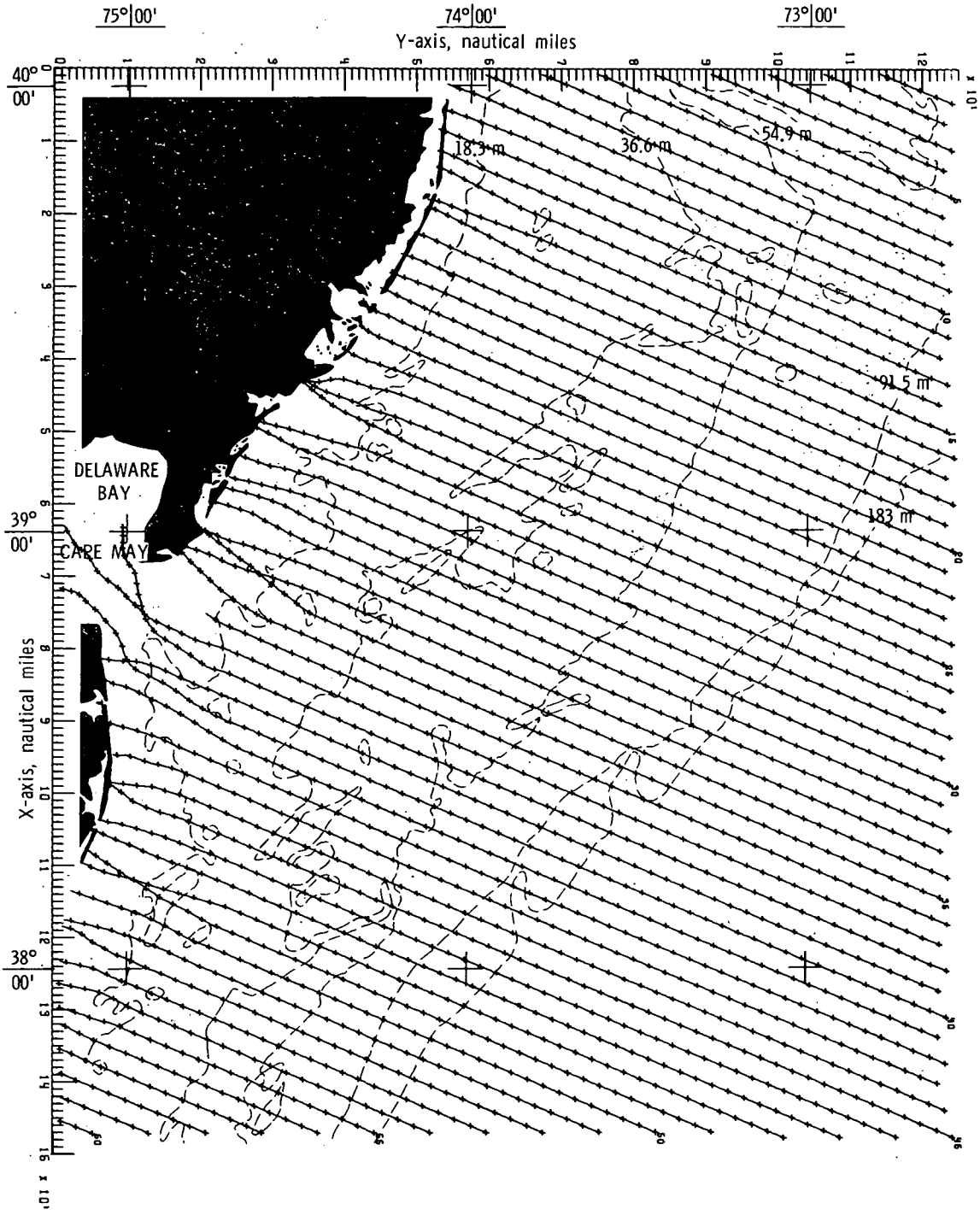


(c) Bottom topography approximated by constrained bicubic interpolation technique.

Figure 30.- Concluded.

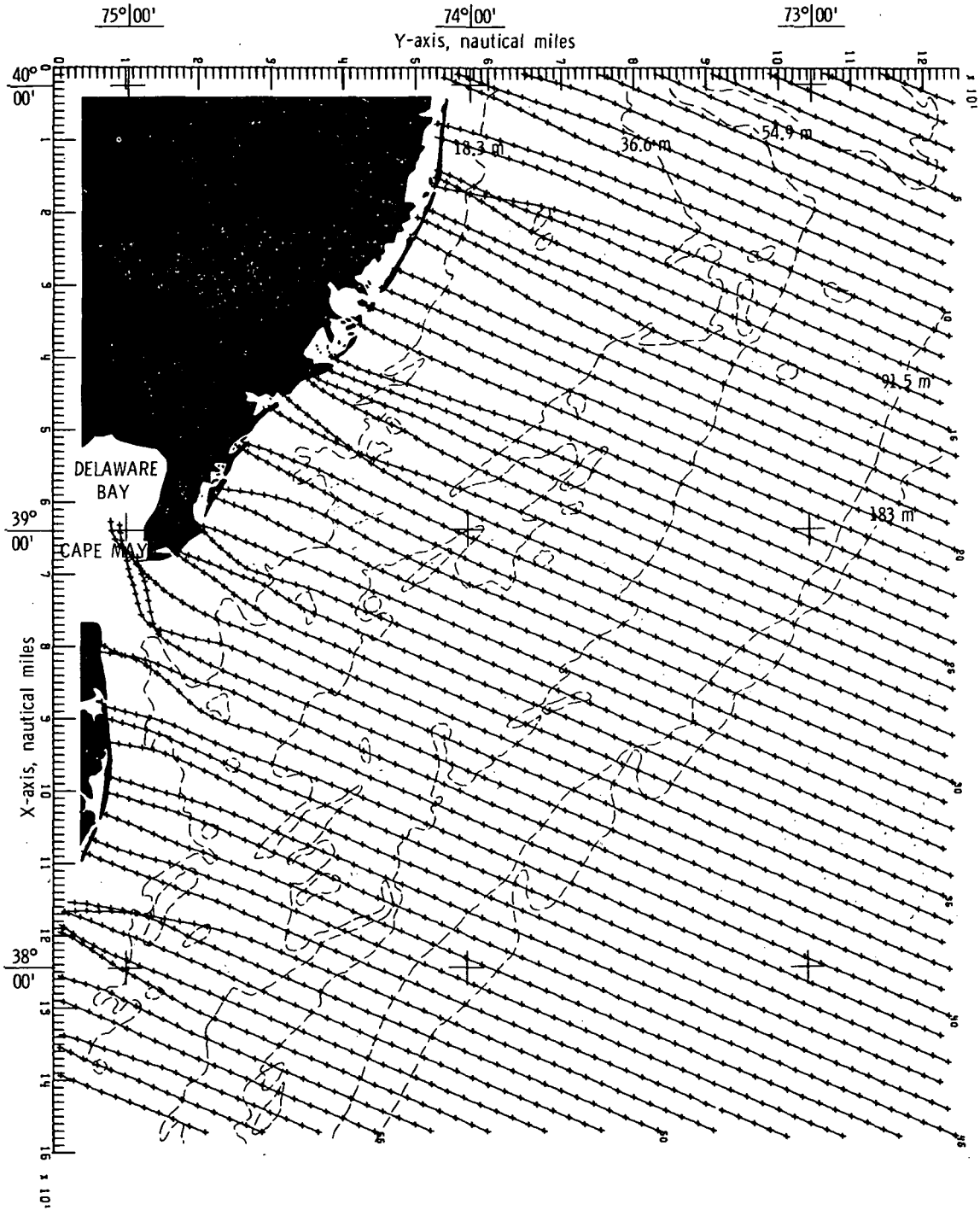


(a) Bottom topography approximated by quadratic least squares technique.

Figure 31.- Wave refraction diagrams. $\alpha = 112.5^{o}$; T = 10 seconds.

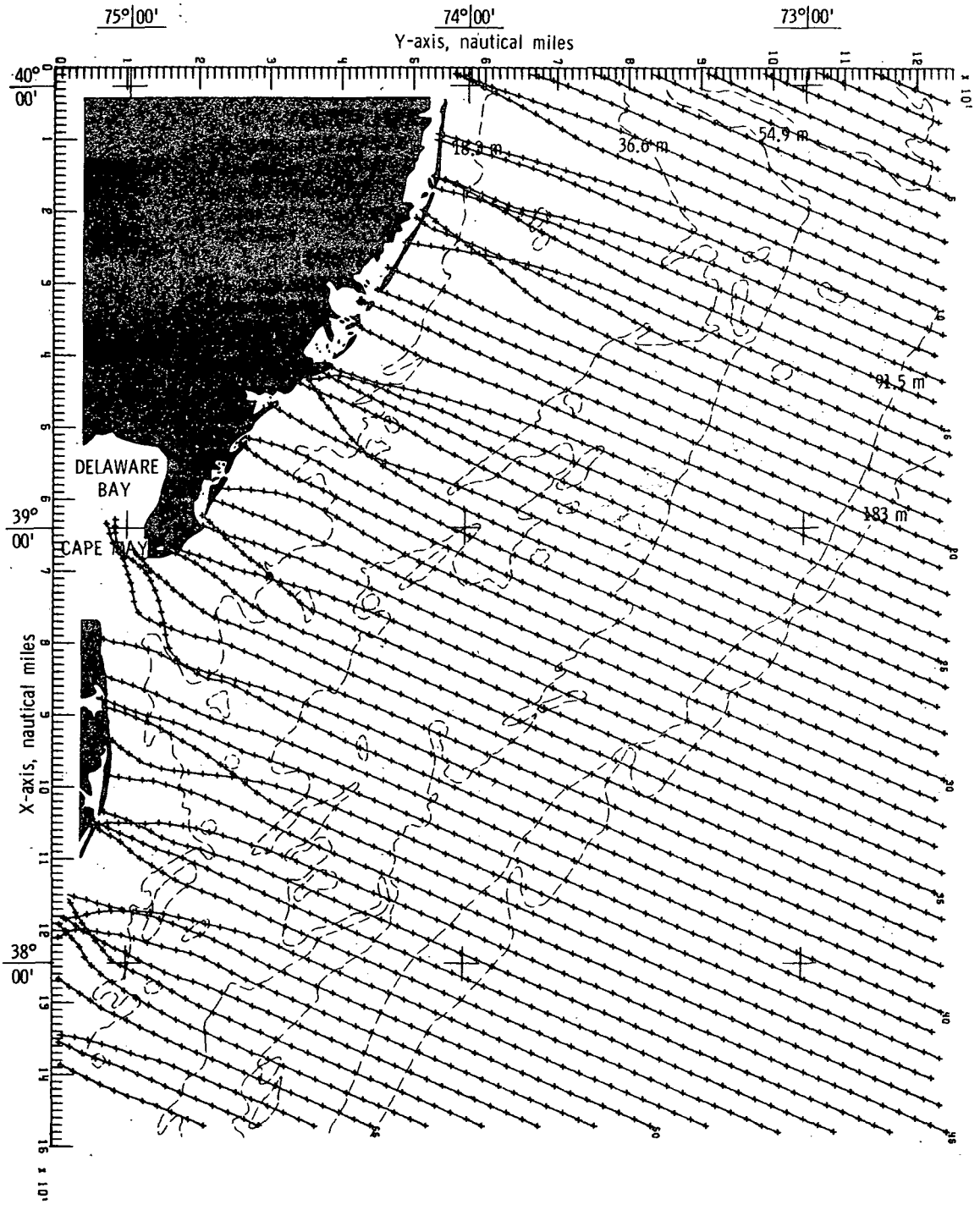


(b) Bottom topography approximated by cubic least squares technique.

Figure 31.- Continued.

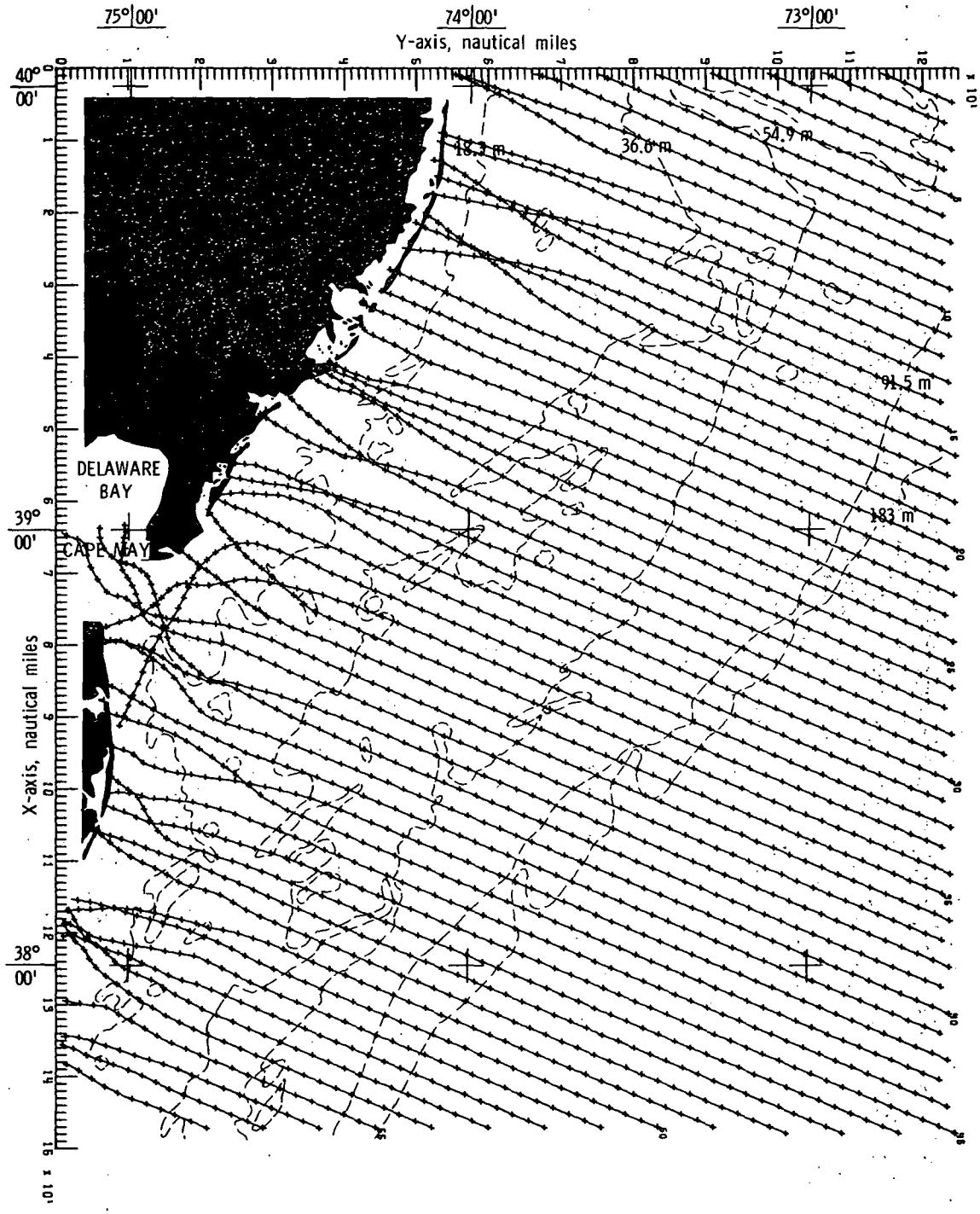


(c) Bottom topography approximated by constrained bicubic interpolation technique.

Figure 31.- Concluded.

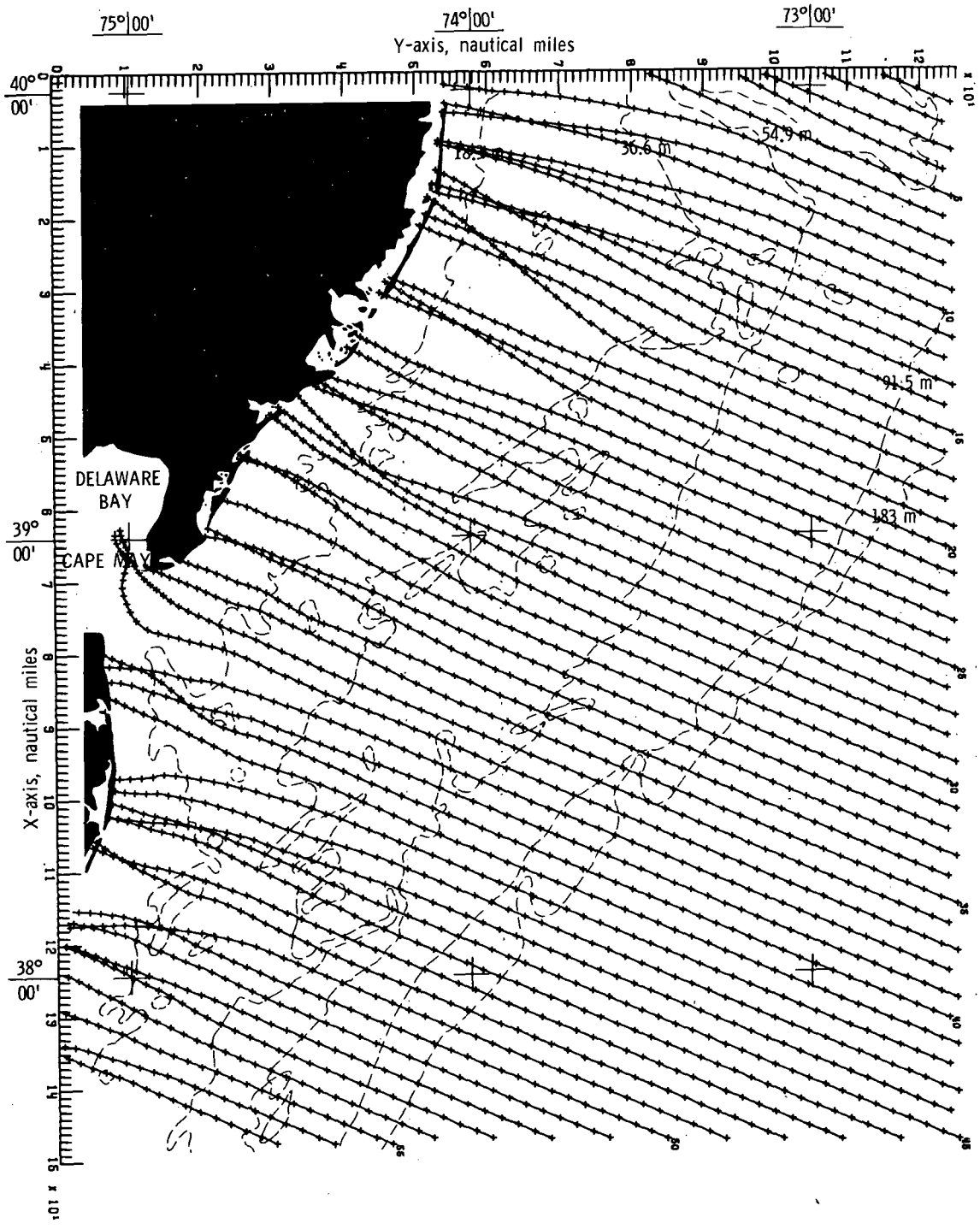


(a) Bottom topography approximated by quadratic least squares technique.

Figure 32.- Wave refraction diagrams. $\alpha$ = 112.5°; T = 12 seconds.

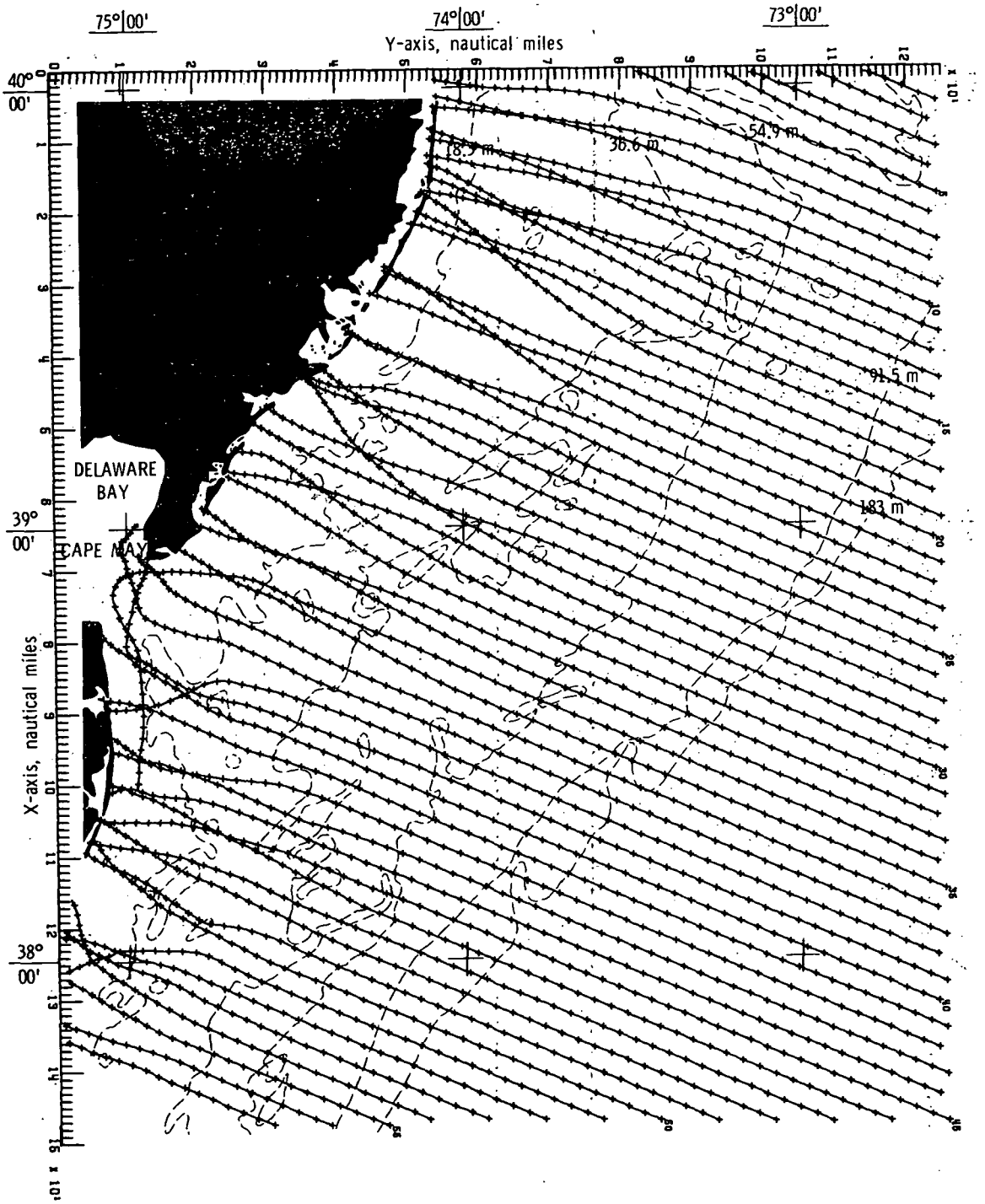


(b) Bottom topography approximated by cubic least squares technique.

Figure 32.- Continued.

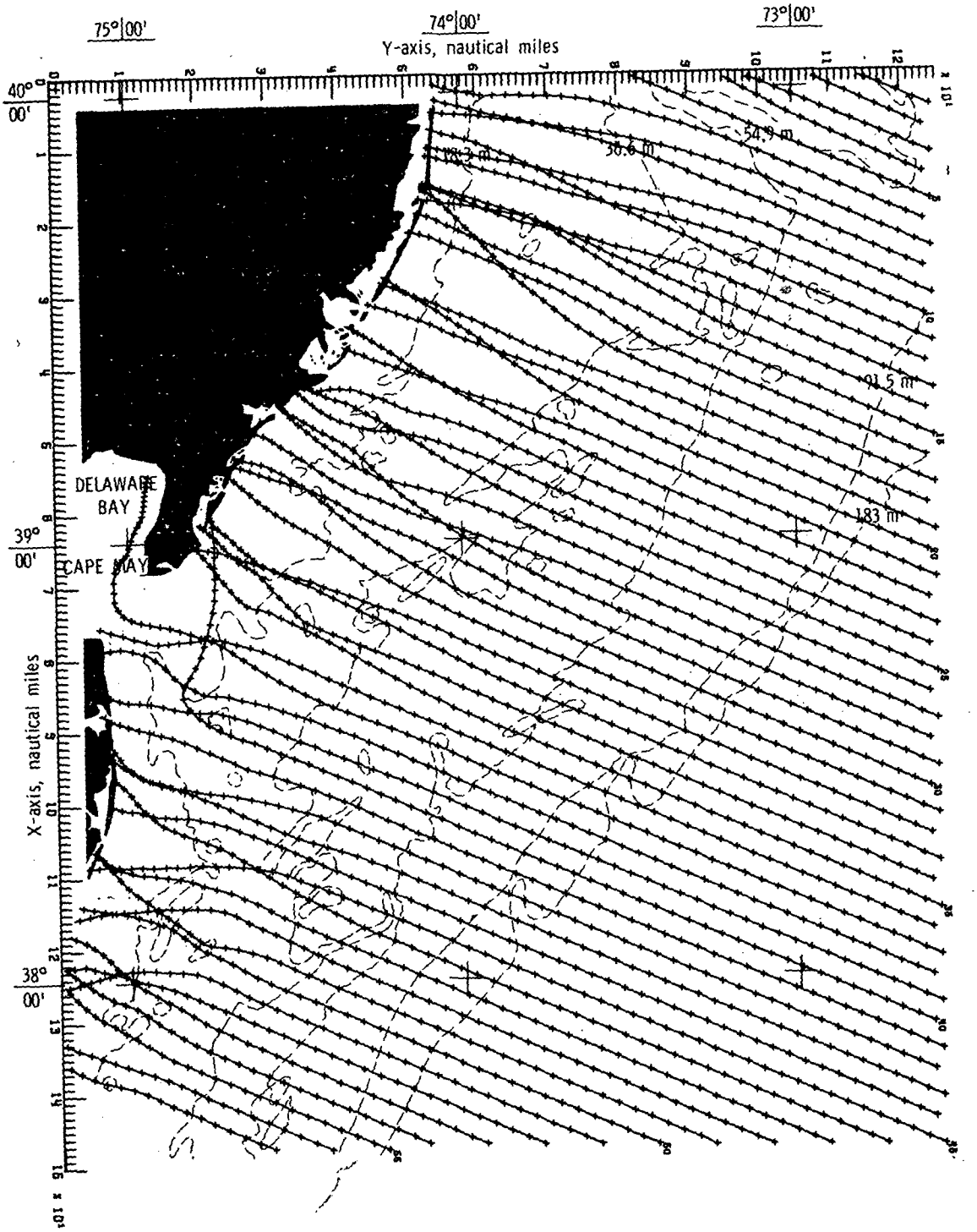


(c) Bottom topography approximated by constrained bicubic interpolation technique.

Figure 32.- Concluded.

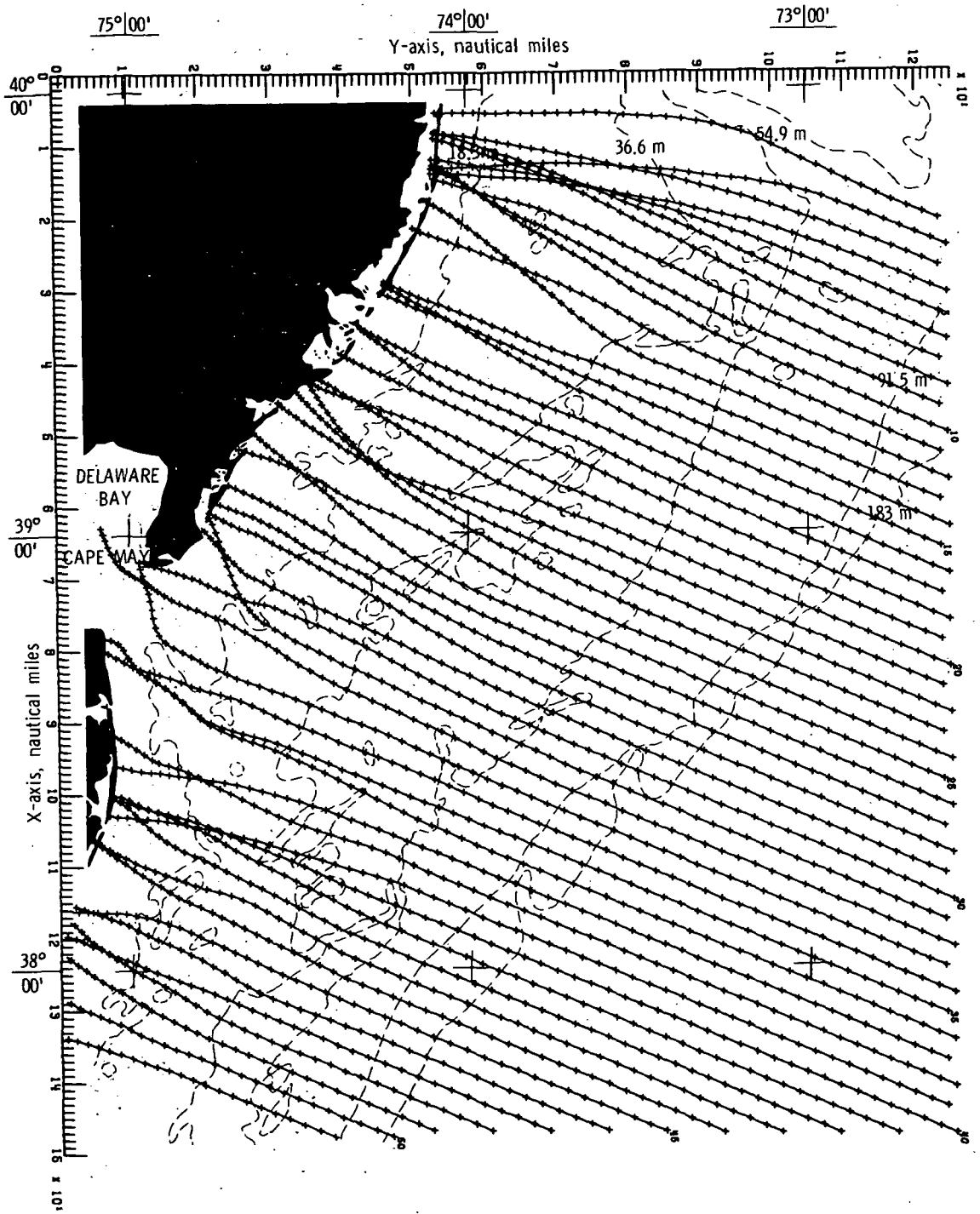


(a) Bottom topography approximated by quadratic least squares technique.

Figure 33.--Wave refraction diagrams. $\alpha$ = 112.5°; T = 14 seconds.

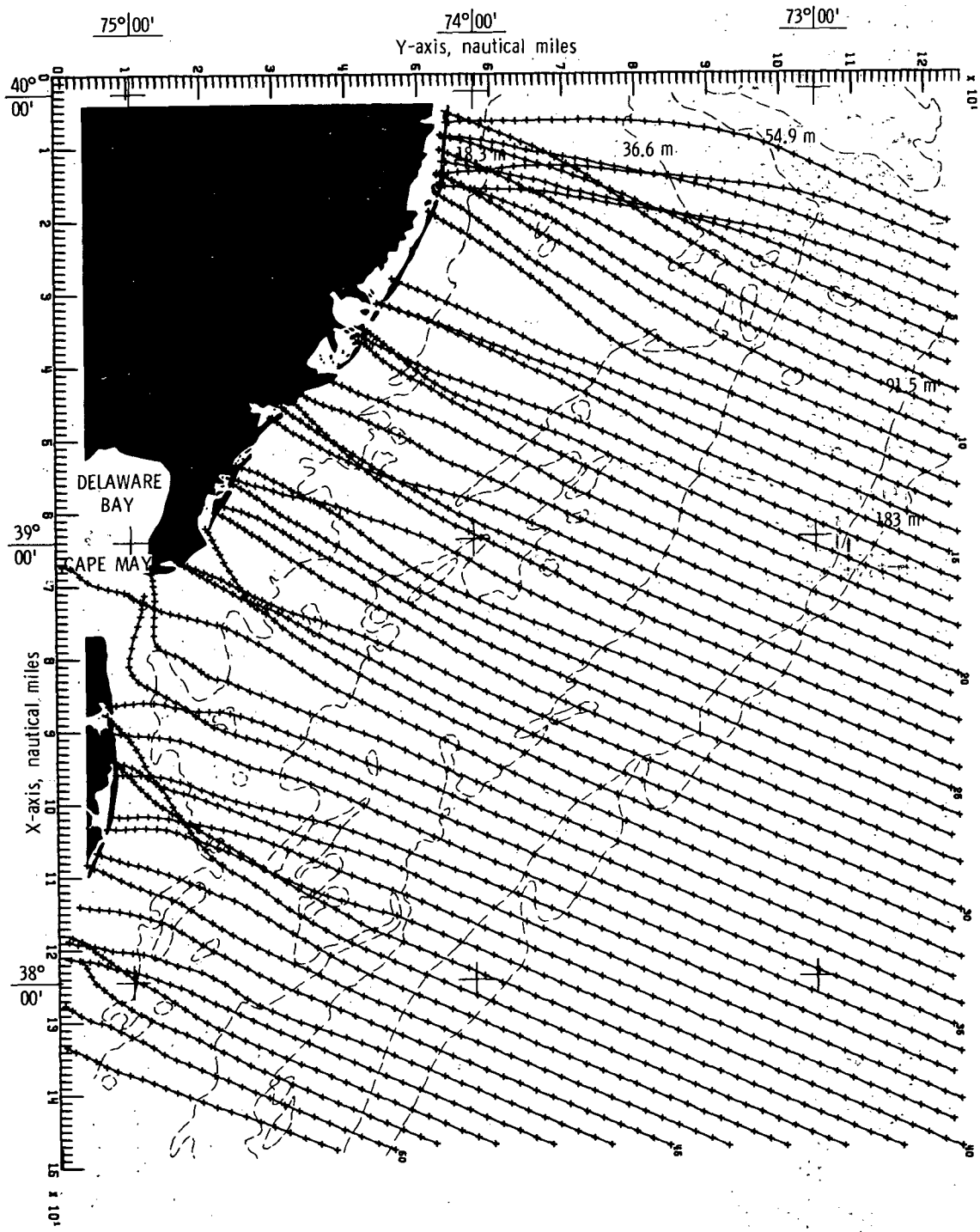


(b) Bottom topography approximated by cubic least squares technique.

Figure 33.- Continued.

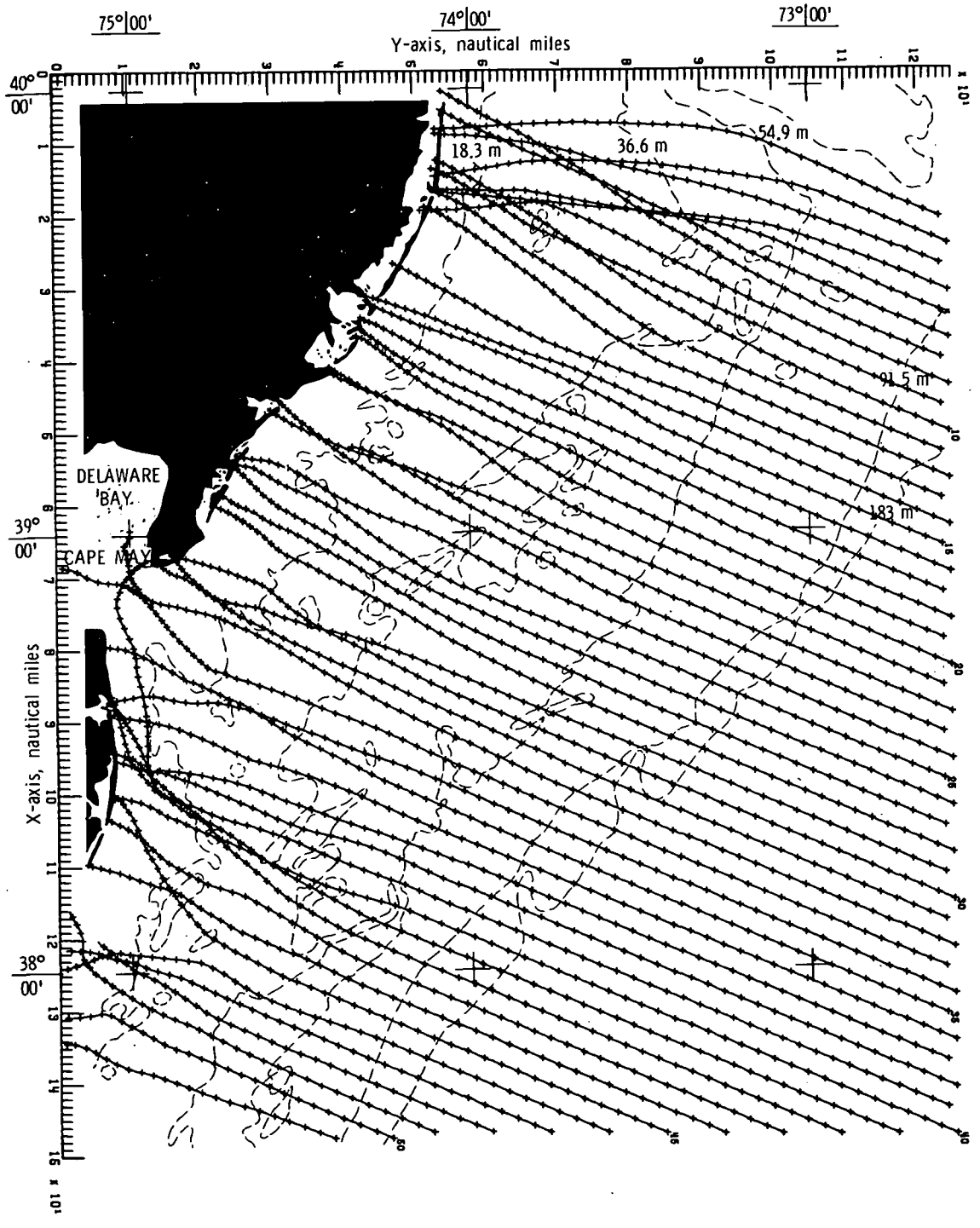


(c) Bottom topography approximated by constrained bicubic interpolation technique.

Figure 33.- Concluded.

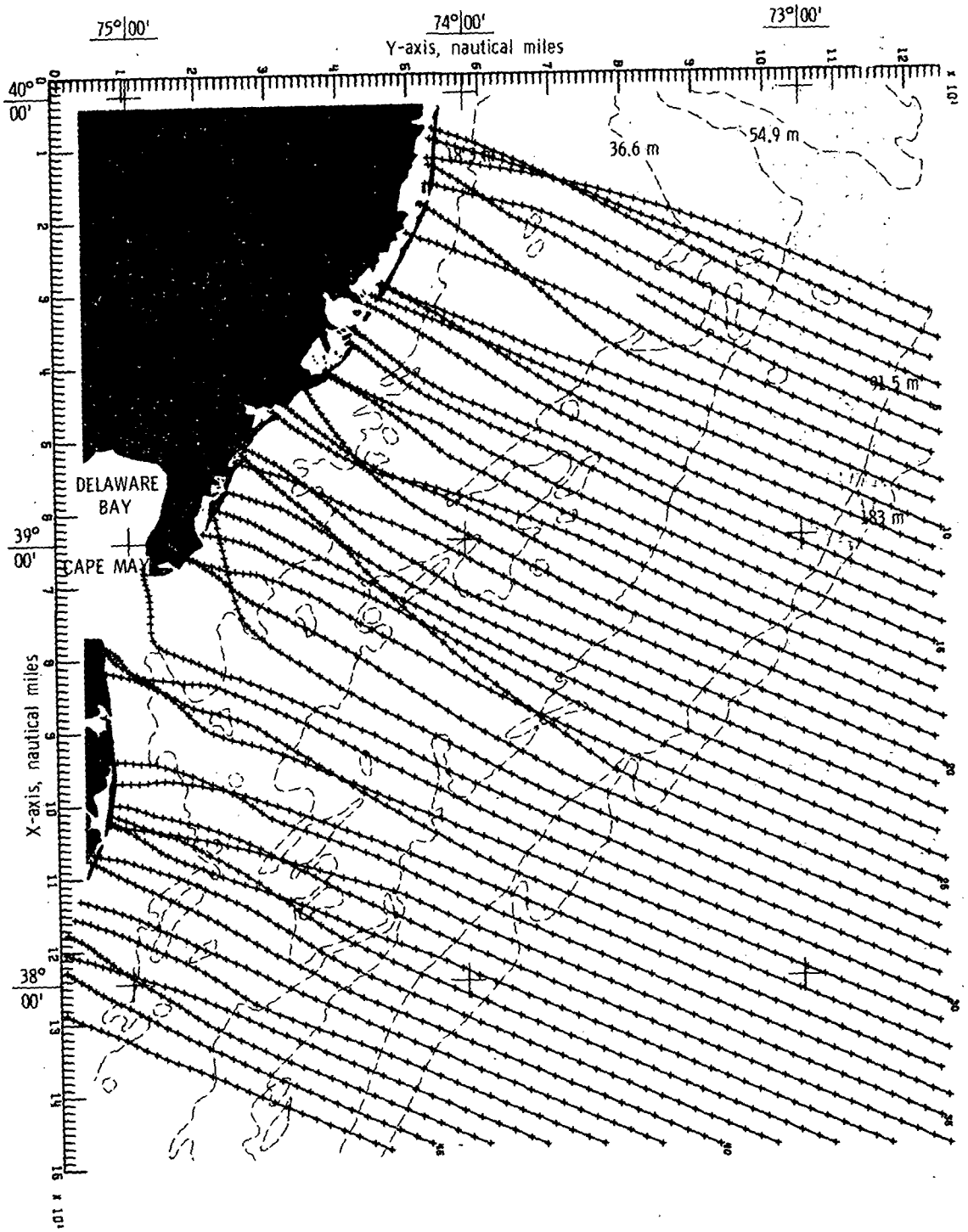


(a) Bottom topography approximated by quadratic least squares technique.

Figure 34.- Wave refraction diagrams. $\alpha = 112.5^{\circ}$; T = 16 second

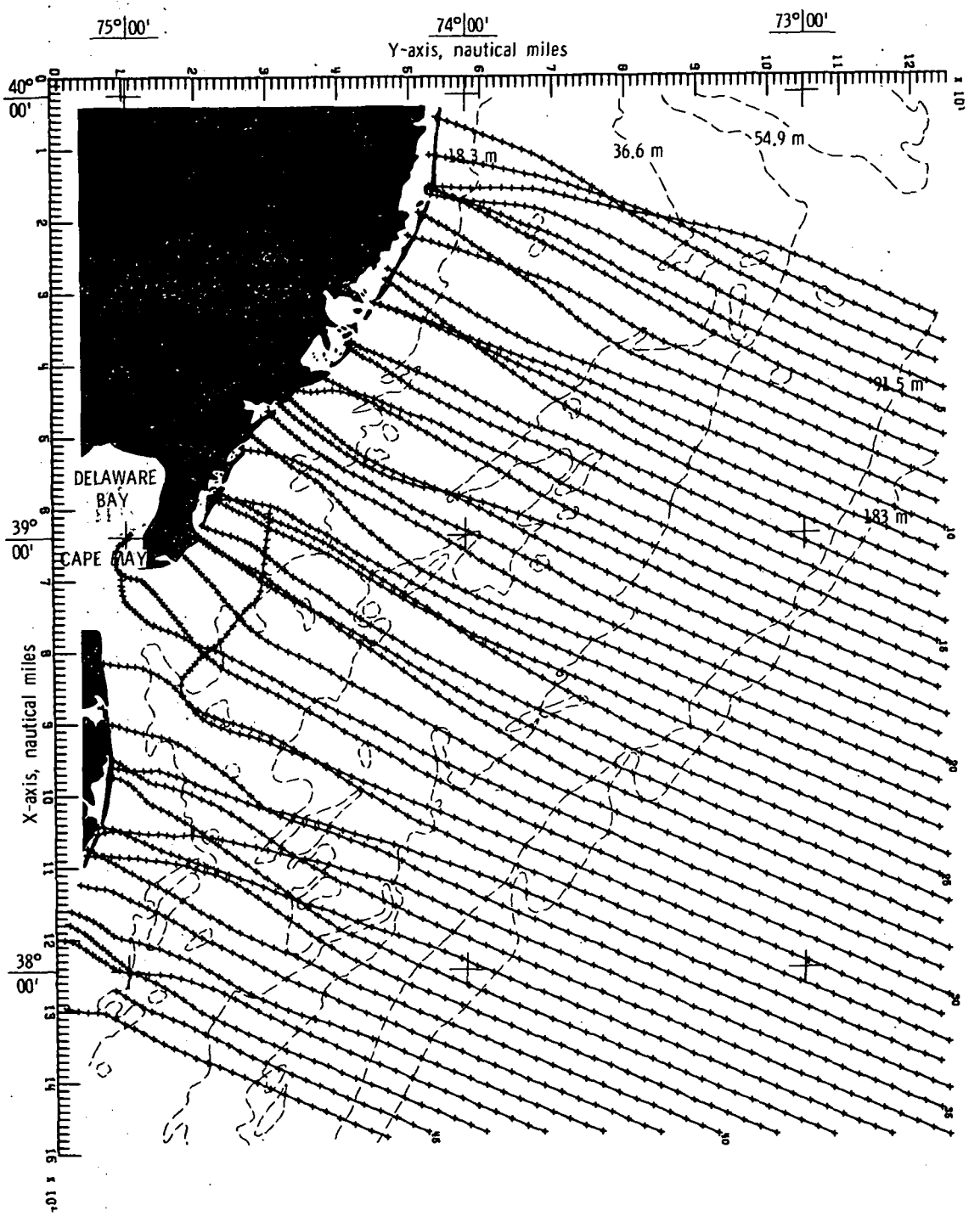


(b) Bottom topography approximated by cubic least squares technique.

Figure 34.- Continued.

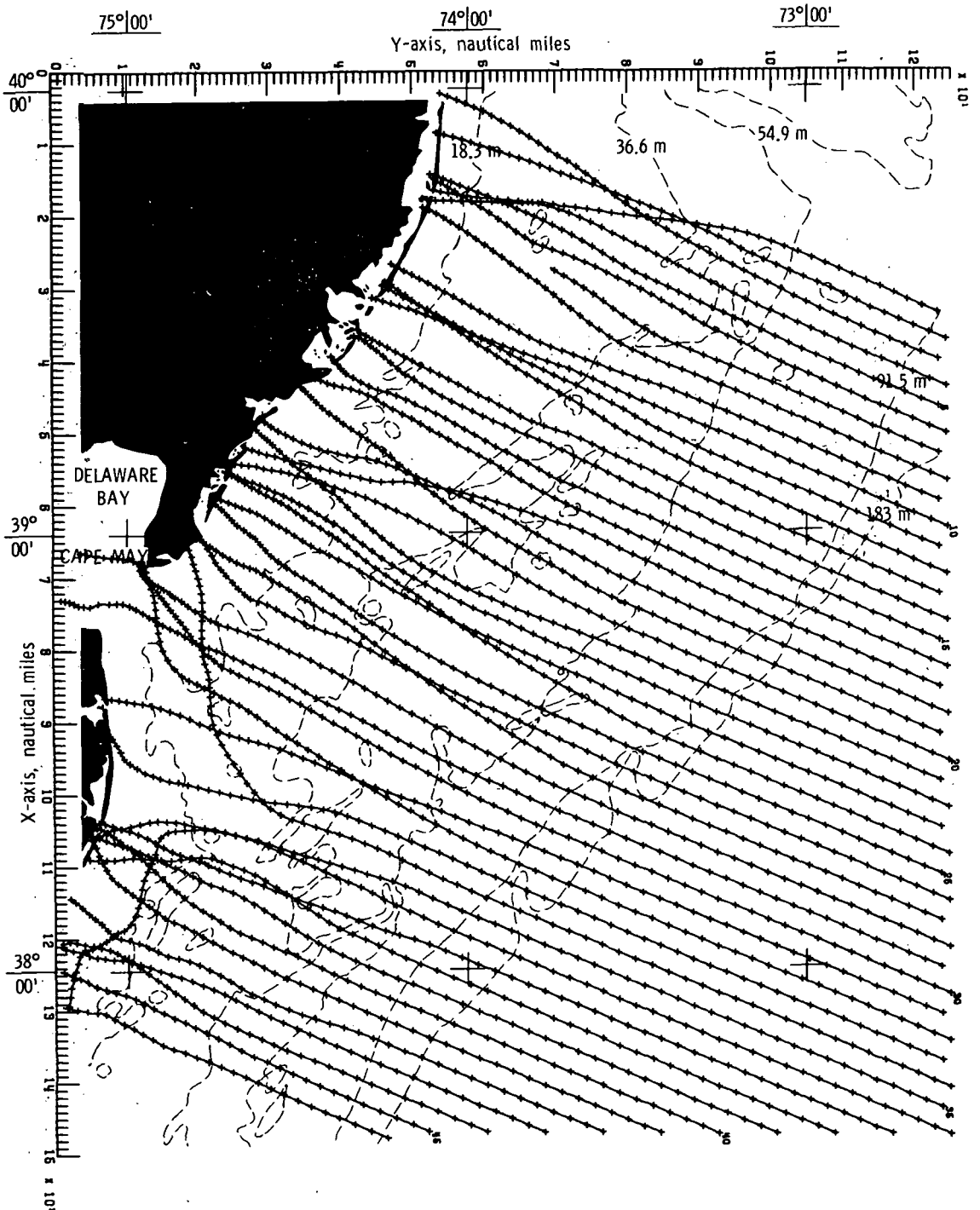


(c) Bottom topography approximated by constrained bicubic interpolation technique.

Figure 34.- Concluded.

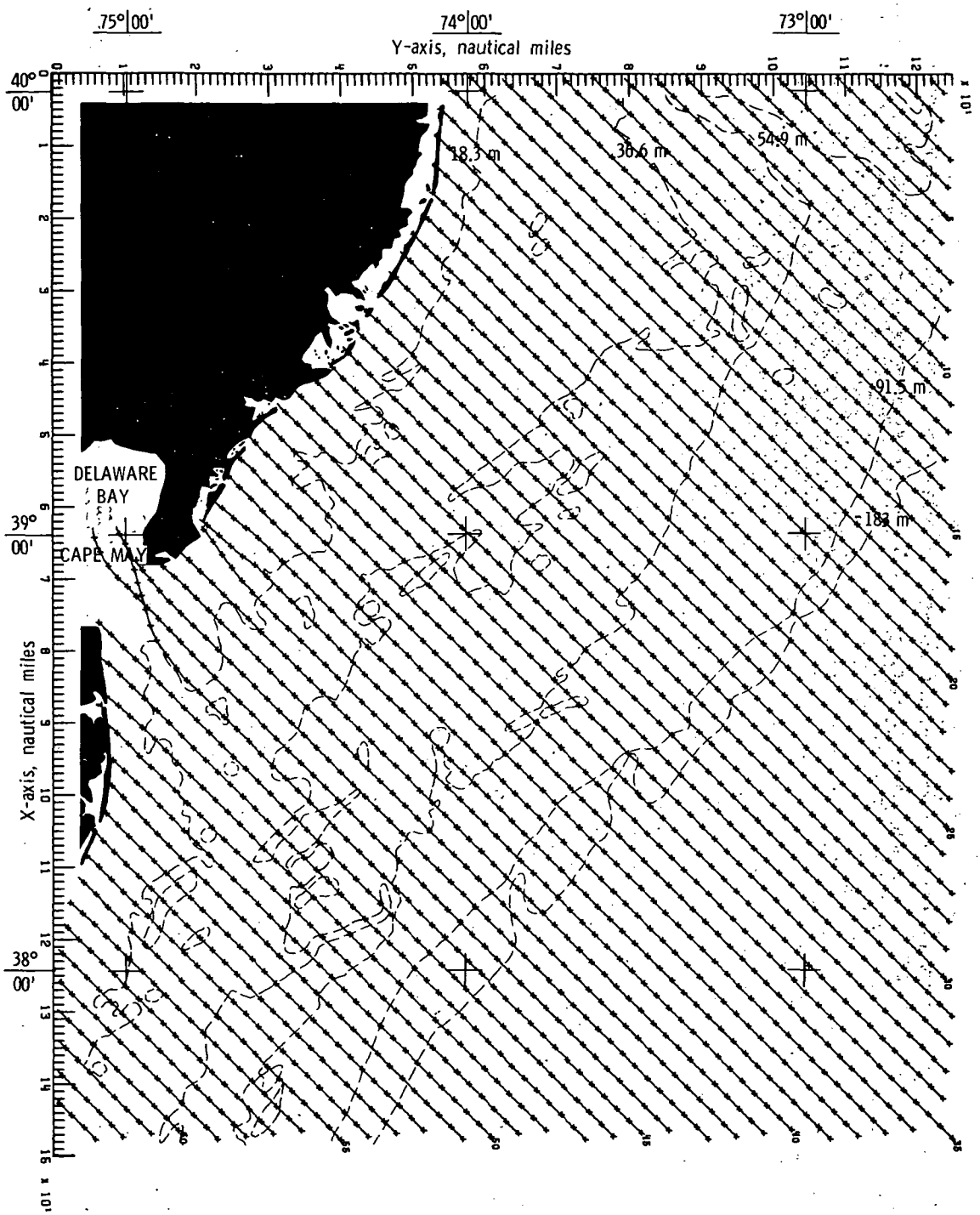


(a) Bottom topography approximated by quadratic least squares technique.

Figure 35.- Wave refraction diagrams. $\alpha = 135^{o}$; T = 6 seconds.

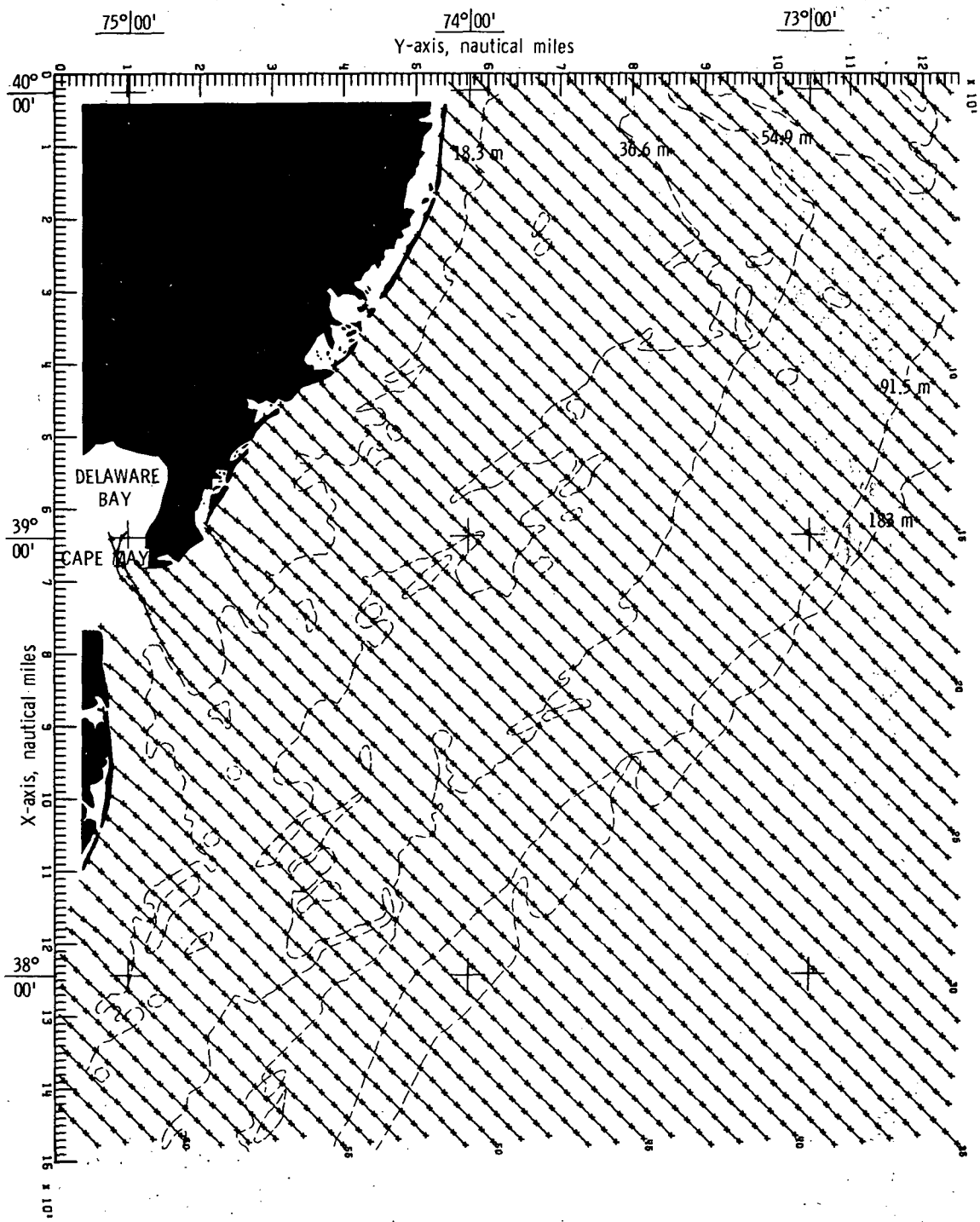


(b) Bottom topography approximated by cubic least squares technique.

Figure 35.- Continued.

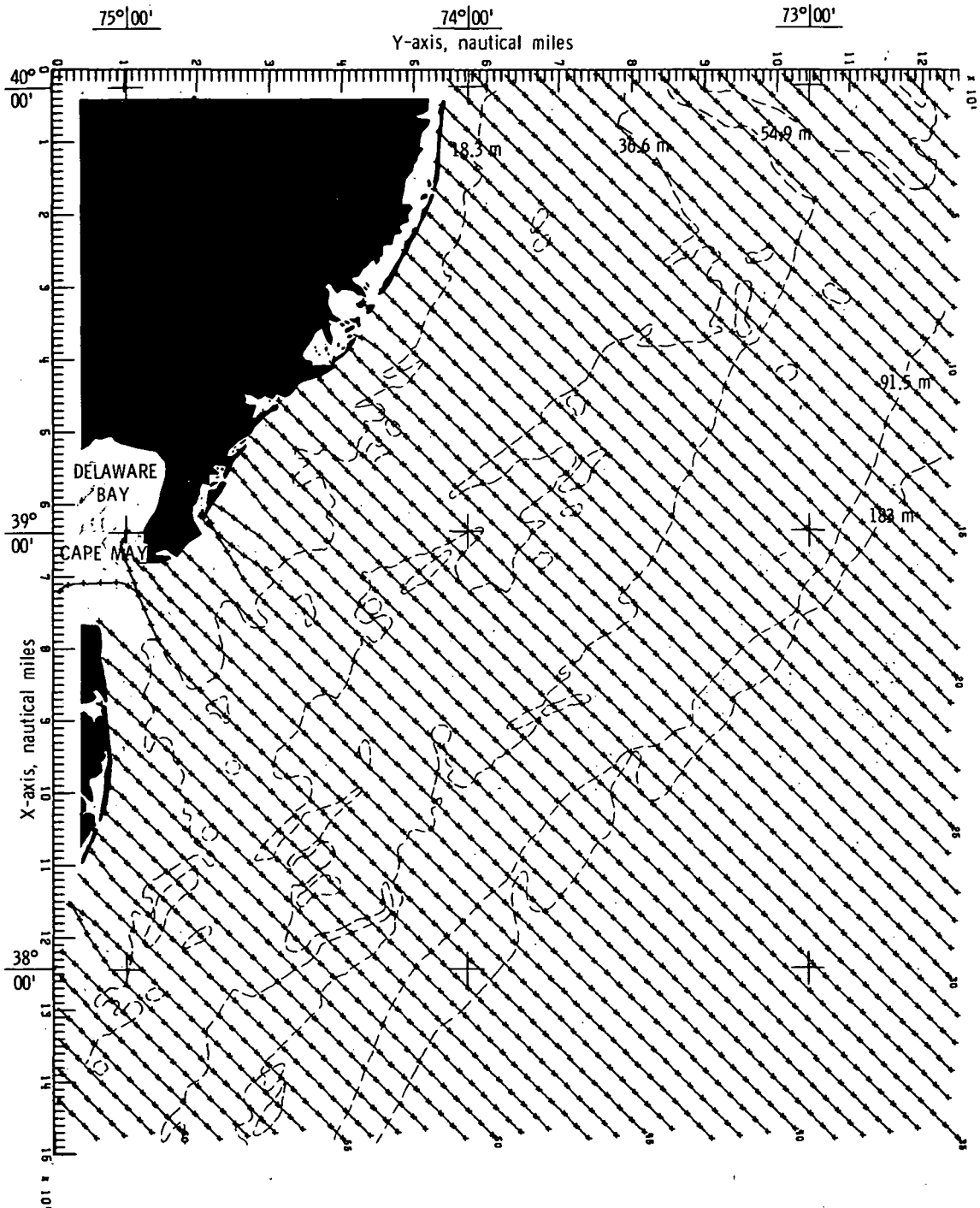


(c) Bottom topography approximated by constrained bicubic interpolation technique.

Figure 35.- Concluded.


(a) Bottom topography approximated by quadratic least squares technique.

Figure 36.- Wave refraction diagrams. $\alpha = 135^{\circ}$; T = 8 seconds.

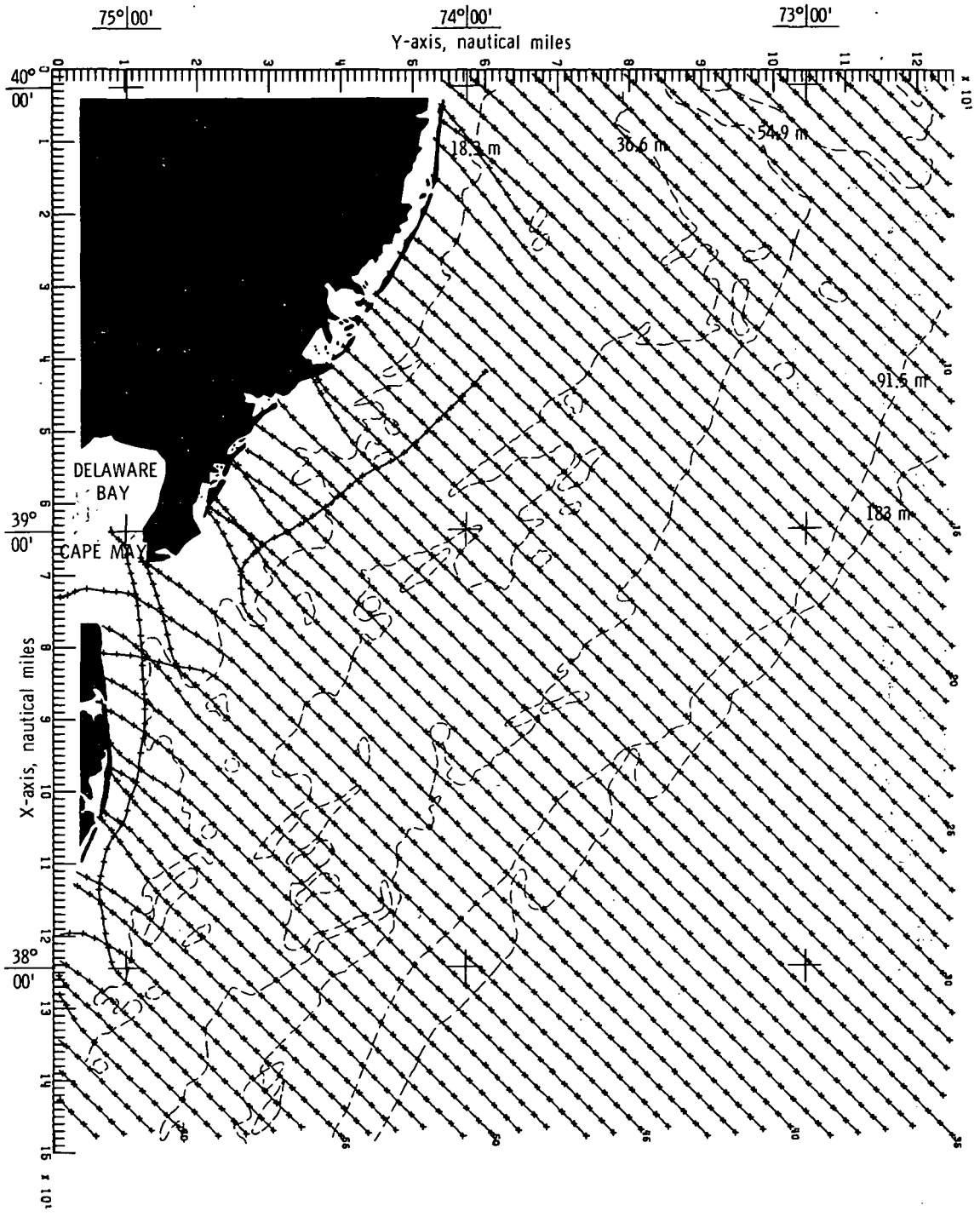


(b) Bottom topography approximated by cubic least squares technique.

Figure 36.- Continued.

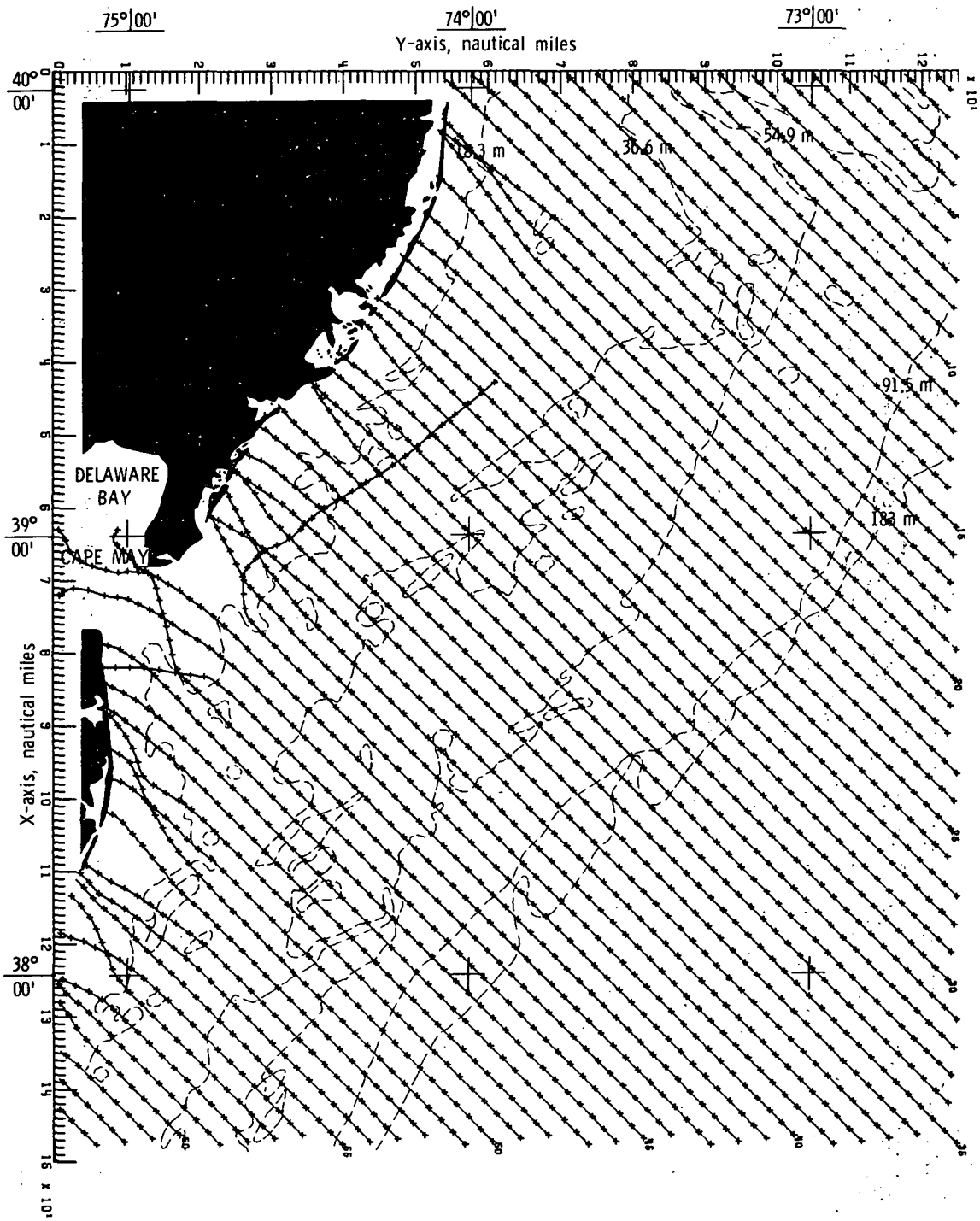


(c) Bottom topography approximated by constrained bicubic interpolation technique.

Figure 36.- Concluded.

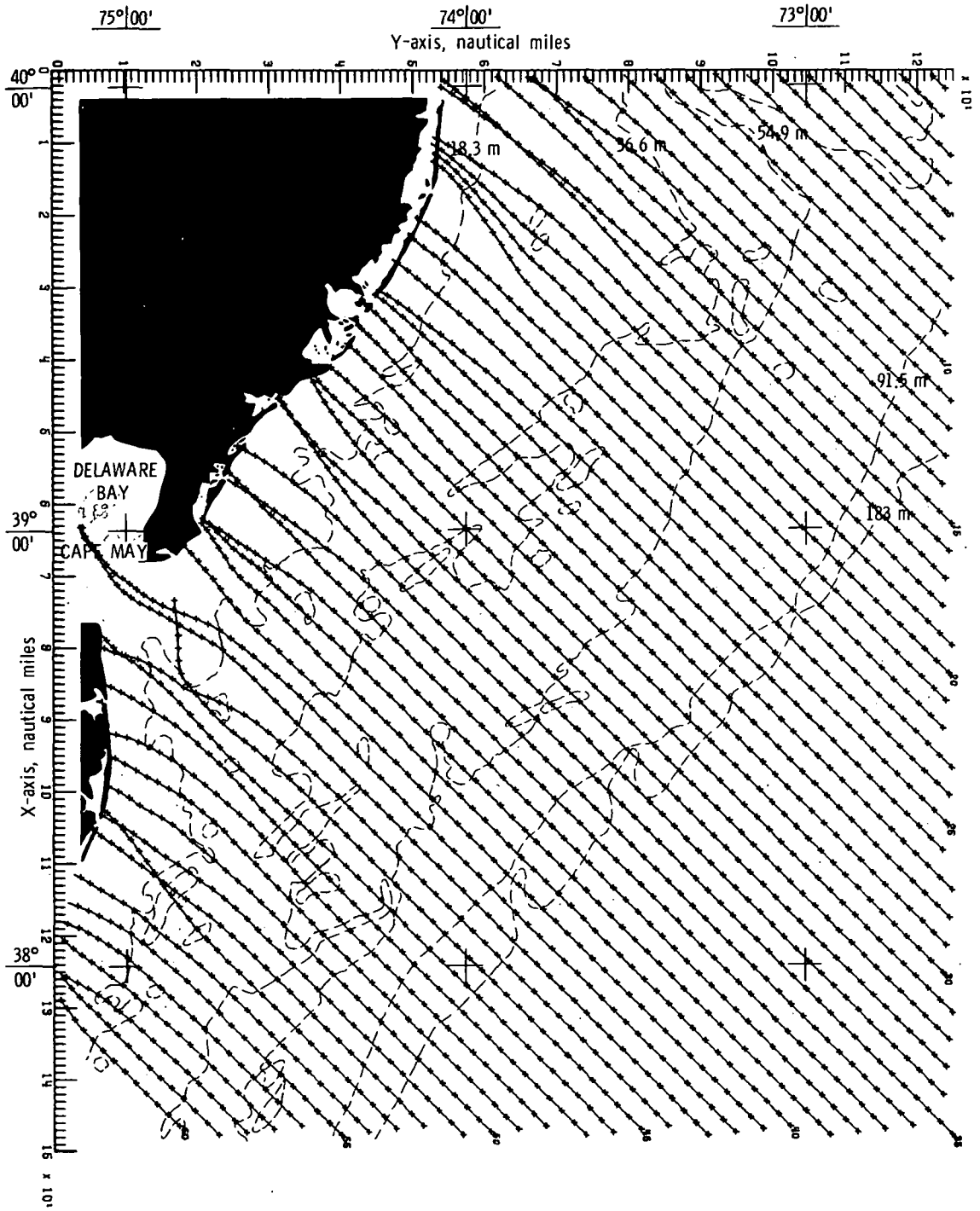


(a) Bottom topography approximated by quadratic least squares technique.

Figure 37.- Wave refraction diagrams. $\alpha = 135^{o}$; T = 10 seconds.

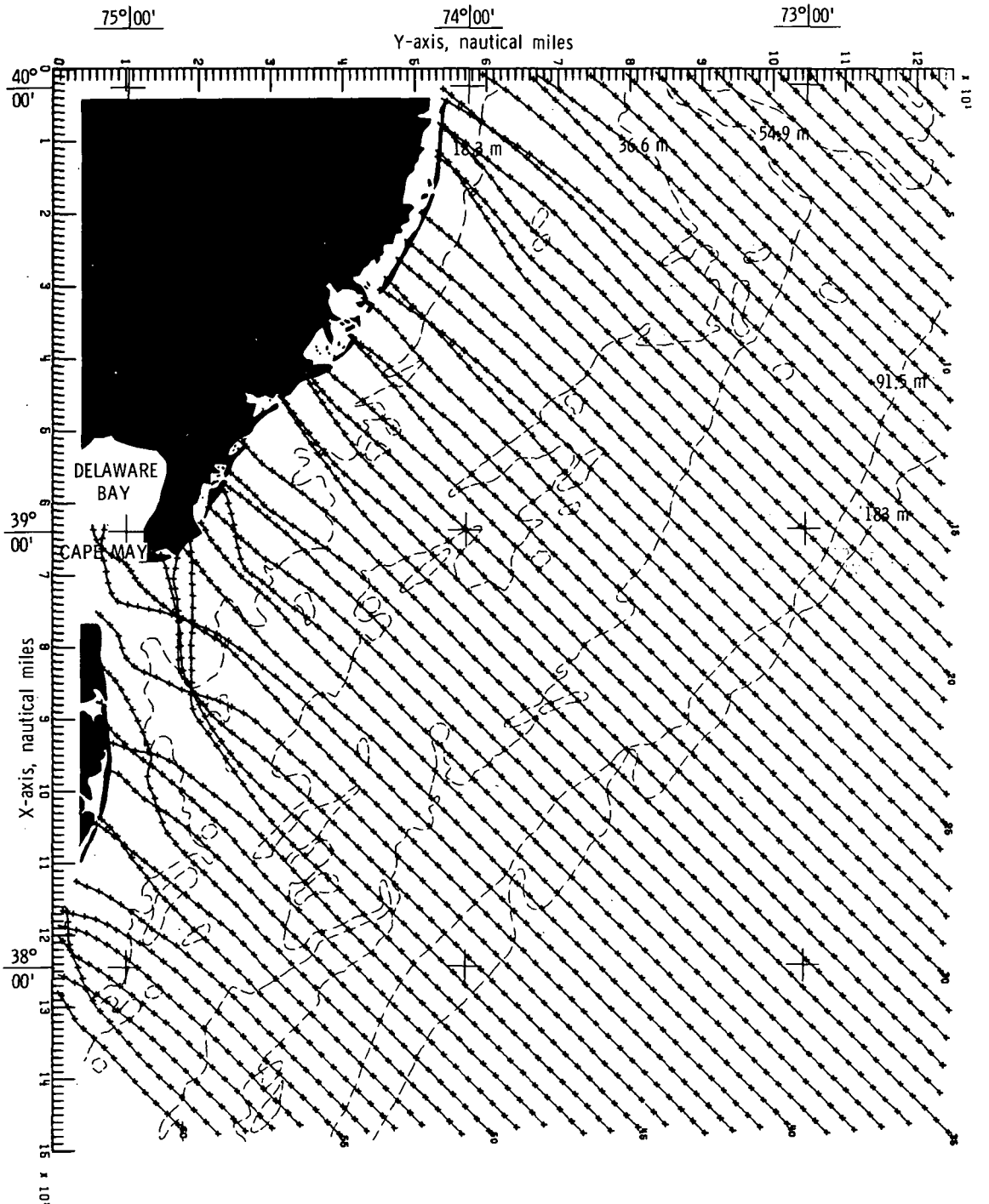


(b) Bottom topography approximated by cubic least squares technique.

Figure 37.- Continued.

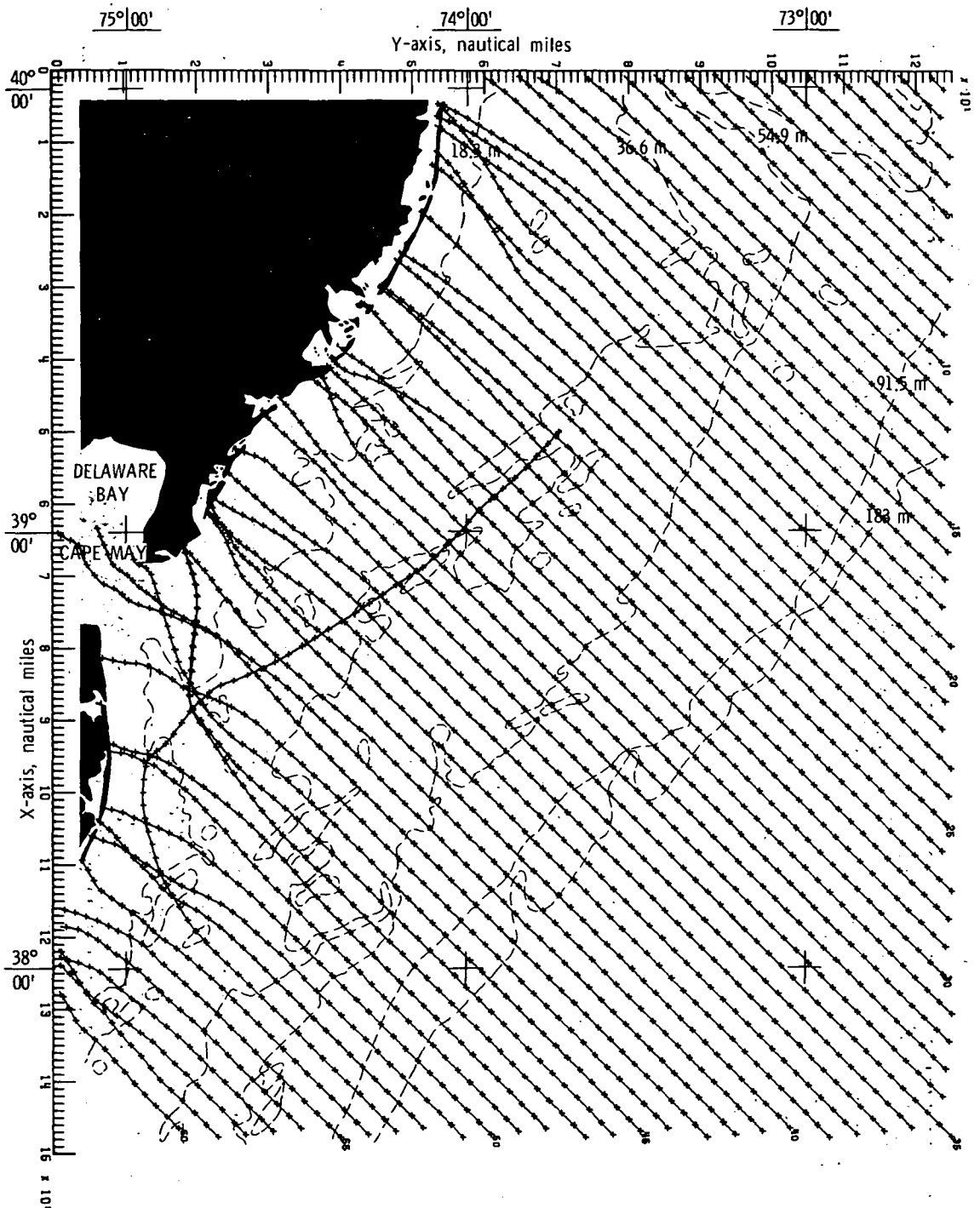


(c) Bottom topography approximated by constrained bicubic interpolation technique.

Figure 37.- Concluded.

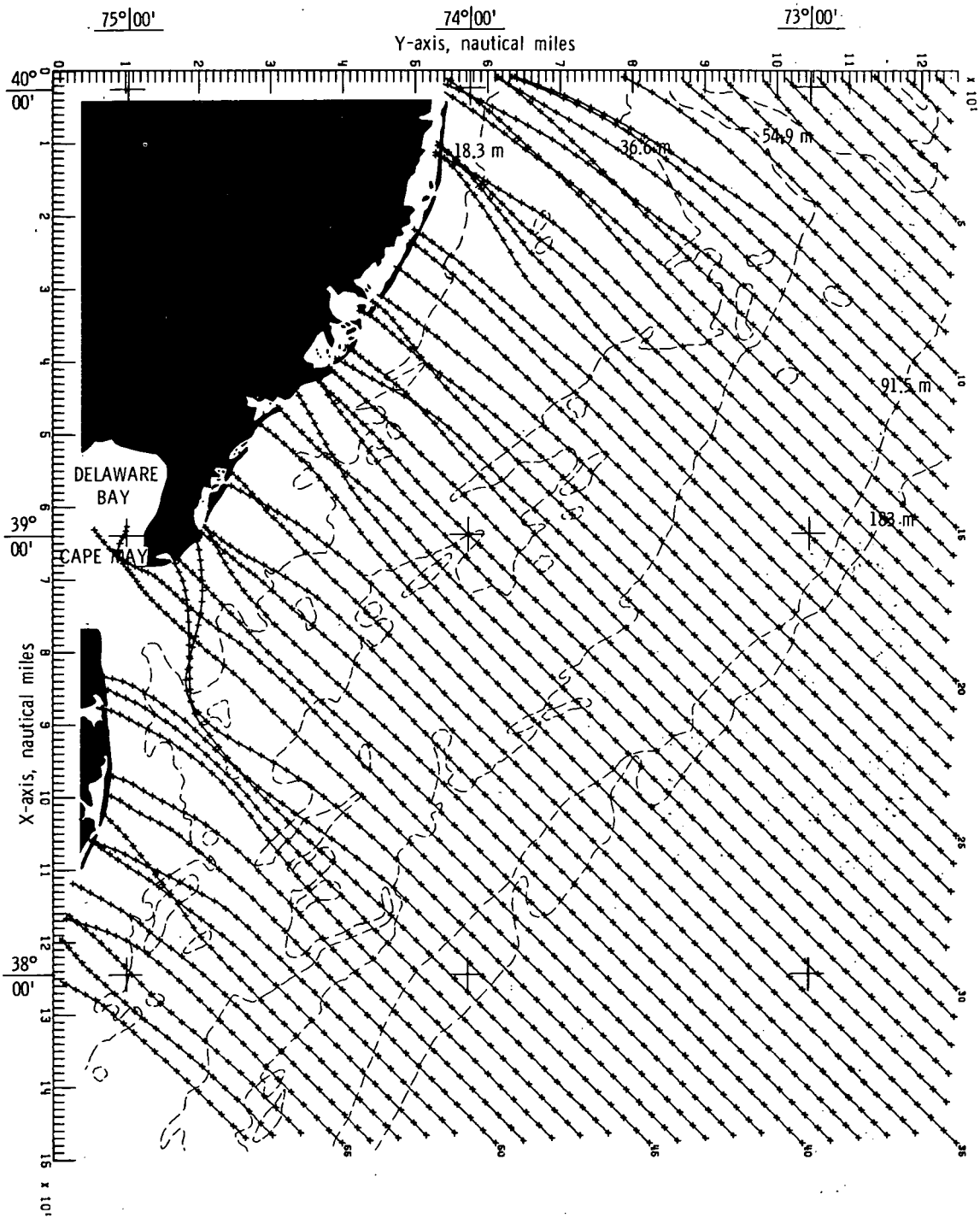


(a) Bottom topography approximated by quadratic least squares technique.

Figure 38.- Wave refraction diagrams. $\alpha = 135^{o}$; T = 12 seconds.

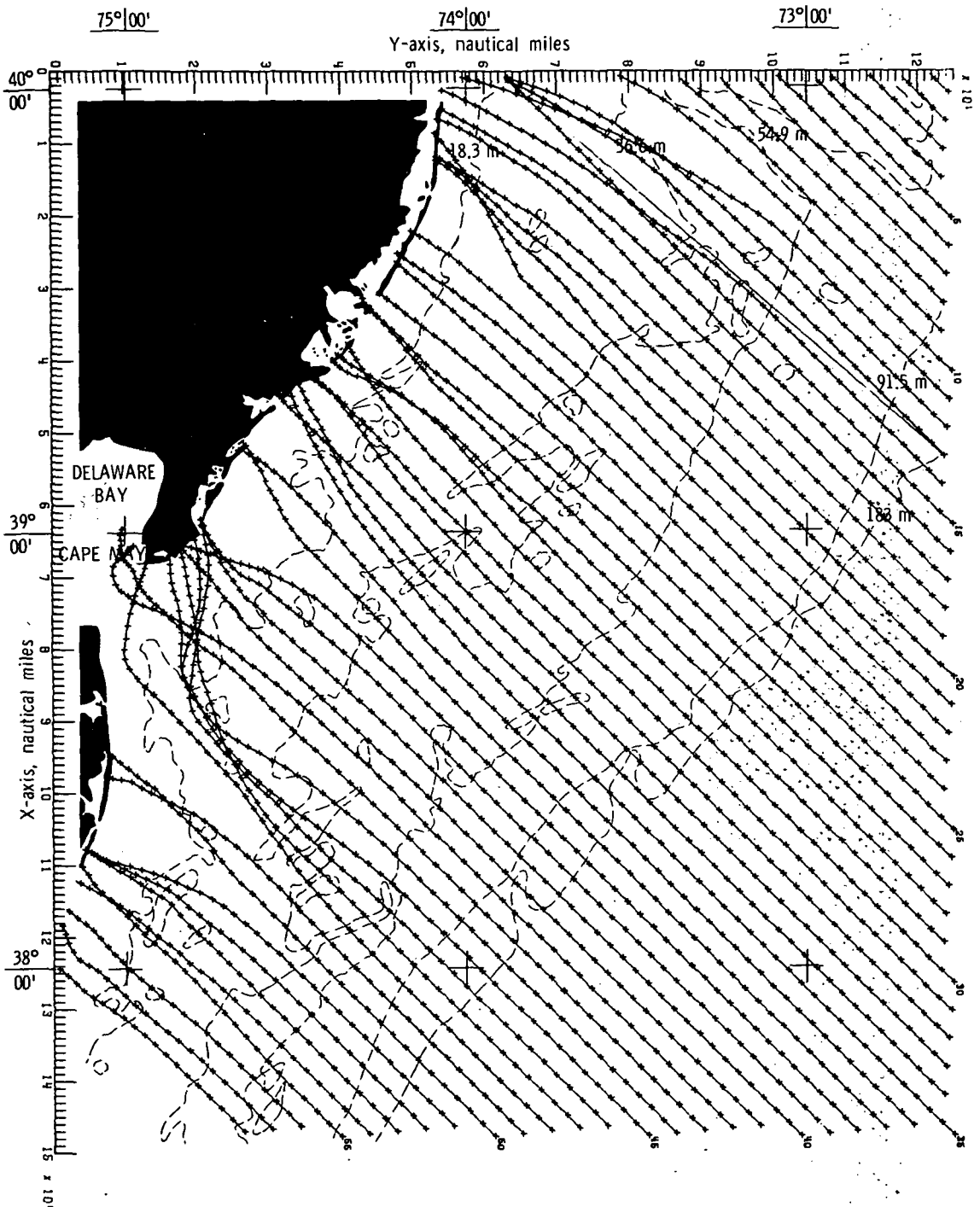


(b) Bottom topography approximated by cubic least squares technique.

Figure 38.- Continued.

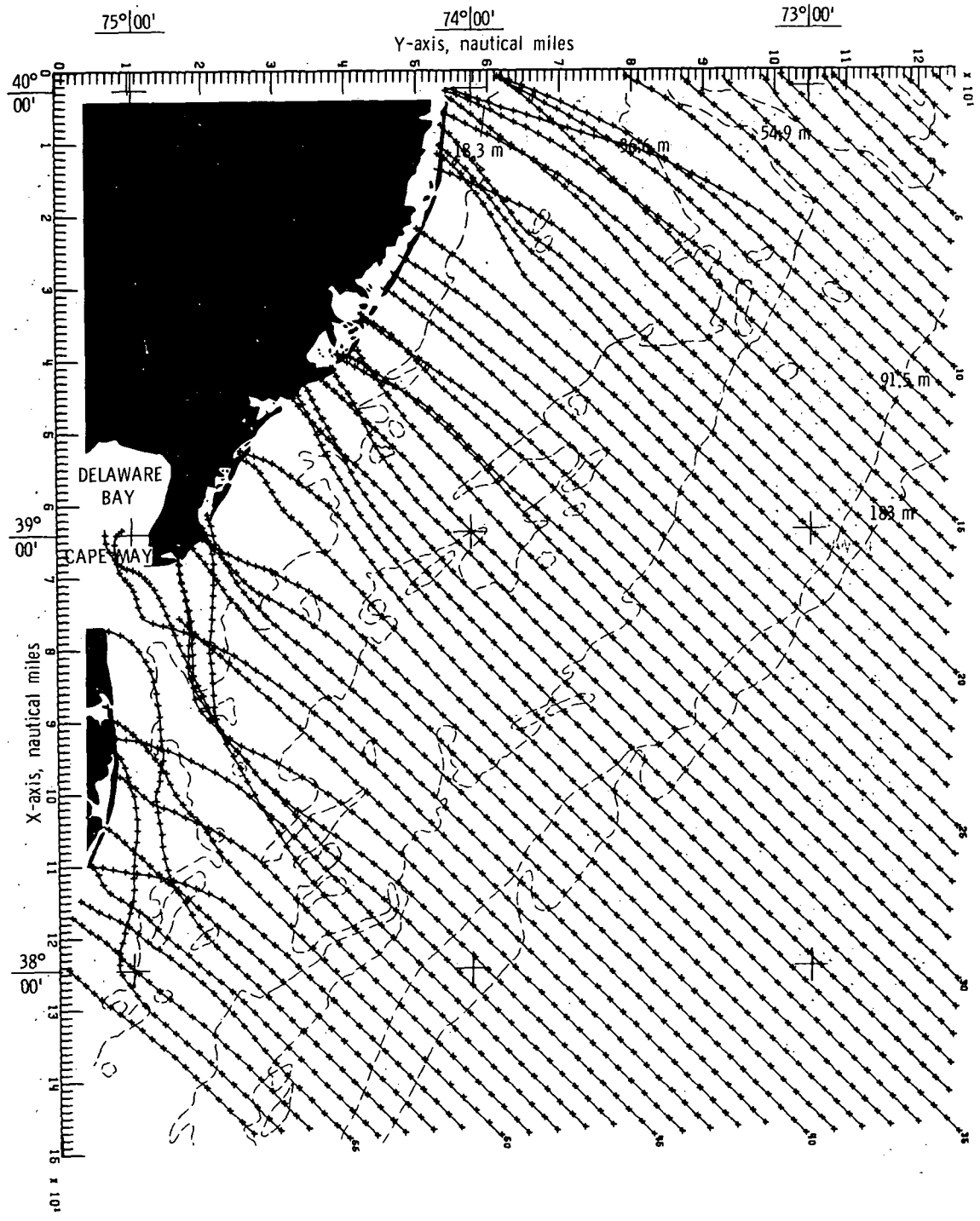


(c) Bottom topography approximated by constrained bicubic interpolation technique.

Figure 38.- Concluded.

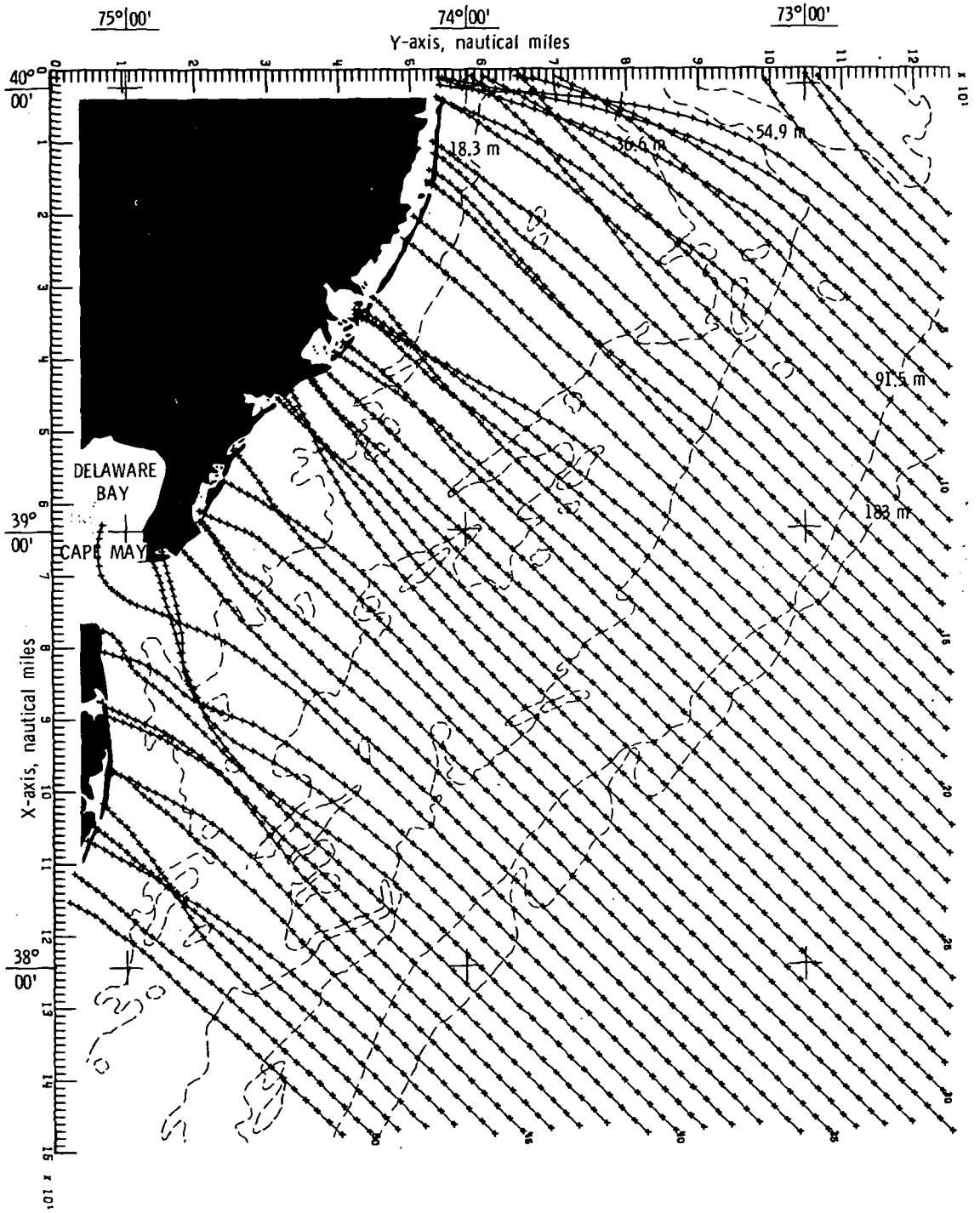


(a) Bottom topography approximated by quadratic least squares technique.

Figure 39.- Wave refraction diagrams. $\alpha = 135^{o}$; $T = 14$ seconds.

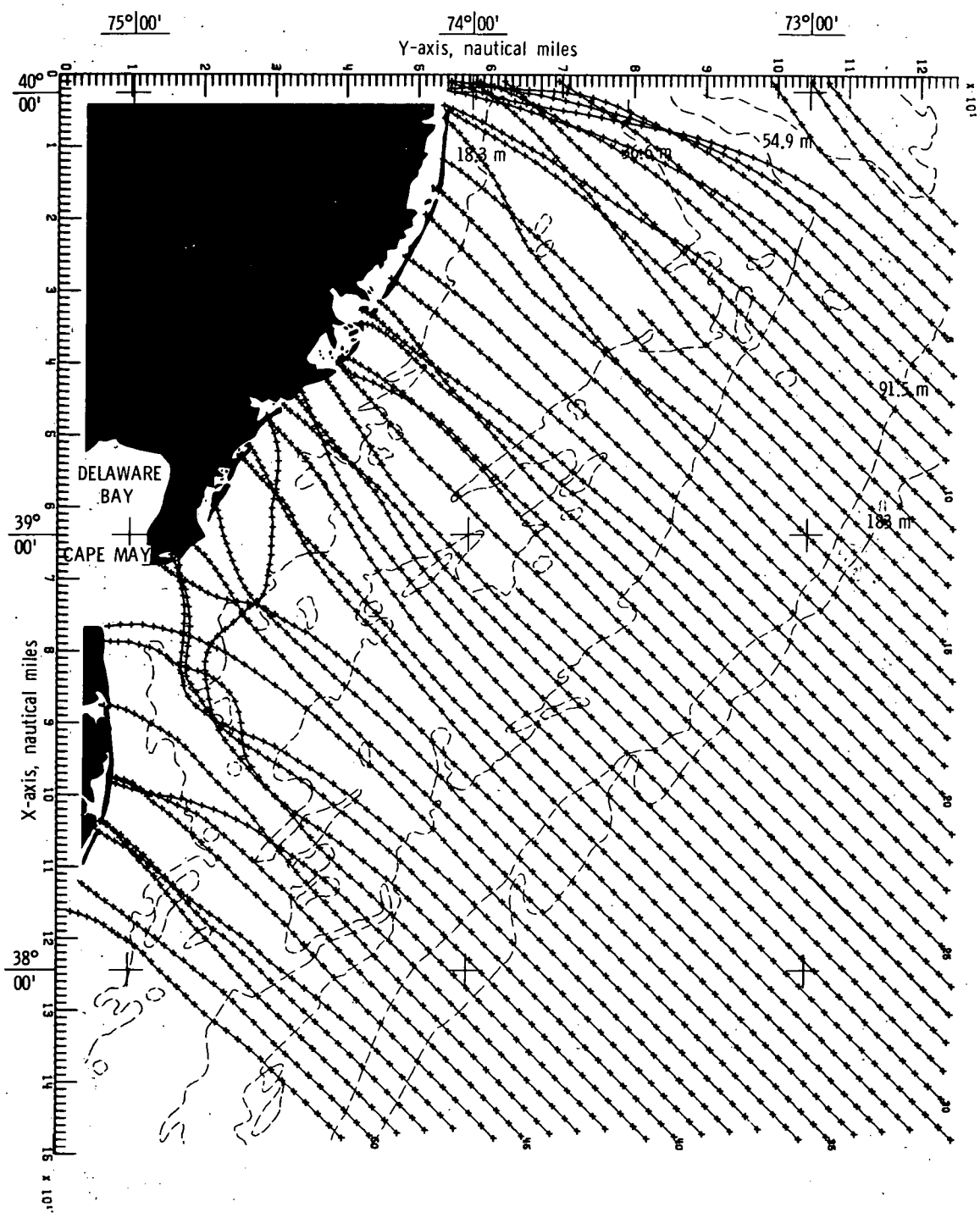


(b) Bottom topography approximated by cubic least squares technique.

Figure 39.- Continued.

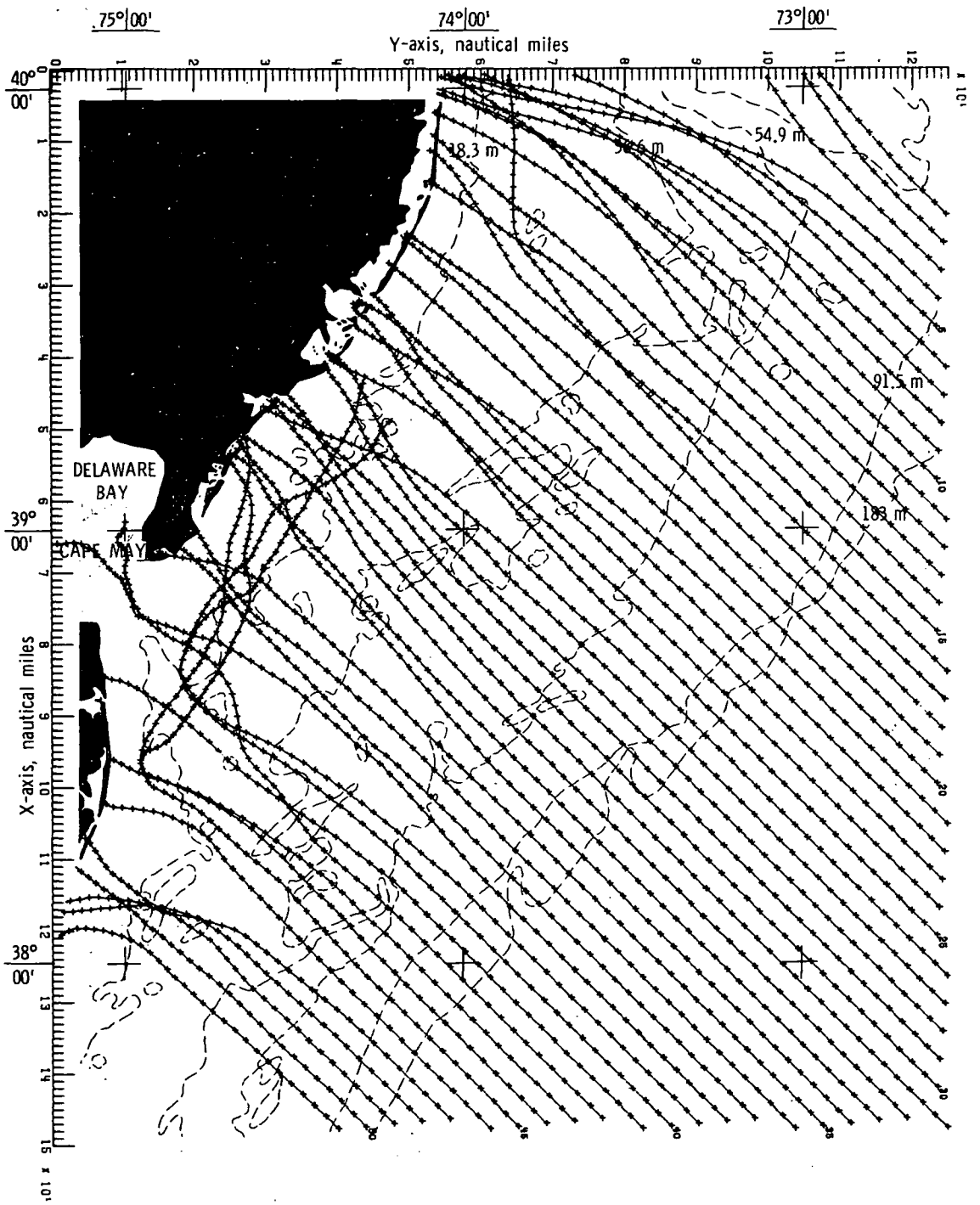


(c) Bottom topography approximated by constrained bicubic interpolation technique.

Figure 39.- Concluded.

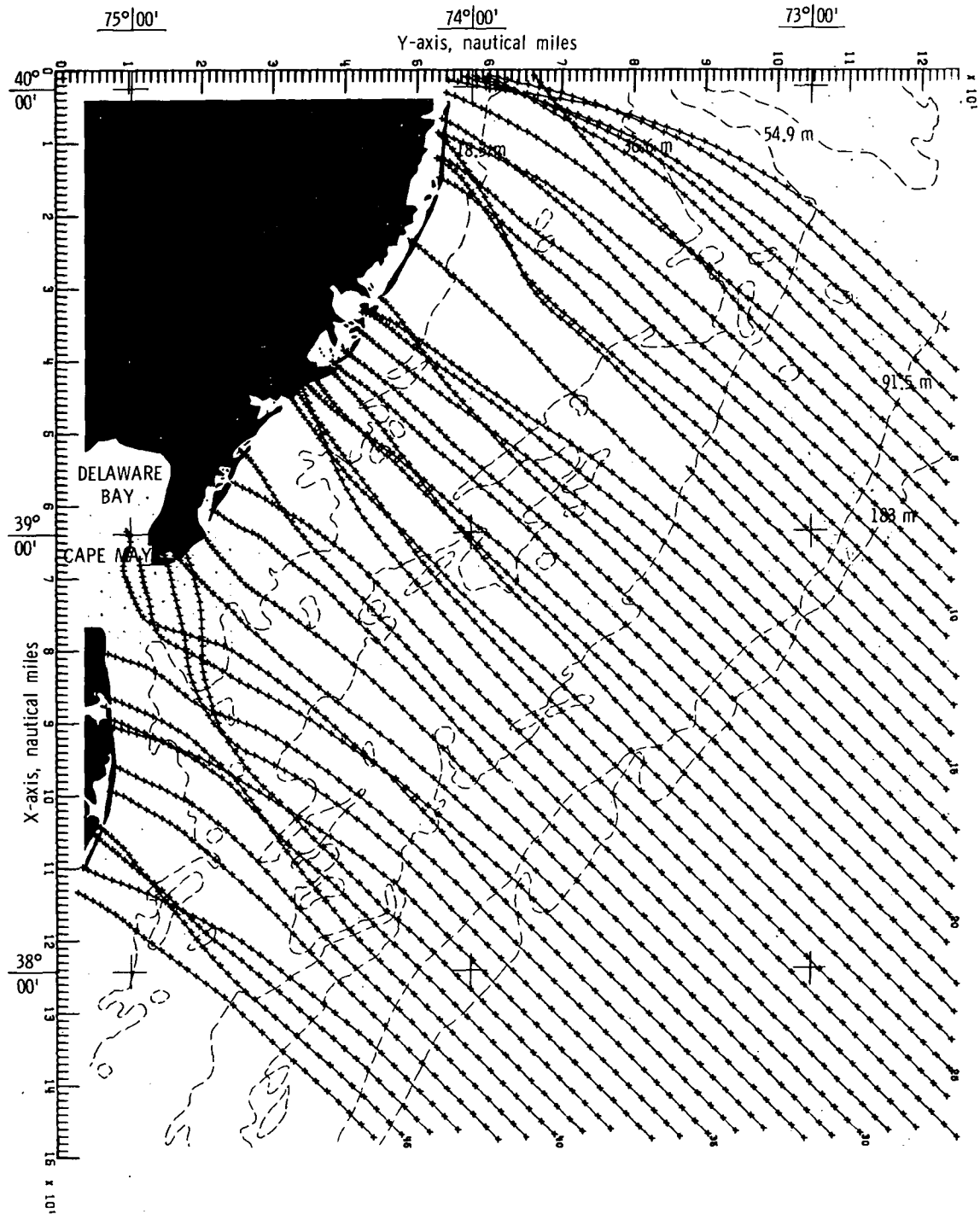


(a) Bottom topography approximated by quadratic least squares technique.

Figure 40.- Wave refraction diagrams. $\alpha = 135^{o}$; T = 16 seconds.

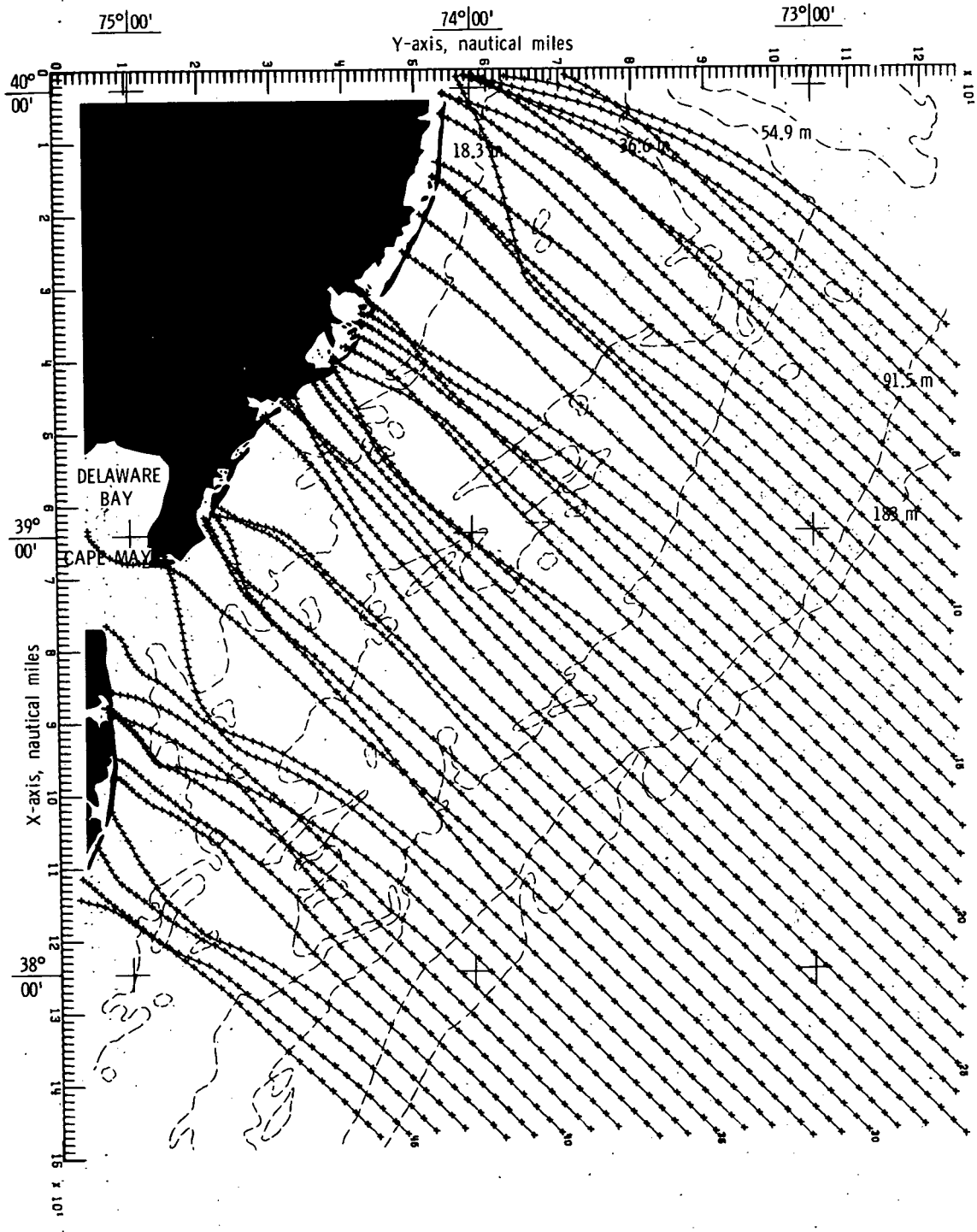


(b) Bottom topography approximated by cubic least squares technique.

Figure 40.- Continued.

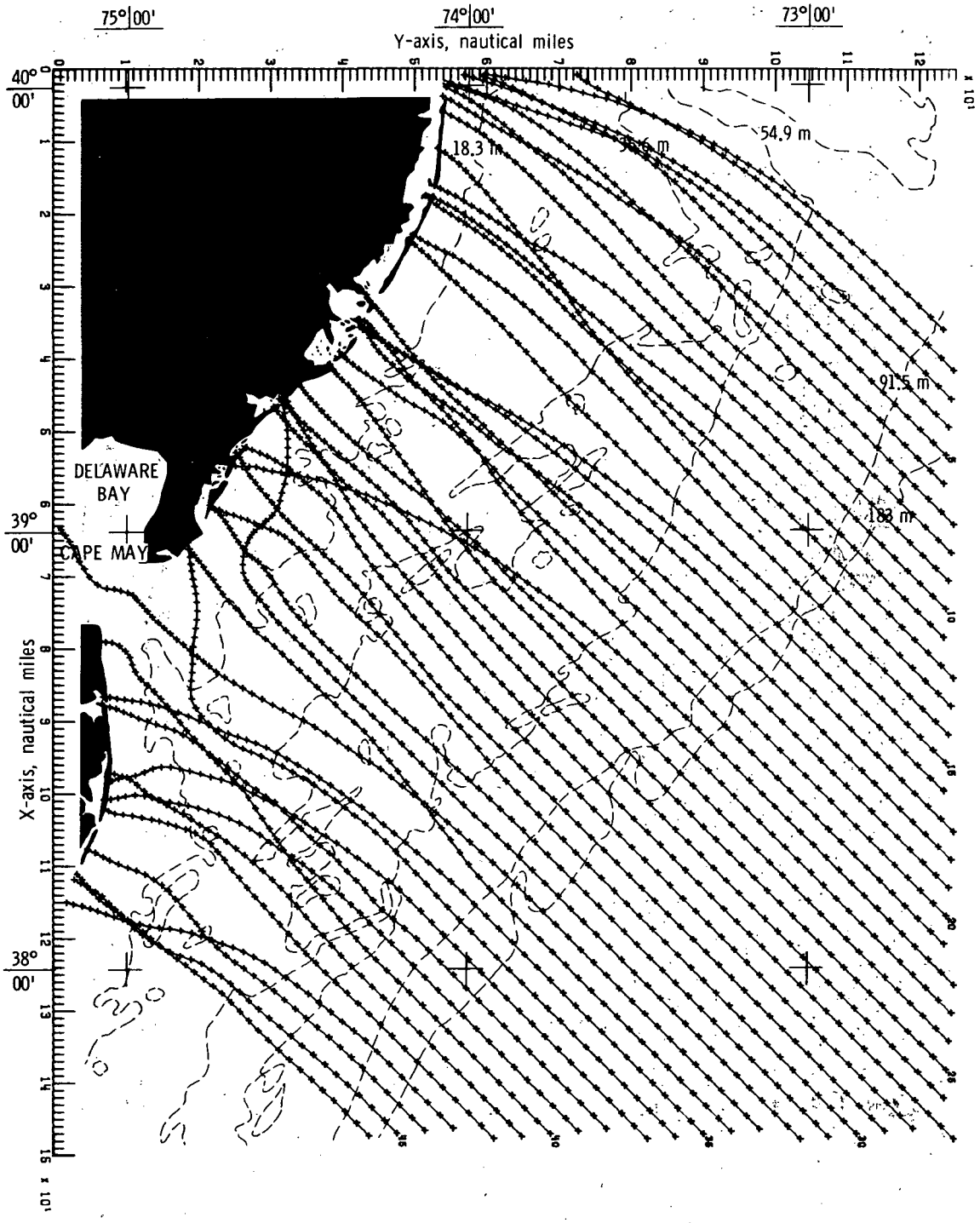


(c) Bottom topography approximated by constrained bicubic interpolation technique.

Figure 40.- Concluded.

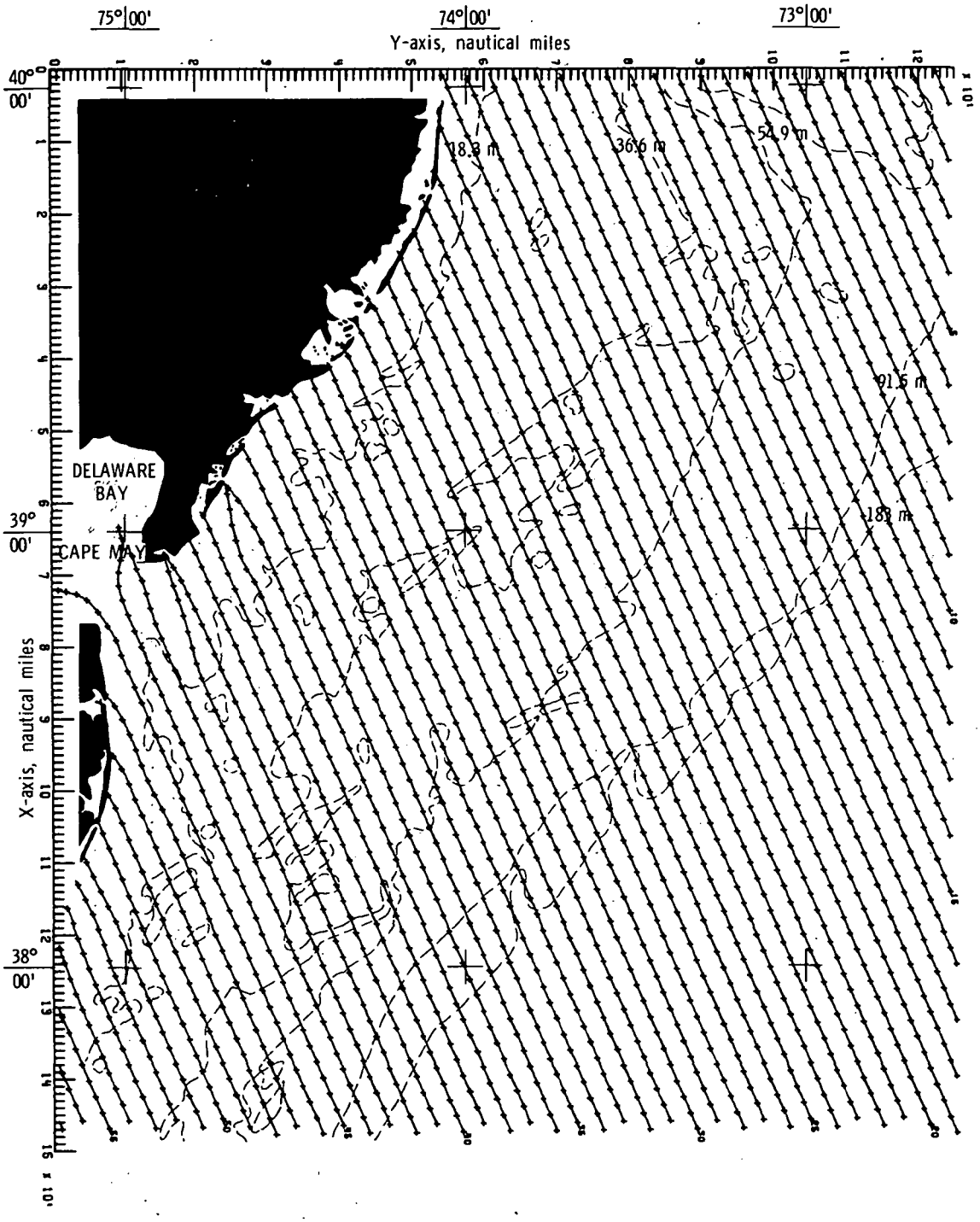


(a) Bottom topography approximated by quadratic least squares technique.

Figure 41.- Wave refraction diagrams. $\alpha = 157.5^{o}$; T = 6 seconds.

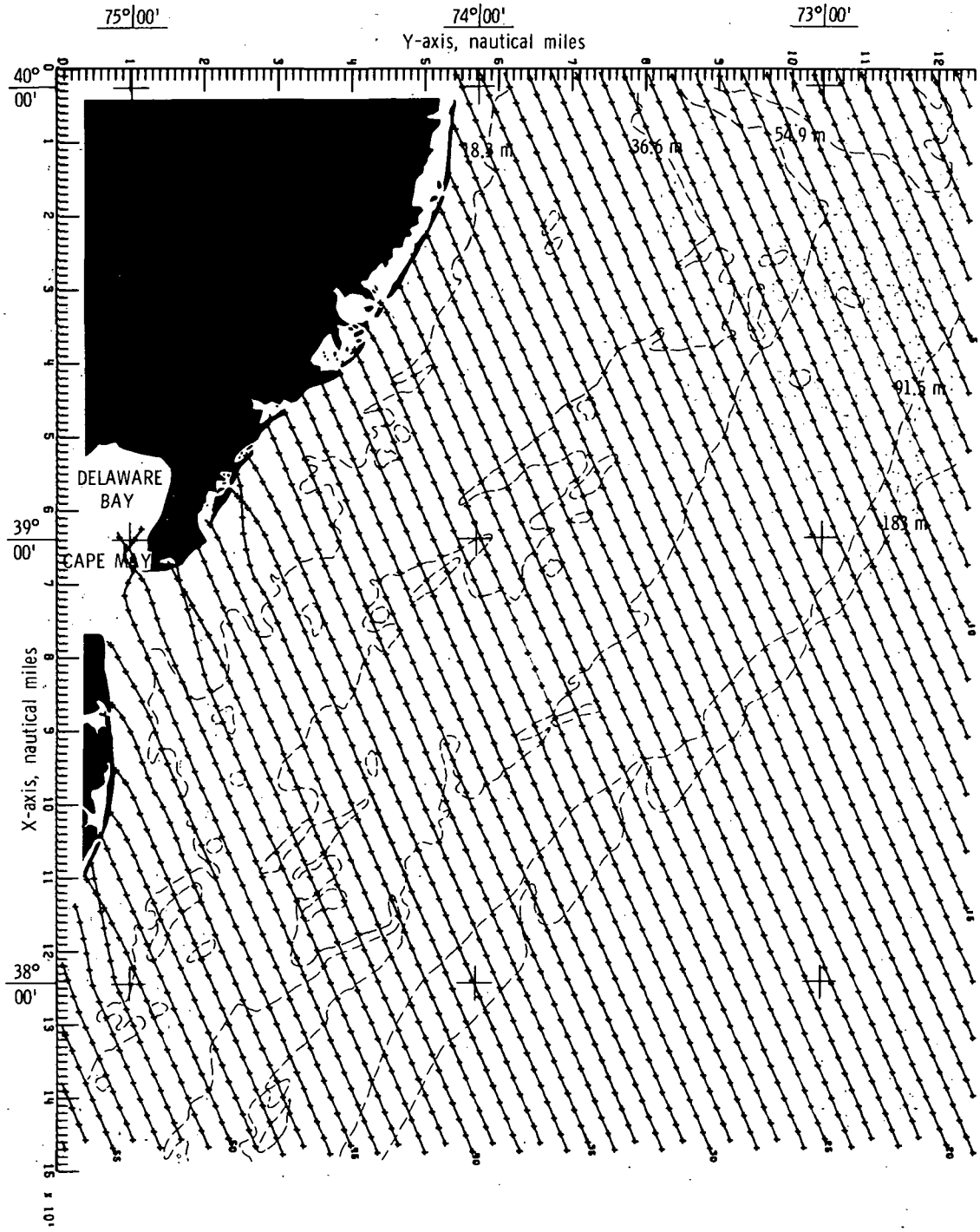


(b) Bottom topography approximated by cubic least squares technique.

Figure 41.- Continued.

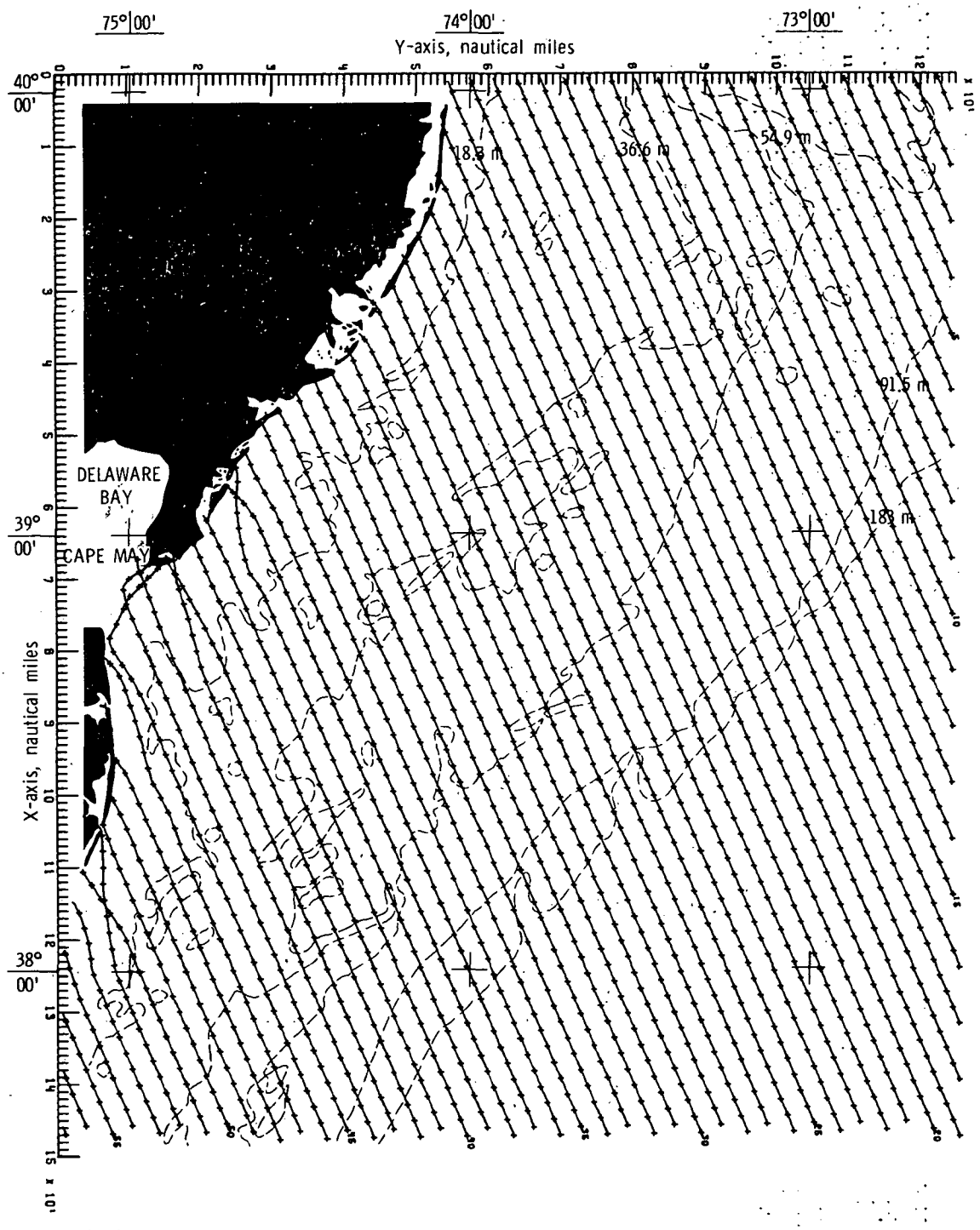


(c) Bottom topography approximated by constrained bicubic interpolation technique.

Figure 41.- Concluded.

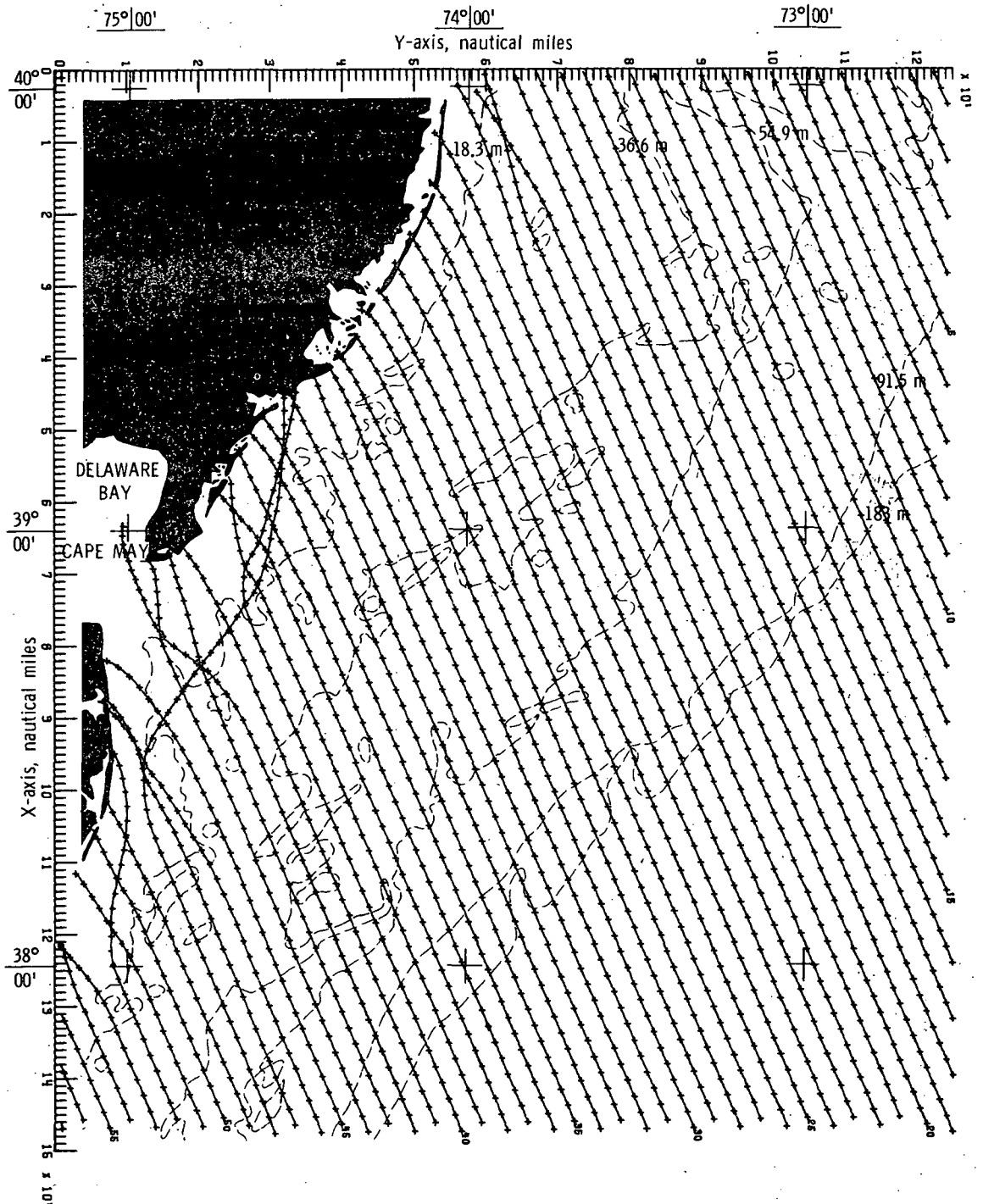


(a) Bottom topography approximated by quadratic least squares technique.

Figure 42.- Wave refraction diagrams. $\alpha$ = 157.5°; T = 8 seconds.

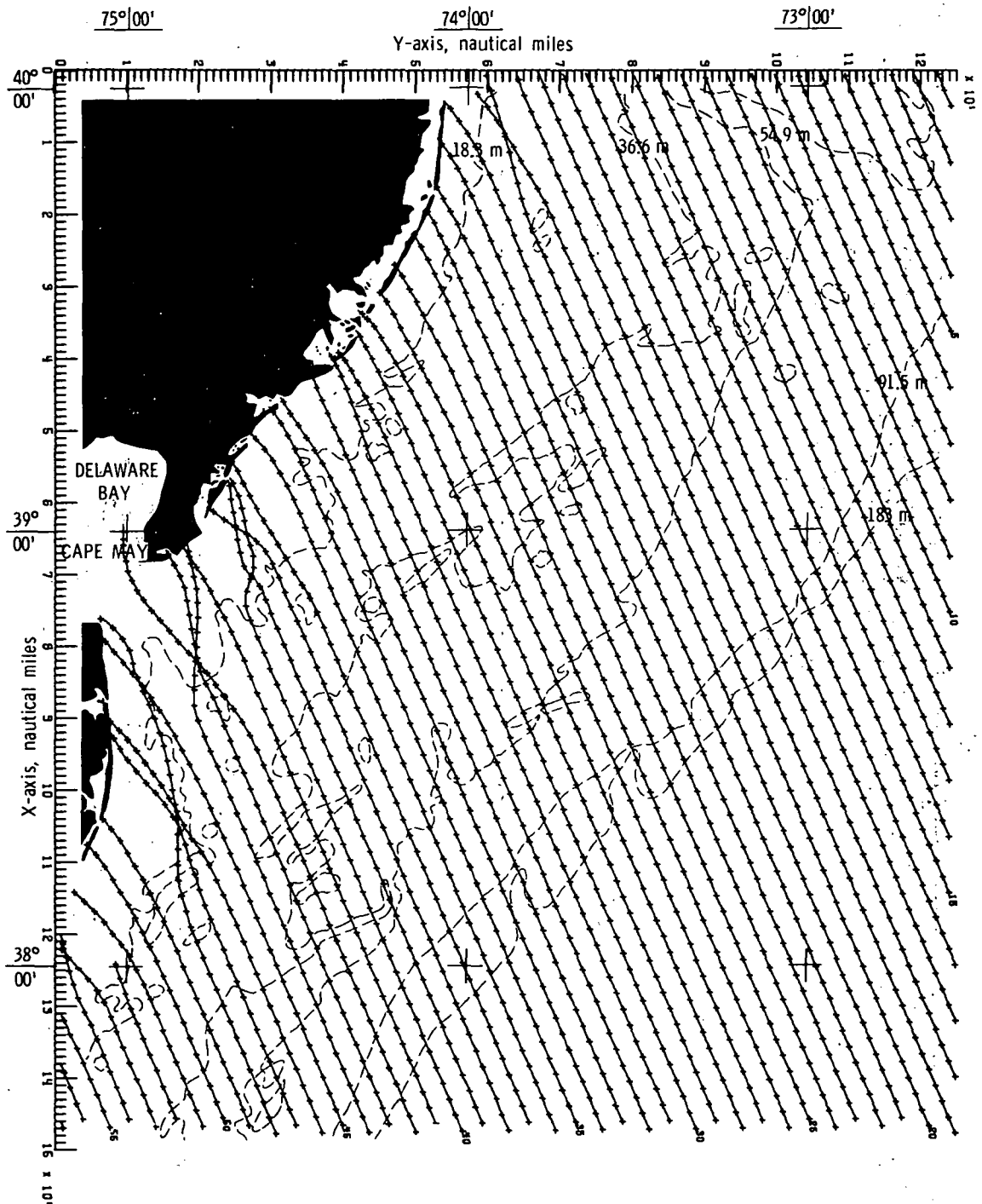


(b) Bottom topography approximated by cubic least squares technique.

Figure 42.- Continued.

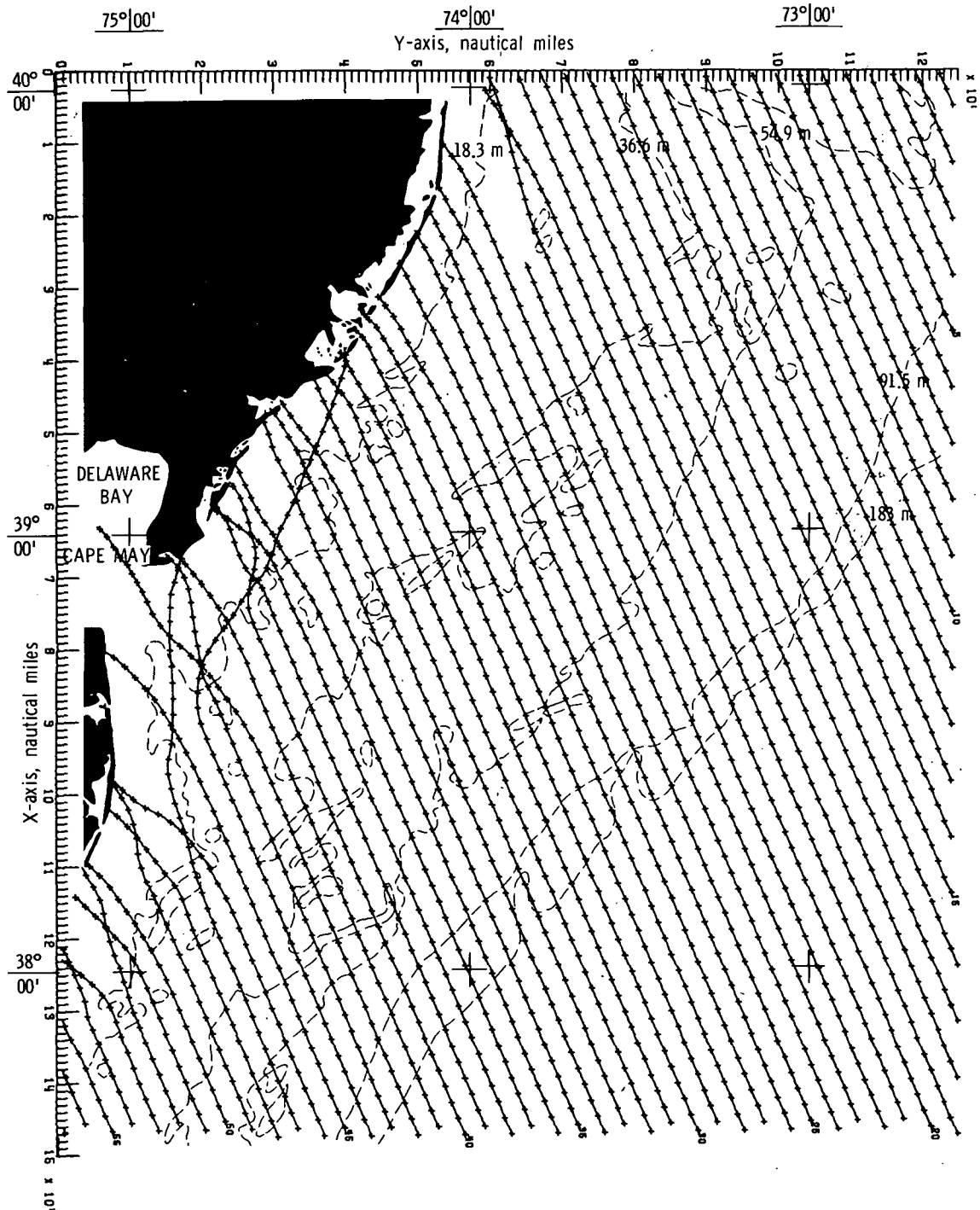


(c) Bottom topography approximated by constrained bicubic interpolation technique.

Figure 42.- Concluded.

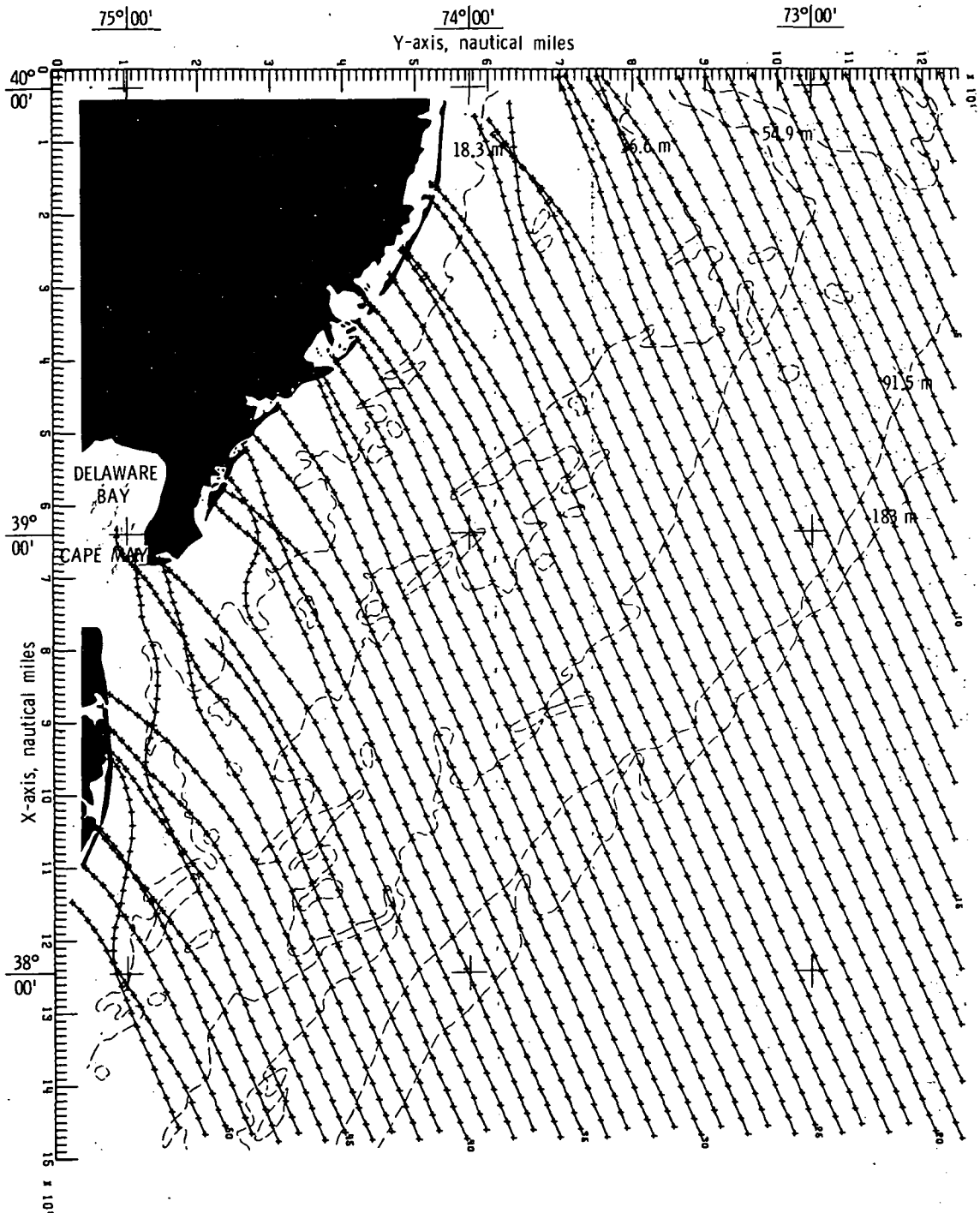


(a) Bottom topography approximated by quadratic least squares technique.

Figure 43.- Wave refraction diagrams. $\alpha = 157.5^{o}$; T = 10 seconds.

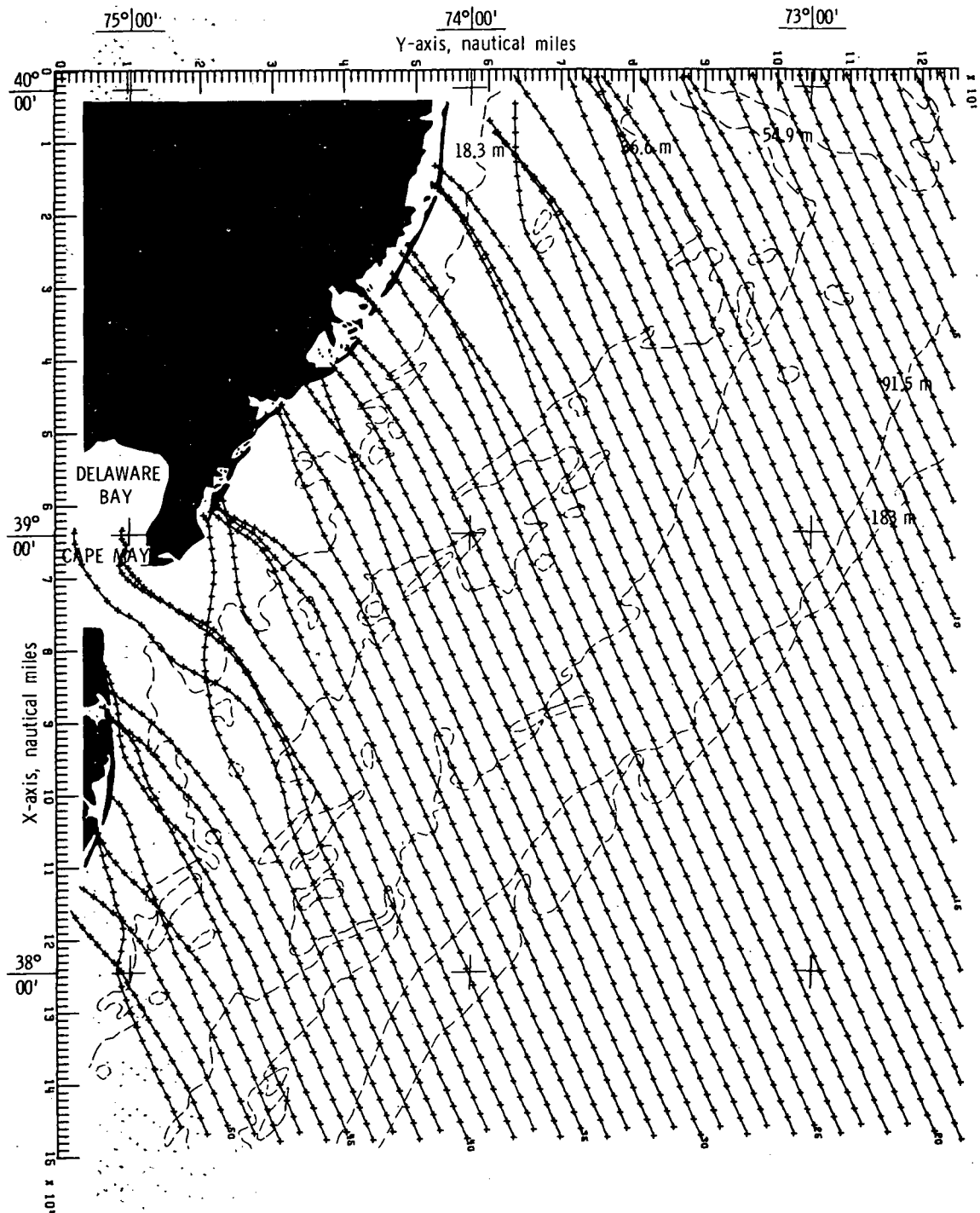


(b) Bottom topography approximated by cubic least squares technique.

Figure 43.- Continued.

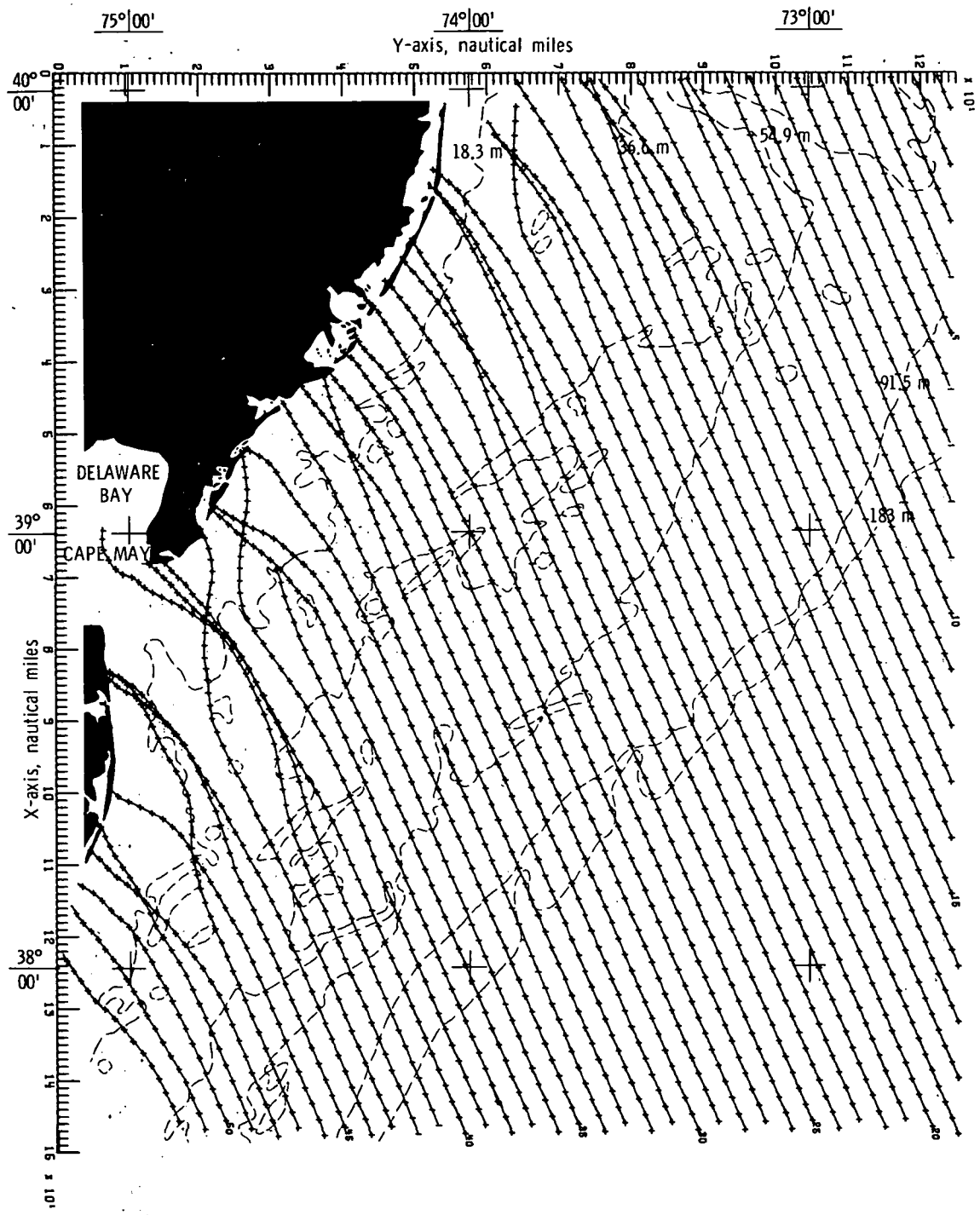


(c) Bottom topography approximated by constrained bicubic interpolation technique.

Figure 43.- Concluded.

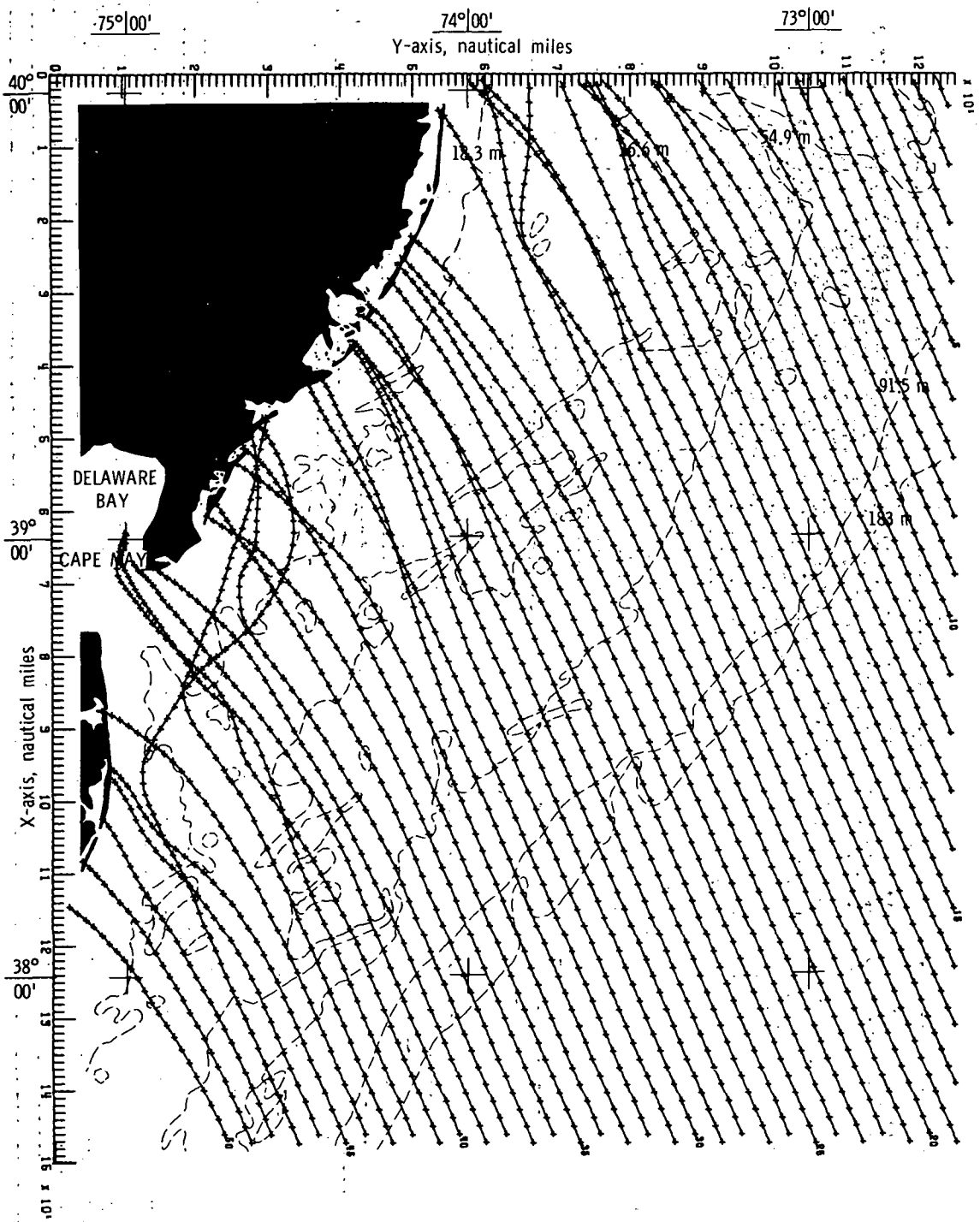


(a) Bottom topography approximated by quadratic least squares technique.

Figure 44.- Wave refraction diagrams. $\alpha = 157.5^{\circ}$; $T = 12$ seconds.

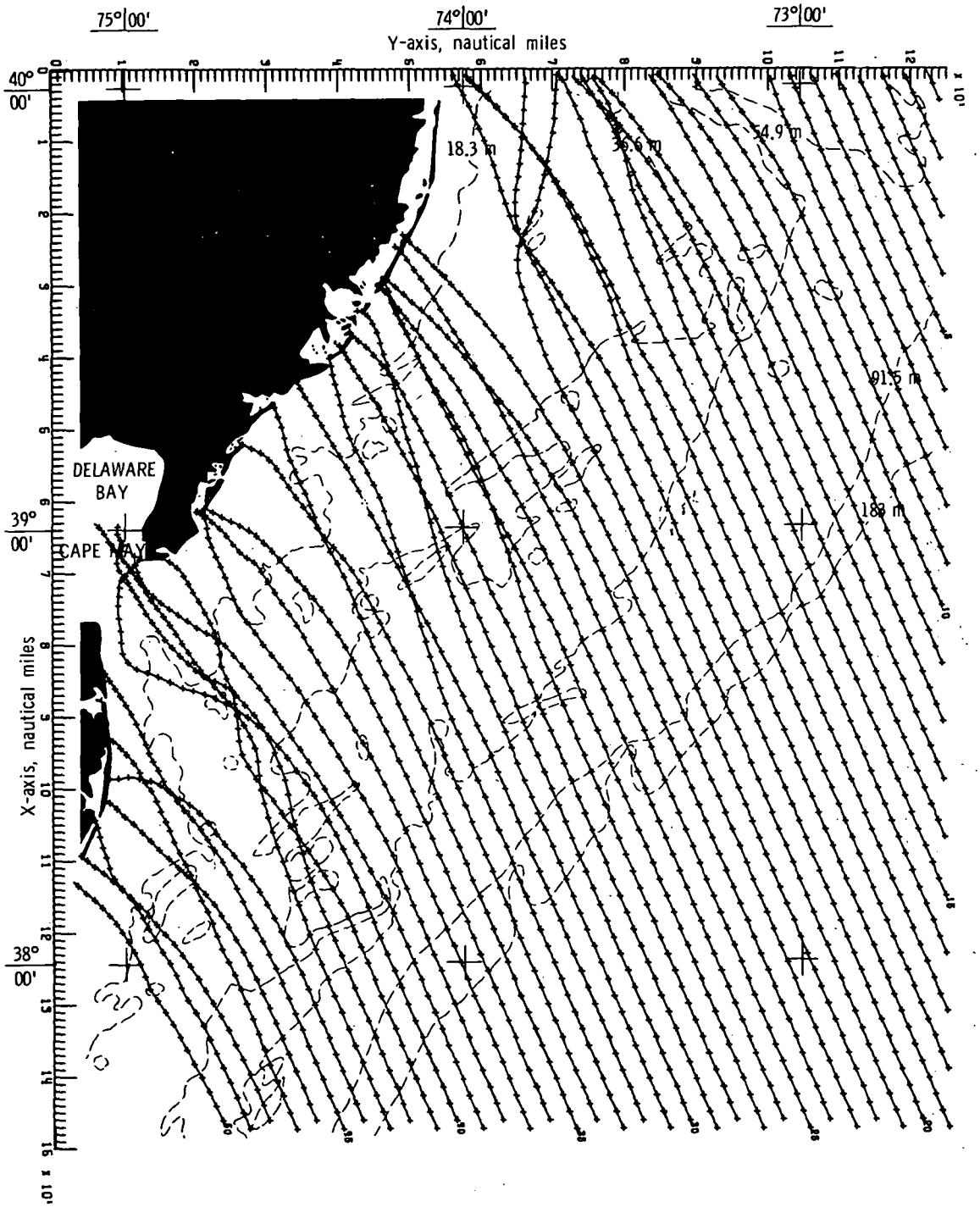


(b) Bottom topography approximated by cubic least squares technique.

Figure 44.- Continued.

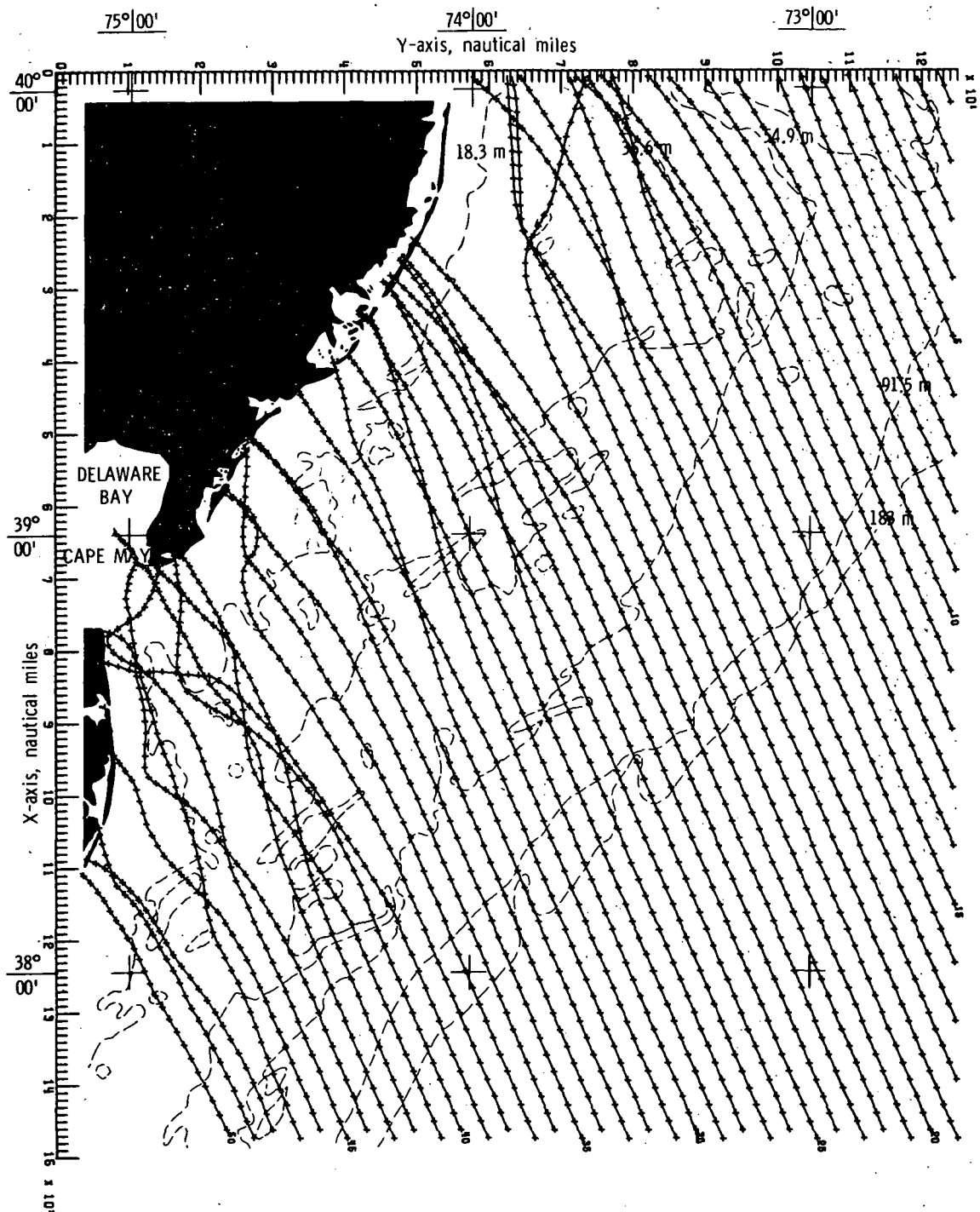


(c) Bottom topography approximated by constrained bicubic interpolation technique.

Figure 44.- Concluded.

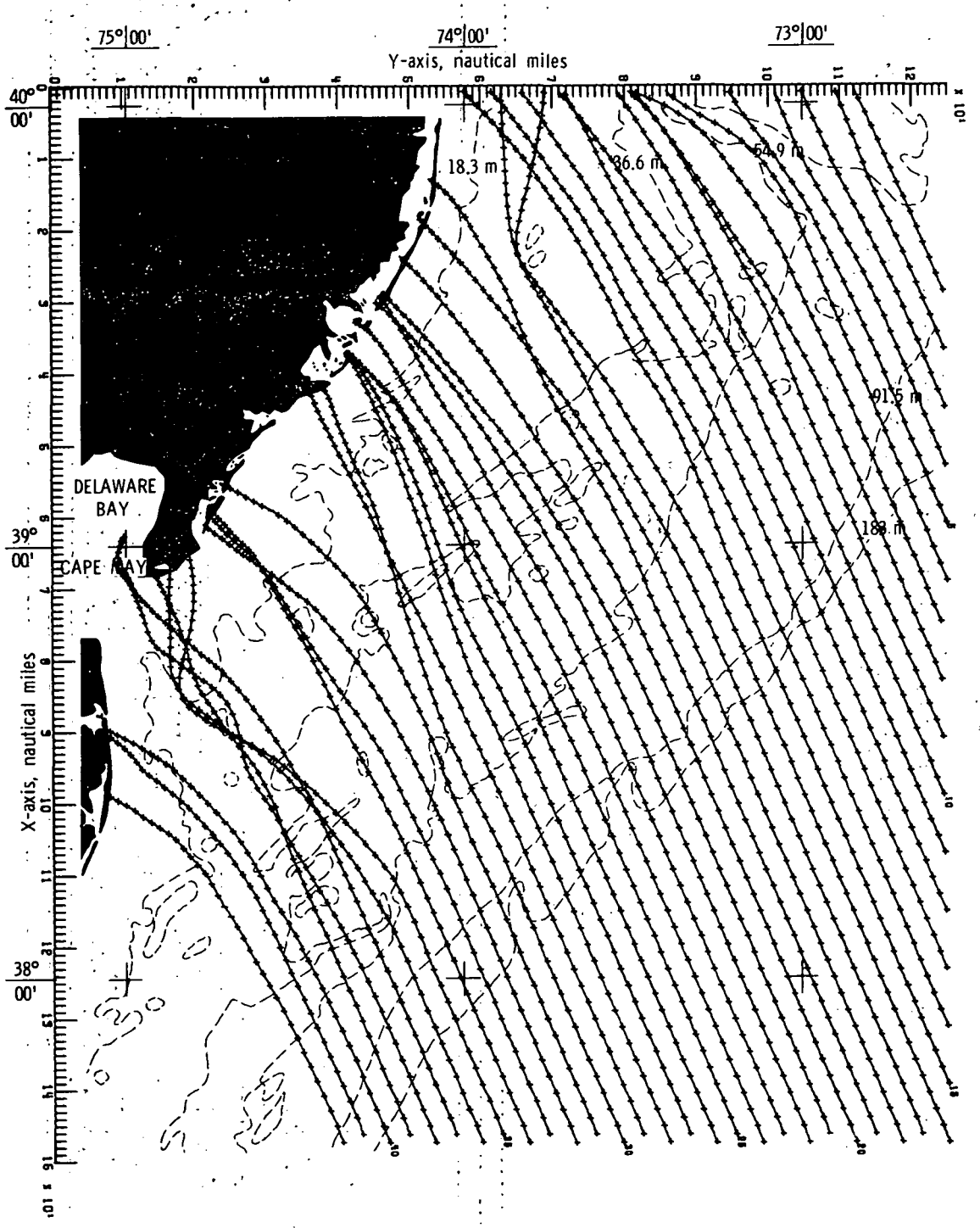


(a) Bottom topography approximated by quadratic least squares technique.

Figure 45.- Wave refraction diagrams. $\alpha = 157.5^{o}$; T = 14 seconds.

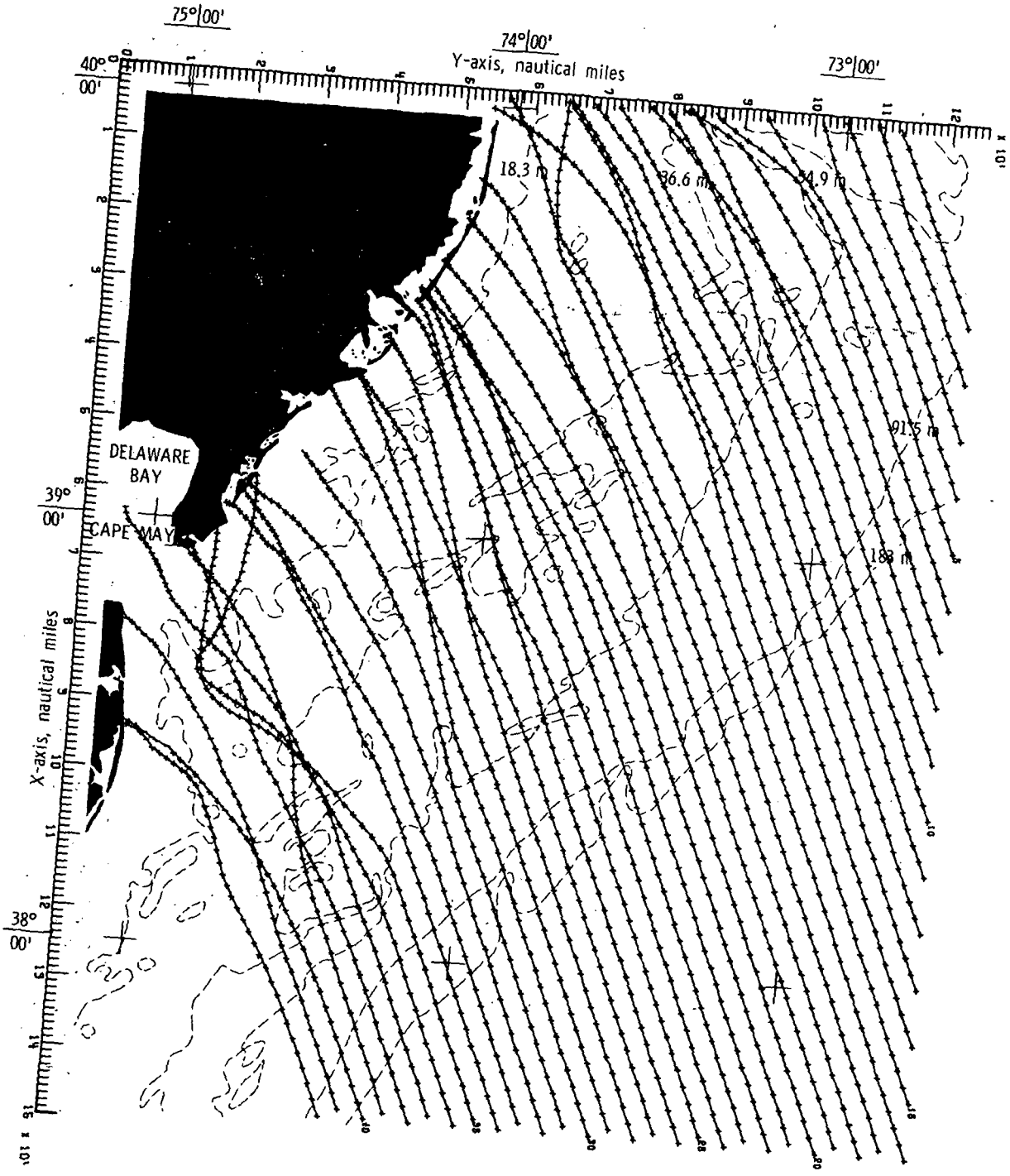


(b) Bottom topography approximated by cubic least squares technique.

Figure 45.- Continued.

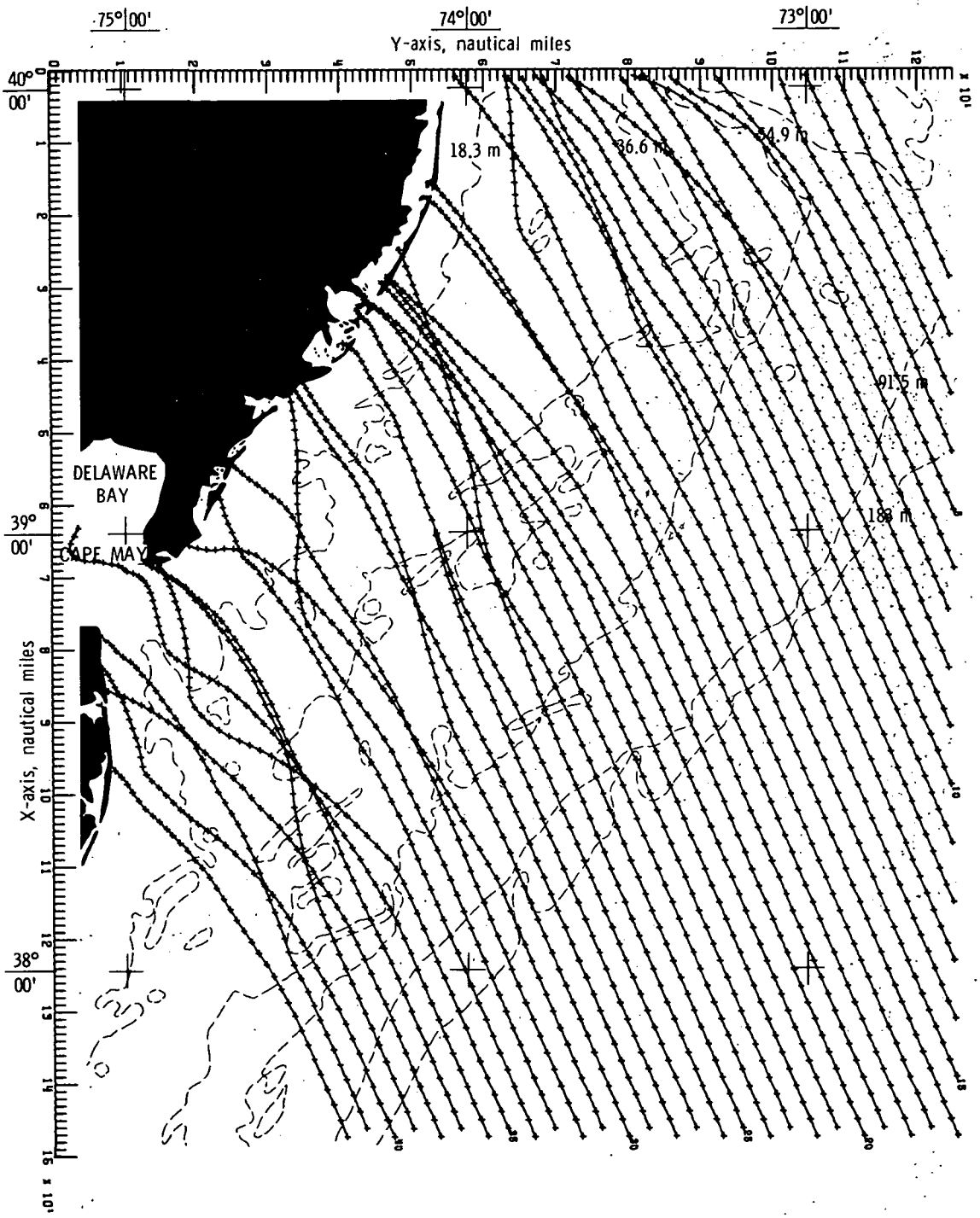


(c) Bottom topography approximated by constrained bicubic interpolation technique.

Figure 45.- Concluded.

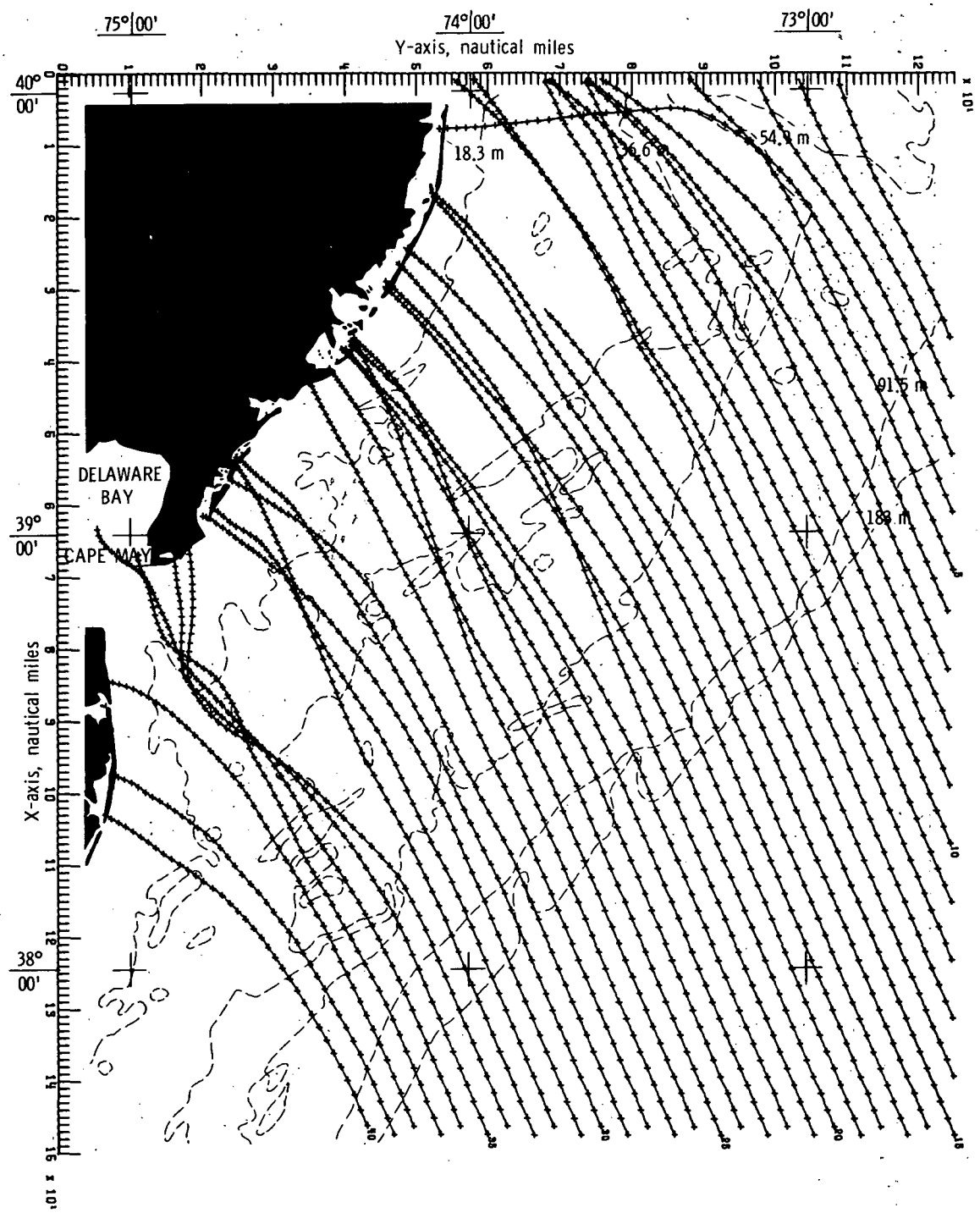


(a) Bottom topography approximated by quadratic least squares technique.

Figure 46.- Wave refraction diagrams. $\alpha$ = 157.5°; T = 16 seconds.

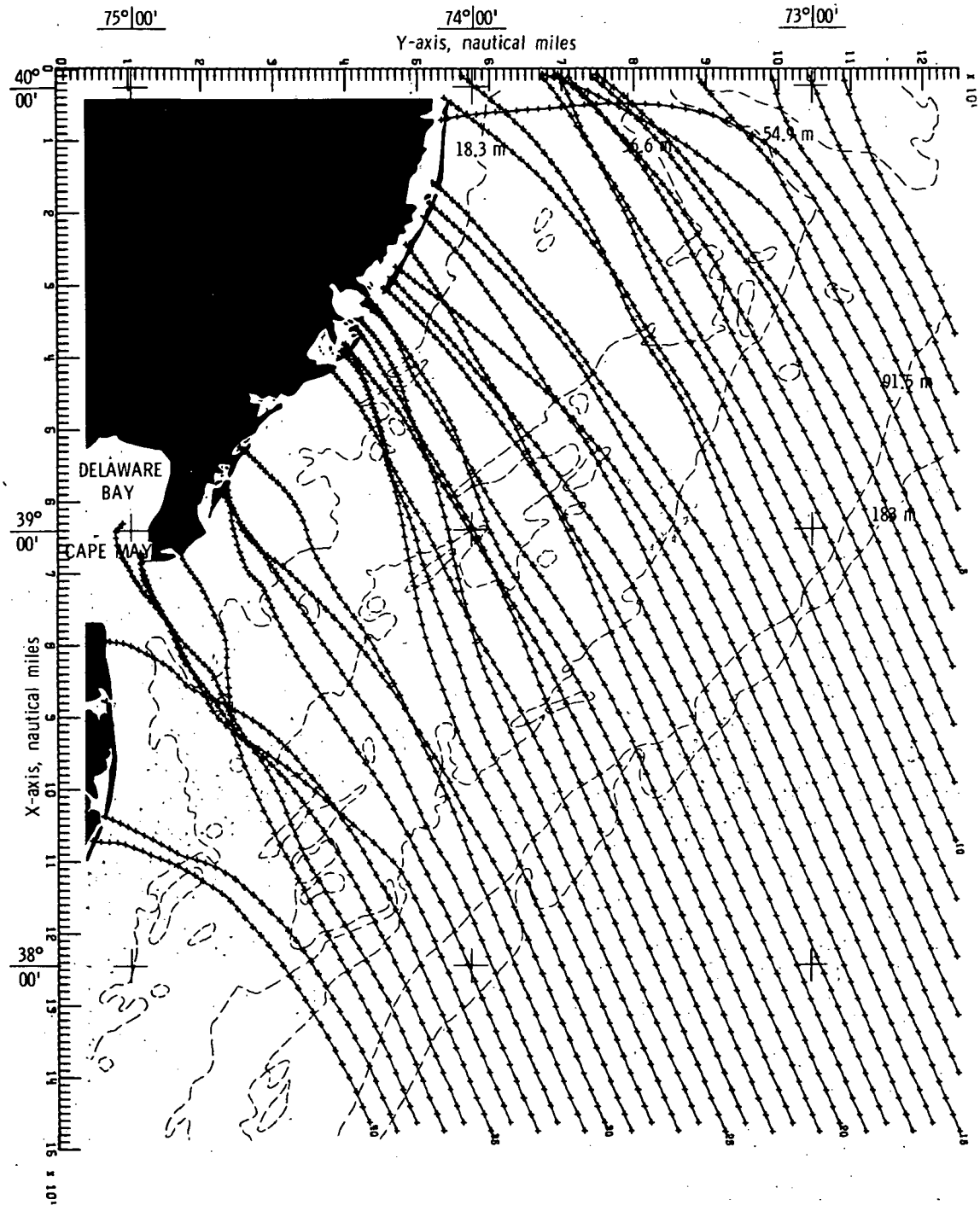


(b) Bottom topography approximated by cubic least squares technique.

Figure 46.- Continued.

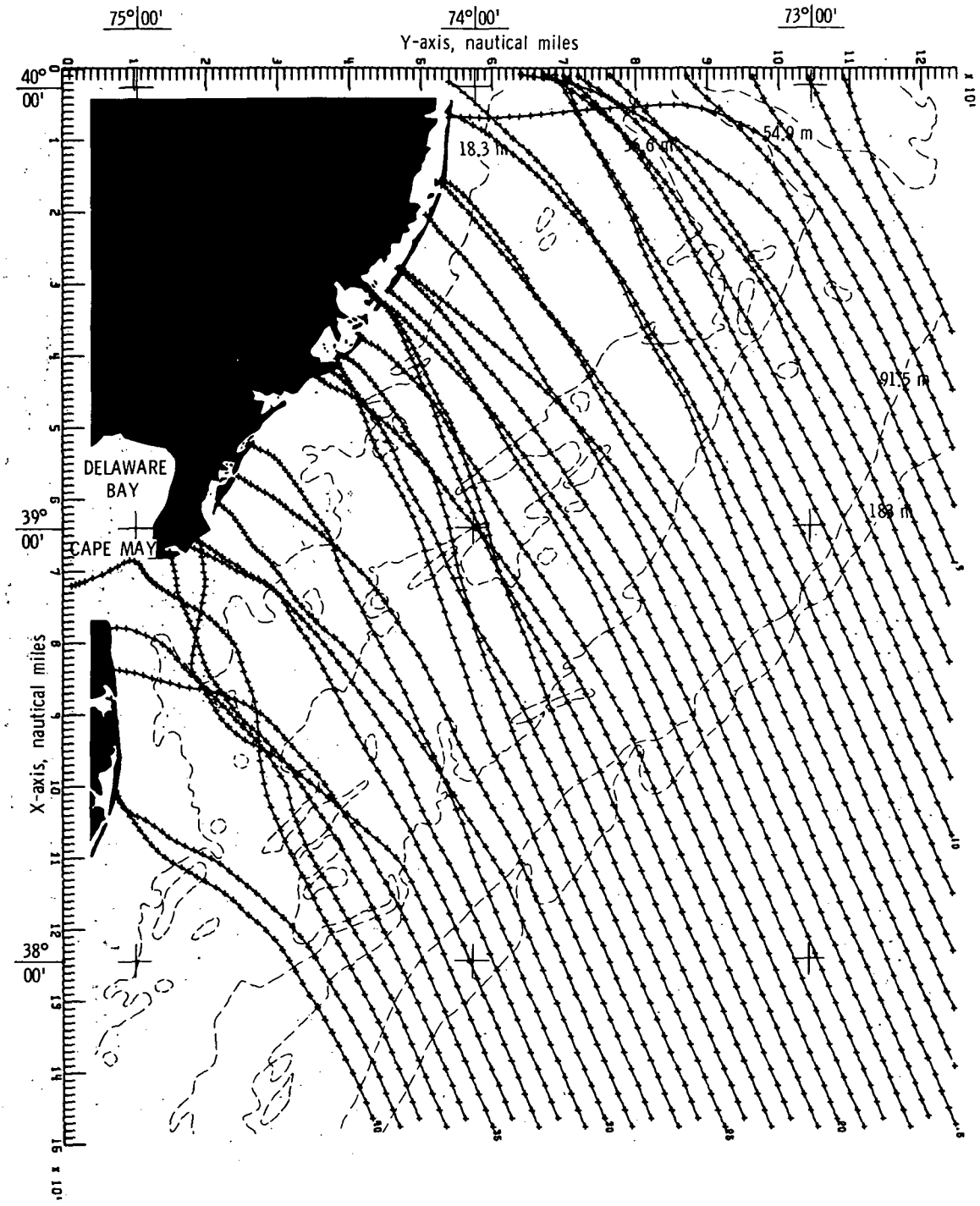


(c) Bottom topography approximated by constrained bicubic interpolation technique.

Figure 46.- Concluded.

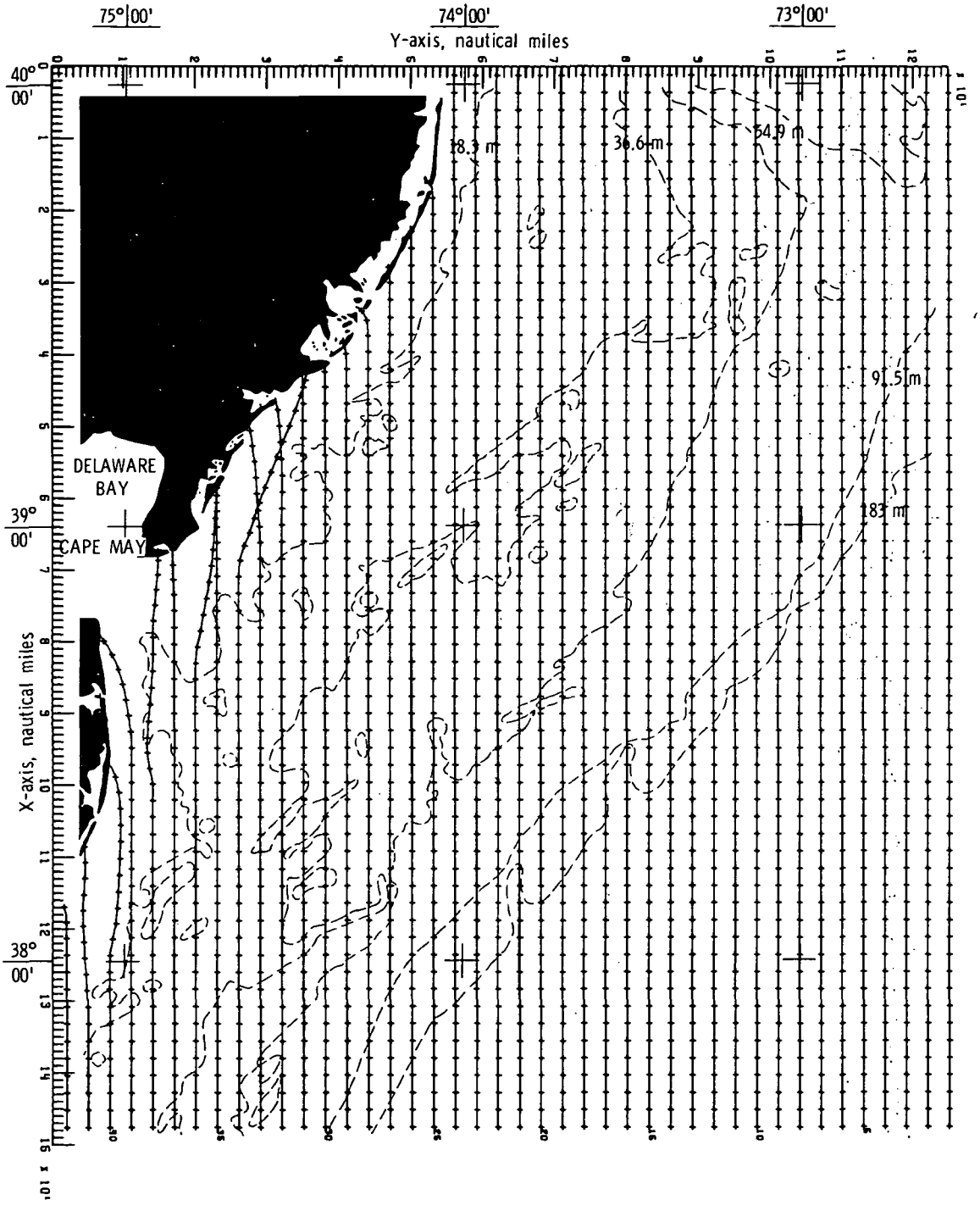


(a) Bottom topography approximated by quadratic least squares technique.

Figure 47.- Wave refraction diagrams. $\alpha = 180^{o}$; T = 6 seconds.

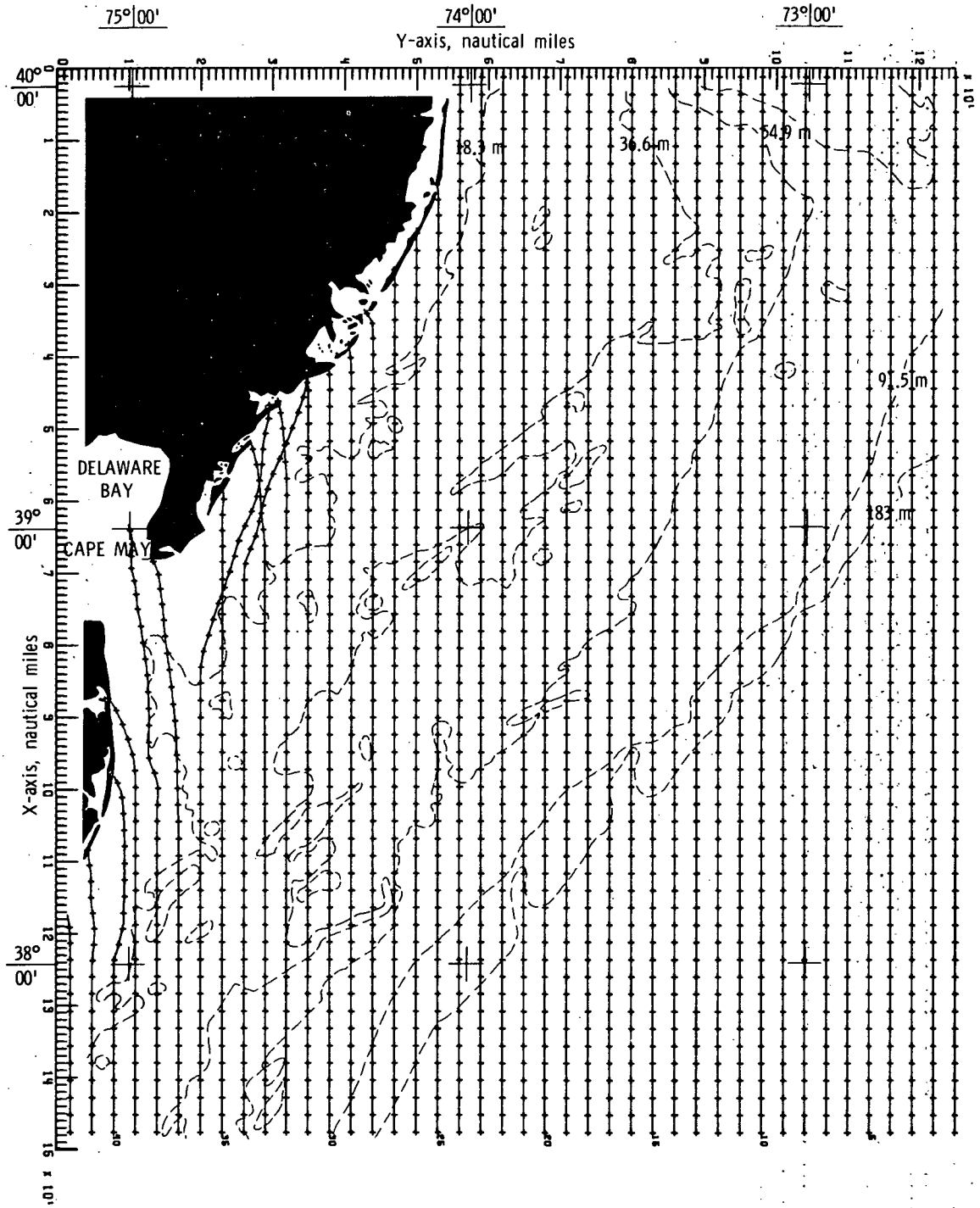


(b) Bottom topography approximated by cubic least squares technique.

Figure 47.- Continued.

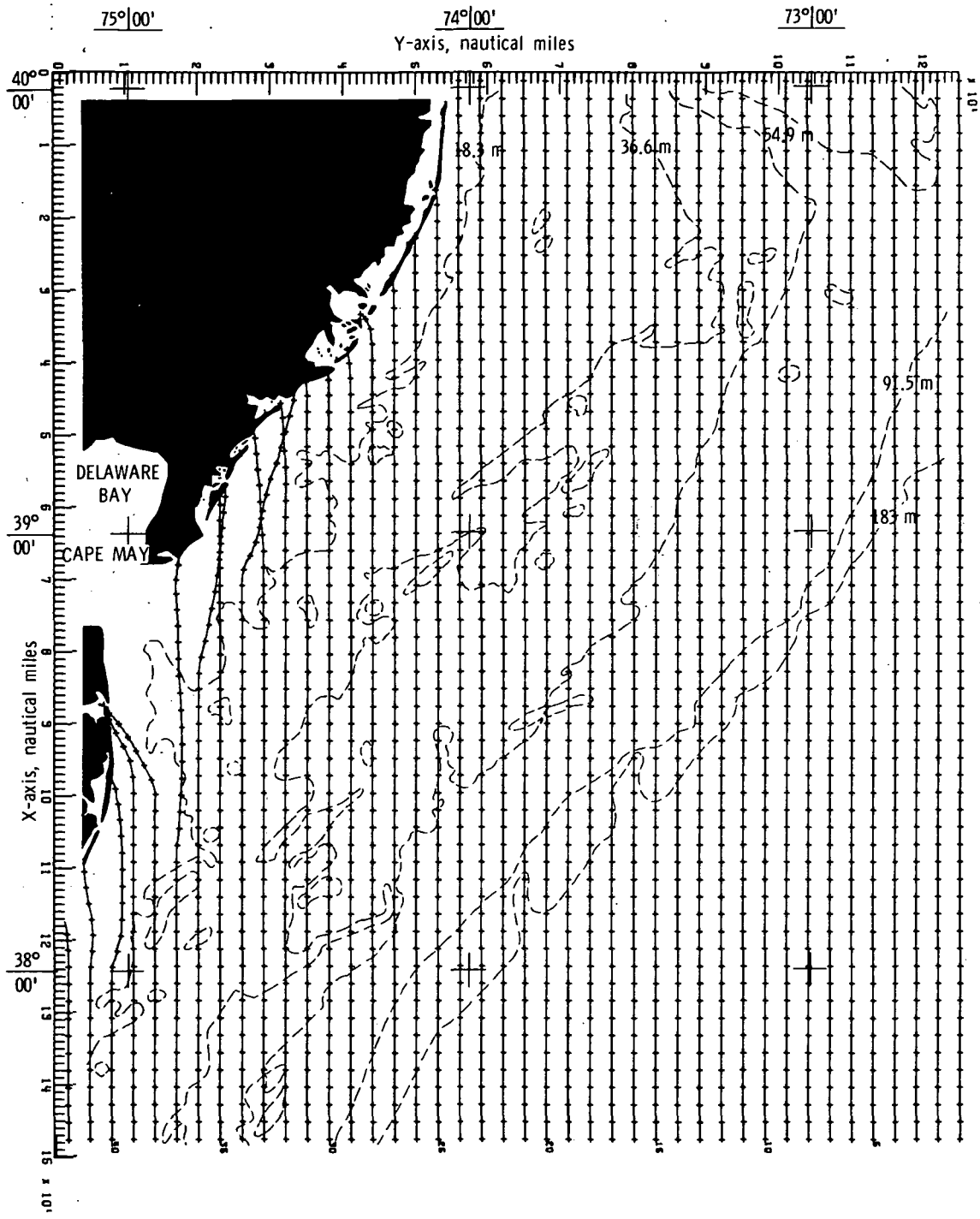


(c) Bottom topography approximated by constrained bicubic interpolation technique.

Figure 47.- Concluded.

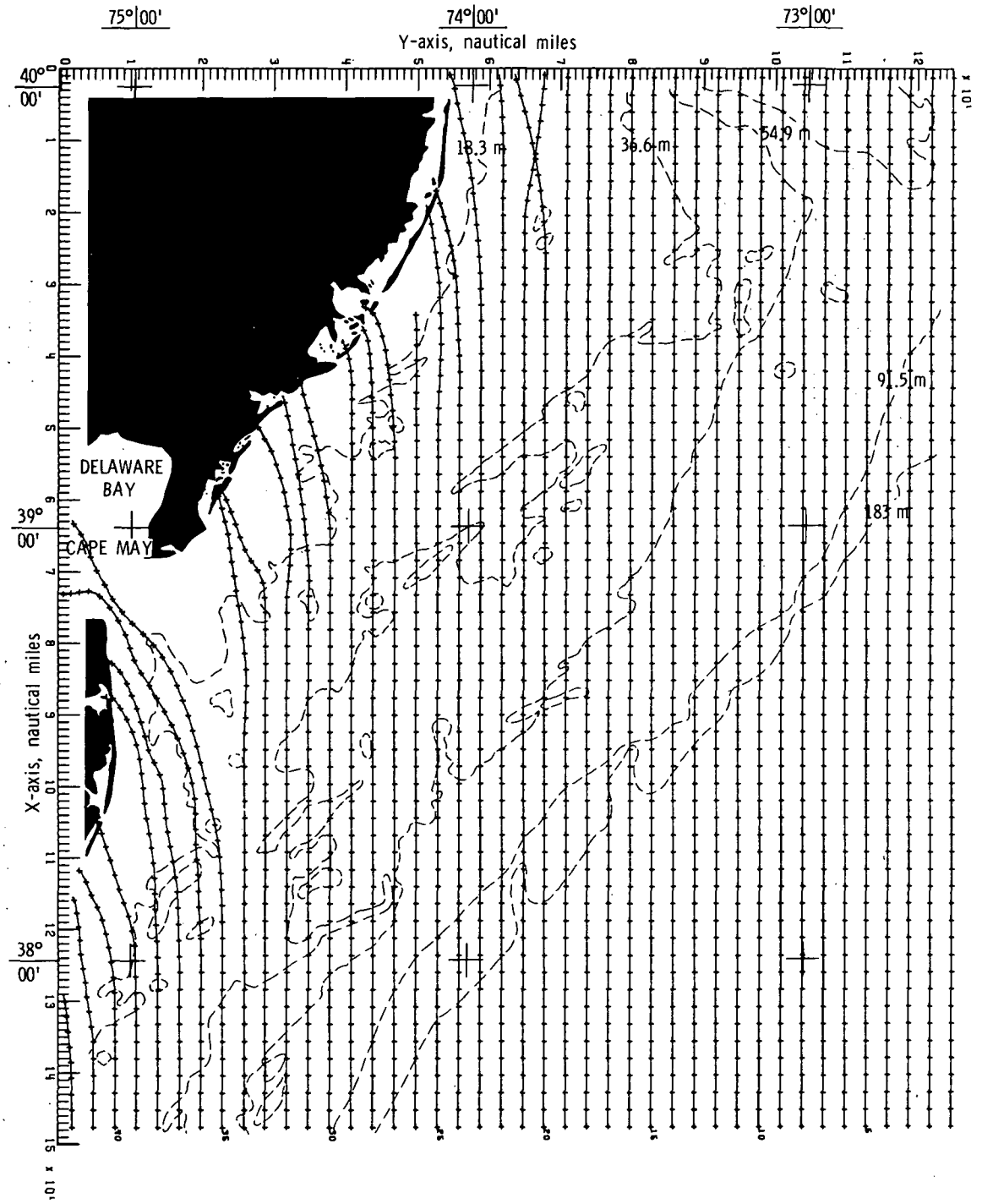


(a) Bottom topography approximated by quadratic least squares technique.

Figure 48.- Wave refraction diagrams. $\alpha = 180^{\circ}$; T = 8 seconds.

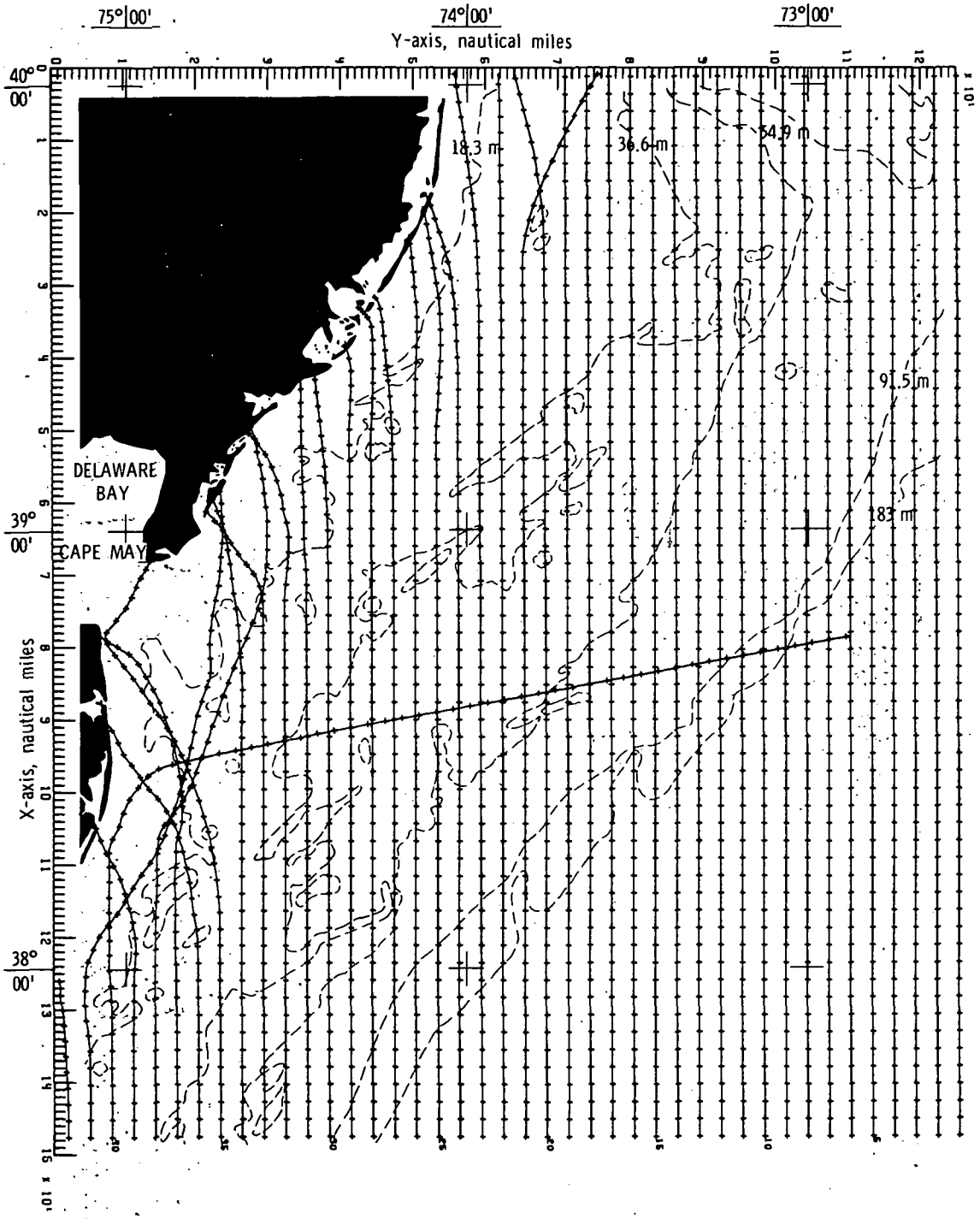


(b) Bottom topography approximated by cubic least squares technique.

Figure 48.- Continued.

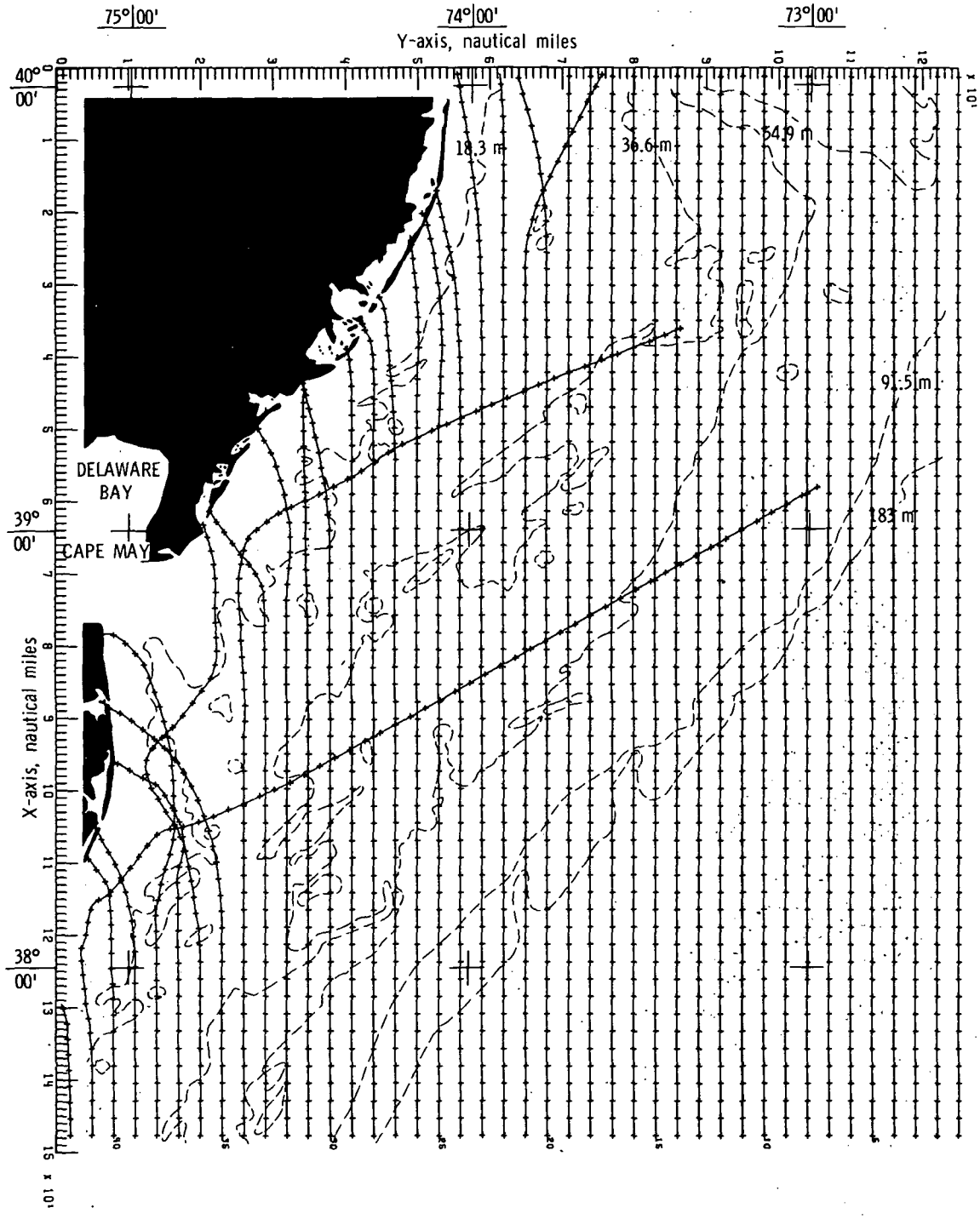


(c) Bottom topography approximated by constrained bicubic interpolation technique.

Figure 48.- Concluded.

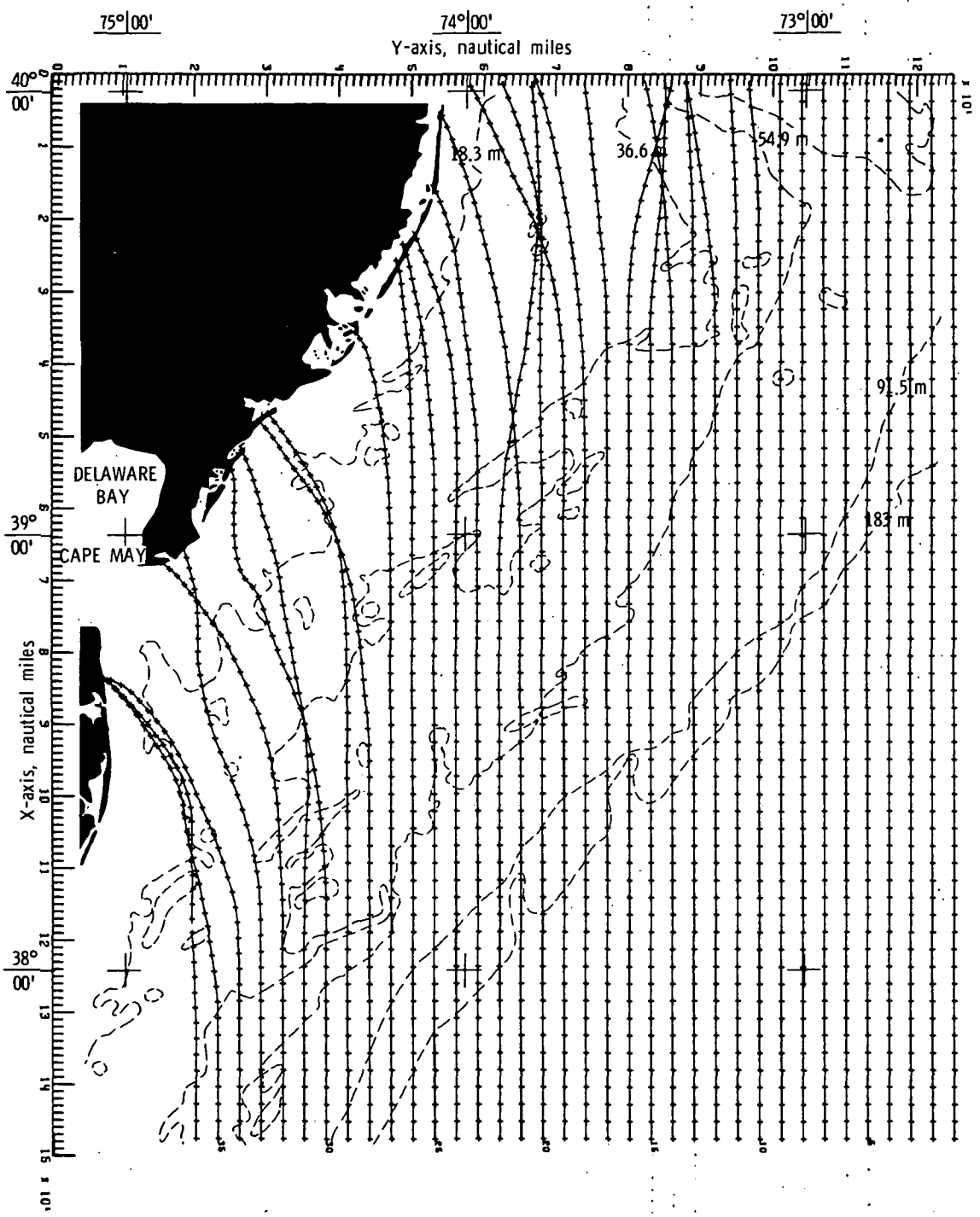


(a) Bottom topography approximated by quadratic least squares technique.

Figure 49.- Wave refraction diagrams. $\alpha$ = 180°; T = 10 seconds.

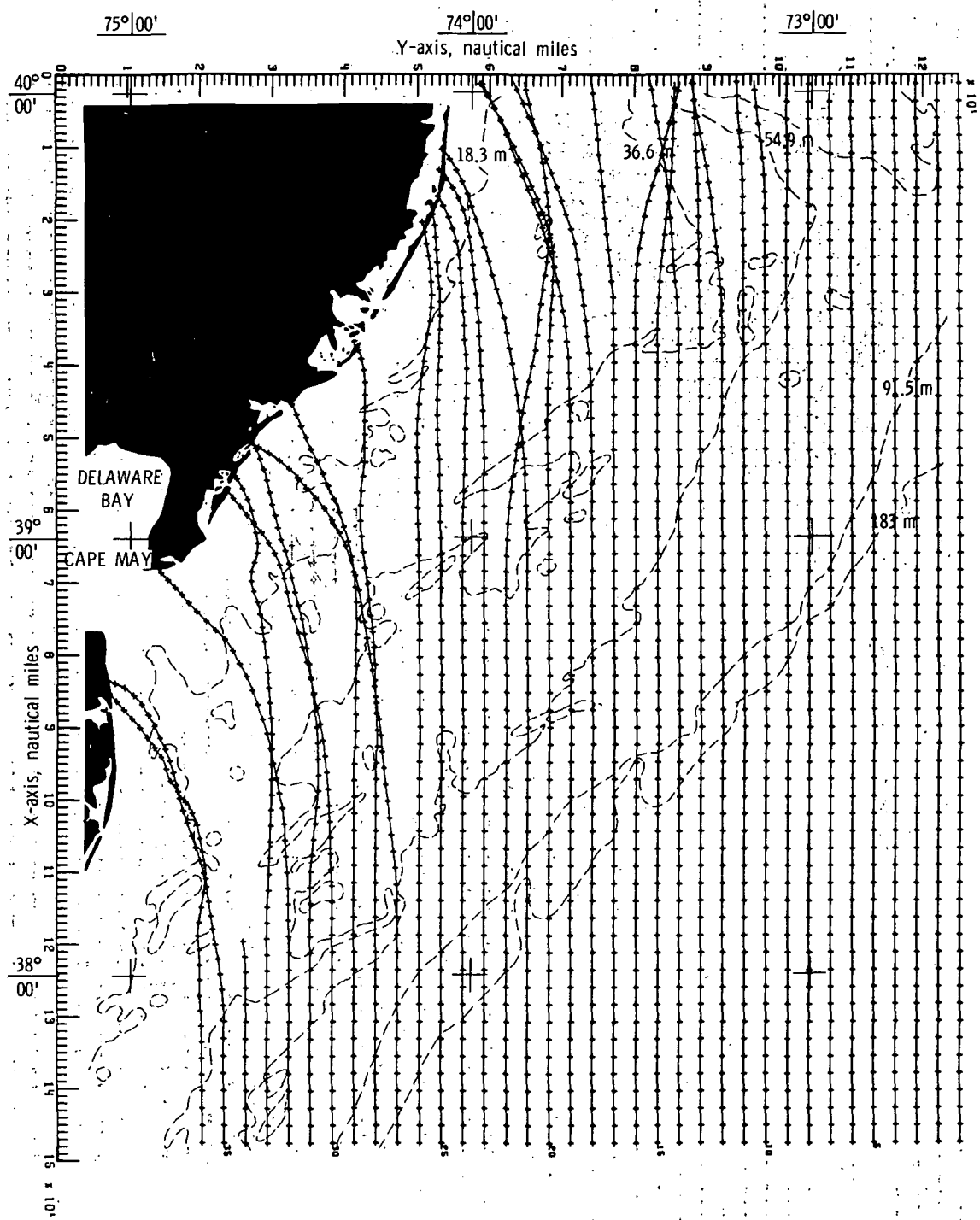


(b) Bottom topography approximated by cubic least squares technique.

Figure 49.- Continued.

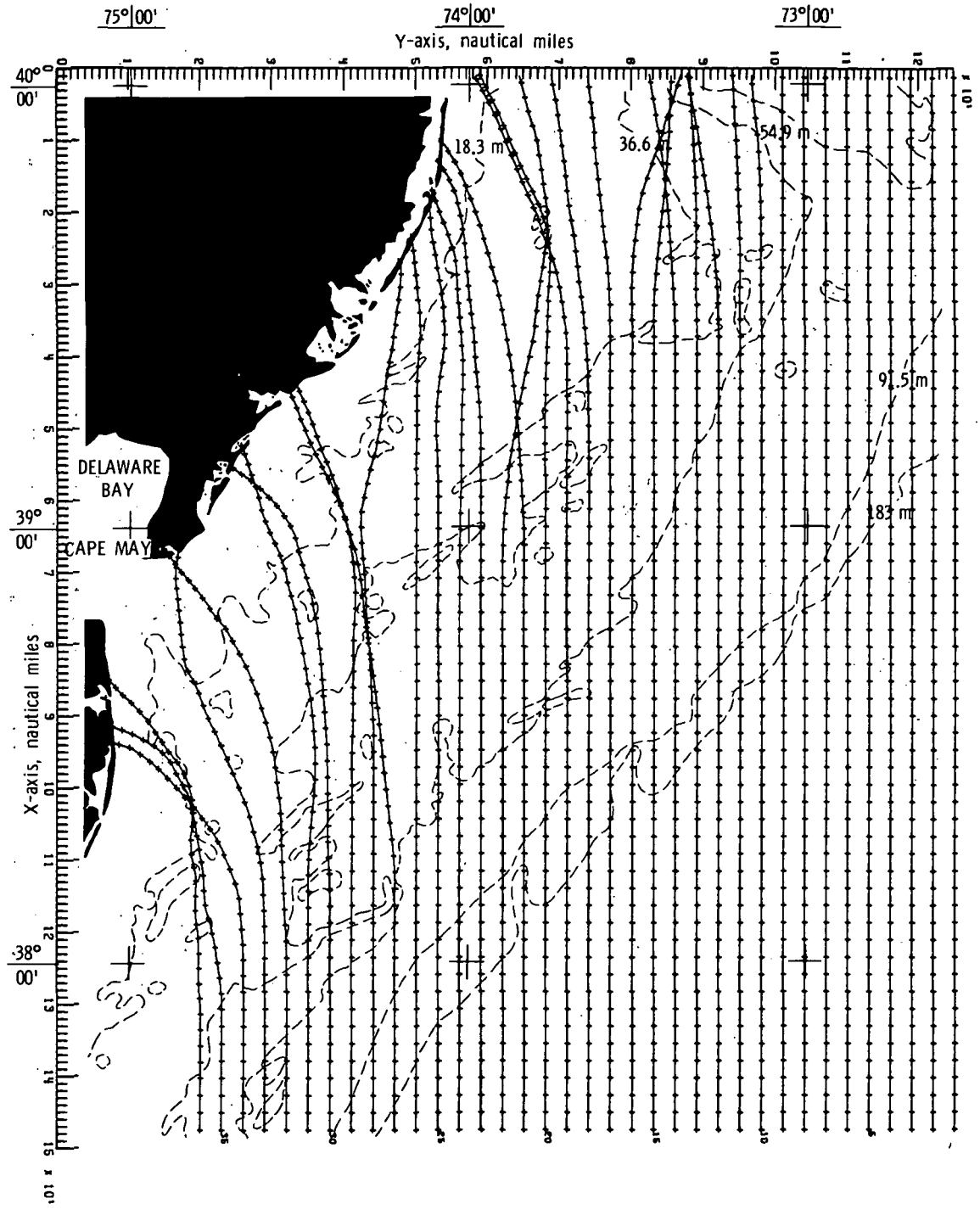


(c) Bottom topography approximated by constrained bicubic interpolation technique.

Figure 49.- Concluded.

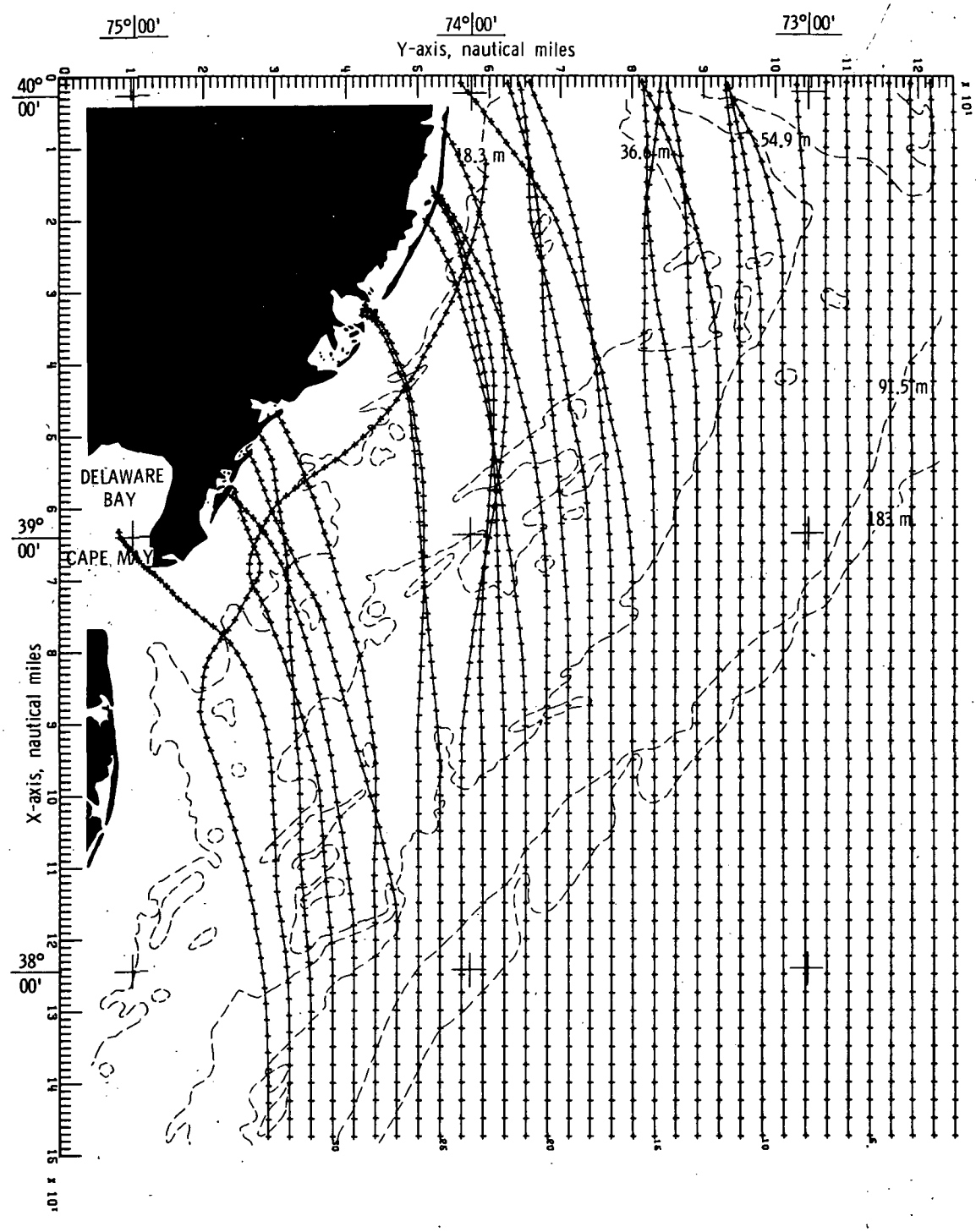


(a) Bottom topography approximated by quadratic least squares technique.

Figure 50.- Wave refraction diagrams. $\alpha = 180^{\circ}$; T = 12 seconds.

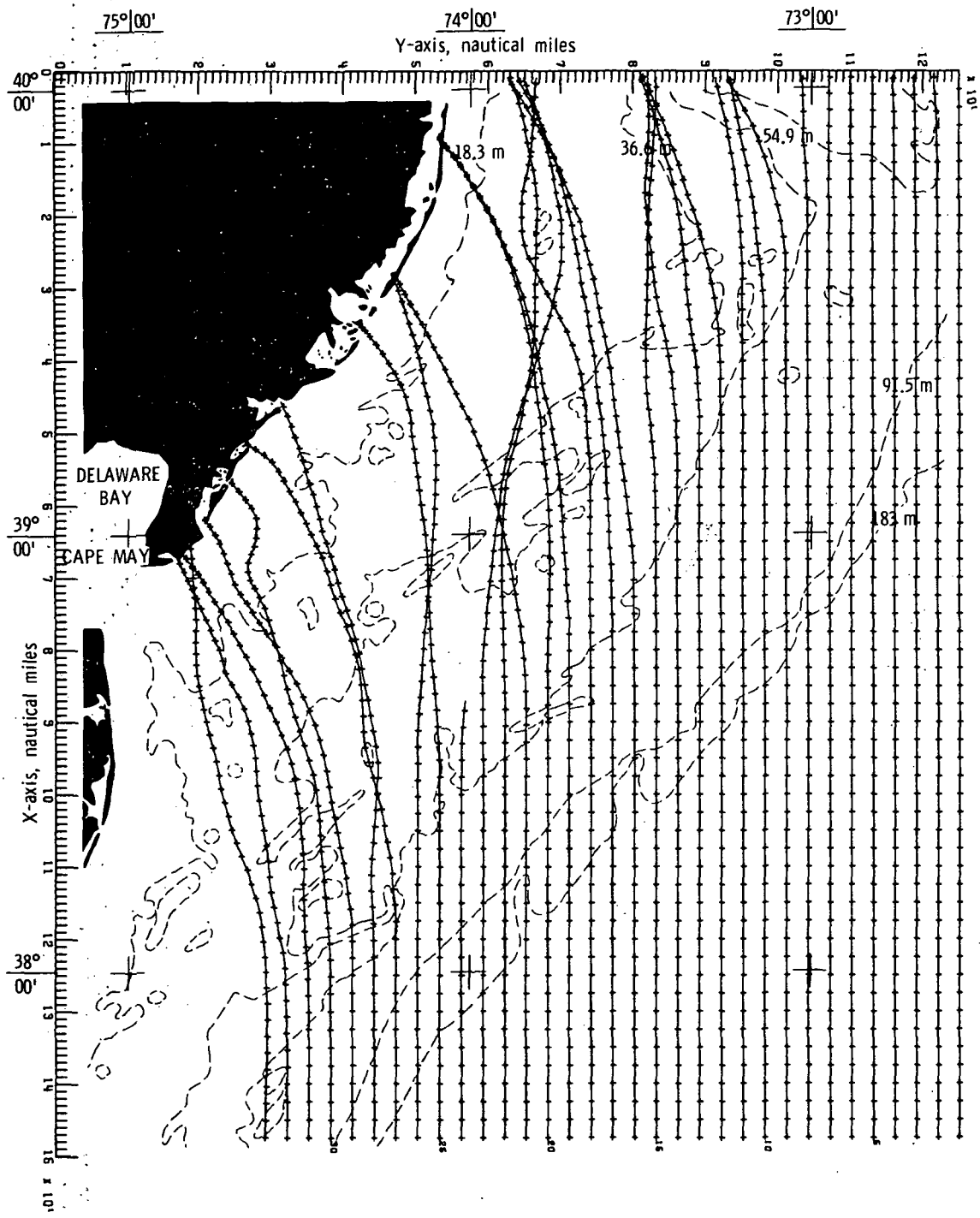


(b) Bottom topography approximated by cubic least squares technique.

Figure 50.- Continued.

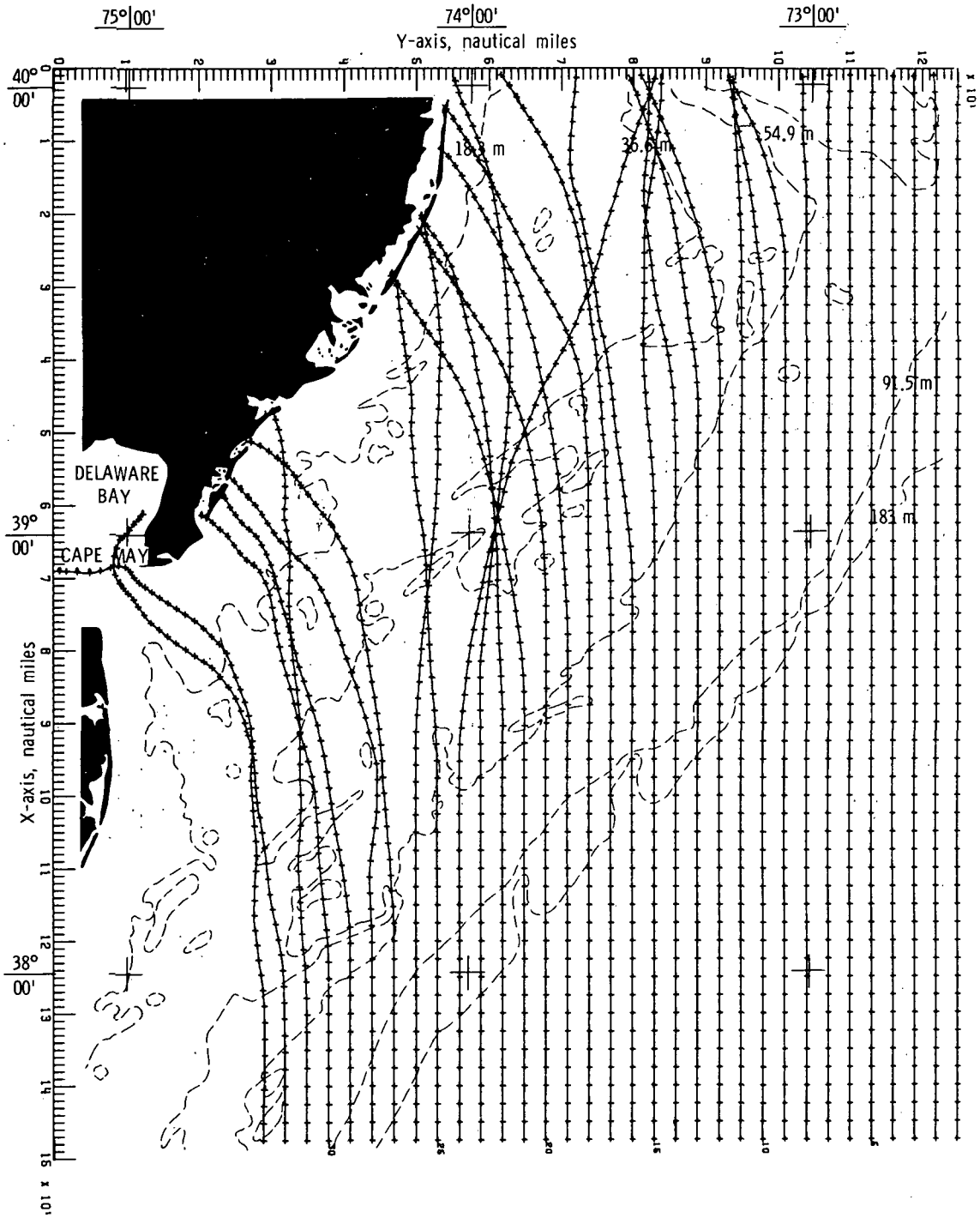


(c) Bottom topography approximated by constrained bicubic interpolation technique.

Figure 50.- Concluded.

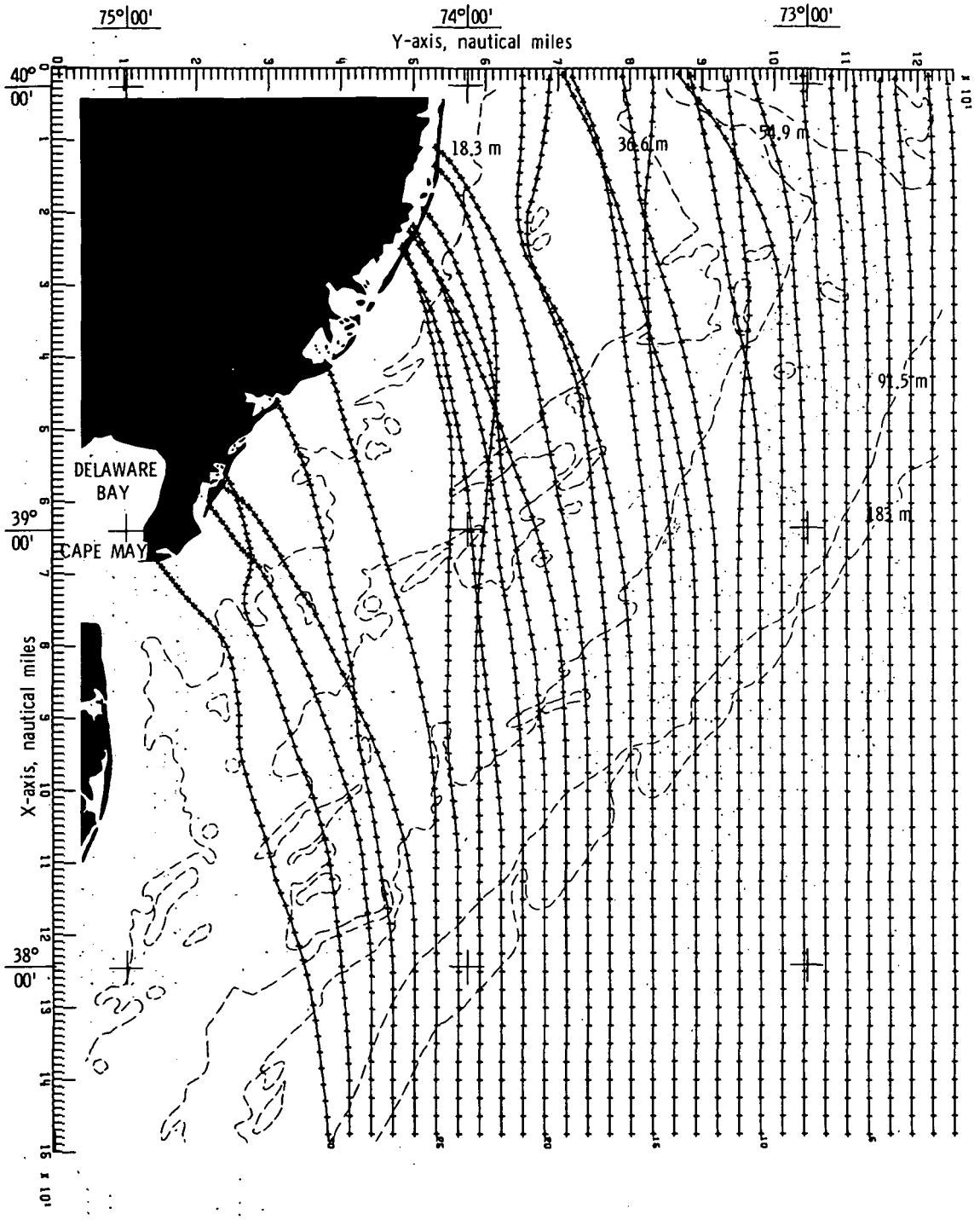


(a) Bottom topography approximated by quadratic least squares technique.

Figure 51.- Wave refraction diagrams. $\alpha = 180^{\circ}$; T = 14 seconds.

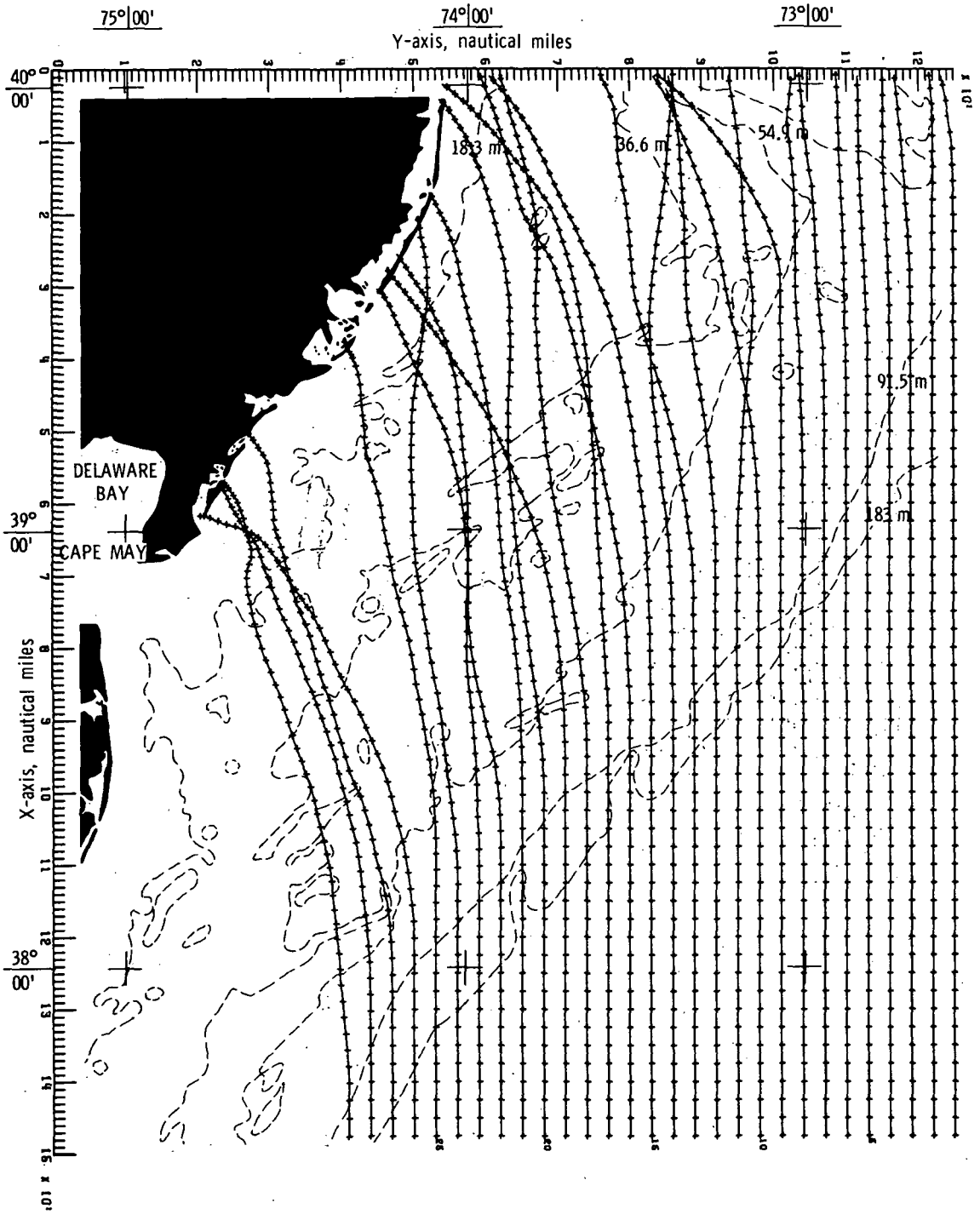


(b) Bottom topography approximated by cubic least squares technique.

Figure 51.- Continued.

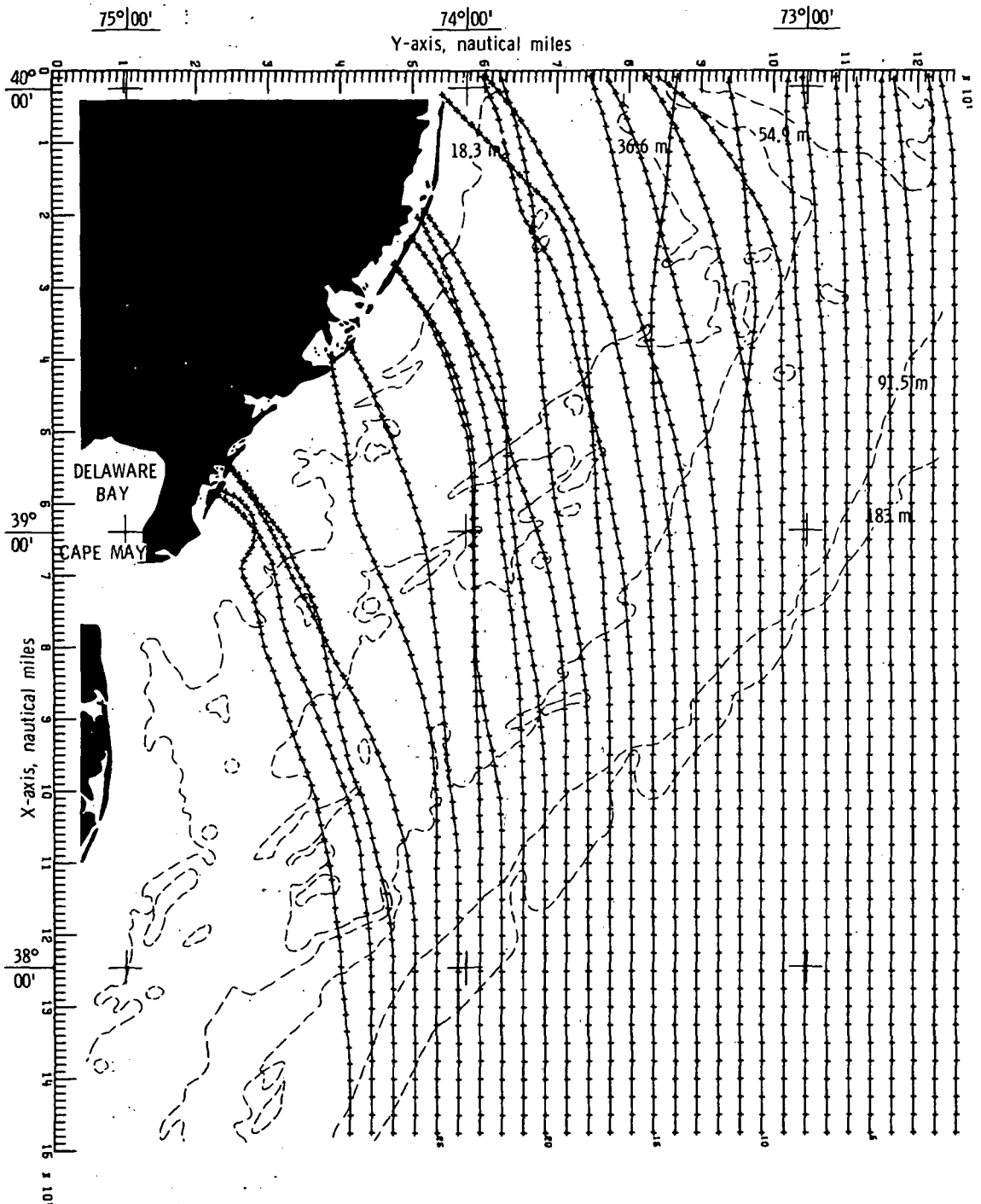


(c) Bottom topography approximated by constrained bicubic interpolation technique.

Figure 51.- Concluded.

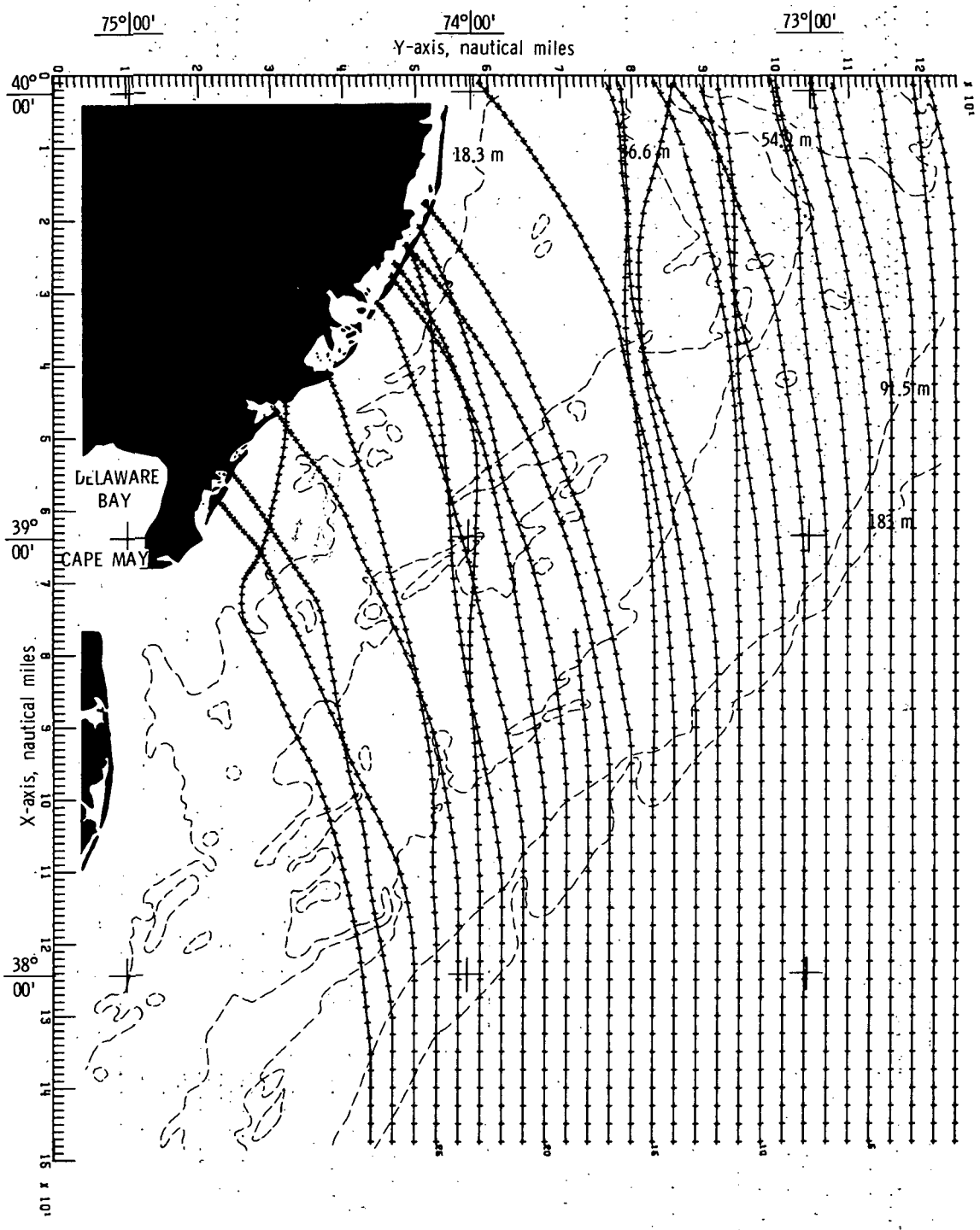


(a) Bottom topography approximated by quadratic least squares technique.

Figure 52.- Wave refraction diagrams. $\alpha = 180^{o}$; T = 16 seconds.

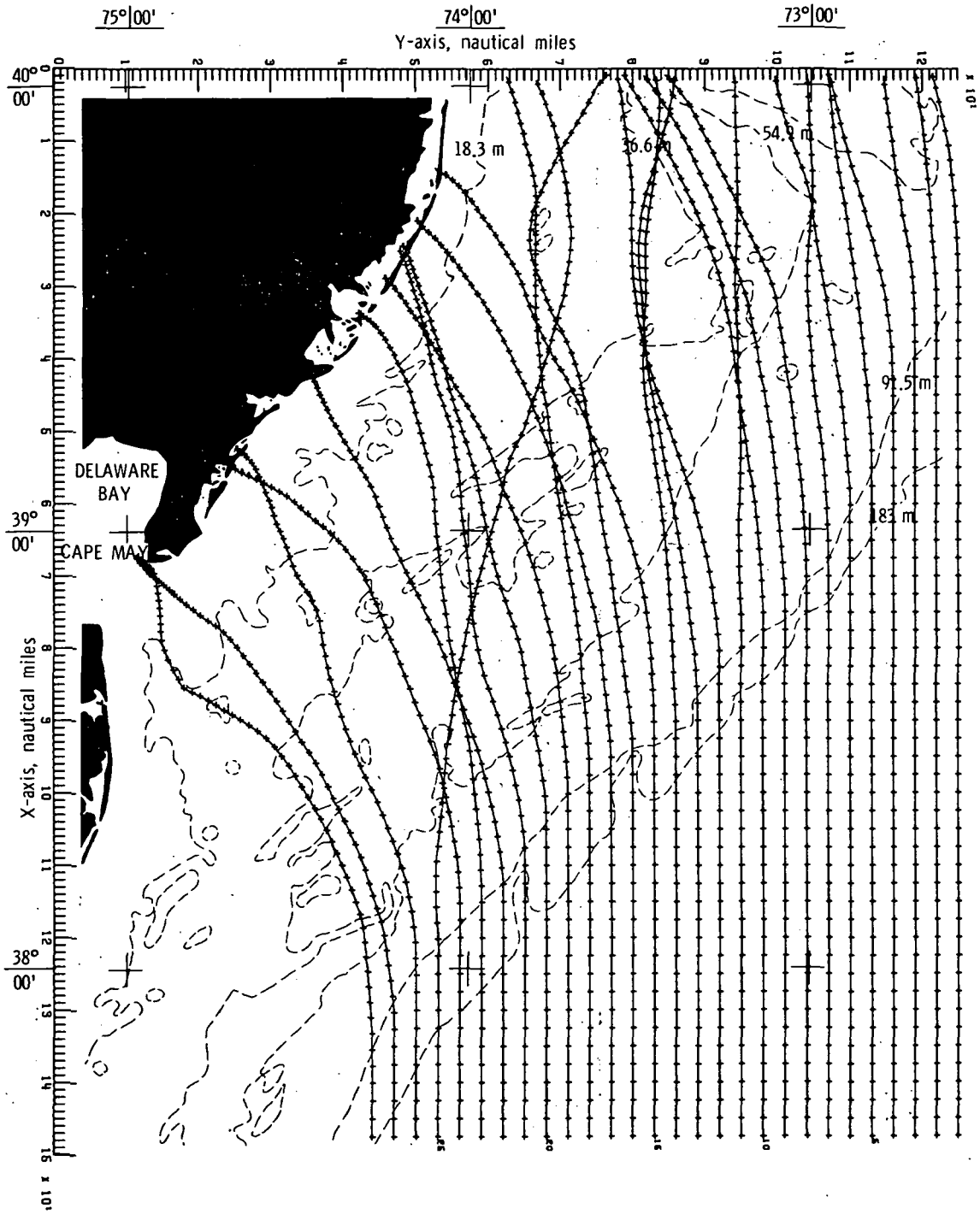


(b) Bottom topography approximated by cubic least squares technique.

Figure 52.- Continued.

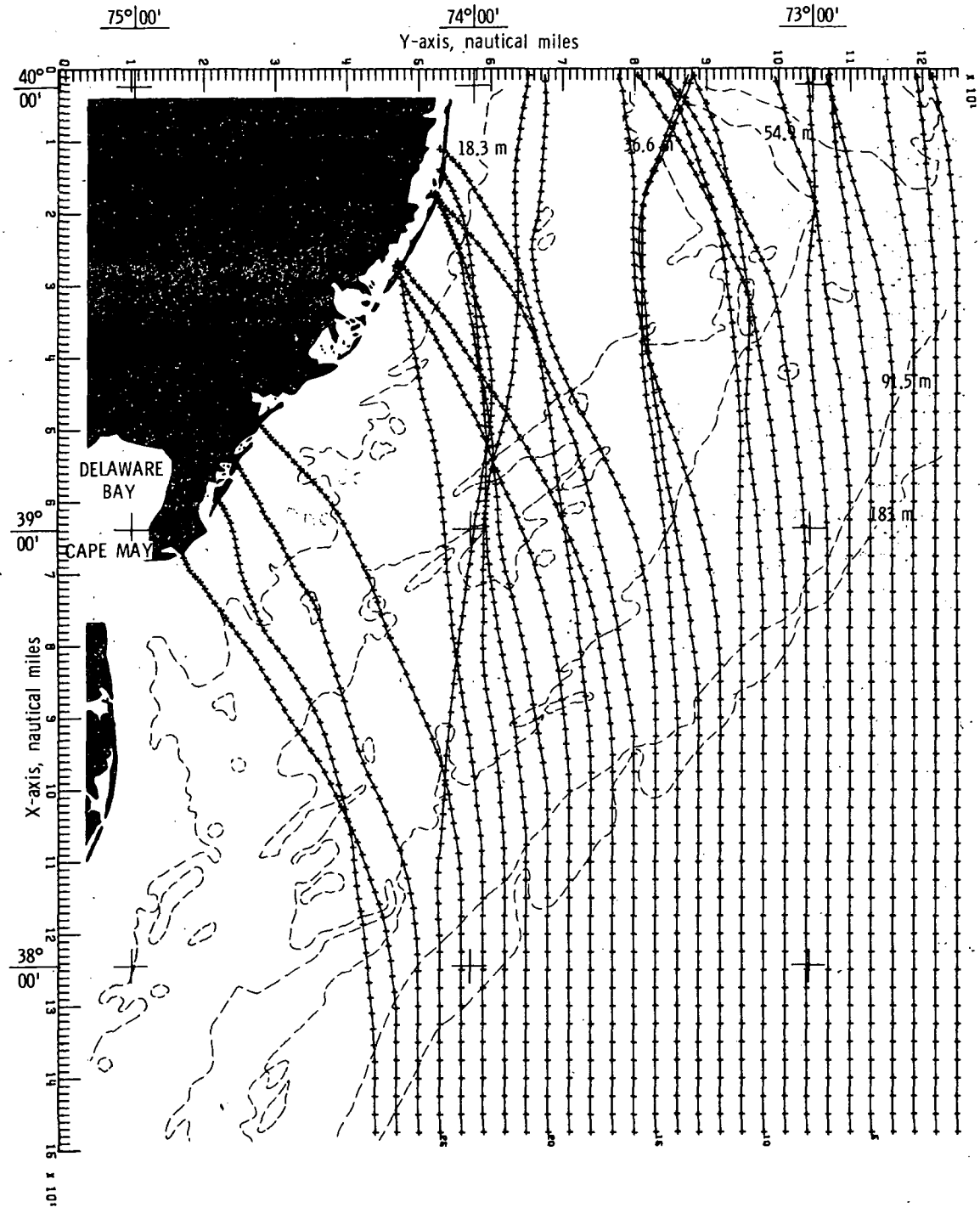


(c) Bottom topography approximated by constrained bicubic interpolation technique.

Figure 52.- Concluded.

## REFERENCES


1. Goldsmith, Victor; Morris, W. Douglas; Byrne, Robert J.; and Whitlock, Charles H.: Wave Climate Model of the Mid-Atlantic Shelf and Shoreline (Virginian Sea) - Model Development, Shelf Geomorphology, and Preliminary Results. NASA SP-358, VIMS SRAMSOE No. 38, 1974.
2. Poole, Lamont R.: Random-Access Technique for Modular Bathymetry Data Storage in a Continental-Shelf Wave-Refraction Program. NASA TM X-3018, 1974.
3. Poole, Lamont R.: Comparison of Techniques for Approximating Ocean Bottom Topography in a Wave-Refraction Computer Model. NASA TN D-8050, 1975.
4. Goldsmith, Victor: Shoreline Waves, Another Energy Crisis. VIMS Contrib. No. 734 to First Annual Conference of the Coastal Society (Arlington, Virginia), Nov. 1975.



Langley Research Center
National Aeronautics and Space Administration
Hampton, VA 23665

September 8, 1976


*U.S. GOVERNMENT PRINTING OFFICE: 1976 - 735-004/8

NATIONAL AERONAUTICS AND SPACE ADMINISTRATION
WASHINGTON, D.C. 20546

OFFICIAL BUSINESS
PENALTY FOR PRIVATE USE $300

SPECIAL FOURTH-CLASS RATE BOOK

POSTAGE AND FEES PAID
NATIONAL AERONAUTICS AND SPACE ADMINISTRATION
451

U.S.MAIL

POSTMASTER: If Undeliverable (Section 158 Postal Manual) Do Not Retur

*"The aeronautical and space activities of the United States shall be conducted so as to contribute . . . to the expansion of human knowledge of phenomena in the atmosphere and space. The Administration shall provide for the widest practicable and appropriate dissemination of information concerning its activities and the results thereof."*

—NATIONAL AERONAUTICS AND SPACE ACT OF 1958

# NASA SCIENTIFIC AND TECHNICAL PUBLICATIONS

TECHNICAL REPORTS: Scientific and technical information considered important, complete, and a lasting contribution to existing knowledge.

TECHNICAL NOTES: Information less broad in scope but nevertheless of importance as a contribution to existing knowledge.

TECHNICAL MEMORANDUMS: Information receiving limited distribution because of preliminary data, security classification, or other reasons. Also includes conference proceedings with either limited or unlimited distribution.

CONTRACTOR REPORTS: Scientific and technical information generated under a NASA contract or grant and considered an important contribution to existing knowledge.

TECHNICAL TRANSLATIONS: Information published in a foreign language considered to merit NASA distribution in English.

SPECIAL PUBLICATIONS: Information derived from or of value to NASA activities. Publications include final reports of major projects, monographs, data compilations, handbooks, sourcebooks, and special bibliographies.

TECHNOLOGY UTILIZATION PUBLICATIONS: Information on technology used by NASA that may be of particular interest in commercial and other non-aerospace applications. Publications include Tech Briefs, Technology Utilization Reports and Technology Surveys.

***Details on the availability of these publications may be obtained from:***

**SCIENTIFIC AND TECHNICAL INFORMATION OFFICE**

**NATIONAL AERONAUTICS AND SPACE ADMINISTRATION**

**Washington, D.C. 20546**